PNL-8500, Pt. 1
UC-408

Pacific Northwest Laboratory Annual Report for 1992 to the DOE Office of Energy Research

Part 1: Biomedical Sciences

J. F. Park and Staff

June 1993

Prepared for
the U.S. Department of Energy
under Contract DE-AC06-76RLO 1830

Pacific Northwest Laboratory
Richland, Washington 99352

Preface

This 1992 Annual Report from Pacific Northwest Laboratory (PNL) to the U.S. Department of Energy (DOE) describes research in environment and health conducted during fiscal year 1992. This year the report consists of four parts, each in a separate volume.

The four parts of the report are oriented to particular segments of the PNL program, describing research performed for the DOE Office of Health and Environmental Research (OHER) in the Office of Energy Research. In some instances, the volumes report on research funded by other DOE components or by other governmental entities under interagency agreements. Each part consists of project reports authored by scientists from several PNL research departments, reflecting the multidisciplinary nature of the research effort.

The parts of the 1992 Annual Report are:

Part 1: Biomedical Sciences		
Program Manager: J. F. Park		J. F. Park, Report Coordinator S. A. Kreml, Editor
Part 2: Environmental Sciences		
Program Manager: R. E. Wildung		L. K. Grove, Editor
Part 3: Atmospheric Sciences		
Program Manager: W. R. Barchet		R. E. Schrempf, Editor
Part 4: Physical Sciences		
Program Manager: L. H. Toburen		L. H. Toburen, Report Coordinator W. C. Cosby, Editor

Activities of the scientists whose work is described in this annual report are broader in scope than the articles indicate. PNL staff have responded to numerous requests from DOE during the year for planning, for service on various task groups, and for special assistance.

Credit for this annual report goes to the many scientists who performed the research and wrote the individual project reports, to the program managers who directed the research and coordinated the technical progress reports, to the editors who edited the individual project reports and assembled the four parts, and to Ray Baalman, editor in chief, who directed the total effort.

T. S. Tenforde
Health and Environmental Research Program

Previous reports in this series:

Annual Report for

1951	HW-25021, HW-25709
1952	HW-27814, HW-28636
1953	HW-30437, HW-30464
1954	HW-30306, HW-33128, HW-35905, HW-35917
1955	HW-39558, HW-41315, HW-41500
1956	HW-47500
1957	HW-53500
1958	HW-59500
1959	HW-63824, HW-65500
1960	HW-69500, HW-70050
1961	HW-72500, HW-73337
1962	HW-76000, HW-77609
1963	HW-80500, HW-81746
1964	BNWL-122
1965	BNWL-280, BNWL-235, Vol. 1-4; BNWL-361
1966	BNWL-480, Vol. 1; BNWL-481, Vol. 2, Pt. 1-4
1967	BNWL-714, Vol. 1; BNWL-715, Vol. 2, Pt. 1-4
1968	BNWL-1050, Vol. 1, Pt. 1-2; BNWL-1051, Vol. 2, Pt. 1-3
1969	BNWL-1306, Vol. 1, Pt. 1-2; BNWL-1307, Vol. 2, Pt. 1-3
1970	BNWL-1550, Vol. 1, Pt. 1-2; BNWL-1551, Vol. 2, Pt. 1-2
1971	BNWL-1650, Vol. 1, Pt. 1-2; BNWL-1651, Vol. 2, Pt. 1-2
1972	BNWL-1750, Vol. 1, Pt. 1-2; BNWL-1751, Vol. 2, Pt. 1-2
1973	BNWL-1850, Pt. 1-4
1974	BNWL-1950, Pt. 1-4
1975	BNWL-2000, Pt. 1-4
1976	BNWL-2100, Pt. 1-5
1977	PNL-2500, Pt. 1-5
1978	PNL-2850, Pt. 1-5
1979	PNL-3300, Pt. 1-5
1980	PNL-3700, Pt. 1-5
1981	PNL-4100, Pt. 1-5
1982	PNL-4600, Pt. 1-5
1983	PNL-5000, Pt. 1-5
1984	PNL-5500, Pt. 1-5
1985	PNL-5750, Pt. 1-5
1986	PNL-6100, Pt. 1-5
1987	PNL-6500, Pt. 1-5
1988	PNL-6800, Pt. 1-5
1989	PNL-7200, Pt. 1-5
1990	PNL-7600, Pt. 1-5
1991	PNL-8000, Pt. 1-5

Foreword

This report summarizes progress in OHER biological research and general life sciences research programs conducted at PNL in FY 1992. The research develops the knowledge and fundamental principles necessary to identify, understand, and anticipate the long-term health consequences of energy-related radiation and chemicals. Our continuing emphasis is to decrease the uncertainty of health risk estimates from energy-related technologies through an increased understanding of the ways in which radiation and chemicals cause biological damage.

The sequence of this report of PNL research reflects the OHER programmatic structure. The first section, **Biological Research**, contains reports of biological research in laboratory animals and *in vitro* cell systems, including research with radiation, radionuclides, and chemicals. The next section, **General Life Sciences Research**, reports research conducted for the OHER human genome research program.

Biological Research

Life-span studies in beagles with inhaled $^{239}Pu(NO_3)_4$ were in the 15th postexposure year. All 105 plutonium-exposed dogs are dead; 28 dogs had bone tumors, 34 had lung tumors, and 14 had liver tumors. Bone or lung tumors were also the primary plutonium-exposure-related causes of death in beagles with inhaled $^{238}PuO_2$ initial lung depositions (ILD) $\geq$0.67 kBq. Six of the dogs had liver tumors; however, liver tumors were the cause of death in only 1 dog. Although liver tumors were not a primary cause of death, chronic increased levels of serum alanine aminotransferase (ALT), indicating liver damage, were observed in dose-level groups with ILD $\geq$2.9 kBq 9 years after exposure, 4 years earlier than the median survival time of the group.

The "National Radiobiology Archives" project is a comprehensive effort to gather, organize, and catalog data, documents, and tissues related to life-span radiobiology studies for future research and analyses. The scope of the information system has been expanded to include dose-effect information on approximately 7,000 beagles and 10,000 mice from seven laboratories. An introduction to the system is available on diskette.

Dose-effect-relationship studies on inhaled $^{239}PuO_2$ in rats are in progress to obtain lung tumor incidence data at lifetime lung doses of 0.05 to 55 Gy. The incidence of lung tumors was 0.32% in 1877 rats receiving $\leq$1 Gy to the lung, 42% in 229 rats receiving $\geq$1 Gy, and 0.19% in 1052 controls. Although 1% of deposited plutonium was found in subepithelial locations of upper airways, the dose calculated to upper-airway epithelium from subepithelially located particles was small, and no tumors were observed in the bronchi, trachea, or larynx. No significant difference in tumor frequency, location, or type was found between control and exposed rats, other than for tumors in the lung.

Rats exposed by inhalation to radon, radon progeny, and uranium ore dust are being evaluated to determine the influence of dose, dose rate, and cigarette smoke in lung cancer incidence. The overall trend in lung tumor incidence decreases in proportion to the decrease in cumulative radon exposure and remains elevated at exposures less than 100 working-level months (WLM), levels comparable to those found in houses. Rats exposed to uranium ore dust alone showed no tumors in the lung, suggesting minimal involvement of ore dust in carcinogenicity of mixed exposures to radon progeny and uranium ore dust. Rats exposed to radon (320 WLM) and cigarette-smoke mixtures showed hyperplasia of nonciliated cells with thickening of tracheal epithelium at 25 weeks of exposure; the epithelium recovered to within control values by 27 weeks after exposure.

After *in vitro* x-irradiation or radon exposure, the largest category of CHO-HGPRT mutation types obtained was full deletions of the gene. The percentage of full deletions obtained from both levels of radon (25 to

77 cGy) and the 300-cGy x-ray exposure were similar (44% to 48%) compared to 14% spontaneous deletions.

Studies are in progress to determine the relationships between *in vivo* radon-exposure levels and radiation dose to cells of the respiratory tract by comparing cellular damage induced by alpha particles both *in vivo* and *in vitro*. Studies on radon-induced micronuclei in rat lung fibroblasts determined that a 1-WLM exposure *in vivo* resulted in an amount of chromosome damage similar to that from a 0.6-mGy *in vitro* dose. Studies on chromosomes aberration frequency in rat tracheal epithelial cells determined that a 1-WLM exposure *in vivo* resulted in an amount of chromosome damage similar to a 2.2-mGy *in vitro* ^{238}Pu alpha-particle dose.

Microdosimetric dose–effect relationship modeling of *in vitro* rat lung epithelial cells exposed to ^{238}Pu alpha particles showed that a cell whose nucleus received a single alpha hit has a 50% probability of not showing any micronuclei. Most cells exhibiting more than two micronuclei had experienced multiple hits.

Physiologically based pharmacokinetic (PBPK) models to predict the uptake and retention of radon, thoron, and their progeny were refined to more accurately predict individual variation following ingestion exposure and then compared with human data. A new model was developed to predict uptake and retention of lead.

A recirculating animal exposure system that simulates the ultrafine (unattached) fraction of radon-progeny potential alpha energy in homes was designed. Our ultrafine radon progeny size-spectrometer and low-pressure impactor, both employing CR-39 track-etch technology, are used to monitor and measure the conversion coefficient between exposure and dose during a representative period and at low levels of exposure.

We are examining the role of oncogenes and tumor suppressor genes in lung cancer in rats and dogs that had inhaled radon progeny or plutonium and in leukemic dogs that were exposed to whole-body irradiation. We have identified activating *ras* mutations in leukemic dog spleen tumors, in lung tumors from plutonium-exposed dogs, and in lung tumors from radon-progeny-exposed rats. We also have identified *ras* second-exon mutations that have not been documented previously as *ras* activating and have characterized the p53 suppressor gene. The rat gene lacks one intron that occurs in the human and mouse gene. The sizes of the exons, introns, and splice junction are similar for all species.

Research on the potential interaction of mutated oncogenes with ^{239}Pu and the organic solvent CCl_4 in the production of liver cancer in mice showed an increase in liver nodules and liver cancer and decreased survival in animals that received combined exposure relative to those exposed to single insults. Analysis of liver nodules indicated that the cells in the nodules expressed either K-*ras* or *neo* genes and were clonal in origin.

Studies are in progress to determine whether benzo[a]pyrene diolepoxide (BPDE) adduct locations and frequency of adduction are altered in plasmid DNA reconstituted into nucleosomes. When reconstituted supercoiled pGEM-5S plasmid was incubated with (±)-anti-BPDE, less binding was observed on reconstituted DNA than on naked plasmid, suggesting that interactions between the DNA and histones protected the DNA from BPDE modifications. When a site-specific BPDE-modified oligomer was incubated with a polymerase, a significant amount of synthesis past the lesion was observed. The position of polymerase blockage and the amount of translesional synthesis varied with the polymerase used.

In a new project, we are examining the effects of DNA structure and chemical microenvironment in free radical-induced DNA damage. Liquid chromatography–thermospray mass spectrometric analysis of an irradiated sample of 2′-deoxyadenosine revealed formation of (R)- and (S)-8,5′-cyclodeoxyadenosine and 8-oxodeoxyadenosine in addition to radiolytic base release. Completion of these analyses coupled with

our ongoing effort to synthesize 8,5′-cyclodeoxyadenosine provides the essential background to quantitate these products in irradiated samples of DNA using mass spectrometry.

General Life Sciences Research

Pacific Northwest Laboratory is developing a computer information system to graphically display and manipulate the vast amounts of information in genome databases. GnomeView is an interface to databases rather than a data repository. It integrates information across databases and between different levels in the mapping hierarchy. In GnomeView Version 1.0 Beta, entry at the chromosome level is to Genome Data Base and entry at the sequence level is to GenBank. Other possible entry levels including restriction enzyme, contig, and linkage mapping are inactive in Version 1.0 Beta. As more cross-referenced databases containing the appropriate data became available, entry at these levels will be incorporated into the system.

Biomedical research at PNL is an interdisciplinary effort requiring scientific contributions from many research departments throughout the laboratory. Personnel in the Life Sciences Center are the principal contributors to this report.

Requests for reprints from the list of publications will be honored while supplies are available.

Contents

Biological Research

Inhaled Plutonium Oxide in Dogs

Principal Investigator: *J. F. Park*

Other Investigators: *R. L. Buschbom, G. E. Dagle, E. S. Gilbert, G. J. Powers, C. R. Watson, and R. E. Weller*

Technical Assistance: *R. F. Flores and B. G. Moore*

This project is concerned with long-term experiments to determine the life-span dose-effect relationships of inhaled $^{239}PuO_2$ and $^{238}PuO_2$ in beagles. This report describes dose-effect relationships in the liver of beagle dogs receiving a single exposure of $^{238}PuO_2$ aerosols to obtain dose-level groups of 20 dogs with mean initial lung depositions (ILD) of 0.061, 0.67, 2.9, 13, 51, and 192 kBq. Bone or lung tumors were the primary plutonium-exposure-related causes of death in dose-level groups with ILDs ≥ 0.67 kBq. Approximately 20% of ILD was translocated to the liver. Six of 116 dogs had liver tumors; however, liver tumors were the cause of death in only 1 dog. Although liver tumors were not a primary cause of death, increased levels of serum alanine aminotransferase (ALT), which indicates liver damage, were observed in dose-level groups with ILD ≥ 2.9 kBq as compared to control dogs. In the lowest dose-level group with increased ALT, the level of serum ALT was first observed to be higher than that of controls 9 years after exposure, 4 years earlier than the median survival time of the group. At 9 years after exposure, the mean cumulative dose to the liver was 0.2 Gy; the mean dose rate was 0.03 Gy/yr, and the concentration of plutonium in the liver was 1.2 Bq/g.

To determine the life-span dose-effect relationships of inhaled plutonium, 18-month-old beagle dogs were exposed to aerosols of $^{239}PuO_2$ [mean activity median aerodynamic diameter (AMAD), 2.3 μm; mean geometric standard deviation (GSD), 1.9], prepared by calcining the oxalate at 750°C for 2 hours; or to $^{238}PuO_2$ (mean AMAD, 1.8 μm; mean GSD, 1.9), prepared by calcining the oxalate at 700°C and subjecting the product to $H_2{}^{16}O$ steam in argon exchange at 800°C for 96 hours. This material, referred to as pure plutonium oxide, is used as fuel in space nuclear-power systems.

One hundred thirty dogs exposed to $^{239}PuO_2$ in 1970 and 1971 were selected for long-term studies; 14 dogs were periodically sacrificed to obtain plutonium distribution and pathology data, and 116 were assigned to life-span dose-effect studies (Table 1). The 116 dogs exposed to $^{238}PuO_2$ in 1973 and 1974 were selected for life-span dose-effect studies (Table 2), and 21 additional dogs were exposed for periodic sacrifice. The Appendix (which follows Part 1 of this *Annual Report*) shows the status of the dogs in these experiments. The *Pacific Northwest*

TABLE 1. Life-Span Dose-Effect Studies with Inhaled $^{239}PuO_2$ in Beagles[a]

Exposure-Level Group	Number of Dogs		Initial Lung Deposition[b]	
	Male	Female	kBq[c]	Bq/g Lung[c]
Control	10	10	0	0
1	10	11	0.12±0.05	0.93±0.39
2	11	11	0.69±0.14	6.2±1.3
3	11	10	2.7±0.5	23±4
4	12	12	11±2	95±17
5	10	10	41±6	349±46
6	3	5	213±120	2130±1160
	67	69		

(a) Exposed in 1970 and 1971.
(b) Estimated from external thorax counts at 2 and 4 weeks after exposure, and from estimated lung weights (0.011 x body weight).
(c) Mean ± 95% confidence intervals around mean.

TABLE 2. Life-Span Dose-Effect Studies with Inhaled $^{238}PuO_2$ in Beagles[a]

Exposure-Level Group	Number of Dogs		Initial Lung Deposition[b]	
	Male	Female	kBq[c]	Bq/g Lung[c]
Control	10	10	0	0
1	10	10	0.061±0.036	0.48±0.28
2	11	10	0.67±0.12	5.9±1.2
3	12	10	2.9±0.4	24±3
4	10	10	13±3	106±21
5	10	10	51±10	403±68
6	7	6	192±51	1651±443
	70	66		

(a) Exposed in 1973 and 1974.
(b) Estimated from external thorax counts at 2 and 4 weeks after exposure, and from estimated lung weights (0.011 x body weight).
(c) Mean ± 95% confidence intervals around mean.

Laboratory Annual Report for 1989 to the DOE Office of Energy Research, Part 1, summarized the results of the $^{239}PuO_2$ study, and the results of the $^{238}PuO_2$ study were summarized in the *Annual Report for 1990*. Because liver damage was one of the effects of inhaled $^{238}PuO_2$, this year we focused on evaluating dose-effect relationships of inhaled $^{238}PuO_2$ in the liver.

Bone tumors or lung tumors were the primary plutonium-exposure-related causes of death in dose-level groups 2, 3, 4, 5, and 6 (Table 3). Bone tumors were the primary cause of death in dose levels 4, 5, and 6, and they were usually fatal; that is, the dogs were euthanized because of the bone tumor. Although lung tumors were observed in 14 of 33 dogs euthanized because of bone tumors, the bone tumors were the cause of death. Lung tumors were observed in dose-level groups 2 and 3 at dose levels lower than those at which bone tumors were observed. The lung tumors were fatal in 6 of the 10 dogs with lung tumors in dose-level groups 2 and 3. Six dogs had liver tumors; however, liver tumor was the cause of death in only 1 dog, and that dog died of a hepatocellular carcinoma; 3 dogs had bile-duct adenomas and 2 had bile-duct carcinomas; 1 dog died of liver abscesses. No other deaths were associated with liver damage, and none of the dogs had clinical signs related to liver dysfunction. However, increases in serum alanine aminotransferase (ALT) levels, indicating liver damage, were observed in the four highest dose-level groups as compared to controls.

The plutonium content in the liver at death for each dog, measured by radiochemical analysis, was expressed as percent initial lung deposition (ILD), determined by *in vivo* counting, to obtain a liver uptake and retention function fitted by nonlinear regression (Figure 1). The liver retention equation was $y = 22.2(1-e^{-0.00109t})$ where y = percent ILD in liver and t = days after

TABLE 3. Primary Lung, Bone, and Liver Tumors in Dogs After Inhalation of $^{238}PuO_2$

Dose-Level Group	Mean Initial Lung Deposition, kBq	Median Survival After Exposure, days	Number of Dogs	Number of Dogs with Tumors					
				Lung Tumors		Bone Tumors		Liver Tumors	
				Total	Fatal[a]	Total	Fatal	Total	Fatal
Control	0	4974	20	1	1	0	0	1	0
1	0.061	4548	20	1	1	1	1	0	0
2	0.67	4752	21	8	5	0	0	1	0
3	2.9	4640	22	2	1	0	0	2	0
4	13	4244	20	4	1	7	6	3	1
5	51	2780	20	5	0	17	17	0	0
6	192	1899	13	9	3	9	9	0	0

(a) Fatal tumors causing death or euthanasia.

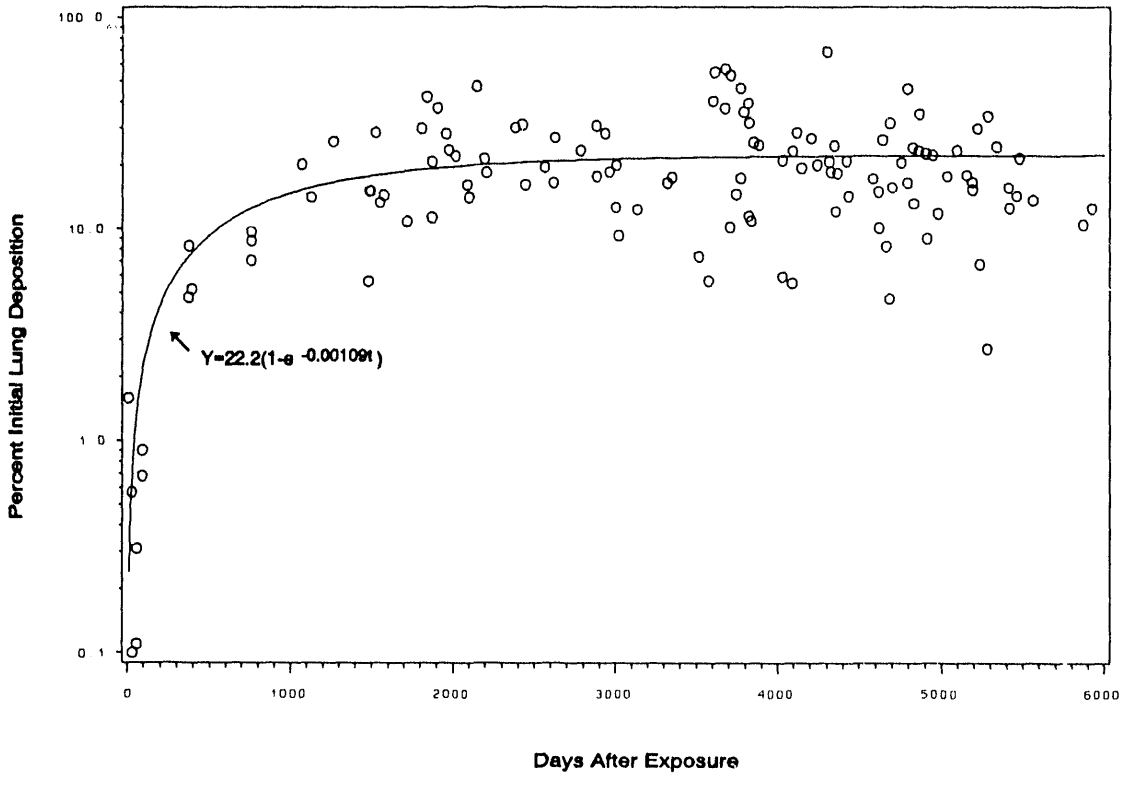

FIGURE 1. Liver Retention of Inhaled $^{238}PuO_2$ Determined by [(final liver burden of plutonium)/(initial lung deposition of plutonium)] x 100.

exposure. Approximately 20% of the ILD was translocated to the liver by 1500 days after exposure, and this amount was retained in the liver until death.

Cumulative dose to the liver was estimated by integrating the liver retention function and multiplying by the appropriate factors. Figure 2 shows the cumulative dose to the liver for a 10-kg dog with an ILD of 37 Bq. Dose rates to the liver were estimated by taking the derivative of the cumulative dose equation. Figure 3 shows the dose rate to the liver for a 10-kg dog with an ILD of 37 Bq. Cumulative radiation dose to the liver continued to increase throughout the lifetime of the dog; however, dose rate was relatively constant by 1500 days after exposure.

Blood samples for serum ALT analyses to assess liver damage were collected before exposure and every 4 months thereafter throughout the life of the dogs. Figure 4 shows the median serum ALT values for dose-level groups compared to the upper and lower 95% confidence limits of control animals. Serum ALT values were higher than those of the controls in dose-level groups 3, 4, 5, and 6; ALT values increased soonest after exposure in the highest dose-level group, group 6, and increased at increasingly later times after exposure for lower dose-level groups 5, 4, and 3. When ALT values for a dose-level group increased relative to controls, they remained elevated. Dogs with liver tumors, hyperadrenal corticism, or hypoadrenalcorticism treated with glucocorticoids were not included in these

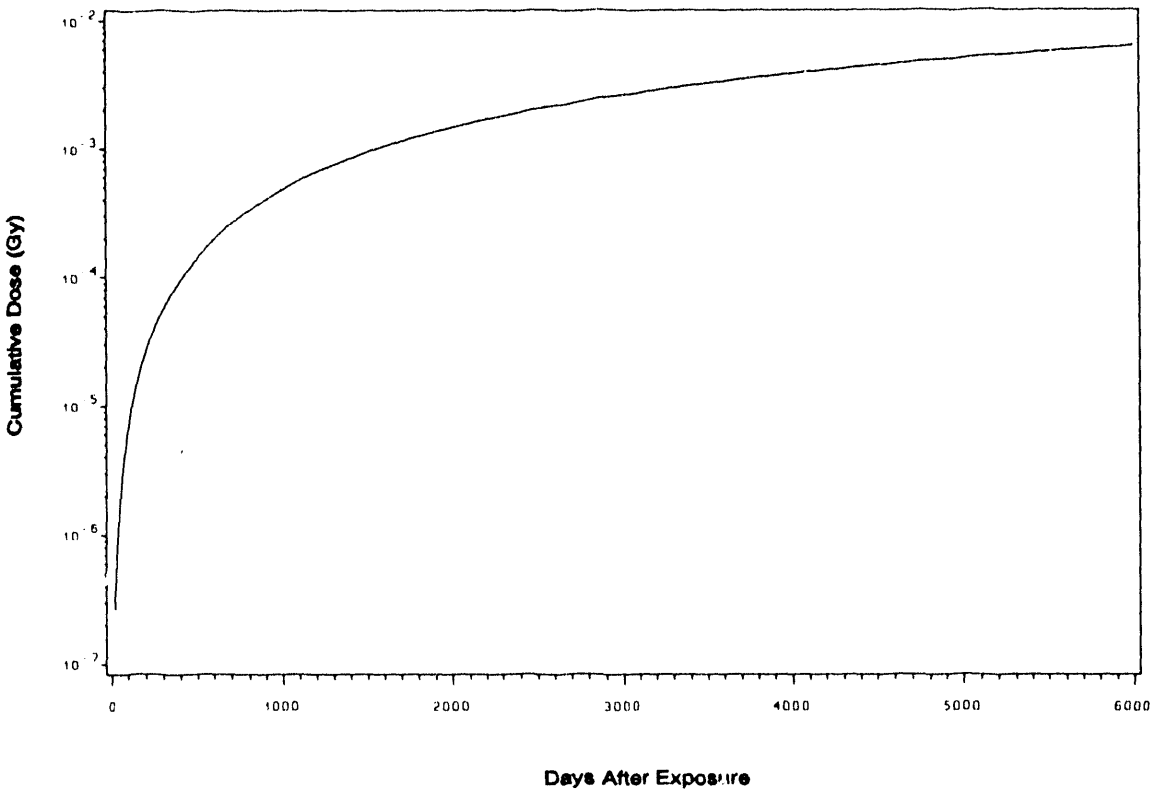

FIGURE 2. Cumulative Dose (Gy) to the Liver Calculated for 10-kg Dog with 37-Bq $^{238}PuO_2$ Initial Lung Deposition (ILD) and the Liver Retention Equation in Figure 1.

evaluations because marked increases in ALT levels are associated with these conditions.

Cumulative radiation dose to the liver for the mean ILD for each dose-level group (3, 4, 5, and 6) with increased serum ALT levels was calculated to the time after exposure for each dose-level group when the median ALT values were first observed to be significantly higher ($p < 0.05$, Wilcoxon rank-sum test) than the control group median ALT at the same time after exposure (Table 4). For dose-level groups (1 and 2) with no increase in ALT values, cumulative radiation dose was calculated to the mean survival time after exposure. For these calculations, 5% of mean body weight of the dose-level group at the time of exposure was used to estimate liver weight because the ratio of body weight to liver weight was frequently abnormal at death. Increased levels of ALT were observed in dose- level groups (3, 4, 5, and 6) with a cumulative dose to liver of 0.2 Gy and higher (Table 4). Dose-level groups 1 and 2, with a cumulative dose of 0.076 Gy and less, did not have increased serum ALT. In dose-level group 3, increased ALT levels were not observed until 9 years after exposure, 4 years earlier than the mean survival time of the group. At 9 years after exposure, 17 of the 18 dogs were alive for ALT measurements.

The dose rate to the liver at the time that serum ALT values first increased was 0.03 Gy/yr or higher for dose-level groups 3, 4, 5, and 6 (see Table 4). The liver dose rate at death for dose-level groups 1 and 2, which did not exhibit

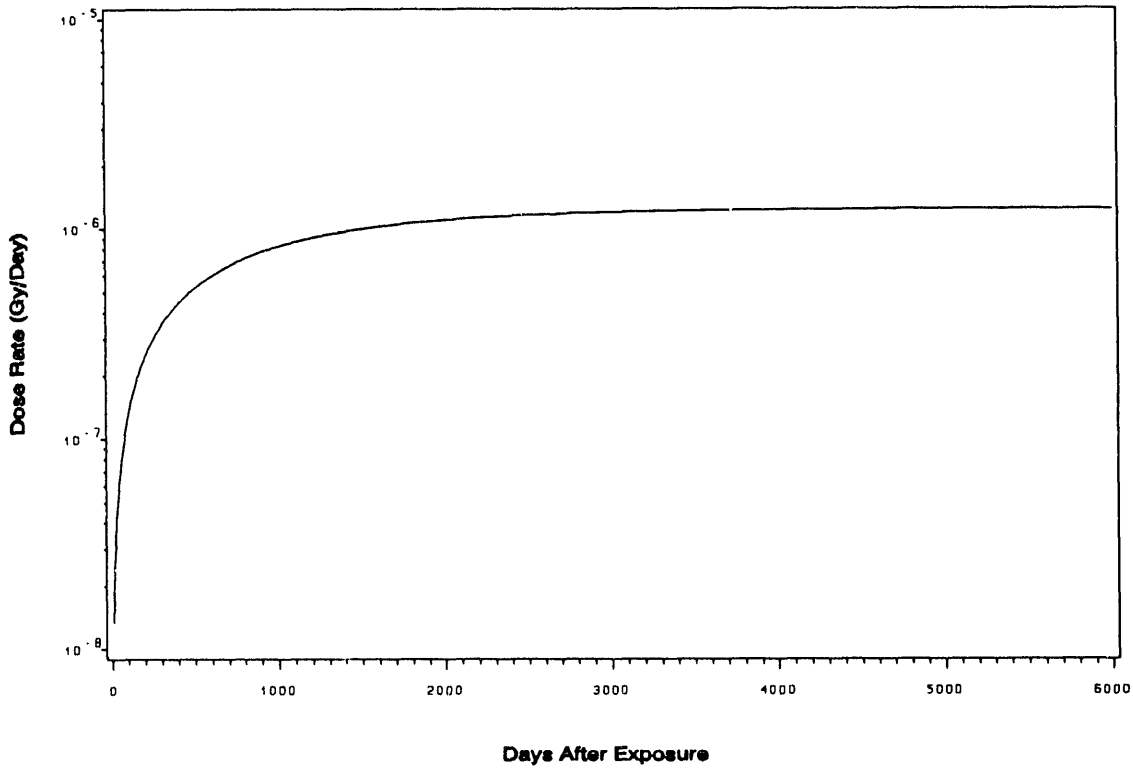

FIGURE 3. Dose Rate (Gy/day) to the Liver Calculated for 10-kg Dog with 37-Bq $^{238}PuO_2$ Initial Lung Deposition (ILD) and the Liver Retention Equation in Figure 1.

increased serum ALT levels, was less than 0.0075 Gy/yr. The mean plutonium concentration in the liver at death for dose-level groups 3,4, 5, and 6, which had increased serum ALT values, was 1.2 Bq/g liver or more (see Table 4). For dose-level groups 1 and 2, which did not have increased ALT levels, the plutonium concentration in the liver was less than 0.26 Bq/g liver.

Table 5 compares the mean dose rate at death for each dose-level group calculated using the liver retention equation (Figure 1) and the ILD of each dog with the dose rate at death as calculated from the plutonium liver concentration at death for the individual dog. The mean values for each dose-level group were similar for both methods of calculating dose rate. The dose rates at death were similar to those calculated for the dose rates at the time of increased serum ALT values in Table 4, which were calculated using the liver retention equation. As shown in Figure 3, liver dose rate was expected to be nearly constant from 1500 days after exposure until death. Therefore, dose rate at death would also predict dose rate at earlier times when ALT was increased.

Sulfobromophthalein sodium (BSP) retention test was performed in 10 dogs with marked increased ALT values to assess whether the increased enzyme activity reflected functional impairment; the BSP retention test revealed no evidence of functional impairment.

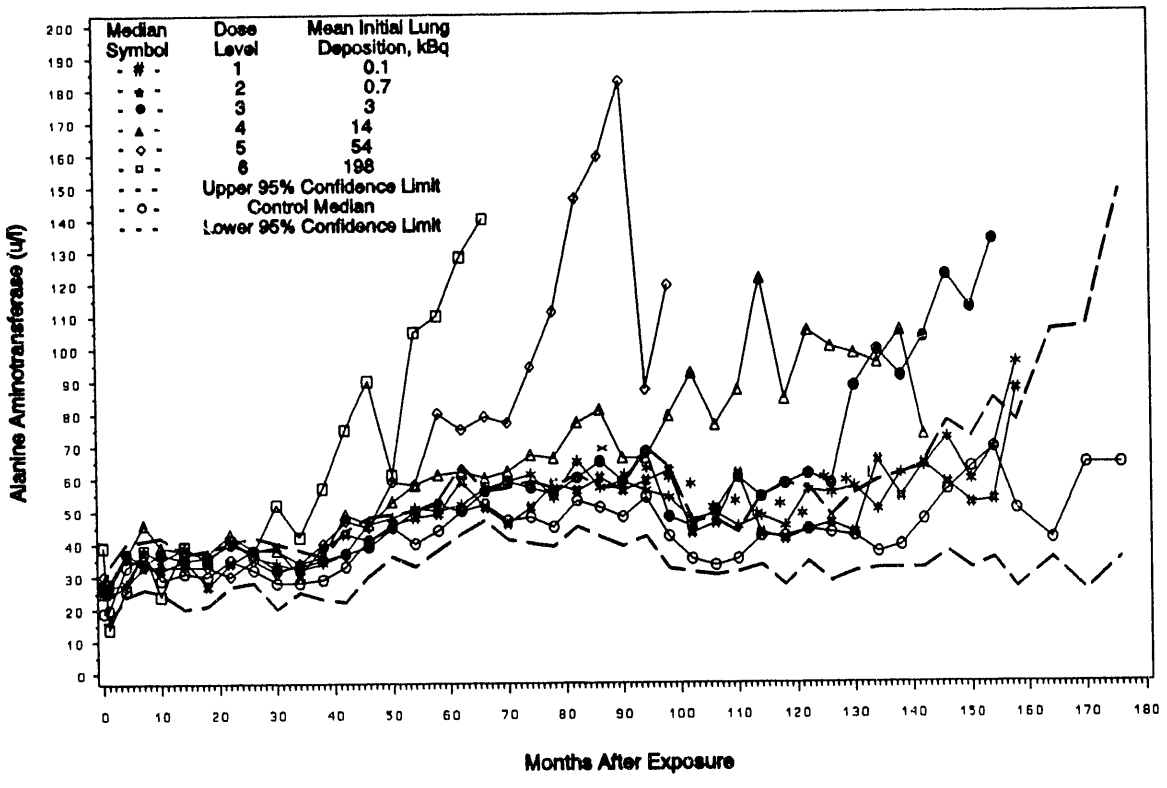

FIGURE 4. Serum Alanine Aminotransferase (ALT) Values in Dogs After Inhalation of $^{238}PuO_2$.

TABLE 4. Time After Exposure, Cumulative Dose, Dose Rate, and Plutonium Concentration in Liver When Alanine Aminotransferase Values Were First Observed to Be Increased Compared to Controls

Dose-Level Group	Number of Dogs	Mean Initial Lung Deposition, kBq	Mean Survival After Exposure, days	ALT Increase After Exposure, days	Cumulative Dose, Gy	Dose Rate, Gy/yr	Liver, Bq/g
Control	17	0	4760	None	0	0	0
1	19	0.081	4501	None	0.0089	0.00091	0.036
2	20	0.67	4589	None	0.076	0.0075	0.26
3	18	2.7	4788	3346	0.20	0.030	1.2
4	16	14	3808	2129	0.58	0.15	4.9
5	18	54	2853	1643	1.4	0.5	20
6	12	198	1961	1034	2.5	1.5	67

The most common histopathological liver lesion in these dogs was adenomatous hyperplasia, which was graded 0 (none) to 5 (most severe) in each dog. The number of dogs with lesions and the average grade per dose-level group are shown in Table 6. The fraction of dogs with lesions and the severity grade were higher for dose-level groups 2 through 6 than for controls or dose-level group 1. Adenomatous hyperplasia is not unusual in old dogs; it is generally considered a regenerative change in response to liver damage.

Liver lesions were not severe, and there was no evidence of liver function impairment. However, the dose-related levels of serum ALT increased compared to controls, indicating that liver damage that was observed several years before death should be considered in evaluating noncancer effects of inhaled $^{238}PuO_2$.

TABLE 5. Liver Dose Rate (Gy/yr) at Death Calculated from the Liver Retention Curve and from Liver Plutonium Concentration (Bq/g) Measured at Death (mean ± SD)

Dose-Level Group	Liver, Bq/g	Liver Concentration, Gy/yr	Liver Retention Curve, Gy/yr
1	0.036±0.028	0.0010±0.00076	0.00086±0.00069
2	0.26±0.17	0.0072±0.0048	0.0079±0.0036
3	1.2±0.7	0.035±0.021	0.030±0.0091
4	4.9±2.6	0.14±0.07	0.15±0.06
5	20±13	0.54±0.36	0.53±0.18
6	67±28	1.8±0.8	1.9±0.7

TABLE 6. Liver Adenomatous Hyperplasia in Dogs After Inhalation of $^{238}PuO_2$

Dose-Level Group	Number of Dogs	Median Survival After Exposure, days	Adenomatous Hyperplasia	
			Number of Dogs	Mean Severity Grade[a]
Control	20	4974	11	1.4
1	20	4548	13	1.8
2	21	4752	18	2.2
3	22	4640	20	2.8
4	20	4244	17	2.5
5	20	2780	16	2.3
6	13	1899	12	2.2

(a) 0 (none) to 5 (most severe).

Inhaled Plutonium Nitrate in Dogs

Principal Investigator: *G. E. Dagle*

Other Investigators: *R. R. Adee, R. L. Buschbom, K. M. Gideon, E. S. Gilbert, G. J. Powers, H. A. Ragan, C. O. Romsos, S. K. Smith, C. R. Watson, and R. E. Weller*

Technical Assistance: *B. M. Colley, K. H. Debban, R. F. Flores, B. B. Kimsey, B. G. Moore, C. R. Petty, M. A. Pope, and R. P. Schumacher*

The major objective of this project is to determine dose-effect relationships of inhaled plutonium nitrate in dogs to aid in predicting health effects of accidental exposure in man. For life-span dose-effect studies, beagle dogs were given a single inhalation exposure to $^{239}Pu(NO_3)_4$ in 1976 and 1977. All the 105 plutonium-exposed dogs died or were euthanized by 15 years after exposure; 28 dogs had bone tumors, 34 had lung tumors, and 14 had liver tumors. Additional plutonium-induced changes included radiation pneumonitis, tracheobronchial lymphadenopathy, radiation osteodystrophy, hepatopathy, and hematologic alterations.

The skeleton is generally considered the critical tissue after inhalation of "soluble" plutonium (e.g., plutonium nitrate), on the assumption that the plutonium will be rapidly translocated from the respiratory system to the skeleton. In several rodent studies, however, inhalation of "soluble" plutonium has resulted primarily in lung tumors. Skeletal tumors were seen less often, perhaps because they were not expressed within the short life span of the rodents. Therefore, beagle dogs were chosen for this study to compare relative risks with those from intravenously injected radionuclides in beagles at the University of Utah, inhalation studies with beta-, gamma-, and alpha-emitting radionuclides at the Inhalation Toxicology Research Institute (Lovelace), and external irradiation at the University of California (Davis) and at Argonne National Laboratory. More specifically, this study can be compared with inhaled $^{239}PuO_2$ and $^{238}PuO_2$ studies in beagle dogs at PNL (see *Inhaled Plutonium Oxide in Dogs*, this volume).

Six dose groups (105 dogs) were exposed, in 1976 and 1977, to aerosols of $^{239}Pu(NO_3)_4$ for life-span observations (Table 1). In addition, 20 dogs were exposed to nitric acid aerosols as vehicle controls; 25 dogs were exposed to aerosols of $^{239}Pu(NO_3)_4$ for periodic sacrifice to obtain plutonium distribution and pathogenesis data in developing lesions; 7 dogs were selected as controls for periodic sacrifice; and 20 dogs were selected as untreated controls

TABLE 1. Life-Span Dose-Effect Studies with Inhaled $^{239}Pu(NO_3)_4$ in Beagles[a]

Dose-Level Group	Number of Dogs		Initial Lung Deposition[b]	
	Male	Female	kBq[c]	Bq/g Lung[c]
Control	10	10	0	0
Vehicle	10	10	0	0
1	10	10	0.062 ± 0.033	0.48 ± 0.26
2	10	10	0.32 ± 0.06	2.6 ± 0.6
3	10	10	2.2 ± 0.3	19 ± 4
4	10	10	11 ± 1	91 ± 15
5	10	10	63 ± 11	518 ± 106
6	3	2	202 ± 84	1772 ± 747

(a) Exposed in 1976 and 1977.
(b) Estimated from external thoracic counts at 2 weeks post exposure and estimated lung weights (0.011 x body weight).
(c) Mean ± 95% confidence intervals around mean.

for life-span observations. The Appendix (at the end of this volume of the *Annual Report*) shows the current status of each dog on these experiments.

All the plutonium-exposed dogs had died or had been euthanized by 15 years after exposure. Plutonium analyses of tissues were completed on all the dogs (Table 2). The average amount of plutonium in the lungs decreased to approximately 1% of the final body burden in dogs surviving 5 years or more. More than 90% of the burden translocated to the liver and skeleton; only about 1% translocated to thoracic and abdominal lymph nodes. This was in contrast to dogs that inhaled $^{239}PuO_2$; in these dogs, approximately 50% of the final body burden was present in thoracic lymph nodes, but only about 2% in the skeleton at 10 to 11 years after exposure.

The earliest observed biological effect was on the hematopoietic system: lymphopenia occurred at the two highest dose levels at 4 weeks after exposure to $^{239}Pu(NO_3)_4$. Total leukocyte concentrations were reduced significantly in the two highest dose groups, that is, Group 5 (mean initial lung deposition, 63 kBq) and Group 6 (202 kBq).

The reduction in white cells in Groups 5 and 6 resulted from an effect on most leukocyte types (neutrophils, lymphocytes, monocytes, and eosinophils). This is in contrast to the effects of both $^{239}PuO_2$ and $^{238}PuO_2$, which significantly depressed lymphocyte concentrations in groups with initial lung burdens of approximately 3 kBq or more. The lymphopenia at lower dose levels of plutonium oxides may be related to the more extensive translocation of plutonium oxide to the tracheobronchial lymph nodes and subsequent higher dosage levels to lymphocytes circulating through those lymph nodes.

Serum enzyme assays have been performed throughout the postexposure period in an attempt to identify specific damage to liver or bone by plutonium translocated from the lung. Evaluation of these data has revealed a biphasic elevation of serum alkaline phosphatase (ALP) and serum glutamic pyruvic transaminase (GPT) in individual dogs. An early increase was followed by a return to control values, and a later effect was characterized by persistent, increased elevations of both ALP and GPT. Calculation of the cumulative average radiation dose to mean time after exposure, when serum chemistry values were first observed to be different from controls for dose-level Group 5 dogs, revealed a mean dose to liver of 2.8 Gy for the late effect, which occurred 4.1 years post exposure. At this time, the dose rate was 60 to 70 cGy per year. GPT and ALP values in dose-level Groups 3 and 4 were significantly higher ($p \leq 0.05$) than those for the control group.

Table 3 summarizes, by dose-level group, the mortality and lesions associated with deaths through the 15 years after exposure to $^{239}Pu(NO_3)_4$. All five dogs at the highest dose level (Group 6) died from radiation pneumonitis 14 to 41 months after exposure. Histopathological examination of the lungs of these dogs revealed interstitial fibrosis, alveolar epithelial hyperplasia, increased numbers of alveolar macrophages, occasional small emphysematous cavities and, at times, very small nodules of squamous metaplasia at the termini of respiratory bronchioles. One dog at the highest dose level had a small bronchioloalveolar carcinoma as well as radiation pneumonitis.

All the dogs in dose-level Group 5 died or were euthanized 34 to 92 months after plutonium exposures. The principal cause of death at this exposure level was osteosarcoma, which occurred in 17 of 20 dogs. Other deaths in dose-level Group 5 were caused by radiation pneumonitis (2 dogs) and multiple lung tumors (1 dog). The multiple lung tumors, in different lobes, were papillary adenocarcinomas, combined epidermoid and adenocarcinoma, and bronchioloalveolar carcinoma; metastases were present in the tracheobronchial lymph nodes.

Malignant but nonfatal lung tumors were also present in nine dogs from dose-level Group 5

TABLE 2. Tissue Distribution of Plutonium in Beagles After Inhalation of $^{239}Pu(NO_3)_4$

Dog Number	Time After Exposure, months	Final Body Burden, Bq	Percent of Final Body Burden					Cause of Death
			Lungs	Thoracic Lymph Nodes[a]	Abdominal Lymph Nodes[b]	Liver	Skeleton	
1359M	0.1	2966	90.50	0.15	0.06	2.46	3.20	Sacrifice
1375F	0.1	2708	89.61	0.14	0.01	0.97	4.68	Sacrifice
1407F	0.1	3398	51.87	0.41	0.13	10.99	18.70	Sacrifice
1389M	0.5	1964	24.07	0.38	0.08	41.28	26.21	Sacrifice
1390M	0.5	1898	24.62	0.32	0.11	20.05	44.45	Sacrifice
1445F	0.5	2096	26.42	0.32	0.11	21.28	44.73	Sacrifice
1329F	1	17935	70.05	0.16	0.04	8.28	18.79	Sacrifice
1346M	1	33388	76.81	0.32	0.03	10.45	10.30	Sacrifice
1347F	1	25851	71.71	0.36	0.08	9.33	14.09	Sacrifice
1336M	1	1199	71.38	0.22	0.05	5.72	19.73	Sacrifice
1341F	1	883	64.43	0.29	0.10	12.92	18.63	Sacrifice
1344F	1	1959	58.68	0.25	0.04	21.87	16.09	Sacrifice
1335M	1	102	19.52	0.07	0.06	6.68	25.04	Sacrifice
1339F	1	51	19.08	0.13	0.08	20.92	45.47	Sacrifice
1351M	1	74	40.68	1.22	0.09	17.09	28.89	Sacrifice
1522F	3	2175	54.68	0.57	0.10	11.52	28.24	Sacrifice
1529F	3	1811	51.68	0.40	0.07	18.48	23.74	Sacrifice
1539M	3	2647	52.45	0.31	0.05	18.58	25.03	Sacrifice
1564F	12	1358	18.00	1.27	0.11	33.53	42.63	Sacrifice
1571F	12	1957	22.37	1.47	0.11	28.76	42.91	Sacrifice
1588M	12	1950	13.14	0.40	0.12	35.85	46.18	Sacrifice
1424M	14	171111	33.10	1.43	0.16	26.49	36.88	Radiation pneumonitis
1517F	16	148928	18.99	0.94	0.18	29.51	47.88	Radiation pneumonitis
1510F	17	69587	22.00	1.15	0.05	20.71	52.00	Radiation pneumonitis
1420M	25	59811	16.51	0.86	0.20	7.77	70.06	Radiation pneumonitis
1471M	34	50893	9.25	0.73	0.12	26.92	58.34	Radiation pneumonitis
1518M	42	69587	6.87	0.24	0.07	21.34	67.51	Radiation pneumonitis, lung tumor
1512M	42	79051	4.31	0.60	0.08	49.93	42.66	Bone tumor
1508M	43	64022	3.24	0.62	0.08	41.53	52.70	Bone tumor
1459F	51	57971	4.40	0.15	0.12	30.86	61.41	Radiation pneumonitis, lung tumor
1492F	52	44480	2.81	0.20	0.17	27.02	66.38	Bone tumor
1485F	54	38928	0.82	0.35	0.07	31.13	63.94	Bone tumor
1502F	55	115170	0.80	0.39	0.09	33.33	62.51	Bone tumor, lung tumor
1387F	55	6170	1.41	0.22	0.12	45.48	49.10	Bone tumor
1429M	59	42891	4.14	0.35	0.10	37.06	54.70	Bone tumor, lung tumor
1598F	60	2136	0.90	0.14	0.17	24.44	31.62	Sacrifice
1576M	60	2411	1.54	0.36	0.13	46.23	39.15	Sacrifice
1605F	60	954	1.87	0.11	0.12	52.32	39.37	Sacrifice
1646F	60	29815	0.72	0.20	0.40	46.92	48.42	Bone tumor
1619F	62	50394	0.55	0.59	0.13	37.87	58.63	Bone tumor
1589F	63	1088	0.68	0.04	0.13	46.43	50.32	Sacrifice
1636M	66	23475	1.21	0.27	0.52	53.97	39.09	Bone tumor
1652F	68	24356	1.46	0.23	0.29	50.47	44.32	Bone tumor, lung tumor
1498F	69	31277	0.59	0.32	0.13	26.63	53.37	Bone tumor, lung tumor
1659F	69	27229	1.14	0.34	0.40	38.90	55.89	Bone tumor
1640M	76	6540	4.01	0.64	0.63	54.41	36.59	Lung tumor
1419M	76	32296	0.69	0.28	0.39	44.06	50.70	Bone tumor, lung tumor
1660M	82	31601	0.76	0.53	0.53	37.51	56.17	Bone tumor, lung tumor
1621M	84	31074	0.94	0.56	0.29	40.87	54.55	Bone tumor, lung tumor
1655M	88	18705	1.05	0.22	0.93	41.83	52.14	Lung tumor, bone tumor

TABLE 2. Continued

Dog Number	Time After Exposure, month	Final Body Burden, Bq	Percent of Final Body Burden					Cause of Death
			Lungs	Thoracic Lymph Nodes[a]	Abdominal Lymph Nodes[b]	Liver	Skeleton	
1501M	92	71	1.62	0.50	0.79	38.05	48.41	Thyroid tumor
1648M	92	23661	1.12	0.25	0.73	42.83	50.61	Bone tumor, lung tumor
1641M	92	32169	0.78	0.24	0.48	45.72	48.89	Lung tumor
1408F	93	6704	0.60	0.19	0.37	49.47	45.52	Bone tumor
1404M	93	8041	0.82	0.28	0.72	46.24	48.62	Pleuritis
1470F	95	49	1.11	0.48	0.34	43.21	50.23	Meningioma
1489F	98	82	1.23	0.73	0.70	41.36	48.52	Esophageal tumor
1565F	101	31	0.77	1.55	0.87	43.62	44.09	Hemangiosarcoma
1385M	101	13399	0.62	0.51	0.42	46.38	49.36	Bone tumor, lung tumor
1364M	102	13704	1.13	0.32	0.40	49.46	46.17	Lung tumor
1503F	103	271	0.37	0.64	0.25	60.15	35.37	Thyroid tumor
1645F	105	6749	0.73	0.41	0.46	55.96	40.70	Lung tumor
1587M	106	1013	0.65	0.74	0.51	20.11	74.97	Hemangiosarcoma, lung tumor
1534M	106	7443	0.96	0.43	0.49	50.78	43.95	Congestive heart failure
1521F	106	5407	0.88	0.34	0.36	51.77	44.41	Bone tumor, lung tumor
1599F	106	268	0.69	0.54	0.48	34.04	60.60	Adrenal tumor
1413F	109	966	1.16	0.39	0.51	58.06	37.78	Malignant lymphoma
1391M	111	1383	1.21	0.34	0.47	50.40	45.49	Thyroid tumor, lung tumor
1581M	111	57	0.52	0.95	0.31	38.21	56.46	Hemangiosarcoma
1602M	111	231	1.95	1.29	0.97	42.80	46.45	Epilepsy
1428F	114	8492	0.72	0.62	0.56	35.16	60.14	Bone tumor, lung tumor
1386M	116	1068	1.59	0.26	0.82	56.40	38.62	Hemangiosarcoma
1568M	116	1270	0.93	0.50	0.54	42.27	52.10	Pneumonia
1590F	119	109	0.48	0.35	1.00	59.61	31.23	Mammary tumor
1530F	122	651	0.89	0.77	0.84	42.50	50.30	Bone tumor, lung tumor
1570F	122	51	0.34	0.91	0.42	30.80	63.13	Stomach tumor
1535F	122	5373	0.62	0.67	0.74	19.27	73.73	Bone tumor, lung tumor
1446F	123	6102	0.40	0.56	0.63	27.06	67.94	Pyometra, liver tumor
1540M	124	1384	0.61	0.45	0.38	39.21	55.37	Lung tumor
1414F	126	4479	1.29	0.42	0.54	44.44	49.50	Bone, lung, and liver tumors
1569F	126	1146	0.53	0.42	0.31	50.23	45.17	Lung tumor
1575M	128	137	0.43	0.54	0.51	55.53	37.17	Prostate tumor
1456F	132	1522	0.33	0.60	0.49	41.34	52.74	Pneumonia
1637M	132	3873	1.22	0.64	0.31	45.50	49.64	Lung tumor
1607M	135	38	0.53	1.80	0.44	37.49	55.95	Liver tumor
1363M	135	1715	0.51	0.69	0.44	55.62	40.23	Pneumonia, adrenal/liver tumor
1582F	136	1266	0.64	0.69	4.82	31.22	57.87	Mammary tumor, liver tumor
1380M	136	1502	0.57	0.70	0.82	34.11	58.90	Pneumonia
1618F	140	4990	0.38	0.23	1.05	38.34	56.67	Bone tumor
1439F	143	1230	0.41	0.69	0.75	25.65	68.09	Malignant lymphoma
1379M	144	7459	0.56	0.72	0.85	25.30	67.38	Liver, lung, and bone tumors
1507M	144	90	1.69	0.38	0.58	51.27	38.98	Malignant melanoma
1639F	145	3449	0.84	0.70	0.73	35.42	57.73	Radiation pneumonitis, lung
1647M	146	5741	0.78	0.46	0.17	45.84	51.38	Lung tumor, liver tumor
1591M	147	266	0.68	0.56	0.70	31.49	59.61	Malignant lymphoma
1585F	148	192	1.03	0.80	0.85	28.77	60.90	Thyroid tumor
1490F	149	494	0.45	0.42	0.34	46.01	49.06	Mammary tumor
1583F	149	29	1.20	3.65	1.33	29.96	57.51	Thyroid tumor
1592F	150	38	0.63	0.47	0.48	44.39	50.24	Pneumonia
1595M	154	1109	0.61	0.68	0.53	43.98	50.01	Nephropathy
1362M	155	6207	0.45	0.44	0.61	36.97	58.06	Bone, liver, and lung tumor
1465F	156	45	1.71	0.37	1.31	45.84	44.12	Nephropathy

TABLE 2. Continued

Dog Number	Time After Exposure, month	Final Body Burden, Bq	Percent of Final Body Burden					Cause of Death
			Lungs	Thoracic Lymph Nodes[a]	Abdominal Lymph Nodes[b]	Liver	Skeleton	
1604M	156	1190	0.91	0.72	0.58	21.71	70.83	Encephalopathy
1423M	157	362	0.83	0.49	0.65	27.97	58.67	Panophthalmitis
1567M	157	129	0.56	0.34	0.88	35.26	58.91	Nephritis
1579M	157	237	0.51	0.17	0.89	53.11	41.14	Hepatocellular carcinoma
1656M	157	2845	1.21	0.66	0.51	42.64	50.80	Pneumonia; lung tumor
1600F	158	37	0.86	0.69	0.86	22.77	72.87	Nephropathy
1606F	158	140	0.68	0.54	0.51	36.11	58.65	Hemangiosarcoma, spleen
1417M	160	399	0.37	0.37	0.26	64.40	32.21	Malignant lymphoma
1427F	160	1273	0.79	0.79	0.56	32.90	60.50	Malignant melanoma, oral cavity
1458F	160	83	0.71	0.26	0.61	30.68	62.00	Malignant pheochromocytoma, adrenal
1573M	160	36	0.31	0.36	0.45	47.84	41.85	Gastric dilatation
1574M	160	1140	0.60	0.54	0.41	54.97	40.47	Lung tumor
1472F	162	225	0.47	0.81	0.62	39.29	52.78	Nephropathy; carcinoma, bile duct
1415M	163	130	0.82	0.63	0.54	40.58	54.07	Transitional carcinoma, urinary bladder
1466F	163	410	0.23	0.50	0.41	44.52	50.88	Nephropathy
1603M	164	37	0.46	0.80	0.46	24.89	68.59	Nephropathy
1416M	165	46	0.25	0.13	0.78	64.53	30.75	Heart failure
1444F	168	1715	0.70	0.23	0.37	23.89	68.60	Transitional carcinoma, urinary bladder
1520M	168	367	0.33	0.53	0.70	37.73	57.58	Carcinoma, bile duct
1487F	169	50	0.44	0.51	0.30	35.91	58.55	Gastric dilatation
1519M	169	97	0.72	0.13	1.16	24.84	68.40	Nephropathy
1596M	170	31	0.48	0.73	0.65	40.62	52.90	Senility
1513M	172	219	0.48	0.59	0.49	46.03	49.21	Hepatitis; lung tumors
1422F	173	1765	0.70	0.35	0.77	27.36	66.38	Lung tumor; adenoma, bile duct
1484F	173	158	0.81	0.96	0.64	12.45	79.95	Malignant lymphoma
1523F	173	1089	0.54	0.66	0.57	28.81	65.68	Metastatic sarcoma
1515M	174	57	0.30	0.11	0.44	56.93	39.77	Urethral carcinoma; hepatocellular carcinoma
1580F	176	123	1.06	0.59	0.45	46.39	47.75	Transitional carcinoma, urinary bladder

(a) Includes tracheobronchial, mediastinal, and sternal lymph nodes.
(b) Includes hepatic, splenic, and mesenteric lymph nodes.

that died from osteosarcomas and in one dog that died from radiation pneumonitis. Typically, these arose subpleurally, proximal to areas of interstitial fibrosis or small cavities communicating with bronchioles. They consisted of bronchioloalveolar carcinomas in four dogs; papillary adenocarcinomas in two dogs; both bronchioloalveolar carcinoma and papillary adenocarcinoma in one dog; both papillary and tubular adenocarcinomas in one dog; a combined epidermoid and adenocarcinoma in one dog; and a bronchioloalveolar carcinoma, a papillary adenocarcinoma, and a mixed lung tumor in one dog. No metastases of these lung tumors were observed.

In dose-level Group 4, all the dogs died or were euthanized 54 to 157 months after plutonium exposure. The causes of death, probably related to plutonium exposure, included bone tumors (9 dogs), lung tumors (5 dogs), a delayed-onset radiation pneumonitis (1 dog),

TABLE 3. Lesions in Beagle Dogs 15 Years After Inhalation of $^{239}Pu(NO_3)_4$

	Dose Group							
	6	5	4	3	2	1	Vehicle	Control
Number of Dogs/Group	5	20	20	20	20	20	20	20
Number of Dead Dogs/Group	5	20	20	20	20	20	17	18
Condition[(a)]								
Radiation pneumonitis	4	1						
Radiation pneumonitis and lung tumor	1	1	1					
Bone tumor		8	3					
Bone and lung tumor		9	4	1				
Bone, lung, and liver tumor			2					
Lung tumor		1	4	3				
Liver, lung, and bone tumor			1					
Lung and liver tumor			1	1				
Hemangiosarcoma and lung tumor				1				
Thyroid and lung tumor				1				
Pneumonia and lung tumor			1					
Hepatitis and lung tumor						1		
Pyometra and liver tumor			1					
Pneumonia and liver tumor				1				1
Mammary and liver tumor				1				
Nephropathy, liver tumor					1			
Liver tumor					2	1		
Pneumonia or pleuritis			1	3		1		3
Lymphoma				2	3		4	
Thyroid tumor					2	2		2
Meningeal tumor						1		
Status epilepticus/encephalopathy				1	1			1
Congestive heart failure			1			1	1	
Hemangiosarcoma				1	1	2		
Adrenal tumor					1	1		1
Esophageal/stomach tumor						2		
Intervertebral disc protrusion							2	2
Mammary tumor					2		3	
Cerebral hemorrhage								1
Urinary bladder/urethral tumor				1	3	1		1
Pyometra								1
Mastocytoma							1	
Splenic tumor								1
Endocarditis								1
Nephropathy				1		5	3	
Malignant melanoma (oral)				2	1		1	
Nephritis					1			
Panophthalmitis					1			
Gastric dilatation					1	1		
Skin tumor (lung metastasis)							1	
Hypothyroidism							1	
Pituitary tumor								1
Ovarian tumor								1
Senility and liver tumor						1		
Unknown								1

(a) Number of dogs with lesions associated with death.

and a bile duct carcinoma (1 dog). Intrahepatic bile duct tumors were present in the livers of 4 additional dogs that died of other causes. Nonfatal lung tumors were present in 9 dogs that died of other causes.

In dose-level Group 3, all the dogs died or were euthanized 106 to 173 months after plutonium exposure. Four dogs died of lung tumors, and lung tumors were present in each of 3 additional dogs that died of a bone tumor, a thyroid tumor, and a hemangiosarcoma. Three dogs had nonfatal bile duct tumors.

In the lower dose levels (Groups 1 and 2), all the dogs died or were euthanized by 15 years after exposure, and the incidence of lesions was not clearly different from that of the control groups. Of uncertain relationship to plutonium exposure, however, were bile duct tumors in 3 dogs (2 from dose-level Group 1 and 1 from dose-level Group 2) and hepatocellular carcinomas in 3 dogs (1 from dose-level Group 1 and 2 from dose-level Group 2). Bile duct tumors have not yet been observed in any control dogs, but we have observed a nonfatal hepatocellular carcinoma in a control dog. In addition, a nonfatal lung tumor was present in 1 dog from dose-level Group 1.

The skeleton is generally considered the critical tissue after inhalation of soluble plutonium, and 28 of the exposed dogs died with bone tumors (Table 4). The sites of the bone tumors were lumbar vertebrae (6 dogs), humerus (6 dogs), cervical vertebrae (4 dogs), pelvis (4 dogs), thoracic vertebrae (3 dogs), sacrum (3 dogs), ribs (3 dogs), facial bones (2 dogs), femur (2 dogs), radius (1 dog), scapula (1 dog), and nasal turbinates (1 dog); several dogs had tumors at more than one site, and metastases were frequent. However, 34 of the 105 exposed dogs also had lung tumors, and lung tumors were more frequent than bone tumors in the middle dose-level groups. Fourteen of the exposed dogs had liver tumors compared to 1 of 35 controls. Only 4 of the liver tumors were fatal; however, they were more frequent than lung or bone tumors in the lower dose-level groups.

TABLE 4. Primary Lung, Bone, and Liver Tumors in Dogs 15 Years After Inhalation of $^{239}Pu(NO_3)_4$

Dose-Level Group	Number of Dogs	Median Survival after Exposure	Lung Tumors		Bone Tumors		Liver Tumors	
			Total	Fatal	Total	Fatal	Total	Fatal
6	5	16.6	1	0	0	0	0	0
5	20	62.5	11	1	17	17	0	0
4	20	114.3	14	5	10	9	5	1
3	20	135.8	7	4	1	1	3	0
2	20	157.6	0	0	0	0	3	2
1	20	150.0	1	0	0	0	3	1
Vehicle Control	17	154.4	0	0	0	0	0	0
	18	139.5	0	0	0	0	1	0
Total	—	—	34	10	28	27	15	4

National Radiobiology Archives

Principal Investigator: *C. R. Watson*

Other Investigators: *S. K. Smith, E. K. Ligotke, J. C. Prather, L.G. Smith, and M. T. Karagianes*

The National Radiobiology Archives (NRA) project is a comprehensive effort to gather, organize, and catalog data, documents, and tissues related to radiobiology studies. This archiving activity will provide future researchers with information for statistical analyses to compare results of these and other studies and with materials for application of advanced molecular biology techniques. The project concentrated initially on studies of beagle dogs exposed to ionizing radiation at five DOE laboratories, and has been expanded to include similar studies in other species. Three major tasks are associated with this project:

1. implementing an interlaboratory computerized **information system** containing a summarized dose-and-effects database with results for each of more than 5,000 life-span-observation dogs, a collection inventory database, and a bibliographic database. During the past year, database structures were designed and populated. The scope of the information system has been expanded to include about 7,000 beagle and 10,000 mouse records from seven laboratories. An introduction to the system is available on diskette. A NRA-sponsored workshop focused on combining information from control beagles resulted in designation of 1,096 animals as well-characterized representatives of controls in six laboratories.

2. establishing a **document archives** of research materials such as logbooks, clinical notes, radiographic films, and pathologists' observations. The first major collection of documents and radiographs, donated by the University of California at Davis, was received this year.

3. establishing a **specimen archives** for research materials such as tissue samples or histopathology blocks and slides. Tissue specimens, histopathology blocks and slides, serial radiographs, and extensive clinical records from more than 1,000 University of California at Davis dogs are organized and available. In addition, two groups of investigators visited the tissue archives to harvest brain specimens from selected aged dogs to analyze for indicators of Alzheimer's disease.

Many investigations have been conducted into the biological effects of ionizing radiation. The focus has been on understanding the nature of human health effects and the degree of risk. When acute effects of relatively large doses had been characterized, attention shifted to the relationship between lower doses, lower dose rates, and cancer. This focus led to initiation of life-span studies of experimental animals in several DOE-supported laboratories. As DOE radiobiology studies are completed, the National Radiobiology Archives (NRA) provides integration and preservation of this unique body of information and materials, and encourages and facilitates its continued use.

Radiobiology Studies

Nearly 40 years ago, the U.S. Atomic Energy Commission began life-span radiation effect studies in a relatively long-lived animal, the beagle dog. As a consequence, a group of closely related experiments are now coming to fruition. These studies, conducted at the University of Utah (U of Utah), the University of California at Davis (UC Davis), Argonne National Laboratory (ANL), Pacific Northwest Laboratory (PNL), and the Inhalation Toxicology Research Institute (ITRI) were summarized in 1989 by Roy Thompson in *Life-Span Effects of Ionizing Radiation in the Beagle Dog* and became the initial focus of NRA

activities. Another multigeneration study in beagle dogs was conducted by the Food and Drug Administration at Colorado State University (CSU). Information from CSU about effects of gamma rays is being included in the NRA. There have also been many life-span studies of rodents, notably those conducted at Oak Ridge National Laboratory (ORNL), ANL, Brookhaven National Laboratory (BNL), and PNL.

The experiments currently available from NRA are listed in Table 1, showing the NRA study code, the time period over which exposures were conducted, the nature of exposures, and the number of animals held for life-span observation. Information is available on 7,061 life-span beagles and 9,765 mice.

Three tasks are associated with integrating and preserving information from these studies. The computerized **information system** provides electronic access to summary data on each animal, to the document and specimen collection catalogs, and to bibliographic citations about the studies; the **document archives** house and preserve nonbiological materials; and the **specimen archives** house and preserve biological materials.

Advisory Committee

The NRA is guided by the National Radiobiology Archives advisory committee (NRAAC) consisting of five external advisors:

Stephen A. Benjamin, Colorado State University: Dog Studies
J. A. Louis Dubeau, University of Southern California: Molecular Biology
Kenneth L. Jackson, University of Washington: Radiobiology
Elizabeth Sandager, Chemical Heritage Foundation: Archivist
Philip R. Watson, Oregon State University: Databases

and eight participating (or internal) advisors:

Bruce B. Boecker, Inhalation Toxicology Research Institute
Ronald E. Filipy, Washington State University, Tri-Cities
Marvin E. Frazier, U.S. Department of Energy
Thomas E. Fritz, Argonne National Laboratory
Scott C. Miller, University of Utah
James F. Park, Pacific Northwest Laboratory
Otto G. Raabe, University of California at Davis
Roy C. Thompson, Pacific Northwest Laboratory.

A subcommittee of the NRAAC met in December 1991 to plan for implementation of a collaborative database combining information from 1096 control beagles. This reference set will provide baseline information for comparison with experimental groups. The NRA is coordinating this effort, and several reports will be prepared describing information available on control beagles.

Information System

Computer database technology is essential to integrating this broad and diverse collection of information. The NRA is developing several interrelated databases, each of which follows the relational model. There are three major databases: the dose-effects summary, the collection inventory, and the bibliography. These systems are maintained on IBM PC systems at PNL using the Paradox database management system.

The computerized summary database contains dose to and effect on each significant tissue in each animal. The summary database has six major tables:

LAB:	describing each laboratory
STUDY:	describing each study (as shown in Table 1)
GROUP:	describing groups of animals within each study
ANIMAL:	summarizing each animal
TEFFECT:	effect (and diagnosis dates) observed in each significant tissue category
TDOSE:	dose to each significant tissue category at diagnosis dates in TEFFECT.

TABLE 1. Major Life-Span Studies Being Incorporated into the National Radiobiology Archives

NRA Study ID[a]	Dates of Exposures	Description of Study	Number of Life-Span Animals
Beagle Dogs:			
A-01	1956	^{90}Sr, Transplacental	53
A-02	1957	^{90}Sr, SC injection (multiple, various ages)	98
A-03	1960-1964	^{144}Ce, IV injection	49
A-04	1961-1963	^{137}Cs, IV injection	65
A-05	1968-1978	Gamma ray, whole body (continuous to death)	311
A-06	1968-1977	Gamma ray, whole body (continuous to predetermined dose)	343
C-03	1967-1973	Gamma ray, whole body, F_3 and F_4 generations	1680
D-01	1952-1958	X ray, whole body (fractionated)	360
D-02	1961-1969	^{90}Sr, ingested (*in utero* to 540 days)	483
D-03	1964-1969	^{90}Sr, IV injection	45
D-04	1964-1969	^{226}Ra, IV injection (multiple)	335
I-01	1965-1967	$^{90}SrCl_2$, Inhalation	63
I-02	1966-1967	$^{144}CeCl_3$, Inhalation	70
I-03	1966-1967	$^{91}YCl_3$, Inhalation	54
I-04	1967-1971	^{144}Ce (FAP)[b], Inhalation	126
I-05	1968-1969	$^{137}CsCl$, IV injection	66
I-06	1969-1971	^{90}Y (FAP), Inhalation	101
I-07	1970-1971	^{91}Y (FAP), Inhalation	108
I-08	1970-1974	^{90}Sr (FAP), Inhalation	124
I-09	1972-1976	^{144}Ce (FAP), Inhalation (juvenile)	54
I-10	1972-1975	^{144}Ce (FAP), Inhalation (aged)	54
I-11	1972-1975	^{144}Ce (FAP), Inhalation (multiple)	36
I-12	1973-1976	$^{238}PuO_2$, Inhalation (3.0 μm)	84
I-13	1974-1976	$^{238}PuO_2$, Inhalation (1.5 μm)	84
I-14	1977-1979	$^{239}PuO_2$, Inhalation (0.75 μm)	60
I-15	1977-1979	$^{239}PuO_2$, Inhalation (1.5 μm)	108
I-16	1977-1979	$^{239}PuO_2$, Inhalation (3.0 μm)	83
I-17	1977-1978	$^{239}PuO_2$, Inhalation (multiple, 0.75 μm)	72
I-18	1979-1983	$^{239}PuO_2$, Inhalation (juvenile, 1.5 μm)	108
I-19	1979-1982	$^{239}PuO_2$, Inhalation (aged, 1.5 μm)	60
P-01	1959-1962	$^{239}PuO_2$, Inhalation	35
P-02	1967	$^{238}PuO_2$, Inhalation	22
P-03	1970-1972	$^{239}PuO_2$, Inhalation	136
P-04	1972-1975	$^{238}PuO_2$, Inhalation	136
P-05	1975-1977	$^{239}Pu(NO_3)_4$, Inhalation	148
U-01	1952-1974	^{239}Pu, IV injection	285
U-02	1953-1970	^{226}Ra, IV injection	164
U-03	1954-1963	^{228}Ra, IV injection	89
U-04	1954-1963	^{228}Th, IV injection	94
U-05	1955-1966	^{90}Sr, IV injection	99
U-06	1966-1975	^{241}Am, IV injection	117
U-07	1971-1974	^{249}Cf, IV injection	36
U-08	1971-1973	^{252}Cf, IV injection	35
U-09	1972-1978	^{239}Pu, IV injection (juvenile)	75
U-10	1973	^{253}Es, IV injection	5
U-11	1975-1978	^{239}Pu, IV injection (aged)	34
U-12	1975-1978	^{226}Ra, IV injection (juvenile)	53
U-13	1975-1980	^{226}Ra, IV injection (aged)	33
U-14	1977-1979	^{224}Ra, IV injection (multiple)	128
Total:	1952-1983		7061
Mice:			
R-01	1977	Gamma ray, single exposure at 10 wk, BALB/c & RFM females	4728
R-02	1987	Gamma ray, single exposure at 10 wk, C3Hf & C57BL/6, both sexes	5037
Total:	1977-1987		9765

(a) Laboratory codes: A, ANL; C, Colorado State University; D, University of California at Davis; I, ITRI; P, PNL; R, ORNL; U, University of Utah. Study numbers: arbitrarily assigned by NRA.

(b) FAP: radionuclide was adsorbed to an insoluble fused aluminosilicate vector aerosol.

The summary database also includes laboratory-specific supporting tables for information such as serial hematological determinations or clinical observations. Progress toward populating the summary database is shown in Table 2.

The collection inventory database contains information about each of the bar code labels affixed to materials (or containers of materials) in NRA collections. The database defines materials and also tracks the location of items to allow rapid retrieval. About 15,000 items related to 4000 animals are currently managed by this system.

The bibliographic database uses the same bar code label system as the collection inventory database to identify reference materials. Location information about materials is stored in the collection inventory database and a complete bibliographic citation are stored in the bibliography system. The bibliography system includes more than 500 items of a supporting nature; animal-specific documents that arrived in 1992 are being added to the database.

An introduction to the NRA information system is available as a stand-alone application that can be self-loaded from diskette onto a DOS-based microcomputer. The accompanying documentation, "National Radiobiology Archives Distributed Access User's Manual," explains usage and extensively describes fields (Watson et al. 1991; Smith et al. 1992). This document and software are an important summary of the meta-data (information describing data) collected. The introductory subset diskettes have been distributed in conjunction with responses to requests for information about the NRA.

Document Archives

The research document archives collects detailed research findings associated with each study.

TABLE 2. Progress Toward Populating the Summary Database

NRA Lab and Study ID[a]	Status of NRA Database Tables[b]						
	LAB	STUDY	GROUP	ANIMAL	TEFFECT	TDOSE	LAB SPECIFIC
A-01, A-02, A-03	F	C	C	P			
A-04	F	C	C	C	C		C
A-05, A-06	F	C	C	P			
C-03	F	P	P	I	I		
D-01	F	C	C	P			
D-02, D-03, D-04	F	C	C	C	C	C	C
I-01 to I-19	F	C	C	C			
P-01, P-02	F	C	C	P		P	
P-03, P-04, P-05	F	C	C	C	P	P	P
R-01, R-02	F	C	C	C	C	C	C
U-01 to U-14	F	C	C	C	C	C	C
Number of Records:	7	66	486	19,691	63,318	7,911	>200,000

(a) Laboratory Codes: A, ANL; C, Colorado State University; D, University of California at Davis; I, ITRI; P, PNL; R, ORNL; U, University of Utah. Study numbers are defined in Table 1.

(b) Status Codes:
C, Complete: database records are complete; all significant fields have complete information.
F, Final: database records are complete and reviewed by investigator.
I, Incomplete: database tables are partially filled with representative rows.
P, Partial: database records are partially complete; some fields have no information.

Materials include handwritten "raw" data such as exposure logbooks, clinical notes, laboratory analysis forms, hematological profiles, and animal care observations. A significant class of research documents from these studies comprises photographic film, autoradiographs, radiographs, and photographs. "Summarized" data, usually reduced to computer files or publication reprints, are also included. Each document (or document container such as a folder) is given a bar-coded accession number label and is stored in a controlled environment. This material is cataloged in the bibliographic database for rapid selection and retrieval.

The first contribution to the document archives is the extensive collection of supportive documentation that provided the basis for *Radioactivity and Health: A History*, by J. Newell Stannard; about 50 boxes have been accessioned. The UC Davis clinical and radiographic records were donated in June 1992. The NRA accessioning team organized the shipment and supervised the packing and unpacking of almost 10 tons of materials. Documents such as clinical records, radiographs, photographs, and autoradiography preparations, as well as specimens such as organs, histology blocks, and slides, at the U of Utah were accessioned in 1990; these materials will remain in Utah pending completion of the studies.

Specimen Archives

The biological specimen archives contains collected research materials such as tissues preserved in formalin or alcohol, tissue samples embedded in paraffin or plastic for histopathological analysis, microscope slides, and radiographic films. Many materials are radioactive and are associated with hazardous materials such as formalin, alcohol, or paraffin. A building has been renovated to serve as the repository of these specimens. The building contains a specimen manipulation laboratory and storage bays with an automatic fire suppression system. Materials are nominated for donation to NRA by an institution which recognizes that specific completed studies are worthy of consideration for archival preservation.

Collaborations and Retrievals

The cooperation of participating institutions and investigators is essential to achieve the goals of the NRA project. Collaboration has been excellent with the seven institutions that have donated information and materials. NRA staff have participated in, or have been invited to participate in, several site visits; collaborative projects were initiated, and these laboratory directors serve on the NRAAC.

The NRA encourages analysis of studies that examine previous information from a new perspective by applying different analytical approaches or by combining results of studies performed at different institutions. This year, NRA continued our collaboration with ANL and ITRI to combine information from two studies (I-05 and A-04) of injected $^{137}CsCl$. NRA also collaborated with investigators at UC Davis to obtain brain specimens of dogs whose clinical records indicated Alzheimer-like symptoms. The NRA staff retrieved tissues and provided laboratory facilities, and the UC Davis team prepared histopathology slides for staining and interpretation.

In addition, the NRA specimen archives supplied histopathology slides of control beagle stomach to the Veterinary School at the University of California and brain specimens to the University of Tennessee. The information system responded to several requests for detailed subsets.

Future Activities

The NRA will continue the orderly accessioning of life-span beagle study information and shipment of selected specimens and documents to PNL. While these studies are being completed, NRA will play an increasing role in facilitating analyses that cut across studies and species. For example, NRA will compile and publish a combined data set of control animals based on consensus of donating investigators. Because most rodent-based radiobiology studies involved thousands of animals, access to original, unpublished data from them is limited. However, additional rodent

studies, initially those conducted at ANL, ORNL, and PNL, are planned to be included in the NRA information system.

References Cited

Smith, S. K., J. C. Prather, E. K. Ligotke, and C. R. Watson. 1992. *National Radiobiology Archives Distributed Access User's Manual Version 1.1.* PNL-7877, Rev. 1, Pacific Northwest Laboratory, Richland, Washington.

Stannard, N. J. 1988. *Radioactivity and Health: A History*, R. W. Baalman, ed. DOE/RL/10830-T59 (DE88013791), Office of Scientific and Technical Information, Springfield, Virginia.

Thompson, R. C. 1989. *Life-Span Effects of Ionizing Radiation in the Beagle Dog: A Summary Account of Four Decades of Research by the U.S. Department of Energy and Its Predecessor Agencies.* PNL-6822, Pacific Northwest Laboratory, Richland, Washington.

Watson, C. R., J. C. Prather, and S. K. Smith. 1991. *National Radiobiology Archives Distributed Access User's Manual.* PNL-7877, Pacific Northwest Laboratory, Richland, Washington.

Low-Level $^{239}PuO_2$ Life-Span Studies

Principal Investigator: *C. L. Sanders*

Other Investigator: *G. A. Sanders*

Wistar female rats are being examined for spatiotemporal dose-distribution patterns and pathological sequelae leading to lung tumor formation following inhalation of $^{239}PuO_2$. Plutonium lung clearance was dependent on initial lung burden (ILB). To estimate lung dose, a lung clearance function was derived from experimentally determined data for inhaled $^{239}PuO_2$ that represents clearance for each rat in the life-span study. The incidence of lung tumors was 0.32% in 1877 rats receiving <1 Gy to the lung, 42% in 229 rats receiving >1 Gy, and 0.19% in 1052 controls. Scanning electron microscope (SEM) autoradiographic determination of subepithelial $^{239}PuO_2$ showed that many fewer particles concentrated in large bronchioles (>1 mm^2 in diameter) than in small (<1 mm^2 in diameter) bronchioles. Bronchiolar, bronchial, tracheal, and laryngeal epithelial cells did not phagocytize inhaled $^{239}PuO_2$; however, about 1% of deposited $^{239}PuO_2$ was found in subepithelial locations of these upper airways. Particle transport occurred through intercellular gaps of upper airway epithelial cells. The dose calculated to upper airway epithelium from subepithelially located particles was very small. No tumors were observed in the bronchi, trachea, or larynx.

Tumors in the pituitary gland, mammary glands, and uterus, in order of decreasing prevalence, accounted for 91% of all nonpulmonary tumors; uterine tumors composed 54% of all nonpulmonary malignant tumors. Pulmonary metastases were seen in 12% of rats; two-thirds of these were uterine adenocarcinomas that appeared histologically similar to some primary lung adenocarcinomas. Other than those in the lung, no significant difference was found in tumor frequency, location, or type between control and exposed rats.

Introduction

This project is one of only a few that can provide lung cancer risk data from an animal model at radiation doses as low as allowed for nuclear worker limits, using a sufficient number of animals in control and low-dose groups to estimate tumor risk. The determination of lung dose for each animal and the large numbers of animals in control and low-dose groups provide new information for decreasing the uncertainty of carcinogenic risk estimates in the lung. Quantitative light and scanning electron microscopic (SEM) autoradiography, cell kinetics, morphometry, and pathological studies are used to evaluate and quantitate radiation dose received by type II alveolar epithelium, the apparent target cell, as it progresses to carcinoma.

Spatiotemporal dose-distribution patterns in the lung continually change following inhalation of $^{239}PuO_2$. Concentration of $^{239}PuO_2$ in pulmonary macrophages and in aggregates, with the limited penetration of alpha particles in tissue, result in a highly nonhomogeneous dose-distribution pattern in the lung and other respiratory tract tissues.

Lung Dosimetry

Clearance of inhaled $^{239}PuO_2$ from the lung of rats changes as a function of initial lung burden (ILB), with higher deposition levels depressing early clearance (Figure 1). Clearance of inhaled $^{239}PuO_2$ in rats was best described by the sum of two exponentials with half-times of weeks to a few months during the early, rapid clearance phase and of many months to more than a year during the slow clearance phase.

The experimentally derived lung clearance equations for ILBs of 0.4 kBq and 3.9 kBq were

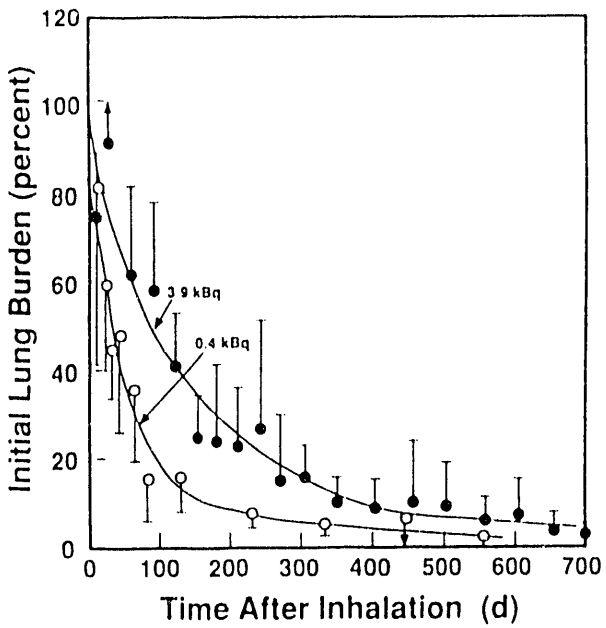

FIGURE 1. Influence of ILB on Clearance of Inhaled $^{239}PuO_2$. Clearance curves from female Wistar rats with ILB values of 0.4 and 3.9 kBq. Values are means ± S.D.

normalized to provide 80% early clearance and 20% late clearance, retaining experimentally determined exponents. Thus initial lung clearance curves were represented by:

$$Y_{0.4}(t) = 0.78\ e^{-0.037t} + 0.22\ e^{-0.0039t}$$

$$Y_{3.9}(t) = 0.81\ e^{-0.0088t} + 0.13\ e^{-0.0014t}$$

Normalized, the lung clearance curves become:

$$Y_{0.4}(t) = 0.80\ e^{-0.037t} + 0.20\ e^{-0.0039t}$$

and

$$Y_{3.9}(t) = 0.80\ e^{-0.0088t} + 0.20\ e^{-0.0014t}$$

We have assumed that there is a mathematically predictable and directly proportional relationship between ILB and $Y_k(t)$ for ILB values of 0.4 kBq and 3.9 kBq. We used this relationship to generate a clearance curve for each life-span ^{239}Pu-exposed rat that was then used to calculate radiation dose to the lung of each rat.

To generate $Y_k(t)$ (where k is ILB in kBq), a percentage of the difference between $Y_{3.9}(t)$ and $Y_{0.4}(t)$ curves is added to the $Y_{0.4}(t)$ curve. This percentage, P(k), is the difference between k [ILB for the calculated Y(t)] and 0.4, compared with the ILB difference between the two experimentally determined curves, or 3.5 (3.9 - 0.4):

$$P(k) = \frac{k - 0.4}{3.5}$$

This gives the function:

$$Y_k(t) = Y_{0.4}(t) + P(k)[Y_{3.9}(t) - Y_{0.4}(t)]$$

For $k > 4.0$, $Y_{4.0}(t)$ is used to calculate dose to lung. Otherwise, for $k < 4.0$, $Y_k(t)$ is used (Table 1). All rats exposed to $^{239}PuO_2$ for life-span study were arranged into lung dose cohorts based on individually determined ILB, survival time, and clearance function. Group mean doses ranged from 0.06 to 55 Gy (Table 2).

TABLE 1. Radiation Dose Estimate to Lung (Gy) at 100 Days and 1000 Days After Inhalation of $^{239}PuO_2$ Based on Clearance Function and ILB

Clearance Function	Lung Dose, Gy			
	ILB, 0.4 kBq		ILB, 3.9 kBq	
	100 days[a]	100 days[a]	100 days[a]	100 days[a]
$Y_{0.4}^{(t)}$	0.69	1.36	--	--
$Y_{3.9}^{(t)}$	--	--	11.5	26.1
$Y_k^{(t)}$	0.67	1.28	12.5	34.5

(a) Post exposure.

Long-Term Retention of Plutonium in Upper Airways

Clearance does not remove all $^{239}PuO_2$ particles initially deposited in the airways of the rat. Published studies indicate that about 1.0% of deposited plutonium particles are found in the walls of the upper airways (bronchi, trachea, and larynx), exhibiting long-term retention in these tissues. In contrast, the respiratory tract

TABLE 2. Survival Time, Lung Dose, and Incidence of Lung Tumors in Female Wistar Rats Following Inhalation of $^{239}PuO_2$[a]

Number of Rats	ILB, kBq	Survival, days after exposure	Lung Dose, Gy	Crude Incidence of Lung Tumors, %
15	8.13 ± 1.27	441 ± 131	55.1 ± 3.7	53.3
17	6.08 ± 0.79	536 ± 148	44.4 ± 3.1	88.2
32	4.70 ± 0.98	566 ± 153	34.5 ± 2.7	65.5
17	4.07 ± 1.66	585 ± 203	25.1 ± 2.7	70.6
33	2.96 ± 1.44	608 ± 216	15.7 ± 3.1	63.6
18	1.65 ± 0.11	727 ± 176	7.99 ± 0.67	33.3
38	1.20 ± 0.11	732 ± 196	5.03 ± 0.60	21.2
58	0.67 ± 0.21	647 ± 177	2.32 ± 0.77	6.9
145	0.22 ± 0.05	722 ± 167	0.62 ± 0.16	0.69
343	0.069 ± 0.032	710 ± 160	0.19 ± 0.09	0.87
1389	0.026 ± 0.005	722 ± 169	0.056 ± 0.020	0.14
1052	0	733 ± 164	0.002[b]	0.19

(a) Values are means ± S.D.
(b) Background dose from alpha emitters.

clearance model proposed by the International Commission for Radiological Protection (ICRP) for the upper airway assumes that only 0.05% of deposited particles are transported to the walls of trachea, larynx, and bronchi.

Particles found in bronchioles, bronchi, or trachea by SEM autoradiography at 1 day after inhalation were mostly on the surface of these structures while particles found at later times were mostly in subepithelial locations. Surface particles in the trachea may have been washed into deeper parts of the lung by the fixation procedure, resulting in an underestimation of surface particle numbers for the trachea. Particles present in subepithelial locations gave a diffuse alpha star formation on SEM autoradiographs; we did not expect that their location would be influenced by the fixation procedure. Absolute counts of fewer than 10 $^{239}PuO_2$ particles, as measured by SEM autoradiography, were found irradiating the total tracheal epithelial surface from subepithelial locations at all times more than 1 day post inhalation after an ILB of 3.9 kBq (Table 3). Occasional $^{239}PuO_2$ particles were found within pulmonary macrophages that were being cleared from the tracheal surface more than 1 day after inhalation.

The larynx is lined by four types of epithelial cells: squamous, squamoid, cuboid, and respiratory. Particularly wide intercellular spaces are found for intermediary cuboid/squamoid epithelial forms that are seen between zones of laryngeal squamous and respiratory epithelial cells (Figure 2).

TABLE 3. Number of Deposited $^{239}PuO_2$ Particles Found Following SEM Autoradiographic Examination of the Total Inner Surface of the Trachea[a]

Time After Inhalation, days	Number of Plutonium Particles
1	47 ± 17
15	8.4 ± 2.0
30	10 ± 1.2
60	8.4 ± 2.7
90	2.6 ± 0.6
120	8.0 ± 5.2
150	3.0 ± 1.3
180	5.0 ± 2.2
210	1.2 ± 1.0
240	1.4 ± 0.7

(a) Most particles seen after 1 day were in subepithelial locations. ILB was 3.9 ± 0.2 kBq (n = 50). Values are mean ± S.E. (n = 5).

Within the respiratory tract is an elaborate network of lymphatics around the bronchi, trachea, and larynx. In the large bronchial wall, a network of lymphatics occurs between the muscular and epithelial layer. Inert particles such as thorium dioxide are removed within lymphatic vesicles and aggregate into vacuoles that become as large as several microns in diameter within the lymphatic endothelium,

FIGURE 2. Transmission Electron Micrograph of Area of Cuboidal/Squamoid Epithelium in the Normal Rat Larynx. Note relatively large intercellular gaps. (x3000)

where they remain for a prolonged time period. A few large $^{239}PuO_2$ particles may be transported within intercellular gaps of epithelial cells in open junctions, finding residence in subepithelial connective tissue lymphatics. Autoradiograms of larynx showed occasional single $^{239}PuO_2$ particles or aggregates of $^{239}PuO_2$ particles in laryngeal subepithelial locations more than 1 year after inhalation (Figure 3). An early inflammatory response caused by the initial radiation dose from inhaled $^{239}PuO_2$ deposited and cleared from the upper respiratory tract airways by the mucociliary escalator may have increased intercellular gap formation and facilitated the uptake of $^{239}PuO_2$ particles into subepithelial regions. No examples of phagocytosis of $^{239}PuO_2$ or other particles by bronchiolar, bronchial, tracheal, or laryngeal epithelium were observed in the current life-span study with inhaled $^{239}PuO_2$ or similar studies. It

FIGURE 3. Light Microscopic Autoradiograph (30-day exposure) of Larynx in Area of Squamous Cell Differentiation. Numerous $^{239}PuO_2$ particles have penetrated the epithelium and lodged in the subepithelial area of fibrous tissue.

is concluded that phagocytosis by nonalveolar respiratory epithelial cells cannot account for subepithelial deposition of inhaled particles in upper respiratory tract airways.

Dose Contribution from Subepithelial $^{239}PuO_2$

Subepithelial particles of $^{239}PuO_2$, seen as diffuse stars on autoradiograms, exposed tracheal epithelial cells to only a few alpha tracks per day. Aggregates of diffuse stars, such as often seen in smaller bronchioles and in occasional sections of larynx, were never seen in the trachea. Fewer than 50 tracheal epithelial cells were within the range of alpha tracks from a single immobilized, subepithelially located $^{239}PuO_2$ particle. Thus, of the several hundred million tracheal epithelial cells, only a few hundred cells were exposed to alpha particles from immobilized subepithelial $^{239}PuO_2$ particles. On the basis of a lung deposition of 75% of inhaled $^{239}PuO_2$ in the upper respiratory tract (exclusive of the nasal cavity) and an alveolar deposition of 6.5%, we estimated that the dose delivered to tracheal epithelial cells is at least 10^5 less from subepithelially located particles than from naked $^{239}PuO_2$ particles or pulmonary macrophages laden with $^{239}PuO_2$ particles being cleared by the mucociliary escalator on the surface of airways. Similar dose relationships are also probable for mainstem bronchi and larynx.

Long-Term Retention of Plutonium in Lower Airways

At an ILB of 3.9 kBq, bronchiolar exposure is delivered in a biphasic manner, first from $^{239}PuO_2$ deposited on the bronchiolar surface and rapidly cleared from the alveoli, and then from $^{239}PuO_2$ retained and aggregated within peribronchiolar alveolar sites. Inhaled $^{239}PuO_2$ deposited in peribronchiolar alveoli was retained or concentrated in these regions. Indeed, no evidence of peribronchiolar alveolar clearance was seen. In contrast, nearly 99% of deposited $^{239}PuO_2$ was cleared from the whole lung by 700 days after exposure.

The number of subepithelial plutonium particles for larger airways (>1 mm^2) was much smaller than that seen for smaller airways (<1 mm^2) (Figure 4), clearly demonstrating that a substantially higher radiation dose is delivered to small bronchiolar airway epithelium than to larger

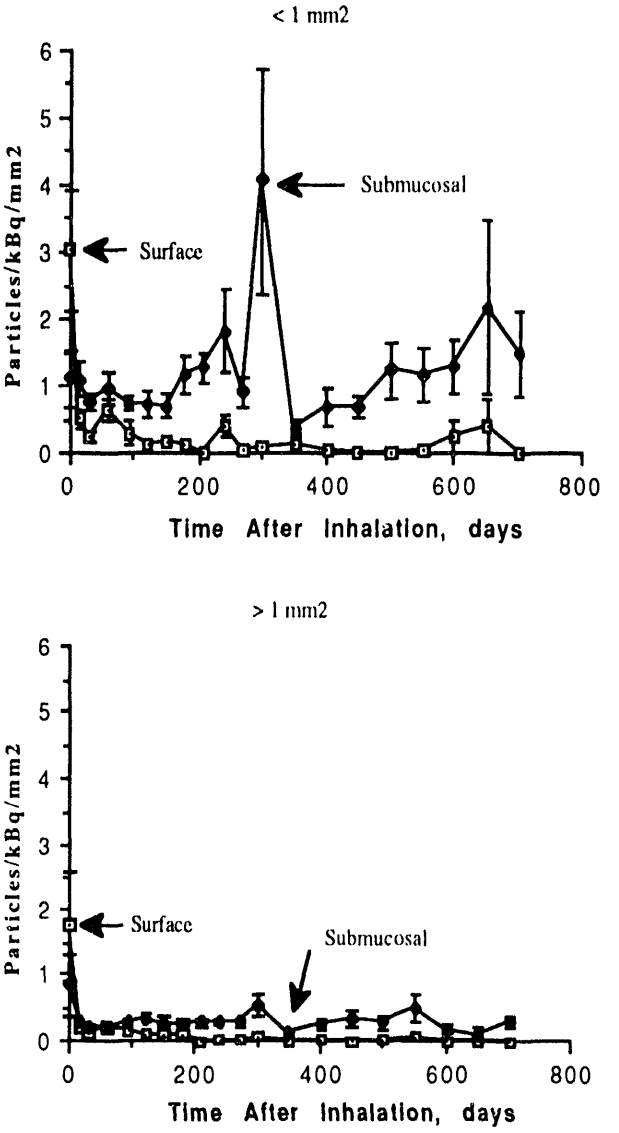

FIGURE 4. Concentration of $^{239}PuO_2$ Particles in Airways with Surface Areas <1 mm^2 or >1 mm^2. Location of particles determined for surface of bronchioles and in adjacent peribronchiolar alveolar or subepithelial regions (submucosal) as a function of time after inhalation; $^{239}PuO_2$ particle concentration determined by SEM autoradiography. ILB, 3.9 kBq; points are means (n = 5) with standard error bars.

bronchiolar and bronchial epithelium from subepithelially located $^{239}PuO_2$.

Transepithelial transport of a variety of insoluble particles, including $^{239}PuO_2$, has been shown for type I alveolar cells. Typically, about 1% of alveolar-deposited particles are phagocytized by

type I cells. Particles of $^{239}PuO_2$ penetrating the alveolar epithelium may be expected to stay in the lung for a long time, and most will be cleared by the lymphatics to the lymph nodes. Several previous light and electron microscopic and autoradiographic studies conducted by the author with various pulmonary-deposited particulates have failed to demonstrate any example of particle phagocytosis by type II alveolar epithelium.

Volumetric measurements from plastic sections were made of focal alveolar regions associated with $^{239}PuO_2$ aggregations photographed under oil immersion with the light microscope. Type II alveolar epithelium, the most probable target cell for carcinomas in the rat lung, accounted for only 3% to 4% of the alveolar surface in the normal rat lung but as much as 100% in some focal regions of plutonium particle aggregation. A marked increase in alveolar histiocytes and macrophages was seen 6 months after exposure, with an increase in type II cell numbers. A greatly increased cellularity of focal alveolar lesions was associated in part with a 20-fold increase in type II cell volume at 600 days after exposure (Figure 5). Increased cell proliferation of type II cells in regions of $^{239}PuO_2$ aggregation is not surprising in view of the vulnerability of type I alveolar epithelium to damage and the requirement of type II cell proliferation to renew type I cells. Proliferation and differentiation of type II cells are the earliest cytological changes associated with carcinoma formation in the lung.

Tumors of the Respiratory Airway Epithelium

Penetration of alveolar epithelium by phagocytosis and aggregation of inhaled $^{239}PuO_2$ particles in alveolar interstitial areas was associated with pulmonary tumor formation. However, inhalation of $^{239}PuO_2$ did not result in tumor formation in bronchi, trachea, or larynx, nor have tumors in these locations been observed by the author in life-span studies with inhaled transuranics with several thousand rats. It may be concluded that even though inhaled $^{239}PuO_2$ is translocated to subepithelial locations associated with bronchi, trachea, or larynx, it does not contribute a carcinogenic dose to the upper respiratory airway epithelium. Likewise, much greater radiation doses to epithelial cells from initially deposited and rapidly cleared $^{239}PuO_2$ failed to induce any tumors in the bronchi, trachea, or larnyx.

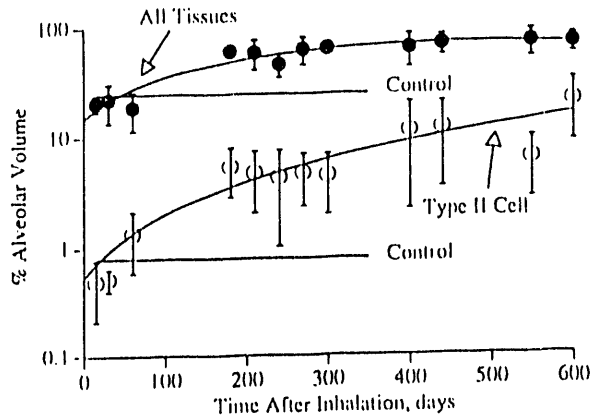

FIGURE 5. Volume Distribution of Alveolar Tissues Following Inhalation of $^{239}PuO_2$. Morphometric measurements were made only in focal alveolar regions exhibiting the greatest pathological or cellular response to plutonium particle aggregation. Measurements include alveolar air spaces; points are means ± S.D.

Primary Lung Tumors

Histopathological analyses have been completed on all female Wistar rats in the first life-span study. To date, the lung tumor incidence was 0.32% in 1877 rats receiving doses to lung between 0 and <1 Gy, 42% in 229 rats receiving lung doses >1 Gy, and 0.19% in 1052 sham-exposed controls. These data clearly indicate that a "practical" threshold dose is about 1 Gy for lung tumor formation from inhaled $^{239}PuO_2$; below this threshold, a tumor is much less likely to develop. The dose-response relationship appears to be well fitted by a pure quadratic function. $^{239}PuO_2$ appears to act as a promoter of type II alveolar epithelial cell-related pulmonary carcinogenesis at lung doses >1 Gy; at such doses, aggregation of plutonium particles leads to a sequence of inflammation, fibrosis, and epithelial metaplasia preceding carcinoma formation.

Pleural Mesothelioma

Pleural mesothelioma was infrequently observed following inhalation of $^{239}PuO_2$. In the current study, only five mesotheliomas were found in 2106 rats exposed to $^{239}PuO_2$ aerosols and one in 1052 control rats. Although the incidence of pleural mesothelioma in exposed rats was about 2.5 times greater than in controls, the difference was not significant. All pleural mesotheliomas were considered to have been lethal. One pleural mesothelioma was of the tubulopapillary type and five were of the mixed spindle cell-epithelial cell type. It was concluded that the lack of $^{239}PuO_2$ aggregation on pleural surfaces is responsible for the small numbers of pleural mesothelioma observed following deposition of $^{239}PuO_2$.

Nonpulmonary Tumors in Control and Exposed Groups

The *Pacific Northwest Laboratory Annual Report for 1991 to the DOE Office of Energy Research, Part 1,* reported data on tumor frequency, mostly occurring in the lungs. In this study, nonpulmonary tumors were evaluated in 2106 exposed and 1052 control rats. No significant differences were noted between control and exposed rats in incidence of nonpulmonary tumors in any organ or tissue, except at the highest doses of radiation to the lung, which shortened the life span (Table 4). Most nonpulmonary tumors were found in three organs: pituitary gland, mammary glands, and uterus. These types of tumors accounted for 88% of all nonpulmonary tumors found in control rats and 91% of all nonpulmonary tumors in exposed rats. Benign tumors were 71% of all tumors in controls and 73% of all nonpulmonary tumors in exposed rats; of these, about 90% were in the mammary gland and pituitary gland. Uterine tumors accounted for 58% of all malignant tumors in control rats and 54% of all nonpulmonary malignant tumors in exposed rats. Of the various uterine tumor types, 6% were adenocarcinoma, 1% squamous carcinoma, 2% leiomyosarcoma, and 43% stroma sarcoma. Tumor incidence was significantly greater (at $p > 0.05$) in exposed rats than in control rats only in the lung. No differences were noted in incidence of thyroid tumor between exposed and control rats. A total of 169 benign and malignant thyroid tumors were seen in control and exposed rats, for an

TABLE 4. Crude Incidence of the Most Prevalent Tumors in $^{239}PuO_2$-Exposed Rats According to Lung Dose[a]

Number of Rats	Survival, days after exposure	Lung Dose, Gy	Crude Incidence of Tumors, %			
			Pituitary Gland	Mammary Gland	Uterus	Lung
15	441 ± 131	55.1 ± 3.7	13.3	6.7	13.3	53.3
17	536 ± 148	44.4 ± 3.1	17.6	17.6	5.9	88.2
32	566 ± 153	34.5 ± 2.7	28.1	28.1	9.4	65.6
17	585 ± 203	25.1 ± 2.7	41.2	41.2	23.5	70.6
33	608 ± 216	15.7 ± 3.1	33.3	36.4	3.0	63.6
18	727 ± 176	7.99 ± 0.67	38.9	50.0	27.8	33.3
38	732 ± 196	5.03 ± 0.60	55.3	28.9	28.9	21.2
58	647 ± 177	2.32 ± 0.77	34.5	36.2	20.7	5.2
145	722 ± 167	0.62 ± 0.16	47.6	44.8	27.6	1.4
343	710 ± 160	0.19 ± 0.09	47.2	46.6	19.2	0.9
1389	722 ± 169	0.06 ± 0.02	46.2	43.2	17.1	0.1
1052	733 ± 164	0.002[b]	47.2	45.1	23.3	0.2

(a) Values are means ± S.D.
(b) Background dose from alpha emitters.

incidence of 5.4%; 33% were follicular adenoma, 39% C-cell adenoma, 14% follicular carcinoma, and 12% medullary adenoma.

An increase in incidence of twofold or more for tumors of the zymbal gland, urinary bladder, brain, and liver was found in exposed rats. Tumor incidence in each organ was less than 1%, and the differences were not significant (Table 5). Despite the finding of nonsignificance, five carcinomas of the bladder in exposed rats and none in control rats suggest an effect from alpha irradiation from $^{239}PuO_2$ cleared in urine. The dose contribution to bladder mucosa from $^{239}PuO_2$ apparently was very low, however, because $^{239}PuO_2$ is very insoluble in tissues. Also, urine constitutes a small source of $^{239}PuO_2$ excretion from the body, and the tumors were found in rats with comparatively low $^{239}PuO_2$ lung deposition.

Pulmonary Metastases

A total of 384 rats, or 12.2%, exhibited pulmonary metastases. No significant differences between control and exposed rats were seen in total incidence of metastases or in pulmonary metastases from any organ site or tumor type, except at the highest lung doses that were associated with reduced life span. About two-thirds of all tumors metastatic to the lung were uterine adenocarcinomas. Pulmonary metastases of some uterine adenocarcinomas, which exhibited extensive confluent growth within the lung and within the pleural cavity, were similar to some primary adenocarcinomas in the lung induced by inhaled $^{239}PuO_2$.

If histological examination is not made of organs of potential metastatic tumor growth to the lung, such as the uterus, misdiagnosis of primary growth from metastatic tumors in the lung is possible. Although careful examination of the lung itself can usually differentiate primary from metastatic tumors, occasional cases have occurred in this study in which such definition was possible only after finding histologically similar tumors in the uterus.

TABLE 5. Crude Incidence of Tumors in $^{239}PuO_2$-Exposed and Sham-Exposed Rats According to Anatomic Location and Lung Doses of <1 Gy and >1 Gy

	Crude Incidence of Lung Tumors, %		
Number of rats	1052	1877	229
Anatomical location	Controls	Lung dose, <1 Gy	Lung dose, >1 Gy
Adrenal gland	3.3	2.6	3.1
Brain	0.57	1.2	0.44
Gastrointestinal tract	0.19	0.33	0.44
Harderian gland	0	0	0.44
Heart[(a)]	0.86	0.32	0.44
Hematopoietic system	0.67	1.1	0.44
Kidney	0.67	0.75	1.7
Larynx	0	0	0
Liver	0.095	0.21	0.44
Lung	0.19	0.32	41.5
Mammary gland	45.1	44.0	31.9
Ovary	0.48	0.48	0.87
Pancreas	1.5	2.2	0
Pituitary gland	47.2	46.5	34.9
Salivary gland	0.48	0.32	0
Skeleton	0.095	0.11	0
Skin	4.7	3.8	0.87
Thymus gland and lymph nodes	3.0	1.9	1.7
Thyroid gland	5.9	4.9	6.1
Trachea	0	0	0
Urinary bladder	0	0.27	0
Uterus	23.3	18.3	17.0
Zymbal gland	0.19	0.43	0.87

(a) Includes endocardial hyperplastic and neoplastic lesions.

Radon Hazards in Homes

Principal Investigator: *F. T. Cross*

Other Investigators: *R. L. Buschbom, G. E. Dagle, K. M. Gideon, and R. A. Gies*

Technical Assistance: *C. R. Petty*

Histopathological data on life-span rats exposed to radon, radon progeny, and uranium ore dust have shown that the overall trend in lung tumor incidence decreases in proportion to the decrease in cumulative radon-progeny exposure and remains elevated at exposures less than 100-working-level months (WLM), levels comparable to those found in typical houses. Histopathological data on rats exposed to only uranium ore dust showed no excess lesions in the nose, larynx, trachea, or kidneys, and no neoplasms in the lungs, when followed throughout their life span. The absence of lung tumors and proliferative epithelial lesions suggests minimal involvement of ore dust in the carcinogenicity of mixed previous exposures to radon progeny and uranium ore dust. The design of a recirculating whole-body animal exposure system, simulating home-environment exposures, was initiated. Testing will proceed in FY 1993 for planned exposures of rats to graded levels of unattached radon progeny such as are found in homes.

Lung cancer incidence and deaths from degenerative lung disease are significantly elevated among uranium miners, but the cause-effect relationships for these diseases are based on inadequate epidemiologic data, thus compromising their utility in determining risks of environmental radon exposures. More recent human data suggest that radon is also implicated in other organ disease, although confirmatory data are lacking in animal systems. This project identified agents or combinations of agents (both chemical and radiological), and their exposure levels, that produced respiratory tract and other system lesions in mine-simulation experiments. The emphasis now is on the development of lung carcinoma and collaborative mechanistic data for environmental exposures. The new project title, "Radon Hazards in Homes," reflects the change in research direction from the former title, "Inhalation Hazards to Uranium Miners."

Wistar Rat Exposure Protocols

The 6000 Series (1000-working level, WL) and 7000 Series (100-WL) mine-simulation experiments (Table 1) are designed to develop the relationships between response and exposure to radon progeny (at two rates of exposure) and to carnotite uranium ore dust. The 8000 Series (100-WL) experiments (Table 2) are designed to extend the exposure-response relationships to cumulative exposure levels comparable to current conditions in uranium mines and to lifetime environmental exposures. The 9000 Series experiments (Table 3) continue the "low-dose" studies at exposure rates comparable to former occupational working levels (10 WL). They will help to further evaluate the hypothesis that the tumor probability per working-level month (WLM) exposure increases with decreasing exposure rate. In addition, concurrent exposure to varying levels of uranium ore dust tests the hypothesis that irritants (both specific and nonspecific) act synergistically with radiation exposures. The exposures of 6000, 7000, and 8000 Series animals are complete. Exposures of 9000 Series animals were suspended with the 80-WLM and 15 mg/m^3 ore-dust exposures to allow analyses of existing data. Exposures of rats to uranium ore dust alone (10,000 Series experiments; Table 4) have been completed.

The ore-dust studies address the potential link of lung cancer to silica and long-lived radionuclide

TABLE 1. Exposure-Response Relationship Study for Radon-Progeny Carcinogenesis in Rats (6000 and 7000 Series Experiments)

Number of Animals[a]		Exposure Regimen[b,c]	Total Exposure, WLM[d]
6000 Series	7000 Series		
64	0	1000-WL radon progeny 15 mg/m^3 uranium ore dust	10,240
56	32	1000-WL radon progeny 15 mg/m^3 uranium ore dust	5,120
56	32	1000-WL radon progeny 15 mg/m^3 uranium ore dust	2,560
56	32	1000-WL radon progeny 15 mg/m^3 uranium ore dust	1,280
88	64	1000-WL radon progeny 15 mg/m^3 uranium ore dust	640
152	128	1000-WL radon progeny 15 mg/m^3 uranium ore dust	320
64	96	Controls	

(a) Number of animals is sufficient to detect the predicted incidence of lung tumors at the 0.05 to 0.1 level of significance, assuming linearity of response between 0 and 9200 WLM (see footnote d) and 0.13% spontaneous incidence.
(b) Exposure rate, 90 hr/wk; planned periodic sacrifice.
(c) Study is repeated at 100-WL rate (without periodic sacrifice) to augment previous limited exposure-rate data (7000 Series experiments).
(d) Working level (WL) is defined as any combination of the short-lived radon progeny in 1 liter of air that will result in the ultimate emission of 1.3×10^5 MeV of potential α energy. Working-level month (WLM) is an exposure equivalent to 170 hours at a 1-WL concentration. Previous exposure at 900 WL for 84 hr/wk to 9200 WLM produced an 80% incidence of carcinoma.

exposures. Exposures of rats to radon progeny, uranium ore dust, and cigarette-smoke mixtures [initiation-promotion-initiation (IPI; 11,000 Series) experiments; see *Mechanisms of Radon Injury* project, this volume] have been completed. These experiments investigate the induction-promotion relationships of radon and cigarette-smoke exposures. Exposures of female rats (12,000 Series experiments; Table 5) are complete. These experiments provide comparative risk data to exposures of male animals using mine-simulation aerosols. Tables 1 through 5 are shown here with the actual numbers of animals (including serial-sacrifice animals) used at each exposure level.

Rat Respiratory Tract Pathology

The development of exposure-response relationship studies were initiated with the 6000 and 7000 Series experiments (see Table 1). Current summaries of primary tumors of the respiratory tract in subsequent experiments (8000 and 9000 Series animals) are shown in Tables 6 and 7. These sampled data show that the incidence of lung tumors decreases in proportion to the decrease in cumulative radon-progeny exposure and, in comparison to an assumed 0.13% spontaneous incidence, remains elevated at exposures comparable to those found in houses (20 to 80 WLM). Histopathological examinations are in

TABLE 2. Low Exposure-Response Relationship Study for Radon-Progeny Carcinogenesis in Rats (8000 Series Experiments)

Number of Animals[a]	Exposure Regimen[b]	Total Exposure WLM[c]
96	100-WL radon progeny 15 mg/m^3 uranium ore dust	640[d]
96	100-WL radon progeny 15 mg/m^3 uranium ore dust	320[d]
192	100-WL radon progeny 15 mg/m^3 uranium ore dust	160
384	100-WL radon progeny 15 mg/m^3 uranium ore dust	80
480	100-WL radon progeny 15 mg/m^3 uranium ore dust	40
544	100-WL radon progeny 15 mg/m^3 uranium ore dust	20
192	Controls	

(a) Number of animals is sufficient to detect lung tumors at the 0.05 to 0.1 level of significance, assuming linearity of response between 0 and 640 WLM (see footnote c) and 0.13% spontaneous incidence.
(b) Exposure rate, 90 hr/wk; planned periodic sacrifice.
(c) Previous exposures indicated a tumor incidence of 16% at 640 WLM. Working level (WL) is defined as any combination of the short-lived radon progeny in 1 liter of air that will result in the ultimate emission of 1.3 x 10^5 MeV of potential α energy. Working-level month (WLM) is an exposure equivalent to 170 hours at a 1-WL concentration.
(d) Repeat exposure is for normalization with Table 1 data.

progress on the remainder of tissues from 8000, 9000, 11,000, and 12,000 Series animals.

Histopathological examination was completed on 10,000 Series young adult male rats exposed to uranium ore dust [15 mg/m^3 concentrations, 2% U_3O_8 by weight; 1.6 μm mass median aerodynamic diameter (MMAD), 2.8 geometric standard deviation (GSD)] for 18 hr/day, 4 days/week, for approximately 15 months. In these experiments, 6 exposed rats, plus 6 sham-exposed control rats, were sacrificed at 6, 12, and 18 months from start of exposures; 75 exposed

TABLE 3. Ultralow Exposure-Rate Study for Radon-Progeny Carcinogenesis in Rats (9000 Series Experiments)

Number of Animals [a]	Exposure Regimen[b]	Total Exposure WML[c]
64	10-WL radon progeny 15 mg/m^3 uranium ore dust	320
64	10-WL radon progeny 3 mg/m^3 uranium ore dust	320
384	10-WL radon progeny 15 mg/m^3 uranium ore dust	80
384	10-WL radon progeny 3 mg/m^3 uranium ore dust	80
512	10-WL radon progeny 15 mg/m^3 uranium ore dust	20
512	10-WL radon progeny 3 mg/m^3 uranium ore dust	20
192	Controls	

(a) Number of animals is sufficient to detect lung tumors at the 0.05 to 0.1 level of significance, assuming linearity of response between 0 and 640 WLM (tumor incidence is approximately 16% at 640 WLM) and 0.13% spontaneous incidence.
(b) Exposure rate, 90 hr/wk; planned periodic sacrifice.
(c) Working level (WL) is defined as any combination of the short-lived radon progeny in 1 liter of air that will result in the ultimate emission of 1.3 x 10^5 MeV of potential α energy. Working-level month (WLM) is an exposure equivalent to 170 hours at a 1-WL concentration.

TABLE 4. Control Study for Uranium Ore-Dust Carcinogenesis in Rats (10,000 Series Experiments)

Number of Animals	Exposure Regimen[a]
96	15 mg/m^3 uranium ore dust
64	Sham-exposed controls

(a) Exposures, 67 weeks at 72 hr/wk; planned periodic sacrifice.

rats, plus 42 control rats, lived out their normal life span. Histopathological examination was made of the nose, larynx, trachea, lung, mediastinal

TABLE 5. Exposure of Female Rats to Radon Progeny and Uranium Ore Dust (12,000 Series Experiments)

Number of Animals	Exposure Regimen[a]
96	100-WL radon progeny; 640 WLM 5 mg/m^3 uranium ore dust
96	Sham-exposed controls

(a) Exposure rate, 72 hr/wk; planned periodic sacrifice. Working level (WL) is defined as any combination of the short-lived radon progeny in 1 liter of air that will result in the ultimate emission of 1.3×10^5 MeV of potential α energy. Working-level month (WLM) is an exposure equivalent to 170 hours at a 1-WL concentration.

lymph nodes, kidney, and all grossly observed lesions. No lesions related to uranium ore-dust exposure were observed in the nose, larynx, trachea, or kidneys, and no neoplasms were observed in the lungs of ore-dust-exposed rats. However, a lower incidence of nonpulmonary neoplasms was noted in rats exposed to uranium ore dust (35%) compared to that in control rats (48%). Table 8 shows the average severity grade of lung and lymph node lesions related to uranium ore-dust exposures of rats. The absence of lung tumors and of proliferative epithelial lesions compatible with preneoplastic changes in rats exposed to ore dust suggests that only the radiation dose from inhaled radon progeny attached to ore dust is responsible for the carcinogenicity of mixed exposures to radon progeny and uranium ore dust.

Recirculating Whole-Body Animal-Exposure System

To increase animal upper-respiratory-tract doses from those employed in previous mine-simulation experiments, and to make them more nearly comparable to those received by humans exposed to indoor radon, the ultrafine (unattached) fraction of home-simulated radon-progeny potential alpha energy needs to be high (>10%). Work was initiated, therefore, to modify the PNL-designed H-2000 chambers (manufactured by Harford Division of Lab Products, Aberdeen, Maryland) previously used in mine-simulation radon animal experiments in the former *Inhalation Hazards to Uranium Miners* project. The modification ensuring uniform exposures of animals throughout the chamber to a high concentration of ultrafine radon progeny, represented by radon-progeny attachment to 5-nm-diameter silver particles, is achieved by recirculating filtered radon-laden air at a moderately high velocity through the chambers (Figure 1). It is expected that a chamber flow rate of 420 liters/min will produce a uniform distribution of the ultrafine radon progeny in the chamber. This will be tested in FY 1993, and the flow rate will be adjusted, if necessary, to reduce spatial variability to less than 10% for planned exposures in FY 1993.

Environmental conditions in the chamber will be maintained by cleaning the recirculated air and adding oxygen when needed. Actual ventilation of the chamber will be only 20 liters/min to maintain a relatively high radon concentration in the chamber atmosphere. Radon progeny generated in this atmosphere will associate rapidly with ultrafine silver particles, which are introduced to the chamber as described in the report *Aerosol Technology Development* (this volume). While the air is being recirculated at 400 liter/min (for a total of 420 liters/min through the chamber), it is filtered by a high-efficiency particulate air (HEPA) filter to remove any particles introduced to the airstream by the rats. This air is blown through the recirculation loop by a fan (see Figure 1). Flow rate will be controlled with a calibrated orifice plate to determine the speed of the fan. Part of the recirculating air goes through a conditioning loop that removes moisture, ammonia, and carbon dioxide. This air-conditioning system (Figure 2) is mounted on a cart adjacent to the exposure chamber. The air then returns to the inlet of the chamber where it is mixed with added radon, radon progeny, and carrier particles.

The chamber environment will be monitored for radon and progeny (see *Aerosol Technology Development* report) and for temperature, humidity, ammonia, carbon dioxide, and oxygen. Temperature will be measured near the center of the chamber. Because the air flow circulates rapidly, this temperature should not become much higher than room air temperature. If the chamber temperature rises above 25°C, chamber walls will be cooled using water jackets. Humidity will be

TABLE 6. Current Summary of Primary Tumors of the Respiratory Tract in Life-Span Animals (8000 Series Experiments)

Nominal Exposure, WLM	Nominal Ore-Dust Concentration, mg/m^3	Extrathoracic Tumors			Lung Tumors							
		Nasal	Laryngeal	Tracheal	Number of Animals Examined	Number of Animals to be Examined	Adenoma	Adeno-carcinoma	Epidermoid Carcinoma	Adeno-squamous Carcinoma	Sarcoma[a]	Animals with Lung Tumors, %
20	15	0/238[b]	0/158	0/230	246	280	1	1	1	0	0	1.2
40[c]	15	0/289	0/167	0/276	306	156	0	4	1	1	1	2.3
80	15	1/184	0/107	0/170	197	169	0	4	4	0	1	4.6
160	15	0/161	0/97	0/158	171	0	4	5	1	0	1	6.4
320	15	0/74	0/56	0/69	77	0	0	1	0	0	1	2.6
640	15	0/72	0/44	0/71	76	0	5	3	2	1	0	13
Controls		0/92	0/68	0/84	96	77	0	0	0	0	0	0

(a) One malignant hemangiopericytoma, one malignant fibrous histiocytoma, and two malignant mesotheliomas considered radon-progeny-exposure related.
(b) Number tumors/number examined.
(c) One malignant oropharyngeal hemangiosarcoma, considered radon-progeny-exposure related; found in tissue not routinely sectioned for histopathology.

TABLE 7. Current Summary of Primary Tumors of the Respiratory Tract in Life-Span Animals (9000 Series Experiments)

Nominal Exposure, WLM	Nominal Ore-Dust Concentration, mg/m^3	Extrathoracic Tumors[a]			Lung Tumors							
		Nasal	Laryngeal	Tracheal	Number of Animals Examined	Number of Animals to be Examined	Adenoma	Adeno-carcinoma	Epidermoid Carcinoma	Adeno-squamous Carcinoma	Sarcoma[a]	Animals with Lung Tumors, %
80	15	0/78[b]	0/59	0/119	126	258	1	0	2	0	0	2.4
320[c]	3	0/50	0/36	0/48	51	0	0	6	1	0	1	16
320	15	0/50	0/41	0/46	52	0	1	4	4	1	0	19
Controls		1/60	0/44	0/66	72	56	0	0	0	0	0	0

(a) One mesothelioma in mediastinum, considered a primary tumor of the lung.
(b) Number tumors/number examined.
(c) One oropharyngeal squamous carcinoma, considered radon-progeny-exposure related; found in tissue not routinely sectioned for histopathology.

TABLE 8. Average Severity Grade of Lung and Lymph Node Lesions Related to Uranium Ore-Dust Exposure of Rats (10,000 Series Experiments)[a]

	Sacrifice Rats[b]			Life-Span Rats	
	6 mo	12 mo	18 mo	Exposed	Control
Lung					
Dust-laden macrophages	2.8	3.0	3.0	3.0	0.0
Interstitial reaction	1.3	1.3	1.8	1.5	0.6
Alveolar proteinosis	1.0	1.0	2.3	1.4	0.0
Nodular fibrosis	0.0	0.0	0.0	0.2	0.0
Mediastinal lymph nodes					
Dust-laden macrophages	3.0	3.8	3.6	3.7	0.0
Reactive hyperplasia	3.0	3.0	3.0	2.2	1.1
Fibrosis	0.2	0.0	0.0	0.2	0.0

(a) Lesions were graded on a scale of 1 through 5: +1 (very slight); +2 (slight); +3 (moderate); +4 (marked); +5 (extreme).

(b) Sacrificed control rats showed only reactive hyperplasia in mediastinal lymph nodes at 12 and 18 months from start of sham exposures; average severity grades were 2.0 and 1.7, respectively.

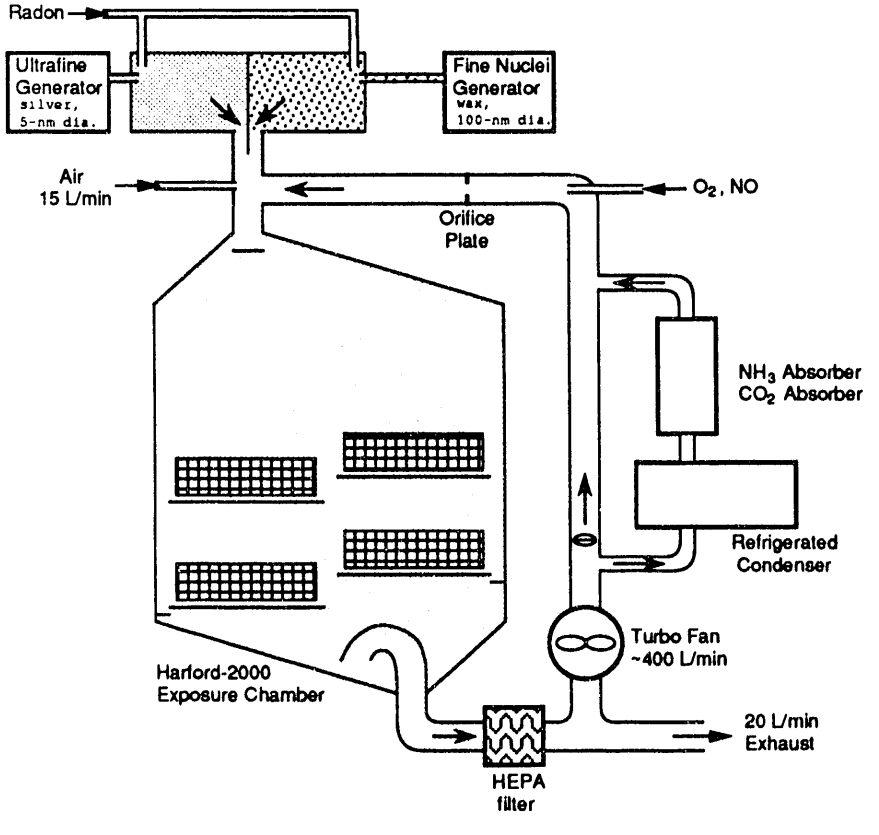

FIGURE 1. Exposure Chamber and Aerosols to Be Used for Exposure of Rats to Simulated Home Radon Environments.

measured by a dew-point hygrometer that will sample air from near the center of the chamber, and will be maintained in the range of 40% to 70% relative humidity by diverting air through the conditioning train in the recirculation loop. Water is removed by condensation, ammonia is absorbed by hydrogen chloride, and carbon dioxide is absorbed by sodium hydroxide. Ammonia and carbon dioxide will be tested by sampling the air between the HEPA filter and the conditioning loop. If ammonia exceeds 50 ppm or carbon dioxide exceeds 5000 ppm, absorbent will be added to the conditioning train; if oxygen in the chamber decreases to less than 19.5%, the oxygen content of the ventilation air will be increased.

The modified chamber and controls should maintain a comfortable environment, ensure normal breathing behavior, and allow the successful conduct of exposures to graded levels of unattached radon progeny.

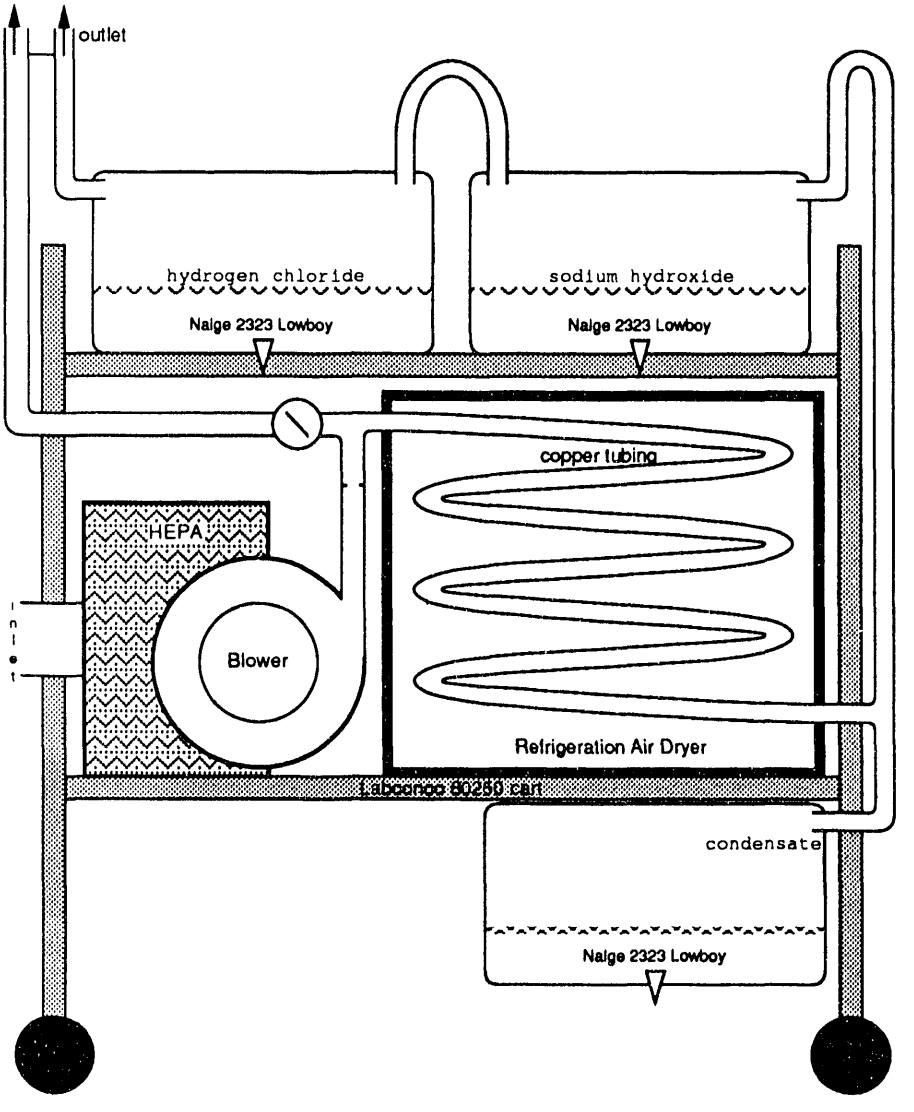

FIGURE 2. Air-Conditioning System for Recirculating Whole- Body Animal Exposure Chamber.

Mechanisms of Radon Injury

Principal Investigator: *F. T. Cross*

Other Investigators: *G. E. Dagle, E. W. Fleck,[a] M. E. Foreman, R. A. Gies, R. F. Jostes, G. L. Stiegler, and L. Stillwell*

Technical Assistance: *T. L. Curry and C. R. Petty*

In this project, we conduct dosimetric, molecular, cellular, and whole-animal research relevant to understanding the mechanisms of radon and radon-progeny injury to the respiratory tract. The work specifically addresses the exposure-rate effect and other major factors influencing radon-progeny carcinogenesis; the induction-promotion relationships associated with exposure to radon and cigarette-smoke mixtures; the role of oncogenes and suppressor genes in radon-induced cancers; and the effects of radon exposure on chromosomal aberrations, mutations, and DNA strand-break production and repair.

Efforts to correlate oncogene data with pathological data derived from animal radon studies continued in FY 1992. Eight *ras* mutations were identified in 15 radon-induced rat lung epidermoid tumors, suggesting that *ras* gene mutations are involved in a subset of radon-induced tumors. Collaborative, mechanistically based cellular studies with researchers at PNL and at other institutions also continued. Collaborations with researchers at other institutions included: (1) Dr. Earl Fleck, Whitman College, on molecular analysis of radon-induced CHO-HGPRT mutations using Southern blot and PCR exon analyses; (2) Dr. Helen Evans, Case-Western Reserve University (CWRU), on mutational response of radiosensitive and radioresistant L5178Y cells as well as the dosimetric evaluation of the CWRU *in vitro* radon exposure system; (3) Drs. James Cleaver and Louise Lutze, University of California, San Francisco (UCSF), on radon exposure of shuttle vectors for molecular analysis of induced mutations; and (4) Drs. Richard Albertini and J. P. O'Neill, University of Vermont, on investigation of the molecular basis of radon-induced mutations at the HGPRT locus in human peripheral blood lymphocytes. A new *in vivo/in vitro* radon mutation study was initiated involving the determination of mutation frequency and molecular analysis of the target sequence in radon-exposed Big Blue™ transgenic mice. Initiation-promotion-initiation experiments in adult male SPF Wistar rats exposed to radon and cigarette-smoke mixtures showed hyperplasia of nonciliated cells with thickening of tracheal epithelium at 25 weeks of exposure; the epithelium recovered to within control values by 27 weeks after exposure ceased.

Oncogene Studies

Research on the molecular basis of radon-induced carcinogenesis in rats continued. Thus far, a total of 20 lung tumors have been analyzed for *ras* oncogene involvement. Of 10 radon-induced epidermoid tumors, 3 were found to have 13th-codon, ras-activating mutations and 1 tumor had a 12th-codon, K-*ras*-activating mutation. The first exon of H-*ras*, and the second exons of H-*ras*, K-*ras*, and N-*ras* have not been examined. K-*ras* and N-*ras* first exons from 5 spontaneous adenocarcinomas in control animals were examined but no 12th- or 13th-codon mutations were identified. The H-*ras* second exon was examined in 5 additional epidermoid tumors, and a 62nd-codon change resulting in an amino acid substitution was found

(a) Whitman College, Walla Walla, Washington.

in 4 of 5 tumors; this mutation has not been documented as a *ras* gene-activation mutation. The other *ras* exons have not been examined in these tumors.

Preliminary data on ras gene mutations associated with radon exposure were published in 1992 (Foreman et al. 1992). On the basis of current data, *ras* gene mutations may be a primary event in a subset of developing epidermoid tumors, and it is equally conceivable that in some tumors *ras* gene mutations are secondary events resulting during tumor progression.

Radon Cell-Exposure System and Molecular/Cellular Studies

In Vitro Radon Studies

The PNL *in vitro* radon cell-exposure system was extensively employed in PNL experiments as well as in several collaborative experiments with other laboratories. The first collaboration is with Dr. Earl Fleck, Whitman College, on molecular analysis of radon-induced CHO-HGPRT mutations using Southern blot and polymerase chain reaction (PCR) exon analyses; all exons except the first were evaluated. A current summary of CHO-HGPRT mutation types is shown in Table 1. Our preliminary work was published in 1992 (Jostes et al. 1992). The largest category of mutation types obtained after x-irradiation or radon exposure is the full deletion (i.e., total deletion of the gene). Further, the percentages of full deletions obtained from both levels of radon exposure, as well as from the 300-cGy x-ray exposure, are essentially the same. The largest category of mutations in the spontaneous population have no changes from the parental cell line that are detectable by Southern blot or PCR exon analysis. This phase of the investigation has been completed and a manuscript is being prepared for submission to *Radiation Research*. We intend to investigate the molecular basis of mutations that exhibit "no change" from the parental cell line by Southern blot or PCR exon analysis. We will examine these mutations by using RNA single-strand conformational polymorphism (rSSCP) to identify the affected exon followed by DNA sequence analysis. If this proves feasible using existing "no-change" mutations, the investigation can be expanded taking advantage of simplified isolation techniques and multiplex exon screening of selected mutations (John Thacker, Medical Research Council, Radiobiology Unit, Didcot, England, personal communication).

The second collaboration is with Dr. Helen Evans, Case-Western Reserve University (CWRU), on mutational response of radiosensitive and radioresistant L5178Y cells as well as the dosimetric evaluation of the CWRU *in vitro* radon exposure system. We have completed experimentation and calculation of the dosimetry for L5178Y cells using three exposure systems (at PNL, CWRU, and the University of Chicago

TABLE 1. Current Summary of CHO-HGPRT Mutation Types[a]

Treatment	Full Deletion[b]	Alteration[c]	No Change[d]	Total
None (spontaneous)	4 (14%)	3 (10%)	22 (76%)	29
Low-dose radon (25 and 30 cGy)	11 (48%)	4 (17%)	8 (35%)	23
High-dose radon (75 and 77 cGy)	11 (44%)	8 (32%)	6 (24%)	25
300-cGy x rays	16 (47%)	8 (24%)	10 (29%)	34

(a) DNA from each mutant cell line was digested with one or more restriction enzymes.
(b) Full deletion, no residual HGPRT-specific coding sequences detectable.
(c) Alteration, loss of bands, and/or appearance of new bands.
(d) No change, banding pattern not different from that of untreated parental controls.

[UC]); Dr. Evans has submitted this work for publication in *Radiation Research*. As a future direction for improving dosimetry, we intend to employ an alpha-probe detector designed at PNL to investigate the buildup of radon and radon progeny in the *in vitro* radon exposure systems at PNL and CWRU.

The third collaboration, with Drs. James Cleaver and Louise Lutze, University of California, San Francisco (UCSF), is radon exposure of shuttle vectors for molecular analysis of induced mutations. This work indicates that a high proportion of radon-induced mutations are large deletions that are not randomly distributed but appear to begin and end in defined regions of the episome. Deletion ends were rejoined by nonhomologous recombination involving as many as 6 base pairs of homology. This work was published in 1992 (Lutze et al. 1992). Dose-response data from UCSF indicated that mutations are induced in the pHAZE shuttle vector in a linear fashion at a rate of approximately 0.22×10^{-6} mutations per cGy with a relative biological effectiveness of 38 compared to x-ray induction of pHAZE mutations; the spontaneous frequency for pHAZE in the RAJI cell line averages 2.9×10^{-5}. The mutation frequency obtained at PNL with the HGPRT locus in CHO cells using the same exposure system is 1.4×10^{-6} mutants per viable cell per cGy. The difference could be caused in part by the recovery of larger deletion events in the HGPRT system. The radon RBE for CHO-HGPRT mutations relative to 300 cGy of x rays was 12. Dr. Lutze is currently restructuring the pHAZE vector to change the relative regions that contain clustered deletion endpoints. In this way we will be able to determine whether damage induction or the subsequent damage repair processes are concentrated in these regions. She is also optimizing the shuttle vector parameters in repair- proficient and repair-deficient human cell lines for investigation with the PNL *in vitro* radon exposure system.

The fourth joint effort, with Drs. Richard Albertini and J. P. O'Neill, University of Vermont, investigates the molecular basis of radon-induced mutations at the HGPRT locus in human peripheral blood lymphocytes. We have completed four *in vitro* lymphocyte exposures for mutation analysis and are currently establishing the dosimetric parameters for isolated G_0 lymphocytes.

Dosimetry of *In Vitro* Radon Exposures

Theoretical models of hit probability require experimental validation. We have used the single-cell gel (SCG) electrophoretic technique to evaluate hit probability calculations based on a dosimetry model (Jostes et al. 1991) developed at PNL. The SCG technique measures DNA strand breaks as increased migration of the DNA out of lysed cells embedded in the middle layer of a three-layer gel formed on a microscope slide. We have used the alkaline SCG technique to estimate the percentage of cell nuclei "hit" by alpha particles after irradiation with an *in vitro* radon exposure system (described in the 1991 *Annual Report, Part I*). This work has been submitted to *Health Physics* for publication. Another dosimetry-related paper submitted to *Health Physics* evaluates the PNL alpha-probe detector for *in vitro* cellular dosimetry.

Radon Mutation Studies in Animals

Radon mutation studies in animals included, first, exposures (320, 640, and 960 WLM) of Big Blue™ transgenic mice. We have initiated mutation frequency determination and molecular analysis of the transgenic target sequence to be performed by Drs. Lutze and Richard Winegar (UCSF and Stanford Research Institute [SRI], respectively) and by Drs. Jostes and Stiegler at PNL. Initially, both laboratories will investigate tissues from the lung. If the induced mutation frequencies are sufficiently greater than background, the target sequence will be excised from the phage and analyzed by restriction fragment-length polymorphism. This will allow an initial determination of the spectrum of mutations induced in different tissues and whether these differ significantly from spontaneous mutations. Other tissues will be studied without duplication of effort. Frequency information will provide the relative mutational damage incurred in the various tissues after *in vivo* radon exposure. Sequence analysis of mutations from the different tissues will provide information on whether

the initial lesions are processed differently, resulting in a different spectra of damage at the base-pair level. It will also be useful to determine whether the process of nonhomologous recombination, which we have found is used to rejoin radon-induced double-strand breaks in cells in culture, is also observed in cells in intact tissues.

A second study included radon exposures of Chinese hamsters comparable to those of the transgenic mice in a pilot study to investigate the feasibility of selecting mutations for molecular analysis at the HGPRT locus in lung cells. If this proved feasible, we would then compare the spectrum of molecular lesions with the existing PNL database from CHO cells exposed *in vitro*. In our initial experiment, cells were processed for mutation analysis in two different protocols for mutation selection. A large number of mutations were obtained in one protocol and none in the other. It is possible that the one protocol resulted in cell death below the induced mutation frequency. This pilot study has been temporarily suspended.

Initiation-Promotion-Initiation Studies

Processing of tissues and analyses of data from initiation-promotion-initiation (IPI) experiments in young-adult, male SPF Wistar rats with radon and cigarette-smoke mixtures continued. The exposure protocols are shown in Table 2.

Radon-progeny exposures were at 100 working-level (100-WL) concentrations with cumulative levels of 320 working-level months (WLM); uranium ore-dust concentrations ranged from about 5 to 6 mg/m^3. Cigarette smoke from Kentucky 1R4F cigarettes, in exposures of 1 hr/day, 5 days/week, for 17 weeks, contained total particulate mass concentrations of about 0.5 mg/liter and carbon monoxide concentrations between 650 and 700 ppm. Mean plasma concentrations of nicotine and cotinine were about 260 and 125 ng/ml, respectively, in cigarette-smoke-exposed animals; carboxyhemoglobin levels were about 29%. Blood samples were obtained within 15 min after exposures ended.

Histopathological examination (reported in the *Annual Report for 1991, Part 1*) was completed

TABLE 2. Initiation-Promotion-Initiation (IPI) Protocol for Radon (R), Dust (D), and Cigarette-Smoke (S) Inhalation Exposure of Rats[a]

	Duration of Exposure, weeks					
Group	0	4	8	17	21	25
1	R+D---------->					
2	R+D----->					R+D->
3	R+D---->S---------->					R+D->
4	R+D---------->	S---------->				
5	S---------->			R+D---------->		
6	D---------->	S---------->				

(a) Moderately low concentrations of uranium ore dust (D) accompany radon exposures as the carrier aerosol for radon progeny; sham-exposed control animals (not shown) are included in each exposure group. Ten animals from each group are killed at 25, 52, and 78 weeks to evaluate developing lesions. Protocol maybe repeated for different radon-progeny and cigarette-smoke exposure rates and levels.

on all IPI series life-span rats exposed to radon, radon progeny, uranium ore dust, and cigarette smoke, as well as on one sham-exposed group of animals. These data were based on our historical protocol examination of one central section per lung lobe, plus any observed lesion at necropsy, rather than the multiple-slicing technique employed in the serially sacrificed rats reported in the *1990 Annual Report, Part 1*. Multiple slicing of the remainder of the IPI life-span rat lungs for histopathological examination continues. Our histopathological analyses of serial-sacrifice rats were published in 1992 (Cross et al. 1992).

Determination of the histomorphological effects of inhaled radon, uranium ore dust, and cigarette smoke in the tracheal epithelium of serially sacrificed IPI rats was initiated in FY 1992. Groups of 5 to 7 rats per exposure group were measured for tracheal epithelium thickness, ciliated cell population density, and non-ciliated cell population density. Table 3 shows a comparison of data at 25 and 52 weeks from start of exposure. Five major conclusions can be derived from these measurements. First, epithelial thickening at 25 and 52 weeks is correlated

TABLE 3. Comparison of Histomorphological Data in the Trachea of Initiation-Promotion-Initiation (IPI) Serial-Sacrifice Rats

Sacrifice Group	Tracheal Measurement	Exposure Group[a] Sham Control	Radon Shelf (Group 1)	Radon Shelf Radon (Group 2)	Radon Smoke Radon (Group 3)	Radon Smoke (Group 4)	Smoke Radon (Group 5)	U Ore Dust Smoke (Group 6)
25 wk	Epithelium thickness, μm	9.8 ± 0.9	10.3 ± 0.7	11.7 ± 1.2	15.0 ± 1.2[b]	12.9 ± 0.8	10.3 ± 0.7	13.4 ± 0.7
	Ciliated cell density, cells/mm	85 ± 9	102 ± 6	88 ± 10	78 ± 7[c]	91 ± 8	123 ± 8	119 ± 9
	Nonciliated cell density, cells/mm	156 ± 16	157 ± 15	181 ± 10	235 ± 29[d]	201 ± 11	154 ± 12	191 ± 9
52 wk[e]	Epithelium thickness, μm	10.4 ± 0.7	10.0 ± 0.7	11.0 ± 0.9	11.1 ± 0.5	10.2 ± 0.8	11.2 ± 0.9	12.1 ± 0.5
	Ciliated cell density, cells/mm	110 ± 10	106 ± 7	124 ± 7	133 ± 7	110 ± 7	146 ± 11	128 ± 7
	Nonciliated cell density, cells/mm	171 ± 15	151 ± 17	174 ± 21	175 ± 10	148 ± 7	167 ± 11	183 ± 12

(a) See Table 2 for further explanation of IPI exposure protocol; data represent the mean and standard error for 5 rats per group at 25 weeks and 7 rats per group at 52 weeks.
(b) Data significantly ($p < 0.05$) different only from sham control, Group 1, and Group 5 data by the HSD test.
(c) Data significantly different only from Group 5 data by the HSD test.
(d) Data significantly different only from sham control, Group 1, and Group 5 data by the HSD test.
(e) No significant group mean differences existed at 52 weeks for epithelium thickness or nonciliated cell density; significant ciliated cell density differences at 52 weeks occurred only between Groups 1 and 5 by the HSD test.

with nonciliated cell density (this group contains target cells for carcinogenesis) but not with ciliated cell density. Second, cigarette-smoke exposures appear to be the predominant cause of increased epithelial thickness and increased density of nonciliated cells in 25-week-sacrifice rats. Third, the timing of smoke exposures is important as the influence of cigarette-smoke exposures diminishes with time following cessation of smoke exposure. This is most clearly seen in 25-week-sacrifice rats from Groups 4 and 5, even though the differences are not significant ($p < 0.05$) by the honestly significant difference (HSD) test. Fourth, split-dose radon, with or without cigarette-smoke exposures, generally increased the thickness of the epithelium and the density of nonciliated cells compared with single-dose radon. The increase, however, was only significant by the HSD test for split-dose radon with cigarette-smoke exposures (Groups 3 and 5, but not Groups 3 and 4). Fifth, the only comparison of exposure group means that was significant at 52 week was for ciliated cell density in rats exposed first to cigarette smoke and then to radon (Group 5 rats), compared with rats exposed to single-dose radon (Group 1). As is true for cigarette-smoke exposures, there also appears to be a time-since-exposure effect (a repair of injury to epithelial tissue) for radon-only exposures.

The histomorphological data overall show a transitory hyperplasia predominantly of nonciliated cells with thickening of the tracheal epithelium. Except for Group 1 exposures, which terminated at 8 weeks, all exposures terminated at 25 weeks. By 52 weeks, the majority of changes noted in exposed, 25-week-sacrifice rats was diminished to values found in control rats. Future histomorphology will complete the measurements on the remainder of sacrifice rats, particularly in the 25- and 52-week groups.

References Cited

Cross, F. T., G. E. Dagle, R. A. Gies, L. G. Smith, and R. L. Buschbom. 1992. Experimental animal studies of radon and cigarette smoke. In: *Indoor Radon and Lung Cancer: Reality or Myth?*, Proceedings of the 29th Hanford Symposium on Health and the Environment, F. T. Cross, ed., Part 2, pp. 821-844. Battelle Press, Columbus, Ohio.

Foreman, M. E., L. S. McCoy, and M. E. Frazier. 1992. Involvement of oncogenes in radon-induced lung tumors in the rat. In: *Indoor Radon and Lung Cancer: Reality or Myth?*, Proceedings of the 29th Hanford Symposium on Health and the Environment, F. T. Cross, ed., Part 2, pp. 649-658. Battelle Press, Columbus, Ohio.

Jostes, R. F., E. W. Fleck, R. A. Gies, T. E. Hui, T. L. Morgan, J. L. Schwartz, J. K. Wiencke, and F. T. Cross. 1992. Cytotoxic, clastogenic and mutagenic response of mammalian cells exposed *in vitro* to radon and its progeny. In: *Indoor Radon and Lung Cancer: Reality or Myth?*, Proceedings of the 29th Hanford Symposium on Health and the Environment, F. T. Cross, ed., Part 2, pp. 555-568. Battelle Press, Columbus, Ohio.

Jostes, R. F., T. E. Hui, A. C. James, F. T. Cross, J. L. Schwartz, J. Rotmensch, R. W. Atcher, H. H. Evans, J. Mencl, G. Bakale, and P. S. Rao. 1991. *In vitro* exposure of mammalian cells to radon: Dosimetric considerations. *Radiat. Res.* 127:211-219.

Lutze, L. H., R. A. Winegar, R. Jostes, F. T. Cross, and J. E. Cleaver. 1992. Radon-induced deletions in human cells: Role of nonhomologous strand rejoining. *Cancer Res.* 52:5126-5129.

In Vivo/In Vitro Radon-Induced Cellular Damage

Principal Investigator: *A. L. Brooks*

Other Investigators: *F. T. Cross, R. F. Jostes, M. A. Khan, J. E. Morris, and K. E. McDonald*

Major research efforts are being conducted, both *in vitro* with model cellular and molecular systems and *in vivo* in whole animals, to understand the health effects of inhaled radon and its progeny. This project provides important links relating the data from mechanistic model studies to those derived from the animal studies, and renders both types of data more useful in predicting health hazards from radon-progeny exposure in homes. The current studies have been designed to define the relationships between inhalation exposure and radiation dose to the cells of the respiratory tract, accomplished by comparing cellular damage induced by alpha particles both *in vivo* and *in vitro*.

Animals were exposed by inhalation to radon and radon decay products. Cellular damage was determined in deep-lung fibroblasts by micronuclei assay, and in epithelial cells of rat trachea by measurement of chromosome aberration frequency, as a function of dose and time after exposure. In chromosome aberration experiments, animals were exposed to either 900- or 320-working-level months (WLM) of radon progeny; aberrations were scored shortly after cells were isolated from the trachea. *In vitro* studies were conducted in the G_0/G_1 stage of the cell cycle using a ^{238}Pu alpha-particle source. The dose–response relationship for induction of aberrations *in vitro* was recorded as aberrations/cell = 0.001 + 0.48 D, where D is in grays (Gy). Using these data, it was possible to estimate the dose/WLM at the two different total radon exposures as 2.2 mGy/WLM and 3.0 mGy/WLM for the high- and low-dose exposures, respectively. *In vivo* dose–response data indicated that micronuclei frequency increased as a linear function of cumulative radon-progeny exposure according to the following equation: micronuclei/1000 cells = 21 + 0.52 WLM. Micronuclei frequency induced in deep lung fibroblasts by 320-WLM exposure was followed for 30 days and was found to decrease with a half-life of about 30 days. These *in vivo* data were related to dose–response relationships derived *in vitro* using a well-defined exposure system. For nonproliferating G_0/G_1 cells, the frequency of induced micronuclei increased linearly: micronuclei/1000 binucleated cells = -14.3 + 8.2 D, where D is in cGy. For cells stimulated to divide in tissue culture, the dose–response curve increased: Micronuclei/1000 binucleated cells = 18.6 + 12.5 D. Using nondividing cells, which better reflect the conditions in the deep lung, it was estimated that a 1-WLM exposure *in vivo* caused the same amount of chromosome damage as would be induced by a 0.6-mGy *in vitro* dose. Additional studies are under way to link exposure, exposure rate, unattached fraction, dose, and species-specific responses to produce data that are useful for defining risk from inhaled radon progeny.

This research is addressing several basic radiobiological questions associated with radon-progeny inhalation to help provide a mechanistic understanding of the action of radon on respiratory tract cells and to develop better estimates of the risk from indoor radon exposure:

1. How do low-level exposures and exposure rates influence cancer risk?
2. What is the relationship between exposure and dose to respiratory cells?
3. How does the unattached fraction influence the distribution of dose and damage in the respiratory tract?
4. What is the biological effectiveness for radon-induced damage relative to low-LET radiation?

Induced chromosome aberrations have been used to detect radiation dose from internally deposited radioactive materials following both experimental and environmental exposure. If chromosome damage is to be a useful indicator of dose, it is essential that damage be measured in the cells at risk or in surrogate cells that receive similar doses. Micronuclei provide a rapid measure of chromosome damage and also are used to evaluate damage in cells exposed either in the whole animal or under well-defined culture conditions. Both chromosome aberrations and micronuclei production are being used as biomarkers of dose in different regions of the respiratory tract.

Experimental Design and Methods

Chromosome aberration frequency was measured in the trachea following either *in vitro* exposure to ^{238}Pu alpha particles or *in vivo* exposure to two levels, 320- or 900-working-level months (WLM), of radon progeny. Aberration frequencies were determined on coded slides 48 hours after short-term culture. The slopes of the dose response relationships from the *in vitro* studies were used to estimate dose to the trachea from inhalation of radon.

The frequency of micronuclei production was measured in rat lung fibroblasts exposed either *in vitro* to radon in suspension cultures or after graded radon-inhalation exposures; both dose response and time response studies were conducted. For *in vitro* exposures, cells were either grown in culture for 16 hours after isolation, providing cells in the G_0/G_1 stages of the cell cycle at the time of exposure, or for 4 days, at which time cells were available in all stages of the cell cycle. Dose/WLM values were estimated by comparing the slopes of dose response in the *in vitro/in vivo* studies. All cells were scored on coded slides.

Results and Discussion

Chromosome Aberrations in Tracheal Epithelium

The results of our studies on chromosome aberration frequency are presented in Figure 1, which illustrates that the slope of the dose response curve after exposure to ^{238}Pu alpha particles is aberrations/cell = 0.001 +0.48 D, where D is in

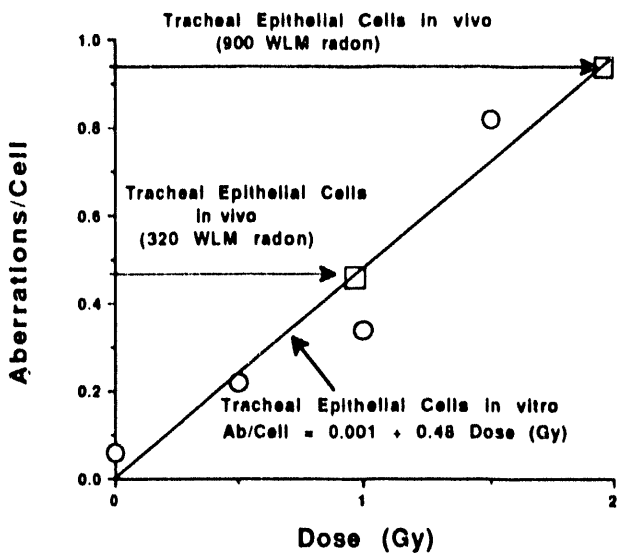

FIGURE 1. Induction of Chromosome Aberrations in Rat Tracheal Epithelial Cells *in Vitro* by ^{238}Pu Alpha Particles and *in Vivo* by Radon Inhalation.

grays (Gy). The figure includes data on the induction of chromosome aberrations following a 900- or 320-WLM *in vivo* exposure. It was calculated that 2.2 or 3.0 mGy from ^{238}Pu alpha-particle exposure resulted in the same amount of chromosome damage as a 1-WLM exposure to radon and its progeny. These data show that the lower exposure level (320 WLM) produces a higher frequency of aberrations than does higher level exposure per working-level month. The explanation could be related to changes in cell cycle kinetics or to a greater degree of cell killing produced by the higher level of radon-progeny exposure.

Micronuclei *In Vivo*

The results of the *in vivo* micronuclei studies are shown in Figure 2. The frequency of micronuclei per 1000 binucleated cells increased linearly with exposure concentration, with a slope of 0.52 micronuclei/1000 binucleated cells/WLM. A linear dose response was observed even though the exposure time was increased for each level, which suggests that there was a very low repair rate compared to the exposure times used in these studies.

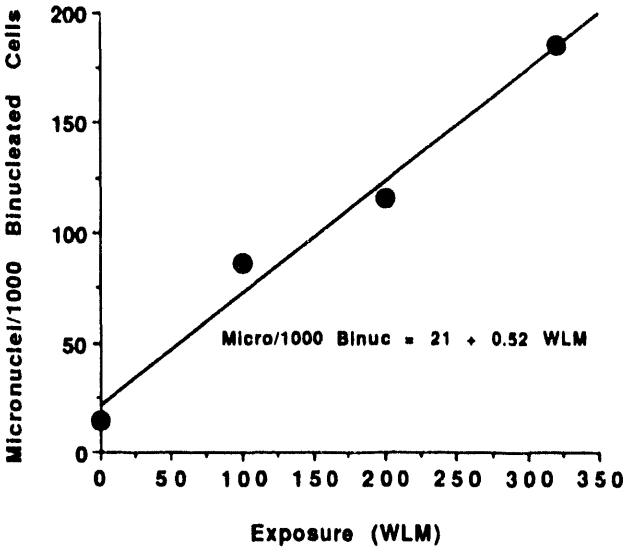

FIGURE 2. Induction of Micronuclei *in Vivo* in Lung Fibroblasts by Inhalation of Radon Progeny.

To evaluate the rate of loss and repair of radon-induced micronuclei from the cell population, animals were sacrificed at 0, 15, and 30 days after exposure to 320-WLM radon progeny, and the frequency of micronuclei measured (Figure 3).

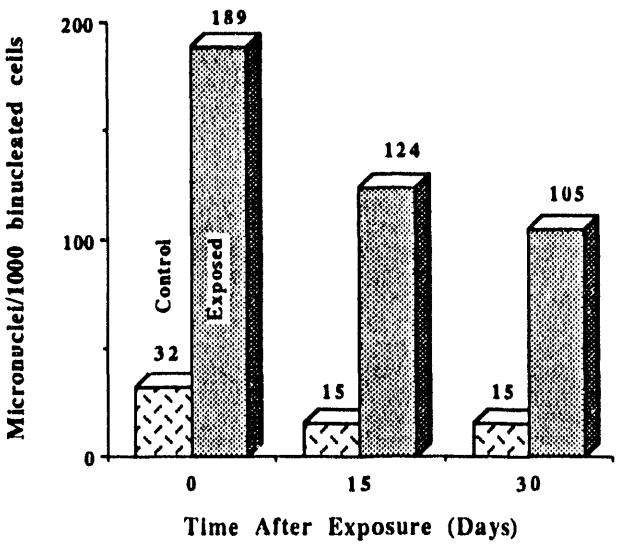

FIGURE 3. Frequency of Micronuclei in Rat Lung Fibroblasts as a Function of Time After Radon-Progeny Inhalation. Animals were sacrificed at 0, 15, and 30 days after inhalation of 320 WLM of radon and its progeny.

Animals sacrificed 30 days after exposure had 105 micronuclei/1000 binucleated cells compared to 189 micronuclei/1000 binucleated cells observed in animals sacrificed at the end of the exposure. This study suggests that cells which are damaged by radon exposure survive in the respiratory tract with a half-life of about 30 days.

Micronuclei *In Vitro*

Cell cycle kinetics for the fibroblasts exposed *in vitro* were determined using a Faxstar Plus flow cytometer. More than 92% of the cells isolated 16 hours before exposure to radon were found to be in the G_0/G_1 stages of the cell cycle, while cells grown in culture for 4 days before exposure were distributed throughout the cell cycle: 43% in G_0/G_1, 46% in S, and 11% in G_2/M stages of the cell cycle. More than 90% of the cells isolated directly from the lung were in the G_0/G_1 stages of the cell cycle, so that it was appropriate to compare the cells grown in culture for 16 hours with those exposed *in vivo*.

In vitro radon exposure of cells produced a linear increase in micronuclei both in cells exposed at 16 hours and in those exposed at 4 days after isolation from animals. The data used to derive the dose-response relationships (Figure 4) illustrate that there was more damage per unit of

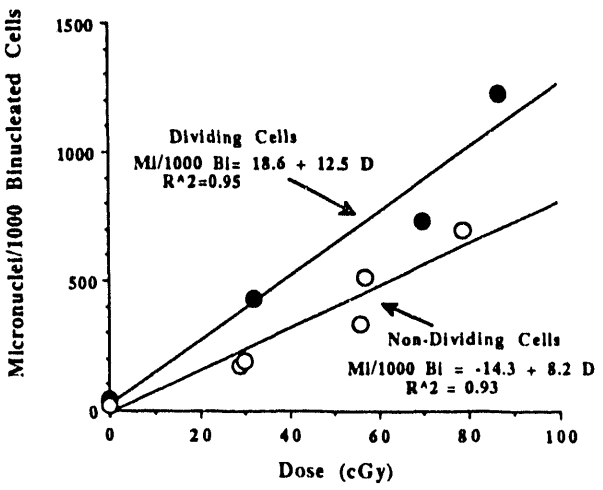

FIGURE 4. Induction of Micronuclei Following *in Vitro* Exposure to Radon Progeny in Dividing and Nondividing Rat Lung Fibroblasts.

dose in dividing cells than was observed in cells in the G_0/G_1 stages of the cell cycle. These data suggest that there are differences in cell-stage sensitivity for the induction of damage by alpha particles.

It was possible to use the frequency of micronuclei induced *in vitro* in lung fibroblasts as a standard biological dosimeter to estimate the radiation dose delivered to deep-lung cells by radon inhalation. When the slope of the dose response relationship for *in vitro* exposure was compared with that for *in vivo* exposure, it was noted that the same amount of damage was induced by 1 WLM of exposure *in vivo* and a 0.6-mGy dose from *in vitro* radon progeny exposure. Models of the dose to the respiratory tract suggest that the dose to the upper-respiratory tract is higher than that in the deep lung. These data will be useful in evaluating models of radiation dose to cells critical for the induction of cancer by radon and its progeny.

Summary

Studies have been conducted that demonstrate the usefulness of cellular damage as biomarkers of radiation dose to the lung. These studies are being expanded to include exposure of cells from different species, including human cells. We also are starting studies that will evaluate the influence of the unattached fraction of radon progeny on dose, dose distribution, and distribution of damage in the respiratory tract. Finally, dose rate studies will be conducted to determine if there is an inverse dose rate effect for radon-induced cellular damage, as has been suggested for high-LET-induced cell transformation and lung cancer induction. Such an approach will help validate the usefulness of micronuclei and chromosome aberration production as markers of radiation dose, and will determine how cellular and molecular changes can be used to improve our understanding of the risk associated with the inhalation of radon progeny.

Dosimetry of Radon Progeny

Principal Investigator: *A. C. James*

Other Investigators: *K. D. Thrall, T. E. Hui, D. R. Fisher, A. Birchall,*[a] *and F. T. Cross*

This project develops and validates cellular dosimetry, microdosimetry of cellular components, and physiologically plausible biokinetic tissue models, and the application of these models to a coherent and comprehensive assessment of human cancer risks from exposures to radon and thoron progeny. We have developed physiologically based pharmacokinetic (PBPK) models to predict the uptake and retention of radon and thoron, and their short-lived progeny, in tissues of experimental animals and in humans. This report describes refinement of these models to more accurately predict individual variation following ingestion exposure and compares the model predictions with rare human data. A new model to predict the uptake and retention of lead in tissues also is described. In addition, we report on research directed toward improving cellular and subcellular dosimetry.

This project develops and validates cellular dosimetry, microdosimetry of cellular components, and physiologically plausible biokinetic tissue models, and the application of these models to a coherent and comprehensive assessment of human cancer risks from exposures to radon and thoron progeny. The major objectives of the ongoing project are (1) to develop state-of-the-art models of human respiratory tract dosimetry for exposures to radon and thoron progeny and to long-lived α-emitters of natural or manmade origin; (2) to apply these models to the review and interpretation of new information on exposure conditions in homes, mines, and other workplaces to improve assessment of human health risk and risk-based standards of radiological protection, provide guidance on environmental monitoring and control, and identify critical research needs; (3) to develop dosimetry of human and experimental animal tissues for short-lived radon and thoron progeny, ^{210}Pb, and ^{210}Po that is based on physiological parameters and experimental data; and (4) to apply comparative tissue dosimetry using epidemiologic data and risk projection models to extrapolate observed carcinogenic risks in humans and experimental animals to radon exposures encountered in homes.

In the *Pacific Northwest Laboratory Annual Report for 1991 to the DOE Office of Energy Research, Part 1*, we reported that we had compared human and laboratory animal data and developed and tested PBPK models to describe tissue uptake and retention of radon, thoron, and their short-lived progeny in experimental animals and in humans following exposure by inhalation or ingestion. In this report, we describe modifications to the PBPK models to more accurately predict individual variations in rate parameters following ingestion exposure. We then compare the model predictions with rare human data. We also describe a new PBPK model, which is based on physiological parameters and developed to predict the uptake and retention of lead in tissues following exposure. In addition, we describe progress in *in vitro* cellular and subcellular dosimetry that will permit us to relate observed cellular *in vitro* radiobiological effects to radon exposures of laboratory animals and humans.

Projecting Lung Cancer Risk from Mines to Homes

During FY 1992, A. C. James participated in committee and task group activities, including

---

(a) Visiting Scientist from the National Radiological Protection Board (NRPB) in the United Kingdom.

the DOE/CEC Radon Risk Strategy Group, and the International Commission on Radiological Protection (ICRP) Task Groups on Measures for Protection Against Radon and on Human Respiratory Tract Models for Radiological Protection. Research conducted in this project provided substantive input to deliberations of the two ICRP Task Groups concerned with limitation of exposures to radon and thoron progeny in workplaces and homes. In addition, the lung dosimetry model developed in this project was applied in the National Research Council's study of "Comparative Dosimetry of Radon in Mines and Homes" (Fisher et al. 1991; James 1992; NRC 1991). This study highlighted new information on environmental and biological parameters generated by the OHER Radon Research Program and was of direct benefit in helping the Environmental Protection Agency (EPA) review radon risk in the home (Oge and Farland 1992).

Modeling Radon-Progeny Doses to Tissues Other Than the Lung

The inert gas model that we developed was based on a model described by Peterman and Perkins (1988), with several modifications. Following the method of Peterman and Perkins, the radon concentration in each organ is assumed to be in equilibrium with that in the blood, which is simultaneously in equilibrium with that in the air spaces of the lungs. Tissue uptake of the inert gas from the blood is a function of the rate at which blood flows through the tissue, divided by the volume of blood in the body. Elimination from each tissue is a function of the rate at which blood flows through each tissue, divided by the volume of the tissue, and also divided by the partition coefficient for the inert gas between blood and the tissue. The partition coefficients for radon and thoron have been reported by Nussbaum and Hursh (1957, 1958).

We have focused on modification of these PBPK models, particularly the model to describe human tissue uptake and distribution of radon following ingestion and those describing tissue distribution of the short-lived progeny. We established a collaboration with C. T. Hess and his colleagues at the University of Maine, who have obtained experimental data on the time-course of radon elimination in breath by studying a large group of subjects (ranging from 9 to 75 years of age) who ingested radon-laden water in their own homes. These data were obtained from volunteers with a wide range of physiological characteristics.

The gastrointestinal tract compartment in the general PBPK model (Figure 1) was modified to include four additional compartments representing the stomach, small intestine, upper large intestine, and lower large intestine. This gastrointestinal tract model contains three parameters that vary dramatically depending on individual characteristics and on postprandial changes: (1) the rate of uptake from the stomach into the blood; (2) the rate of uptake from the small intestine into the blood; and (3) the physical movement of the contents of the stomach into the small intestine. In modifying the radon ingestion model, these three parameters were automatically optimized using an iterative "steepest descent method" (Press et al. 1989) to provide the minimum chi-square fit as compared to the set of human data provided by C. T. Hess (Brown and Hess 1992).

Figure 2 shows the measured and predicted exhalation of radon gas following ingestion of radon-laden water in 3 subjects. Similarly accurate predictions were obtained for most of the other 26 volunteers. The exhalation of radon was found to depend strongly on the subject's breathing rate as well as the quantity of water consumed. We are proceeding, in collaboration with C. T. Hess, to extend the gastrointestinal tract modeling to include the effects of food intake on transit and on uptake through the stomach and small intestine.

In FY 1992, we also refined the previous biokinetic model to describe the uptake and retention of lead in tissues. Developing a PBPK model for lead is complicated by the lack of tissue solubility or partition coefficient information and by the lack of human kinetic data. To overcome these limitations, we have developed

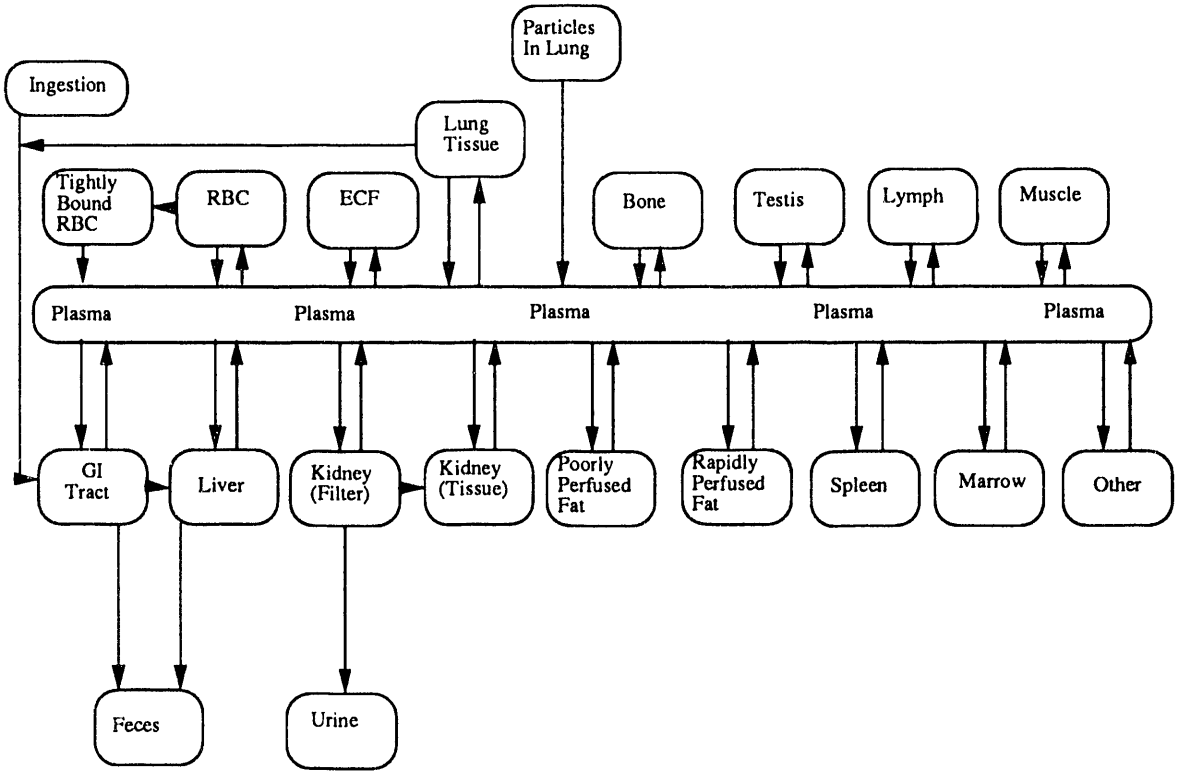

FIGURE 1. General Biokinetic Model for Radon, Thoron, and Their Short-Lived Progeny.

a model similar to that developed for radon. The tissue solubility coefficients were derived using an innovative parameter optimization procedure that we are currently developing (GIGAFIT, or Graphically Interactive General Algorithm for FITting). This enabled us to fit simultaneously all the available kinetic data for tissue uptake and lead excretion in the rat. Figure 3 illustrates that the resulting biokinetic model developed for lead provides a reasonably close representation of the data of Morgan et al. (1977) and also of the additional data obtained by Schubert and White (1952) and Hackett et al. (1982). The GIGAFIT software shows great promise of significantly reducing the tedious task of manually optimizing model parameters to fit experimental data.

The rate constants for tissue uptake and retention of lead atoms determined for the rat can be extrapolated to describe tissue distribution in the human by making the plausible assumption that the partition coefficients from blood to tissue are the same in the human as in the rat. Thus, the appropriate rate constants for tissue uptake and retention in the human are given simply by substituting the documented human values of blood flow rates and tissue volumes. We are further testing the human model against the limited kinetic data available in the literature to verify that this procedure is valid. Our progress in PBPK modeling to date has enabled us to improve the reliability of calculating organ doses from inhalation of the short-lived progeny of radon and thoron, and also those resulting from retention or redistribution of the progeny of radon or thoron decay in body tissues. It may be assumed that the short-lived polonium isotopes produced in tissues by radioactive

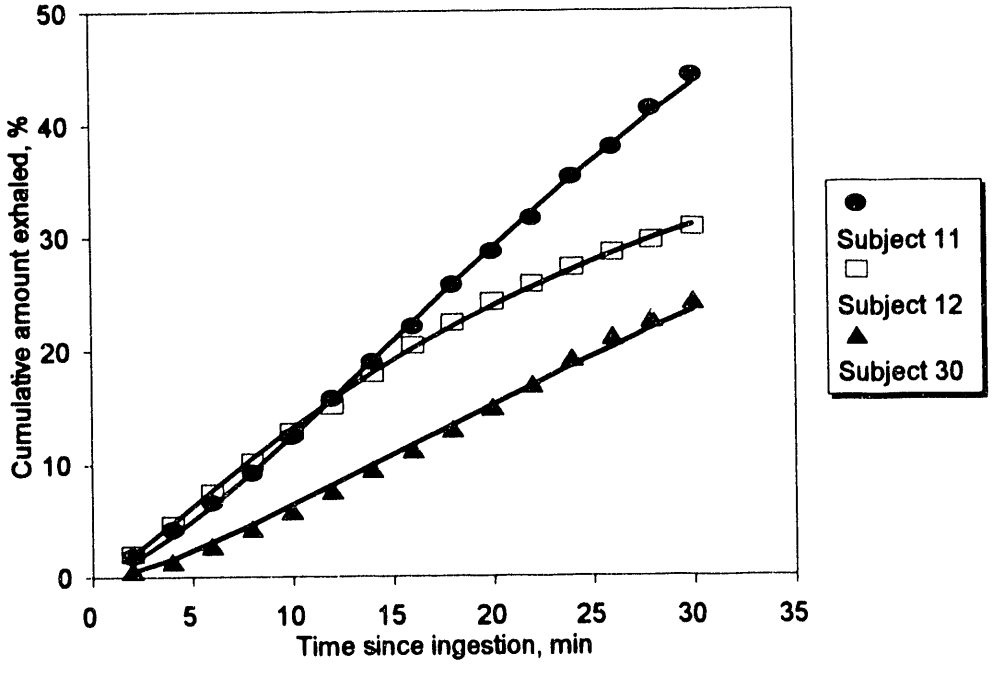

FIGURE 2. Cumulative Amount of ^{222}Rn Exhaled by Three Subjects After Drinking Radon-Laden Water (points) as Predicted by the PNL PBPK Model (lines), Compared with Values Reported by Brown and Hess (1992).

decay of radon, thoron, and their ß-emitting progeny decay *in situ*. Our significant findings are:

1. One may neglect absorption of ^{218}Po from the respiratory tract into the blood in either the "ultrafine" or "attached" forms.

2. The biological half-time for absorption of ^{214}Pb and ^{212}Pb is of the order of 10 hours.

3. There are no data suitable for estimating the absorption rate of bismuth isotopes from the respiratory tract.

Our PBPK modeling also has identified deficiencies in the literature for specific physical or chemical parameters necessary to develop models that are physiologically justified, and thus more reliable. We are directing further research toward testing and verifying some of the critical assumptions involved in the development of these models by means of small-scale experimental studies.

Dosimetry/Microdosimetry for *in Vitro* Cellular Studies

Activity concentrations of α-emitters were measured with an α-probe detector designed for use in the PNL *in vitro* radon cell-exposure system (Jostes et al. 1991). The probe, which consists of a pen-sized body housing a silicon-surface barrier detector, was tested using both chelated and unchelated ^{212}Bi and ^{212}Pb solutions (Hui et al., in press). The detector α-energy spectra, analyzed using a total integration technique, agreed with the solution activity measurement to within 4% to 6%. The congruence of calculated and measured detector response has shown that the α-probe detector will be useful for routine dosimetry of disequilibrium mixtures of radon progeny in the radon cell-exposure systems.

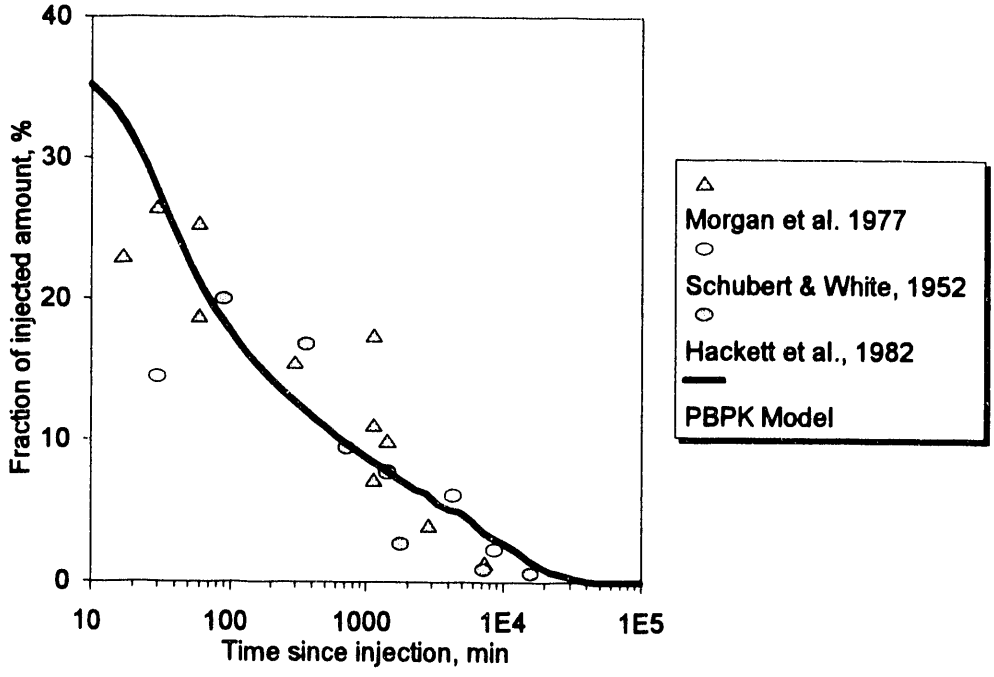

FIGURE 3. Experimental Data on Uptake and Retention of Lead Atoms in Rat Liver Following Intravenous Injection, Compared with Retention Curve Predicted by Biokinetic Model Shown in Figure 1.

In collaboration with PNL investigators in the "Mechanisms of Radon Injury" project, we have analyzed DNA damage to mammalian cells (CHO, A_L, and RAJI) exposed to radon and its progeny *in vitro*. Under single-cell gel (SCG) electrophoresis, DNA damage (single-strand breaks) appears as a comet tail in individual cells. Cells undergoing α-traversals showed increased DNA breakage reflected as greater length-to-width ratios. The histograms of length-to-width ratios of cells exposed to radon and its progeny were biphasic. One peak corresponded to controls, demonstrating that this fraction of the cells was not hit by α-particles. Cells hit showed a marked increase in DNA damage. Hit probabilities were modeled microdosimetrically using the radon and progeny concentrations measured in the suspension medium (Jostes et al. 1991). For example, when CHO cells were given an estimated dose of 0.39 Gy, microdosimetric calculations predicted that 63% of the cell nuclei would be traversed by an α-particle. This prediction was in reasonable agreement with the measured fraction of cells with DNA damage that were placed in the hit category (approximately 51%) (see Figure 4). Similar agreement between measurement and calculation were obtained for A_L and RAJI cells. We concluded that the SCG technique can measure DNA damage from single α-particles and that it supports microdosimetry calculations (Jostes et al., in press).

To apply microdosimetry as an effective tool for predicting radon risk, we also have analyzed the *in vitro* data of cell inactivation and micronuclei induction (Brooks et al. 1990) in rat lung epithelial cells exposed to ^{238}Pu α-particles. This analysis included calculation of dose distribution and hit probability; derivation of dose-response relationships, such as the probability $\lambda(m,n)$ of observing the production of m micronuclei from n α-hits (Table 1); and evaluation of the number of α-traversals required to inactivate a cell (Hui et al., in manuscript). Results show that a cell

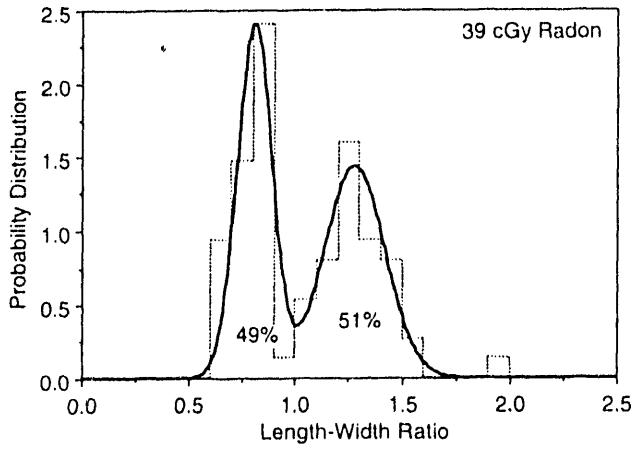

FIGURE 4. Probability Distribution of Cells per Unit Length-to-Width Ratio (total area under curve = 1) of CHO Cells Assayed by Single-Cell Gel (SCG) Technique.

TABLE 1. Probability of Micronuclei Induction as a Function of the Number of Hits to a Cell Nucleus in Lung Epithelial Cell Irradiations

No. of Micronuclei (m)	λ(m,n) No Hit (n = 0)	Single Hit (n = 1)	Multiple Hit (n > 2)
0	0.94	0.50	0.29
1	0.05	0.39	0.25
2	0.01	0.10	0.24
≥3	0[a]	0.01	0.22

(a) Probability less than 0.005.

whose nucleus received a single α-hit has a 50% probability of not showing any micronuclei. Most cells exhibiting multiple ($m > 2$) micronuclei experienced multiple hits ($n > 1$).

The ongoing research to improve our dosimetry techniques will allow us to obtain the distribution of cellular damage and α-particle hits from *in vitro* studies and from *in vivo* animal studies, and to extrapolate these measurements to predict radiobiological effects in humans exposed to radon, thoron, and their progeny.

References Cited

Brooks, A. L., G. J. Newton, L. J. Shyr, F. A. Seiler, and B. R. Scott. 1990. The combined effects of alpha particles and x rays on cell killing and micronucleii induction in lung epithelial cells. *Int. J. Radiat. Biol.* 58:799-811.

Brown, W. T., and C. T. Hess. 1992. Measurement of the biotransfer and time constant of radon from ingested water by human health analysis. *Health Phys.* 62(2):162-170.

Fisher, D. R., T. E. Hui, and A. C. James. 1991. Model for assessing radiation dose to epithelial cells of the human respiratory tract from radon daughters. *Radiat. Prot. Dosim.* 38:73-80.

Hackett, P. L., J. O. Hess, and M. R. Sikov. 1982. Effect of dose level and pregnancy on the distribution and toxicity of intravenous lead in rats. *J. Toxicol. Environ. Health* 9:1007-1020.

James, A. C. 1992. Dosimetry of radon and Thoron exposures: Implications for risks from indoor exposure. In: *Indoor Radon and Lung Cancer: Reality or Myth?*, F. T. Cross, ed., Part 1, pp. 167–200, Proceedings of the 29th Hanford Symposium on Health and the Environment, Richland, Washington. Battelle Press, Columbus, Ohio.

Hui, T. E., A. C. James, R. F. Jostes, J. L. Schwartz, K. L. Swinth, and F. T. Cross. Evaluation of an alpha probe detector for *in vitro* cellular dosimetry. *Health Phys.* (in press).

Jostes, R. F., T. E. Hui, and F. T. Cross. Use of the single-cell gel technique to support hit probability calculations in mammalian cells exposed to radon and radon progeny. *Health Phys.* (in press).

Jostes, R. F., T. E. Hui, A. C. James, F. T. Cross, J. L. Schwartz, J. Rotmensch, R. W. Atcher, H. H. Evans, J. Mencl, G. Bakele, and P. S. Rao. 1991. In vitro exposure of mammalian cells to radon: Dosimetric considerations. *Radiat. Res.* 127:211-219.

Morgan, A., A. Holmes, and J. C. Evans. 1977. Retention, distribution, and excretion of lead by the rat after intravenous injection. *Br. J. Ind. Med.* 34:37-42.

National Research Council (NRC). 1991. *Comparative Dosimetry of Radon in Mines and Homes.* Report by a scientific panel. National Academy Press, Washington, D.C.

Nussbaum, E., and J. B. Hursh. 1957. Radon solubility in rat tissues. *Science* 125:552-553.

Nussbaum, E., and J. B. Hursh. 1958. Radon solubility in fatty acids and triglycerides. *J. Phys. Chem.* 62:81-84.

Oge, N. T., and W. H. Farland. 1992. Radon risk in the home. *Science* 255:1194.

Peterman, B. F., and C. J. Perkins. 1988. Dynamics of radioactive chemically inert gases in the human body. *Radiat. Prot. Dosim.* 22:5-12.

Press, W. H., B. P. Flannery, S. A. Teukolsky, and W. T. Vetterling. 1989. *Numerical Recipes: The Art of Scientific Computing.* Cambridge University Press, New York.

Schubert, J., and M. R. White. 1952. Effect of sodium and zirconium citrates on distribution and excretion of injected radiolead. *J. Lab. Clin. Med.* 39:260-266.

Aerosol Technology Development

Principal Investigator: *A. C. James*

Other Investigators: *J. K. Briant, M. A. Parkhurst, and A. Birchall*[a]

The purpose of this project is to develop and transfer aerosol technology for basic and applied research in biology and chemistry, especially in the areas of health and environmental effects of energy-related materials. We report here the development of special radon-progeny aerosols and exposure systems for the controlled and well-characterized exposure and dosimetry of experimental animals in studies relating cellular damage to radon carcinogenesis. Our ultrafine radon progeny size-spectrometer (URPSS) and low pressure impactor, both employing CR-39 track-etch technology, are used to measure the conversion coefficient between exposure and dose in a home, indoor workplace, or underground mine during a representative period and at low levels of exposure. New methods of data analysis are described for extracting the most useful information from particle-size measurements.

The ongoing objectives of this project are (1) to improve systems for the control, monitoring, and characterization of exposures of laboratory animals to toxic aerosols, gases, and vapors; (2) to develop simpler and more widely applicable techniques to characterize ultrafine and attached radon progeny in domestic and occupational settings, especially to transfer Pacific Northwest Laboratory (PNL) CR-39 (poly-[ethylene glycol *bis*-(allyl)]carbonate) track-etch and analysis technology to improve the monitoring and characterization of occupational and environmental exposure to radon progeny and other alpha (α) emitters; and (3) to deploy these techniques in the field to obtain representative data for human dosimetry and risk assessment.

Animal Exposure to Radon in a Recirculating Atmosphere

Whole-Body Exposure System

To mimic human exposure to radon indoors, animals will be exposed in a manner such that the ultrafine (unattached) fraction of radon progeny potential alpha energy is at least 20%, for which dosimetric modeling indicates that most of the dose to sensitive cells in the respiratory tract epithelium arises from the deposition of unattached radon progeny (NRC 1991). Ultrafine progeny plate out rapidly on exposure chamber surfaces, so we need to provide facilities to maintain and monitor these special radon progeny conditions in the H-2000 chambers (manufactured by Harford Division of Lab Products, Aberdeen, Maryland). Uniform exposures of animals to a high concentration of ultrafine radon progeny will be achieved by recirculating filtered radon-laden air at moderately high velocity through the chambers, as described in the report for *Radon Hazards in Homes*. Aerosol-particle concentration has been demonstrated in the H-2000 to be uniform with three full tiers of animals in the chamber at the normal flow rate of 283 liters/min (10 volume changes per hour) (Beethe et al. 1979; Moss et al. 1982). Other work in this laboratory with reactive, highly diffusive gases has demonstrated the need for a higher flow rate to achieve uniform distribution of these gases to the animals (*Pacific Northwest Laboratory Report for 1989 to the Office of Energy Research, Part 1*, pp. 87-88). The ultrafine (unattached) radon progeny should require an intermediate flow rate. We expect that a chamber flow rate of 420 liters/min will give uniform distribution of the 5-nm ultrafine radon progeny. This flow rate will be tested and increased if necessary to reduce spatial

(a) Visiting scientist from the National Radiological Protection Board (NRPB) in the United Kingdom.

variability to less than 10% for two tiers of exposure cages housing a total of 64 rats in each chamber.

Ultrafine radon progeny will be controlled in association with ultrafine silver particles to present progeny for inhalation at a size that deposits activity in the nasal, pharyngeal, and tracheobronchial regions of the respiratory tract. Monodisperse silver particles are introduced to the ventilation air by vaporization-condensation (Gotoh et al. 1990; Scheibel and Portendörfer 1983). The silver-particle number concentration will be generated at 10 times the expected progeny number concentration, which ensures that most of the progeny will associate with the silver particles rather than plate out on other surfaces. Even at this high number concentration ($\sim 10^6/cm^3$), the airborne mass concentration of silver ($<1\ \mu g/m^3$) will be well below the level of any inhalation toxicity effect. These particles will pass through an aging chamber, with a mean residence time of 1 hour, to allow buildup of radon progeny on the ultrafine silver particles before they enter the exposure chamber. Particle number concentration will be measured in the exposure chamber by a condensation nucleus counter.

Some progeny will be attached to wax aerosol particles of about 0.1-μm diameter, generated by evaporation-condensation (Tu 1982). Ultrafine silver particles with associated progeny will tend to attach to the wax particles, in addition to the attachment of freshly generated progeny. Adjustment of the wax-particle concentration will be used to control the unattached fraction. A preliminary experiment achieved 16% unattached progeny during recirculation with animals in the chamber and a condensation nucleus concentration of $3000/cm^3$. Reducing the carrier aerosol-particle concentration to about $2000/cm^3$ should raise the unattached fraction into the desired range. Again, the airborne mass concentration will be very low ($<10\ g/m^3$). Total mass concentration will be measured by a continuous air sample collected on a filter for gravimetric determination at the end of each exposure day. As with the ultrafine particles, the wax aerosol particles will pass through an aging chamber to allow buildup of radon progeny attached to the particles. These wax aerosol particles should deposit primarily in the pulmonary region of the lungs, thus completing the distribution of progeny deposition throughout the respiratory tract.

Radon-Progeny Metrology

The concentration of radon gas in the animal exposure chambers is monitored continuously in the PNL facility by a commercial Lucas Cell interfaced through a computer to the radon generator and a control system. The concentrations of the individual radon progeny (^{218}Po, ^{214}Pb, and $^{214}Bi/^{214}Po$) are monitored periodically throughout an exposure by collection on a filter and by alpha spectroscopy. The ultrafine (unattached) fraction of radon progeny and its size distribution will be measured using the ultrafine radon progeny size-spectrometer (URPSS). In the exposure-chamber atmosphere, which is contaminated with vapors and other chemicals from the experimental animals, the ultrafine radon progeny are likely to grow substantially in size. So-called unattached progeny have been observed to grow to a diameter of 10 nm in indoor air that is heavily contaminated with vapors (Hopke 1990). Because dosimetric modeling indicates that even moderate growth of ultrafine radon progeny has a significant impact on doses to respiratory tract tissues (NRC 1991), it is important to characterize both the size distribution and the concentration of unattached progeny in the exposure-chamber atmosphere. This will be achieved by deconvolution of the recorded profile of alpha activity deposited along the length of the CR-39 strip in the URPSS.

Attached radon-progeny particle size will be measured by continuously sampling with a low-pressure cascade impactor. The radial-slot impactor (model SE2110, Andersen Instruments, Atlanta, Georgia) will be equipped with CR-39 impaction plates that will record alpha activity deposited on each stage. By diluting the sampled aerosol (Hirano 1987), a sample can be continuously drawn from each chamber, giving an integrated record of attached-activity particle size for each chamber. The primary measurement of total attached-activity aerosol concentration will be determined by the conventional wire-screen sampler (George 1972; James et al. 1972) used periodically during exposure. Radon

concentration, unattached and attached concentration, and size of progeny provide the information needed to model the distribution and dosimetry of inhaled radon-progeny radioactivity.

Ultrafine Radon-Progeny Size Analysis

Analysis of alpha-track density along the channel of the URPSS requires inversion of the data to extract the particle-size distribution of the sampled ultrafine radon progeny. This is accomplished numerically by fitting the data to theoretical formulas for thermodynamic deposition, using the newly developed computer code GIGAFIT (Graphically Interactive General Algorithm for FITting) as developed by A. Birchall. The program resolves the two modes of radon-progeny particle-size distribution typically, that is, the free atoms and ultrafine clusters associated with other vapor molecules. Thus, the so-called unattached progeny are divided into two modes of particle size (Figure 1). Additional modes of particle-size distribution, when present in the data, can be discerned by GIGAFIT.

Measurement of Ultrafine Radon Progeny at Grand Junction

Samples of radon progeny were drawn with the URPSS during air-cleaner tests in the Grand Junction, Colorado radon chamber. The chamber was maintained at a radon-progeny concentration of 1 working level (WL). Size-distribution analysis of a sample collected during a 2-day period with no air cleaning is shown in Figure 1. The small-particle mode (0.77 nm) constitutes only 42% of the total unattached progeny activity. The remaining 58% is associated with an "ultrafine" mode of median particle diameter 12 nm. This finding supports the results obtained with a graded wire screen array (GSA) technique in actual dwellings (Li and Hopke 1991; Wasiolek et al. 1992). A total of 219 quasi-continuous measurements in several normally occupied homes (Wasiolek et al. 1992) showed that, on the average, the so-called "unattached fraction" constitutes about 9% of the total potential α-energy, with an additional 9% carried by particles of diameter between 2 nm and 15 nm (James, submitted). It is also of dosimetric interest to note that GSA aerosol-size measurements in a home while the air was being continuously filtered (Li and Hopke 1991) showed that this cleaning produced a 40% reduction in the concentration of radon progeny in the ultrafine size range (particles between 2 nm and 15 nm in diameter). The reduction achieved for the smaller "unattached" progeny ($\leq$2 nm in diameter) was approximately 10% (James, submitted).

Cascade Impactor Data Analysis

The aerodynamic particle-size distribution of an aerosol is classified by deposition on a series of impactor stages. Measurement of the amount of material deposited on each stage is accomplished by the method best suited to analysis. As reported in *The Pacific Northwest Laboratory Report for 1991 to the Office of Energy Research, Part 1*, we measure uranium alpha activity by recording alpha-radiation tracks on CR-39. To unfold modes of particle size from the data, the numbers of tracks on the stages of the impactors are input to a deconvolution routine (IMPACT-30, S. B. Solomon, Australian Radiation Laboratories, Yallambie, Victoria). This deconvolution is carried out using two different algorithms based on the Twomey method and the expectation-maximization method. These methods give essentially identical results, including median particle size, geometric standard deviation (GSD), and fraction of the total activity for each peak (mode) of the particle-size distribution, under most conditions. The dose-equivalent conversion factor, based on the ICRP-30 model, is also calculated for each of the three retention classes (D, W, and Y) for each peak of the distribution.

Size-distribution data are often presented as a log-probability plot of the cumulative activity. The distribution is commonly approximated by a single log-normal curve, and specified as the median diameter with its GSD. Figure 2 shows this for an impactor sample of uranium aerosol with curves representing the particle-size peaks unfolded by IMPACT-30. Information about the peak at 10 μm, which constitutes 17% of the aerosol activity, would be lost by the simple log-probability presentation as a single distribution. In some cases; information added by resolving

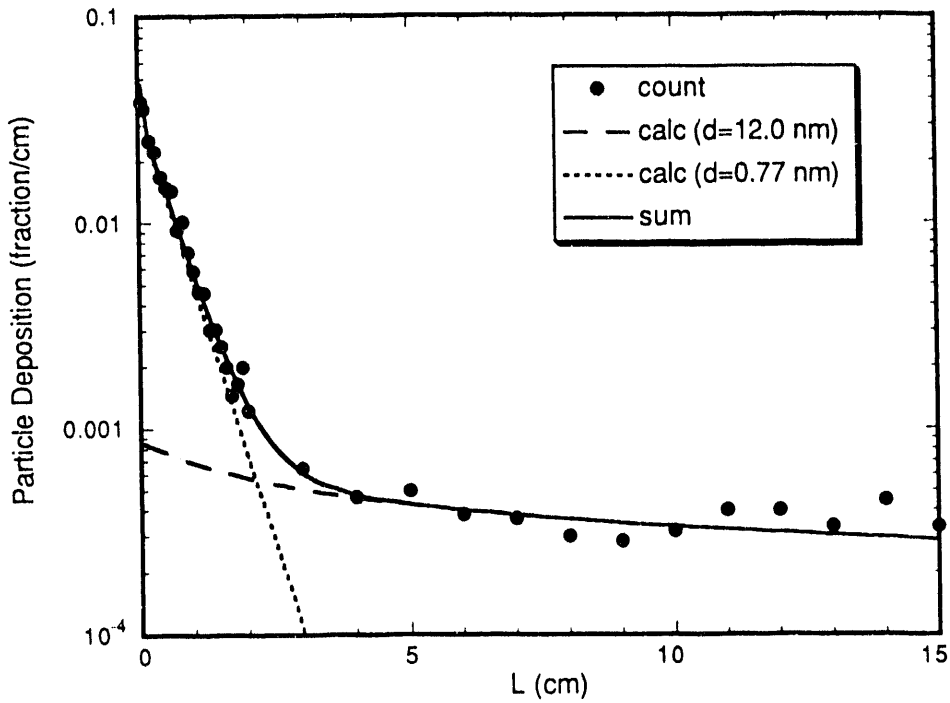

FIGURE 1. Calculated Particle Sizes Are for Two Modes of Distribution of Radon Progeny During Air-Cleaner Operation in the Grand Junction, Colorado, Radon Chamber. Distance L is along the channel of the ultrafine radon-progeny size spectrometer.

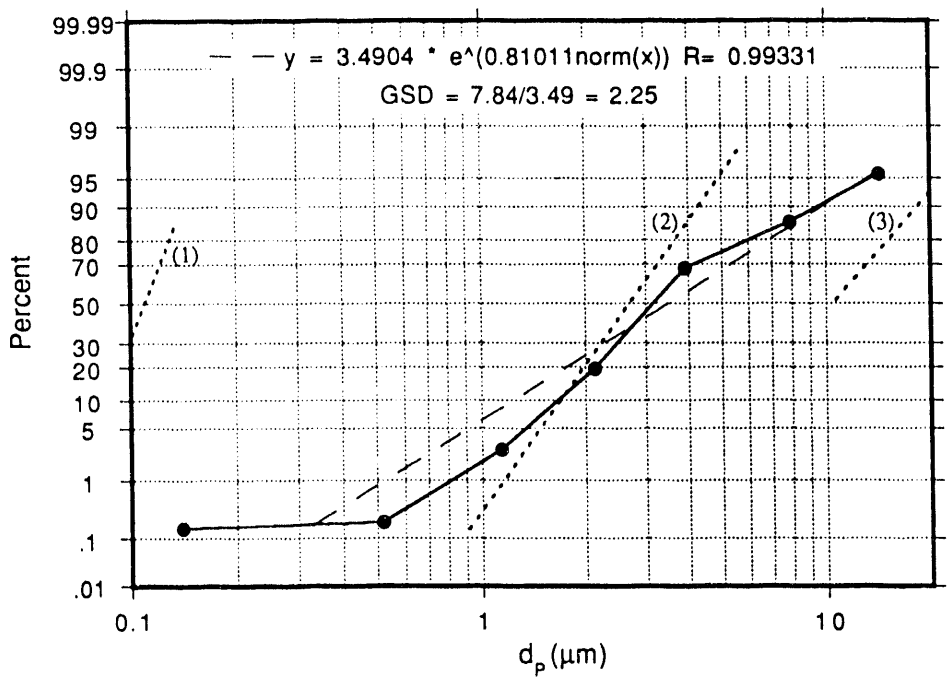

FIGURE 2. Log-Probability of Particle-Size Distribution is Plotted with Graphs of Three Individual Size-Component Peaks Unfolded from the Size Distribution Measured with a Cascade Impactor. A least-squares regression fit is also graphed for nonweighted data.

the size peaks can be important to the dose-equivalent conversion. The small particle-size peak at 0.1 μm may be an artifact of the unfolding procedure, but in any case this has essentially no impact on the overall effective dose equivalent. For this particular sample, the effective dose equivalent per unit intake (H_E/I) is dominated by the peak at 2.7 μm, which is constitutes 83% of the aerosol activity, giving an overall H_E/I equal to 1.54×10^{-5} Sv/Bq for a class Y material.

References

Beethe, R. L., R. K. Wolff, L. C. Griffis, C. H. Hobbs, and R. O. McClellan. 1979. *Evaluation of a Recently Designed Multi-Tiered Exposure Chamber.* LF-67,'NTIS, Springfield, Virginia.

George, A. C. 1972. Measurement of the uncombined fraction of radon daughters with wire screens. *Health Phys.* 23:390-392.

Gotoh, A., H. Ikazaki, and M. Kawamura. 1990. Simple generator of ultrafine particles for tests. *J. Colloid Interface Sci.* 140:535-537.

Hirano, S. 1987. A proportional method for the dilution of submicron hygroscopic aerosols. *Am. Ind. Hyg. Assoc. J.* 48:969-971.

Hopke, P. K. 1990. *A Critical Review of Measurements of the 'Unattached' Fraction of Radon Decay Products.* DE 89ER60878-1, Office of Health and Environmental Research, U.S. Department of Energy, Washington, D.C.

James, A. C., G. F. Bradford, and D. M. Howell. 1972. Collection of unattached RaA atoms using a wire gauze. *J. Aerosol Sci.* 3:243-254.

James, A. C. *The Dosimetry of Human Exposures to Radon, Thoron, and Their Progeny: I. Quantification of Lung Cancer Risk from Indoor Exposure.* DOE/OHER Radon Technical Report Series (in manuscript).

Li, C. S., and P. K. Hopke. 1991. Efficiency of air cleaning systems in controlling indoor radon decay products. *Health Phys.* 61:785-797.

Moss, O. R., J. R. Decker, and W. C. Cannon. 1982. Aerosol mixing in an animal exposure chamber having three levels of caging with excreta pans. *Am. Ind. Hyg. Assoc. J.* 43:244-249.

National Research Council (NRC). 1991. *Comparative Dosimetry of Radon in Mines and Homes.* Report by a scientific panel. National Academy Press, Washington, D.C.

Scheibel, H. G., and J. Porstendörfer. 1983. Generation of monodisperse Ag- and NaCl-aerosols with particle diameters between 2 and 300 nm. *J. Aerosol Sci.* 14:113-126.

Tu, K.-W. 1982. A condensation aerosol generator system for monodisperse aerosols of different physicochemical properties. *J. Aerosol Sci.* 13:363-371.

Wasiolek, P. T., P. K. Hopke, and A. C. James. 1992. Assessment of exposure to radon decay products in realistic living conditions. *J. Exposure Anal. Environ. Epidemiol.* 2:309-322.

Oncogenes in Radiation-Induced Carcinogenesis

Principal Investigator: *G. L. Stiegler*

Other Investigators: *L. C. Stillwell and J. M. Heineman*

We are investigating the role of oncogenes in lung cancer in rats and dogs that inhaled radon progeny or plutonium and leukemia in dogs exposed to whole-body irradiation. Specific *ras* oncogene sequences were amplified by RNA-directed reverse transcriptase polymerase chain reaction (rt-PCR) or by DNA-directed PCR methods. The amplification products were analyzed for base-pair change by the single-strand conformational polymorphism (SSCP) method and by DNA sequence analysis. We have identified activating ras mutations in gamma-radiation-induced leukemic dog spleen tumors, lung and spleen tumors from plutonium-exposed dogs, and radon-induced rat lung tumors. We have also identified *ras* second-exon mutations that have not been documented as *ras* activating. We are initiating quantitative mRNA northern blot analysis using *ras*, c-*myc*, c-*fos*, and c-*jun* gene probes.

The major goal of our research is to identify and characterize genes that are consistently associated with radiation-induced carcinogenesis. The identification of these genes and the molecular definition of their activating lesions will provide genetic markers for radiation damage and also provide a genetic basis for assessing the risk of radiation exposure.

Ionizing radiation damage causes major rearrangements of chromosomal structure such as large deletions, translocations, or chromosomal loss that often result in cell death (Thacker 1985; Thacker and Cox 1983). These effects are an important component of radiation-induced damage, but radiation can also cause less apparent damage such as point mutations, small deletions, and insertions. All these genetic alterations can contribute to the molecular events that lead to cancer.

Two classes of genes have been described as being involved in the induction of cancer: one class acts in a functionally recessive way, and the other in an opposite or dominant mode. Dominant genes are activated by mutational events, and their gene products directly affect the mechanism of cancer. Recessive oncogenes act in a negative, indirect way; their gene products decrease the activity of other genes that regulate growth or differentiation.

The carcinogenic process involves the functional alteration of a critical set of genes (proto-oncogenes) involved in cellular growth control or differentiation; after they are altered, these genes are termed oncogenes. Oncogenes are derived from three broad categories of genes. The first set of gene products acts at the surface of the cell as ligand and ligand receptors (Aaronson 1991). Examples of these oncogenes are *erbB*, *fms*, and *neu*. The altered gene products are involved in cellular processes as growth factors or growth factor receptors. Their aberrant cellular functions result in deregulation of pathways controlling cell division, cytoskeletal structure, and cell metabolism leading to a transformed phenotype. The second set works within the cell cytoplasm as signal transducers carrying signals from the cell surface to the nucleus. The *src* family of tyrosine kinases (Buss et al. 1984) and *ras* family of oncogenes (Hall 1992) are members of this group. Some members of the *src* family physically associate with and are phosphorylated by transmembrane receptors. Other cytoplasmic oncoproteins, such as *ras*, play a more central role in signal transduction by interacting with a variety of cellular growth-related proteins. The third category of cellular oncogene products are the nuclear oncoproteins, such as c-*jun* and c-*fos*. These oncogene products are involved in transcriptional regulation of genes controlling cell growth and differentiation (Landschulz et al.

1988). A number of tumor suppressor genes also express their oncogenic potential by affecting the function of transcriptional regulatory proteins (Weinberg 1991).

Thus, the study of oncogenes and tumor suppressor genes reveals a complex pattern of interactions. Mitogenic signals that begin at the cell surface ultimately result in positive and negative stimuli of nuclear transcriptional factors controlling the tightly regulated genes responsible for differentiation and cell growth. Development of the cancerous phenotype probably requires at least four or five mutational events in key growth-regulating genes.

Because it is not possible to study comprehensively the large number of oncogenes that have been reported in the literature, we are currently focusing our work on a few oncogenes that appear to be more centrally involved in the carcinogenesis process (c-*myc*, c-*fos*, c-*jun*, c-*abl*, and the *ras* oncogene family). Much of our research has concentrated on the dominant-acting *ras* oncogene family, which we chose because its activation has been well characterized and there is a large body of literature describing the molecular mechanism of *ras* oncogene activation. The regions of the *ras* gene family that have been documented as mutational activation sites are at codons 12 and 13 in the first exon and codons 59 and 61 in the second exon of the gene (see review by Barbacid 1987).

We have analyzed the first and second exons of the N-*ras*, H-*ras*, and K-*ras* genes by polymerase chain reaction (PCR) amplification, single-strand conformational polymorphism (SSCP) analysis, molecular cloning of the PCR products, and DNA sequence analysis. An example of *ras* second-exon SSCP analysis is shown in Figure 1; first-exon analysis is summarized in Table 1. We have found, in gamma-radiation-induced canine leukemic spleen tumors, a 12th-codon-activating lesion in both H-*ras* (GCT to ACT) and K-*ras* (GGT to GTT) in one tumor sample and an N-*ras* 13th-codon- (GGT to AGT) activating lesion in another tumor. We have examined a lung tumor from a dog exposed to inhaled plutonium and identified a H-*ras* 13th-codon-activating (GGA to AGA) and a K-*ras* 12th-codon-activating (GGT to GTT) mutation. Examination of lung tumors from radon-progeny-exposed rats has revealed one K-*ras* 12th-codon-activating lesion in which the codon was altered from GGT to GTT. Three 13th-codon activating lesions were identified; the codon was altered from GGC to TGC in two of the lesions and from GGC to GAC in the third. We also found one K-*ras* 12th-codon-activating lesion in a lung tumor from an inhaled-plutonium-exposed rat in which the codon was altered from GGT to GTT.

We have performed PCR amplification and DNA sequence analysis on *ras* gene second exons from canine leukemic spleen tumors induced by whole-body gamma irradiation, lung tumors from dogs exposed to inhaled plutonium, and lung tumors from rats exposed to radon progeny (Table 2). We identified one activating mutation and several second-exon mutations resulting in amino acid substitutions that were not previously identified as activating lesions. To summarize: Examination of seven canine leukemic spleen tumors detected a 64th-codon change in K-*ras* (TAC to CAC) and a 72nd-codon (ATG to ATA) change in N-*ras* in one tumor sample, and a 73rd-codon change (AGG to AGA) in another leukemic spleen. In examining a lung tumor from an inhaled-plutonium-exposed dog, we identified, in the K-*ras* gene, a 61st-codon-activating (CAA to CGA) mutation and changes at the 63rd (GAG to GCG), 64th (TAC to TTC), and 67th (ATG to ACG) codons. In an apparently normal spleen from an inhaled-plutonium-exposed dog we found changes in the N-*ras* gene at codons 55 (ATA to CTA), 70 (CAA to CGA), and 74 (ACA to TCA). The activation of *ras* genes has been reported for specific codons 12 and 13 in the first exon and 59 and 61 in the second exon (Barbacid 1987). The mutations we have identified in codons 55, 62, 63, 64, 67, 70, 72, 73, and 74 have not been documented in the literature as being activating lesions, and their relevance to carcinogenesis is not known. In lung tumors from four radon-progeny-exposed rats, we identified a H-*ras* codon change at position 62 (GAA to GAT).

We are examining gene expression as an additional indicator of oncogene activation using northern blot analysis (Figure 2). We have found increased expression levels of *ras* in total RNA from spleen tissue isolated from a plutonium-exposed dog with splenic malignant lymphoma.

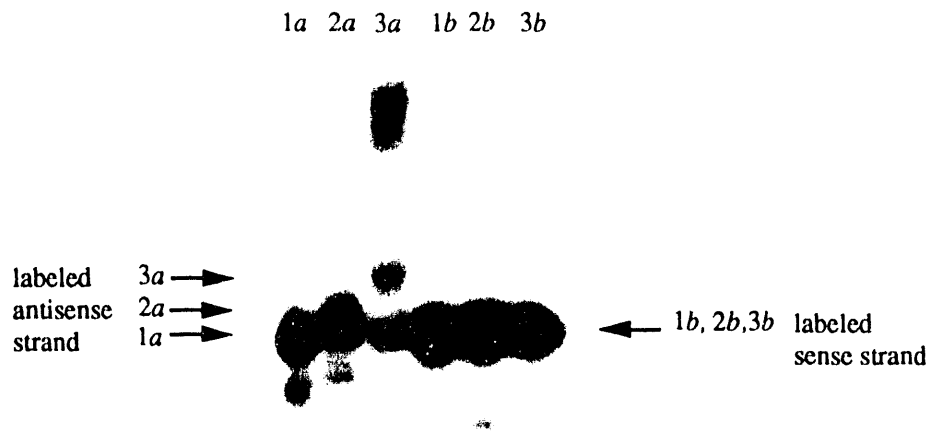

BamHI

1 5'—GGATCC A GAA ACC TGT CTC TTG GAT ATT CTC GAC ACA GCA GGT CAA

2 5'—GGATCC A GAA ACC TGT CTC TTG GAT ATT CTC GAC ACA GCA GGT CAA

3 5'—GGATCC A GAA ACC TGT CTC TTG GAT ATT CTC GAC ACA GCA GGT CAA

1 5'—GAG GCG TAC AGT GCA ATG AGG GAC CAG TAC ACG AGG ACT GGG GAG GGC

2 5'—GAG GAG TAC AGT GCA ACG AGG GAC CAG TAC ATG AGG ACT GGG GAG GGC

3 5' —GAG GAG TAC AGT GCA ATG AGG GAC CAG TAC ATG AGG ACT GGG GAG GGC

1 5'—TTT CTT TGT GTG TTT GCC ATA AAT AAT GGATCC-3'

2 5'—TTT CTT TGT GTG TTT GCC ATA AAT AAT GGATCC-3'

3 5'—TTT CTT TGT GTG TTT GCC ATA AAT AAT GGATCC-3'

BamHI

FIGURE 1. Single-Strand Conformational Polymorphism (SSCP) Analysis of K-*ras* Second-Exon Sequences. Polymerase chain reaction- (PCR-) amplified second-exon sequence differences indicated by closed dot. Top autoradiograph shows single-strand migrational differences attributed to indicated base changes, determined by nucleotide sequence analysis. PCR reactions were individually [^{32}P] 5'-end labeled on sense strand (shown above) or complementary strand (antisense). Labeled PCR reactions were denatured, electrophoresed on 6% nondenaturing polyacrylamide gel, and autoradiographed. Numbers 1, 2, and 3 represent designations for sequences shown above; letters a and b indicate antisense and sense strands, respectively.

The *ras* gene activation is usually not associated with increased expression levels, but it is possible that overexpression of normal *ras* gene product can bring about an aberrant function similar to mutationally activated *ras*.

Summarizing the data from *ras* gene analysis: In examining leukemic spleen samples from seven whole-body, gamma-irradiated dogs, we have identified first-exon *ras*-activating lesions in two dogs (28%). In one dog, *ras* activation was

TABLE 1. First-Exon *ras* Gene Analysis of Tumors from Radiation-Exposed Animals

Exposed Animal	Tissue Type	*ras* Gene	Codon[(a)]	Codon Change
Whole-body gamma-radiation-exposed dog	Spleen	K-*ras*	12	GGT → GTT
		H-*ras*	12	GCT → ACT
Whole-body gamma-radiation-exposed dog	Spleen	N-ras	13	GGT → AGT
Plutonium-exposed dog	Lung	H-*ras*	13	GGA → AGA
		K-*ras*	12	GGT → GTT
Radon-exposed rat	Lung	K-*ras*	13	GGC → TGC
		K-*ras*	12	GGT → GTT
Radon-exposed rat	Lung	K-*ras*	13	GGC → GAC
Radon-exposed rat	Lung	K-*ras*	13	GGC → TGC
Plutonium-exposed rat	Lung	K-*ras*	12	GGT → GTT

(a) Vertical bars indicate that the lesions occurred in the same animal.

observed at the 12th codon in both K-*ras* and H-*ras* genes. In two gamma-irradiated dogs, we identified second-exon point mutations resulting in amino acid substitutions that have unknown significance in carcinogenesis. Mutations were found in four of seven (57%) whole-body, gamma- irradiated dogs, and base transitions occurred in five of the six mutations identified.

In examining 10 rat lung tumors from animals exposed to radon and radon progeny, we identified 3 animals (30%) with first-exon-activating *ras* mutations. One tumor had a mixture of K-*ras* activating mutations at both 12th and 13th codons; the mutations were not found together in the same *ras* gene but were identified in a mixed population of *ras* mutations. K-*ras* 13th-codon mutations were identified in 2 additional tumors. In examining the H-*ras* second exon in radon- exposed rat lung tumors, we identified 4 animals having 62nd-codon mutations that resulted in amino acid substitutions.

Lung tumors examined were obtained from dogs exposed to inhaled plutonium at a heterogeneous mixture of exposure levels, and all these animals were of advanced age at the time tumors were obtained. Of four dogs examined for mutations in the first and second exons of K-*ras*, H-*ras*, and N-*ras* genes, we identified a 12th- and 13th-codon activating lesion in H-*ras* and K-*ras*, respectively, and in a second dog a K-*ras* 61st-codon activating mutation and

TABLE 2. Second-Exon *ras* Gene Analysis of Tumors from Radiation-Exposed Animals

Exposed Animal	Tissue Type	*ras* Gene	Codon[(a)]	Codon Change
Whole-body gamma radiation-exposed dog	Spleen	K-*ras* N-*ras*	64 72	TAC → CAC ATG → ATA
Whole-body gamma radiation-exposed dog	Spleen	K-*ras*	73	AGG → AGA
Plutonium-exposed dog	Lung	K-*ras*	61 63 64 67	CAA → CGA GAG → GCG TAC → TTC ATG → ACG
Plutonium-exposed dog	Normal spleen	N-*ras*	55 70 74	ATA → CTA CAA → CGA ACA → TCA
Radon-exposed rat	Lung	H-*ras*	62 62 62 62	GAA → GAT GAA → GAT GAA → GAT GAA → GAT

(a) Vertical bars indicate that the lesions occurred in the same animal.

additional changes at codons 63, 64, and 67 were observed. We also found N-*ras* mutations at codons 55, 70, and 74 in an apparently normal spleen from a plutonium-exposed dog; these additional mutations may have been associated with the age of this animal or resulted from undetected chronic disease. Finally, two lung tumors from rats exposed to inhaled plutonium yielded a 12th-codon mutation in one of the tumors.

Analyses of these radiation-induced tumors have identified a wide variety of *ras* mutations, considering the small number of tumors studied. Thus far, however, no consistent pattern of mutations specific to radiation-induced tumors has emerged.

References Cited

Aaronson, S. A. 1991. Growth factors and cancer. *Science* 254:1146-1152.

Ainsworth, P. J., L. C. Surh, and M. B. Coulter-Mackie. 1991. Diagnostic single strand conformational polymorphism (SSCP): A simplified non-radioisotopic method as applied to a Tay-Sachs B1 variant. *Nucleic Acids Res.* 19:405-406.

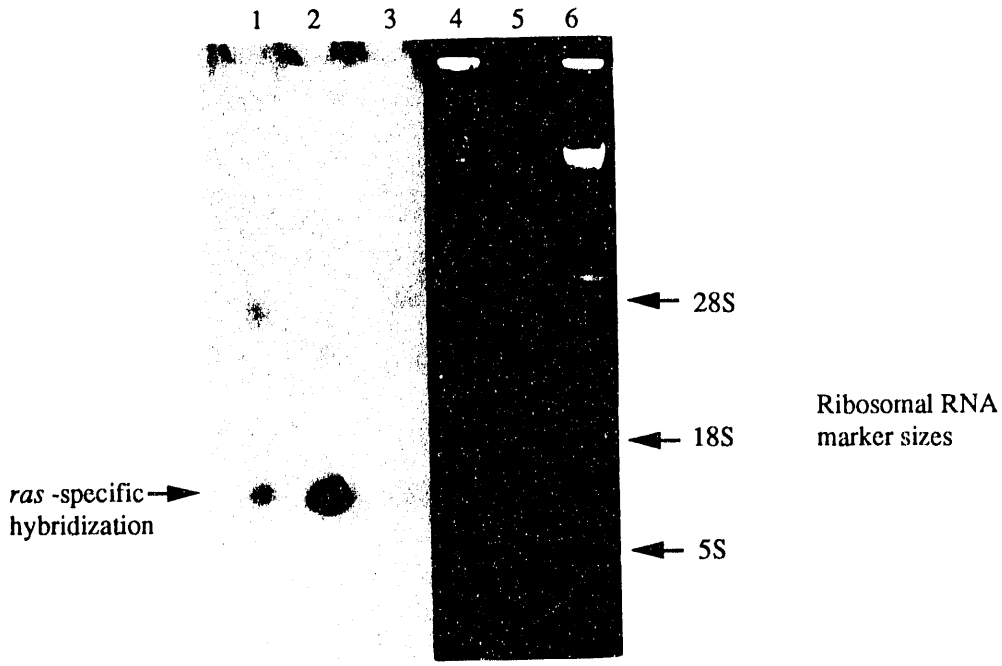

FIGURE 2. Northern Blot Analysis of Total RNA from Normal and Malignant Lymphoma Tumorous Spleen Tissue Isolated from Plutonium-Exposed Dogs. Right: Photograph of total cellular RNA electrophoresed on 2% agarose/urea gel. Left: Nitrocellulose northern transfer autoradiograph of RNA hybridized with [^{32}P]-labeled *ras* probe. Lanes 1 and 2, duplicate tumor samples of differing RNA concentration; lane 3, control of total cellular RNA from normal spleen. Lanes 4, 5, and 6 in gel photograph (right side of figure) correspond to lanes 1, 2, and 3, respectively, of northern blot autoradiograph (left side of figure).

Barbacid, M. 1987. *ras* genes. *Annu. Rev Biochem.* 56:779-827.

Buss, J. E., M. P. Kamps, and B. M. Sefton. 1984. Myristic acid is attached to the transforming protein of Rous sarcoma virus during or immediately after synthesis and is present in both soluble and membrane-bound forms of the protein. *Mol. Cell. Biol.* 4:2697-2704.

Hall, A. 1992. Signal transduction through small GTPases–A tale of two GAPs. *Cell* 69:38-391.

Landschultz, W. H., P. F. Johnson, and S. L. McKnight. 1988. The leucine zipper: A hypothetical structure common to a new class of DNA binding proteins. *Science* 240: 1759-1764.

Thacker, J. 1985. The molecular nature of mutations in cultured mammalian cells. A review. *Mutat. Res.* 150:431-442.

Thacker, J., and R. Cox. 1983. The relationship between specific chromosome aberrations and radiation-induced mutations in cultured mammalian cells. In: *Radiation-Induced Chromosome Damage in Man*, T. Ishihara and M. S. Sasaki, eds., pp. 235-275. Liss, New York.

Weinberg, R. A. 1991. Tumor suppressor genes. *Science* 254:1138-1145.

Mutation of DNA Targets

Principal Investigator: *R. P. Schneider*

Other Investigators: *J. E. Hulla and G. L. Stiegler*

This project is testing the hypothesis that inactivation of tumor suppressor genes is a common mechanism of radiation carcinogenesis. Thus far, we have concentrated our work on characterizing the dog retinoblastoma susceptibility (Rb) and the rat p53 genes. We previously isolated most of the dog Rb cDNA, and this year have defined the structure of the rat p53 gene, including the intron sequences near splice junctions. The rat gene lacks one intron that occurs in the human and mouse gene. The sizes of the exons, introns, and splice junctions are similar for all species. We will now evaluate radon-induced rat lung tumors for mutations of p53 in polymerase chain reaction-amplified DNA. The dog Rb cDNA will be used as probe in northern analysis of dog Rb mRNA in plutonium-induced bone and lung cancer cultured cells and in gamma radiation-induced leukemia.

Mechanistic data are needed to predict the results of exposure to low doses of radiation and chemicals. The information available from epidemiologic data and life-span animal experiments cannot be extrapolated to these low doses with confidence. The principal health effect of chronic, low-dose exposure to ionizing radiation and chemicals is cancer; cancer apparently is caused by mutations or changes in the expression of oncogenes, tumor suppressor genes, or both. Knowledge of which genes are altered, and the nature of such changes, is central to understanding the mechanisms of radiation carcinogenesis.

Tumor Suppressor Genes

Tumor suppressor genes were identified by analyses of the genetics of inherited forms of cancer, chromosomal aberrations, and polymorphic DNA markers of homozygosity. This class of genes is defined by functional criteria; that is, loss of normal function leads to neoplastic growth deregulation. About six of these genes have been described, and one or another has been found to be altered in many types of human cancer. We suspect that inactivation of tumor suppressor genes is a common mechanism of radiation carcinogenesis, because deletions are known to be a major component of genetic damage from ionizing radiation. We are testing this hypothesis by studying, in tumors from animals exposed to ionizing radiation, the two tumor suppressor genes that have been most completely described, the retinoblastoma susceptibility (Rb) and p53 genes.

Defects in the Rb gene are found in retinoblastoma, osteosarcoma, small-cell cancer of the lung (SCCL), some non-small-cell lung cancer, and in breast and bladder cancers in humans. The p53 gene has been found to be altered in almost all types of human cancers. The p53 gene differs from the recessive nature of Rb because mutations can confer a dominant phenotypic expression pattern. Some mutated forms of p53 protein can complex the wild-type gene product from the other nonmutated allele. The gene products of both these genes act in the nucleus, probably by interacting with transcription regulatory factors, and both gene products are inactivated by viral oncoproteins. In infected cells, the viral proteins complex the Rb and p53 gene products and thereby effectively inactivate the genes.

Approach

Our approach is to examine p53 and Rb genes in tumor tissue from life-span animal experiments at PNL and other DOE laboratories. We have a small number of frozen dog lung and bone tumors induced by exposure to inhaled plutonium and radon. We also have a large number of plutonium-induced rat and dog lung tumors that have been fixed in formalin and embedded in paraffin. Myelogenous leukemia cells, from dogs

that were chronically exposed to x rays and gamma radiation at Argonne National Laboratory, are also available. When tissue of sufficient quality is available, we plan to analyze Rb and p53 gene expression by analysis of their mRNA using polymerase chain reaction (PCR) and northern blot methods; the fixed and embedded tissues do not have mRNA or large molecular weight DNA for northern or Southern analysis. Thus, PCR is being used to amplify specific regions of these genes from fixed and embedded tissue for analysis by gel electrophoresis and methods that detect mutations and deletions by changes in electrophoretic mobility.

Preliminary characterization of these genes was required so that we could analyze the dog and rat tumors, because neither the gene structure nor the cDNA sequence of dog p53 or Rb gene is known. The rat p53 cDNA sequence has been published, but its gene structure has not been described. We have therefore focused our efforts on obtaining the location and sequence of splice junctions in rat p53 and generation of DNA probes for most of the Rb cDNA. These data are also of more general interest concerning the relatedness of the genes between species and will aid cancer research with animal models. For example, information describing the p53 structure and the sequences near its splice junctions can be used by other investigators to study the role of this important gene in rats.

Because the Rb gene is commonly defective in human osteosarcomas and some lung tumors, and because dogs exposed to inhaled plutonium developed this form of cancer, we focused on preparing reagents for analysis of the dog Rb gene. We now have generated fragments that include 70% of the coding region of the gene. These gene fragments will serve as probes for northern blots and will provide a means to search for mutations and deletions in experiments planned for FY93.

We previously deduced a tentative structure of the rat p53 gene based on sizes and locations of introns within the mouse and human p53 genes. PCR assays made apparent the occurrence of a p53 pseudogene within the rat genome. We found that the pseudogene is a "processed" sequence; it lacks introns and retains close homology to the cDNA. This year, we completed the definition of the gene structure of the rat p53 gene by using PCR to generate the sequencing templates.

Results

We amplified rat p53 fragments that included each intervening sequence of the gene structure deduced from that of the mouse and human genes. For most PCR assays, two major amplicons were apparent when cDNA primers flanked more than one exon. However when cDNA primers flanking exons 6 and 7 were used, only one amplicon was apparent (Figure 1, lane 7). Each solid line above the gene and below the pseudogene graphics in Figure 1 represents an amplification product that was identified by Southern blotting and probing with cDNA sequences located between the primers.

Using cDNA primers and intron primers, we amplified the region of exon 5 through exon 8 of the deduced structure. As expected, the intron primers yielded only one product amplified from the gene; the cDNA primers yielded both gene and pseudogene amplicons. The sizes of the gene amplicons were consistent with a sequence lacking the 390 bases of intron 6 present in the mouse gene. We sequenced this region directly from PCR products. The templates we isolated were completely homologous with cDNA sequences corresponding to exons 6 and 7 in our deduced gene structure. No intervening sequence occurred between the sequence corresponding to these two exon regions. Although the size and structure of the single amplicon 6 to amplicon 7 sequence is consistent with a product generated from a processed pseudogene template, its sequence does not vary from that of the cDNA, as do pseudogenes. Also, amplification fragments generated using primers that flank exons 5 and 8 or introns 5 and 8 of the deduced structure do not contain intervening sequences between exons 6 and 7, but do contain intron 5 sequences contiguous with the exon 6 to exon 7 region, showing that it is not a pseudogene.

To provide the information needed to synthesize PCR primers for analysis of the gene, we ascertained the intron sequences within 25 bp of each

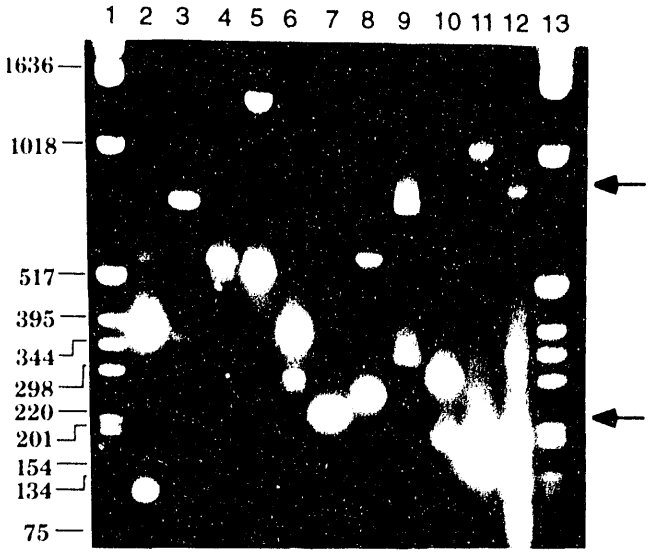

FIGURE 1. Two Major Products Are Amplified Using Primers That Flank More Than One Exon of the Rat p53 Gene. Primers used correspond to cDNA sequences. Regions of gene and pseudo-gene amplified are indicated by lines on graphic representation of deduced structures. Amplification products were electrophoretically separated on 1.5% agarose gel and stained with ethidium bromide. Arrows indicate amplicons in lane 12 that were determined by Southern blot to contain sequences corresponding to exons 10 and 11. Table 1 outlines contents of each lane and expected and observed sizes of amplified fragments. Lanes 1 and 13 contain molecular size markers. Predicted molecular sizes are based on structures of mouse and human p53 genes; sizes are given in numbers of bases, and fragment sizes observed are estimates based on resclution of markers.

Lane	Primers: Flank Exons	Gene Size: Predicted/ Observed	Pseudogene Size: Predicted/ Observed
2	2 and 3	375/380	105/110
3	2 and 4	729/740	369/375
4	2 and 5	1692/1700	552/540
5	4 and 5	1237/1250	457/490
6	5 and 6	397/390	317/310
7	6 and 7	613/220	223/220
8	7 and 8	566/550	246/250
9	7 and 9	741/750	341/340
10	8 and 9	310/320	230/225
11	9 and 10	1013/1020	183/180
12	10 and 11	890/900	190/210

slice junction (Figure 2). The splice junctions downstream of exon 2 were sequenced directly from PCR and from cloned amplification products. The intron 5 sequence adjacent to exon 5 was polymorphic (Figure 2); this was confirmed by sequencing four different amplification products directly and four clones of a fifth one. Each of two sequences contained a single base not present in the other. The sizes of introns 2 through 9 shown in Figure 2 were deduced by comparing sizes of amplicons generated from the p53 gene and processed pseudogene(s) (also see Figure 1).

The two splice junctions upstream from exon 2 were sequenced from a clone of genomic p53 isolated from a rat genomic library. To estimate the size of intron 1, we used cDNA primers from exons 1 and 2 and amplified a 6.5-kb fragment from the lambda clone. The first intron was estimated to be 6.2 kb by subtracting the lengths of exons 1 and 2. The identity of the 6.5-kb fragment was confirmed by blotting and probing individually with cDNA probes specific for exon 1 and exon 2 (Figure 3).

With one exception, cDNA primers flanking more than 1 exon generate amplification products from the gene and at least one processed pseudogene template (see Figure 1). The sizes of these fragments are consistent with the gene and pseudogene structures deduced from the human and mouse gene structures. The sizes of the introns 1 through 9 (Figure 4) were estimated by subtracting the length of exon sequence flanked by the primers from the size of the fragment observed. These were consistent with the sizes of introns in the other two species, except for the single amplicon yielded from cDNA primers flanking exons 6 and 7. The rat p53 gene differs from the mouse, human, and *Xenopus* gene structures in that it has only 10 exons and 9 introns. Despite this difference, the conservation of the gene structure through evolution is remarkable. The sizes of the exons, introns, and locations of splice junctions are similar for all species for which the gene structures are defined. The intron sequences reported here provide primer sites for amplifying selected regions of the rat p53 gene (but not the pseudogene) for detection of mutations within all the exon sequences.

The intron sequences have been used to synthesize a set of primers within introns for amplifying the exons of the rat p53 gene. These primers also have RNA polymerase promoters 5' to the intron sequences. We will amplify the desired exons from radon-induced rat lung tumors and

14
ACTGG:GTAAGTAACTGAGCGTGATGAGTCC...*intron 1 6,200 bp*...CAGTACACAGATGTTCTCTCTGCAG:ATAAC

97
AAACT:GTGAGTGGATCTTACAGGGCCCCTG...*intron 2 260 bp*...CTAATTCTCTGCTCTTGTTCTCCAG:TCTTC

119
TTCTG:GTAAGGAGCCGGGCAAGAGGGGACT...*intron 3 90 bp*...AGGTTCTTCTTTGGCCCATCCACAG:CCCAC

392
GCACG:GTCAGTGGGCCTGAAGAGTTGCTTT...*intron 4 780 bp*...TTTGATTCTTTCTCCTCTCCTACAG:TGACG

576
TGACG:GTGAGCACTGGGCACTGC•TGTGGGG...*intron 5 80 bp*...GCCTCTGACTTATTCTTGCTCTTAG:GCCTG
• C

799
TCCAG:GTAGGAAGCTGTGTGCCAGGTTGGG...*intron 6 320 bp*...CTGTGCCTCCTCTTGTCCCGGGTAG:TGGGA

936
GAGAG:GTGAGCAGGCAGGACAAAGAAGGTG...*intron 7 80 bp*...CACCCCTTGCTCTCTCCTTCCATAG:CACTG

1010
TTAAG:GTACCAAGGTTATTATTGGATTAATA...*intron 8 830 bp*...CTGTCCTACTTCATCCTTGCTACAG:ATCCG

1117
TCCAG:GTGAGTGACCTGGGGCAGCGCCTGG...*intron 9 700 bp*...TCCCTCCCTTTTCTGTATTCCTATAG:CTACC

FIGURE 2. Sequences Adjacent to Splice Sites and Sizes of Intervening Sequences Within Rat p53 Gene. Splice junctions between exon and intron sequences are indicated with colons. Locations of splice junctions in rat cDNA are shown on the left of each line. Sequence polymorphism was detected in Intron 5, adjacent to exon 5. The second intron 5 sequence was homologous to that shown, except where indicated below the line. Each polymorphic sequence contained a single deletion, indicated by a dot.

make T7 (sense) and SP6 (antisense) RNA transcripts of the exons. We will then use these RNA fragments in electrophoresis gels that can detect mutations by virtue of electrophoretic mobility changes. Mutations of p53 will be defined by sequence analysis of the exons that contain them. We plan to identify a spectrum of mutations in p53 in the radon-induced tumors.

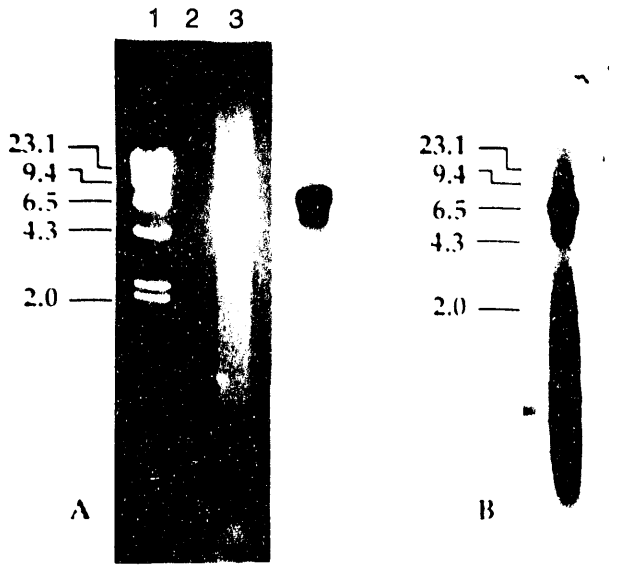

FIGURE 3. Southern Blot Analysis of Amplicon Generated with cDNA Primers Flanking Exons 1 and 2 of Rat p53 Gene. **A.** Lane 1 contains molecular weight markers; lane 2, 10 μl of amplification reaction; lane 3, autoradiograph of sample shown in lane 1 after blotting and probing with exon 1-specific oligonucleotide. **B.** Second autoradiograph of PCR sample that was electrophoretically separated, blotted, and probed with exon 2-specific oligonucleotide.

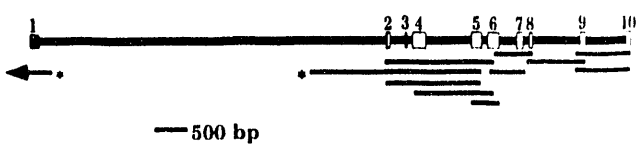

FIGURE 4. Newly Defined Structure of Rat p53 Gene and Representation of Cloned Fragments Used for Determining Intron Sequences Adjacent to Splice Junctions. Noncoding regions of cDNA sequence are shown as solid boxes; open boxes represent coding exon sequences. The PCR template used to generate two clones (asterisk, *) was isolated from rat genomic library; all other PCR template DNA was isolated from fresh rat liver.

Genotoxicity of Inhaled Energy Effluents

Principal Investigator: *A. L. Brooks*

Other Investigators: *W. K. Yang,[a] K. E. McDonald, C. Mitchell, and G. E. Dagle*

The interaction of cellular and genetic damage induced by low- and high-LET radiation damage with that produced by chemicals is being studied to identify health risks associated with the nuclear industry and nuclear waste sites. Mechanistic studies are in progress on the induction of chromosome damage and the role of altered oncogenes in the induction of cancer. Using fluorescent *in situ* hybridization (FISH) techniques, radiation-induced translocations and deletions were seen to have the same dose-response relationships, suggesting that a similar number of "hits" were involved in their induction.

Research on the potential interaction of mutated oncogenes with ^{239}Pu and the organic solvent CCl_4 in the production of liver cancer showed an initial increase in the frequency of liver nodules induced by the combined exposures relative to those exposed to either agent alone. Analysis of early liver nodules indicated that the cells in the nodules expressed either K-*ras* or *neo* and were clonal in origin. Survival was decreased and tumor frequency increased in animals that received the combined exposure relative to those exposed to single insults.

Our research uses both *in vivo* and *in vitro* cellular techniques to investigate potential toxicological interactions between effects produced by radiation and chemicals in the work environment. Several problems are associated with defining health risks associated with mixed wastes in the nuclear industry. First, the site of action and responses may differ for each insult. Second, the dose-exposure terms for radiation and chemicals are hard to express in common units. Finally, it is difficult to convert exposure to biologically significant dose for chemicals and to relate this dose to a measured response.

These factors complicate the comparison of risk from radiation with risk from exposure to carcinogenic chemicals and determination of how these risks interact in combined exposure. Another complication is that damage from two or more carcinogens may be additive, synergistic, or antagonistic, depending on the concentration, time of exposure, biological site of attack, and endpoint evaluated. The important problem of calculating risks for combined exposures requires a range of approaches. Mechanistic understanding is required to identify areas of potential concern from combined exposures.

The relationships between combined exposures and cellular responses, when measured as cell killing, induction of micronuclei, sister chromatid exchanges, chromosome aberrations, and changes in cell cycle, provide preliminary information on potential interactions. The role of chromosome aberrations during cancer induction is well defined. It is also known that stable chromosome aberrations that can survive cell division can be induced by radiation and that these types of abnormalities are present during the progression of cells toward cancer. Information about the mechanisms involved in the production of these aberrations and how well they survive in a dividing cell population is important in understanding the carcinogenic process.

The influence of mutated oncogenes, whether present because of genetic predisposition or induced by environmental insults, can also result in changes that are significant in the carcinogenic progression of cells. The interaction of such changes with those induced by environmental pollution, such as associated with nuclear waste cleanup, needs to be defined.

(a) Oak Ridge National Laboratory, Oak Ridge, Tennessee.

Results and Discussion

Mechanisms Involved in Chromosome Aberration Production

These studies were conducted with A_L cells, a cell line with a single human chromosome 11 in a Chinese hamster background. By using total human genomic probe (Oncore, Inc., Gaithersburg, MD) it is possible to "paint" the human chromosome as shown in Figure 1A. This technique permits following radiation-induced changes in this chromosome very accurately (Figure 1B). Cells were exposed to 0.0, 2.0, 4.0, 8.0, and 12.0 Gy and harvested for chromosome evaluation 24 hr later when most of the cells would have developed chromosome-type aberrations. The frequency, distribution, and types of aberrations involving the human chromosome were evaluated for 100 cells at each dose level.

The dose-response relationship for the induction of both deletions and symmetrical chromosome translocations is shown in Figure 2. This relationship indicates that the induction of these two types of abnormalities follows similar kinetics, suggesting that similar mechanisms are involved in their production.

New information on the basic mechanisms involved in the induction of chromosome damage and cancer is applicable to the evaluation of the health risks of occupational radiation exposure, radiation accidents, and nuclear waste-site cleanup.

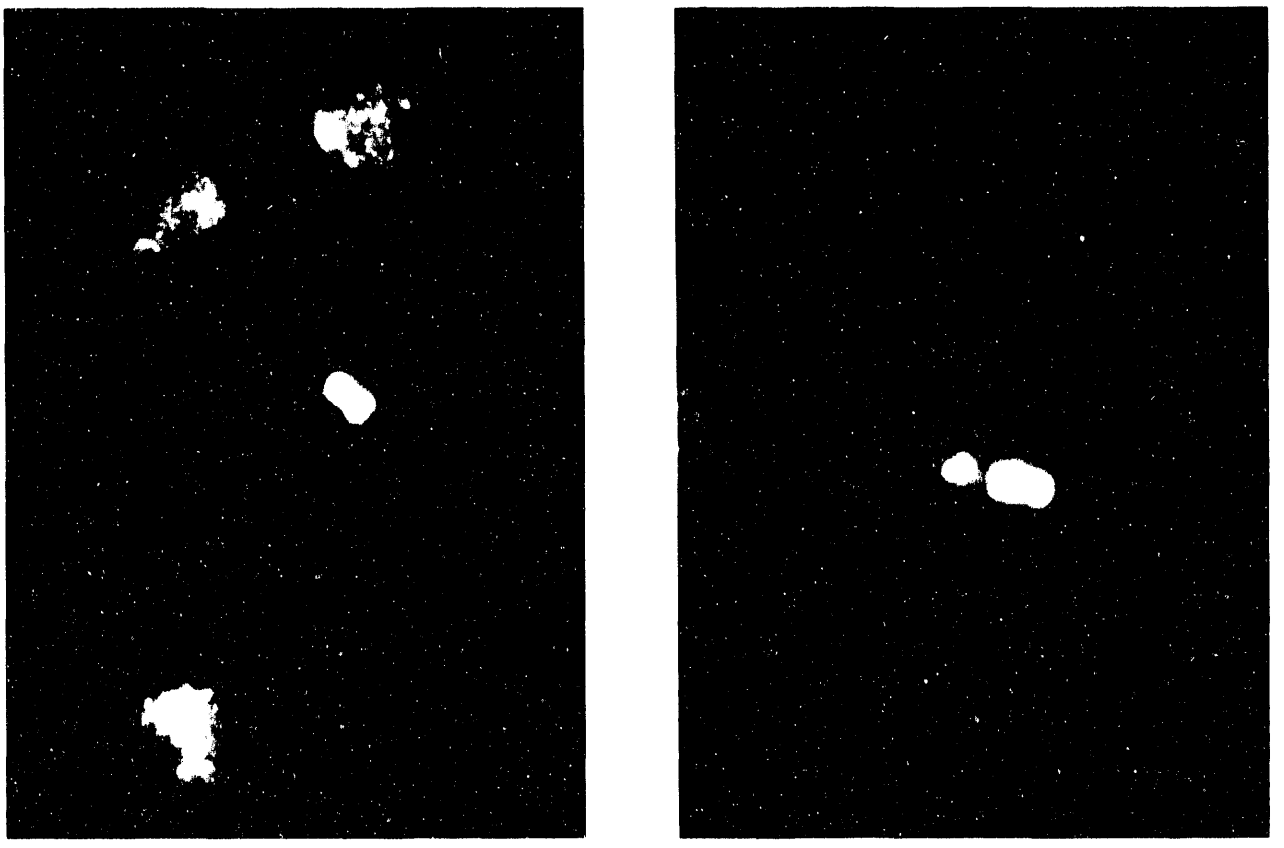

1A 1B

FIGURE 1A and 1B. Karyotype of A_L Cells: Human Chromosome Stained Using Fluorescent *in Situ* Hybridization (FISH) Techniques.

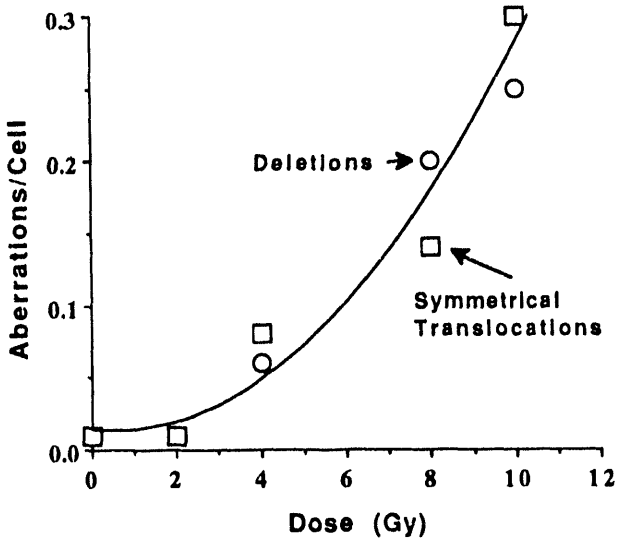

FIGURE 2. Comparison of Radiation-Induced Deletions and Symmetrical Translocations in Chromosome 11 Using FISH-Stained A_L Cells.

Combined Effects of Oncogenes and Plutonium

The experimental design for the study is shown in Table 1.

B_6 C_3 F_1 mice were injected with 27 Bq ^{239}Pu/g body weight either 30 days before or 30 days after the injection of oncogenes in a retroviral vector. This treatment caused an initial liver burden of 110 Bq/g, which was rapidly cleared and resulted in a changing dose rate to the liver (Figure 3). The dose rate was estimated to be 8 mGy/day at day 1 and to decrease to 1.8 mGy/day by 50 days after injection. The total radiation dose to the liver was estimated to be 0.37 Gy by 330 days when the first animals were evaluated for the induction of nodules and tumors. The dose rate had decreased to 0.2 mGy/day at this time and, assuming a constant retention, was calculated to produce an additional 0.058 Gy during the remainder of the study.

The oncogene used in this study was the mutated Ki-v-*ras* gene placed in a retroviral vector. The *neo* gene was placed in the same vector and served as a control. To ensure proper incorporation of the genes into the liver, mice were gavaged with 0.15 ml of 20% CCl_4 in corn oil 24 hours before the oncogenes were given. The CCl_4 caused liver cell necrosis and cell proliferation, thus aiding in the incorporation of retroviral vectors and oncogenes into liver cells.

TABLE 1. Experimental Design: Evaluation of the Effect of Interaction of Oncogenes and Alpha Radiation on Survival and Liver Cancer

Female Mice		
Group 1	Plutonium, 30 days; CCl_4, 1 day; *ras* oncogene	30 mice
Group 2	Plutonium, 30 days; CCl_4, 1 day; *neo* oncogene	30 mice
Group 3	CCl_4, 1 day; *ras* oncogene; 30 days, plutonium	30 mice
Group 4	CCl_4, 1 day; *neo* oncogene; 30 days, plutonium	20 mice
Group 5	CCl_4, 1 day; *ras* oncogene	30 mice
Group 6	CCl_4, 1 day; *neo* oncogene	20 mice
Group 7	Corn oil, 1 day; plutonium	20 mice
Group 8	Corn-oil-only controls	20 mice
Group 9	Cage controls	20 mice
Male Mice		
Group 10	CCl_4, 1 day; *ras* oncogene; 30 days, plutonium	20 mice
Group 11	CCl_4, 1 day; *ras* oncogene	20 mice

At 323, 448, and 629 days after the exposure, 33, 54, and 52 animals, respectively, were sacrificed and evaluated for pathological changes. Animals that died were also studied. Nodules from animals sacrificed at 323 days after the start of the study have been analyzed for the presence of the mutated K-v-*ras* oncogene and the *neo* gene. All the liver nodules expressed either the ras or the *neo* oncogene, but the normal tissue did not express these genes, suggesting the nodules were clonal in nature and that the genes were incorporated in the nodule at an early time.

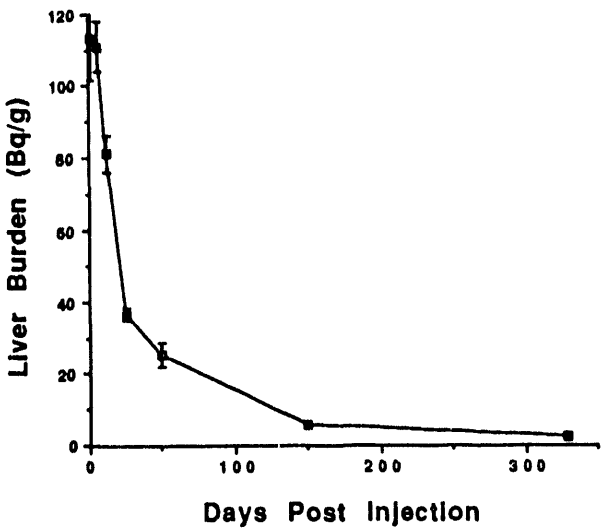

FIGURE 3. Retention of ^{239}Pu Citrate in Liver of $B_6C_3F_1$ Mice.

Survival was evaluated using a life table method to account for animals removed from the study for molecular and pathological evaluation (Figure 4A and 4B). In Figure 4A, nonexposed animals, animals exposed to only one agent, and animals exposed to CCl_4 plus the oncogenes are plotted as a function of time after the start of the study. These data show little life shortening relative to controls with any of the individual exposure schedules but some increase in mortality at long times after exposure. In Figure 4B, survival is followed in the groups that had combined exposures to CCl_4, ^{239}Pu, and oncogenes. These data illustrate an increase in mortality in these animals, with combined exposure to *ras*, CCl_4, and ^{239}Pu being the most effective insult in producing life shortening. A minor effect of the sequence of exposure on survival was suggested; administration of the oncogene before plutonium injection caused greater life shortening than when the sequence was reversed. The mutated oncogene thus seems to initiate changes that are better expressed in animals that are exposed to plutonium.

The pathological results of these studies are summarized in Table 2. Evaluation of the nodules demonstrated that at sacrifice at 323 days no nodules were classified as carcinomas or sarcomas. As the mice became older, the incidence of liver tumors and nodules increased. Table 2 demonstrates that in animals exposed to CCl_4, *ras*, *neo*, or to ^{239}Pu only, had a single hepatocellular carcinoma in 66 animals, about 1.5%. Animals exposed to CCl_4, ^{239}Pu, and the oncogenes demonstrated nine hepatocellular carcinomas in 89 animals or 10%, suggesting that combined exposure caused a sevenfold increase in tumor frequency. No tumors were observed in the 35 cage control animals or those that received corn oil only; no bile duct tumors were observed. Three osteosarcomas were observed, one in an animal that received ^{239}Pu alone and two with ^{239}Pu plus *neo* oncogene.

A similar evaluation showed the presence of liver nodules in 65%, 33%, and 23% of the animals following combined treatment, single treatment, and controls, respectively. Animals receiving either ^{239}Pu (7/17) or *ras* (13/25) singly showed elevated frequency of liver nodules but had only 0 and 1 liver tumor, respectively. Such results suggest that there are multiple steps during the carcinogenic process in liver and that either ^{239}Pu or the *ras* oncogene can cause the cells to progress to the stage at which liver nodules develop. Using the current experimental design, it seems that induction of liver tumors is more effective when both insults are involved, thus providing more of the essential steps toward cancer development. For example, the radiation dose from plutonium exposure was calculated to have produced chromosome aberrations in about 10% of the liver cells. Such damage could cause loss of tumor suppressor genes and cell killing, both of which have been shown to increase cell proliferation. The experiments also suggest that the presence of the *ras* gene at the time of plutonium injection is more effective in producing life shortening but that sequence of exposure does not affect the development of cancer. However, the number of tumors observed is so small that these observations require further additional experimentation.

This line of research helps provide a mechanistic foundation on which the role of the interaction of radiation, oncogenes, and chemicals can be defined in the production of chromosome and cellular damage. Such data provide a background against which health risks in the nuclear industry and during nuclear waste site cleanup may be evaluated.

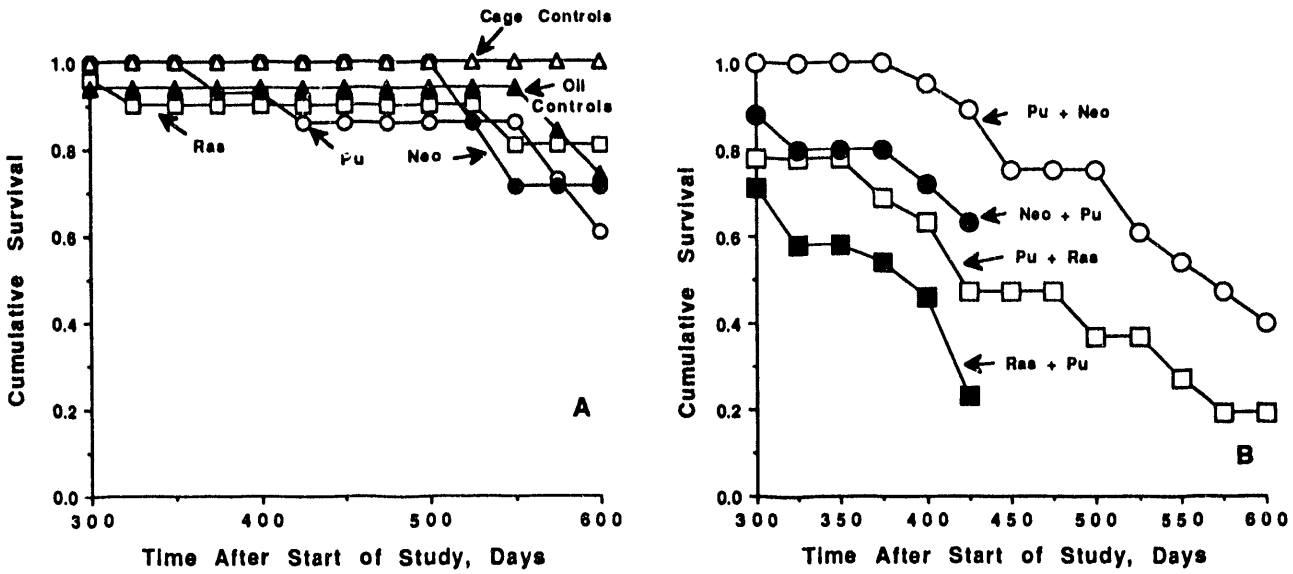

FIGURE 4. A. Life Shortening for Control and $B_6C_3F_1$ Mice Exposed to a Single Insult (K-*ras*, *neo*, or ^{239} Pu). No significant life shortening occurred. **B.** Life Shortening for $B_6C_3F_1$ Mice Exposed to Combined Insults from ^{239} Pu + *neo* or ^{239} Pu + K-*ras*. Significant life shortening occurred regardless of sequence of exposure.

TABLE 2. Histopathological Observations in $B_6C_3F_1$ Mice Exposed to Oncogenes and ^{239}Pu

		Death, day 7-323			Sacrifice, day 323			Death, day 332-448			Sacrifice, day 448			Death, day 448-629			Sacrifice, day 629			Lost to Follow-up	Histopathology		
Experimental Treatment	M	N	C	T	N	C	T	N	C	T	N	C	T	N	C	T	N	C	T		N	C	T
Females																							
Pu + *ras* + CCl_4	30	0	0	3	2	0	4	3	0	5	6	1	6	2	1	2	1	0	1	9	14	2	21
Pu + *neo* + CCl_4	30	0	0	0	1	0	4	0	0	2	3	0	6	1	0	3	6	2	6	9	11	2	21
ras + Pu + CCl_4	30	2	1	4	3	0	3	7	2	7	6	0	6	1	0	1	0	0	0	9	19	3	21
neo + Pu + CCl_4	20	0	0	1	0	0	3	2	0	4	4	0	8	0	0	0	0	0	0	4	6	0	16
ras + CCl_4	30	2	0	2	6	0	7	1	0	1	2	0	6	1	0	1	1	1	8	5	13	1	25
neo + CCl_4	20	0	0	0	0	0	4	0	0	0	1	0	6	0	0	1	1	0	5	4	2	0	16
Pu	20	0	0	0	0	0	4	0	0	2	3	0	6	0	0	0	4	0	5	3	7	0	17
Corn oil	20	0	0	1	0	0	2	0	0	0	1	0	4	0	0	0	3	0	8	5	4	0	15
Cage control	20	0	0	0	0	0	2	0	0	0	0	0	6	0	0	0	4	0	12	0	4	0	20
Males																							
ras + Pu + CCl_4	20	0	0	0	3	0	4							5	2	6				10	8	2	10
ras + CCl_4	20	0	0	0	5	0	6							2	0	2				12	7	0	8

Key: M = Total number of mice
N = Number with nodules
C = Number with cancer
T = Total dead.

Molecular Events During Tumor Initiation

Principal Investigator: *D. L. Springer*

Other Investigators: *D. B. Mann, B. D. Thrall, and C. G. Edmonds*

Benzo[a]pyrene diolepoxide (BPDE), a prototype polycyclic aromatic hydrocarbon, forms a number of covalent modifications to DNA that impede the progression of polymerases. By taking advantage of these polymerase blocks, we determined the frequency and location of adducts on the 5S rRNA gene. Results from studies with several polymerases and the 3′→5′ exonuclease activity of T4 DNA polymerase, using naked DNA that was modified with BPDE, demonstrated that regions rich in deoxyguanine residues are more heavily modified than other regions. Because cellular DNA is associated with a variety of proteins, we developed methods to reconstitute supercoiled pGEM-5S plasmid with core histones. This preparation, which mimics a domain of cellular chromatin, resisted restriction enzyme digestion in the region of the 5S rRNA gene where a nucleosome is expected to form, confirming the presence of this nucleosome. When this reconstituted plasmid was incubated with (±)-anti-BPDE, less binding was observed on reconstituted DNA than naked plasmid, suggesting that interaction between the DNA and histones protected the DNA from BPDE modification. In addition, when a site-specific, BPDE-modified oligomer was incubated with a polymerase, a significant amount of synthesis past the lesion was observed. The position of polymerase blockage and the amount of translesional synthesis varied with the polymerase used. Other efforts were directed at preparing and characterizing core histone from cells grown under conditions that produce modified histones. Characterization of these preparations by electrospray ionization mass spectrometry demonstrated covalent modification (acetylation) of histone H4. Future studies will involve reconstitution of the pGEM-5S plasmid with modified core histones to determine whether accessibility of BPDE to the DNA is altered.

It is well established that damage to DNA, whether from radiation or from chemical adducts, is a necessary, but usually insufficient, requirement for tumorigenesis. Studies with the reactive metabolite of benzo[a]pyrene (i.e., benzo[a]pyrene diolepoxide, BPDE) have demonstrated that BPDE adduction yields a number of stereoisomeric forms and that most of these modifications are to the exocyclic amino group of deoxyguanine (Straub et al. 1977). These modifications impede the progression of DNA and RNA polymerases. We have taken advantage of these blockages to map the location of adducts on the 5S rRNA gene (Thrall et al. 1992). Results from this work demonstrated that regions rich in dG residues were preferred binding sites when naked DNA was modified by BPDE.

Under cellular conditions DNA is closely associated with a number of proteins including histones. These specific interactions function to condense the DNA into chromatin through several types of bonding including hydrophobic interaction, hydrogen and ionic bonds. Transcription of genes is regulated, at least in part, by modification of histones through acetylation, methylation, phosphorylation, and ADP ribosylation. The modification that is best understood is acetylation of basic amino acids, which decreases the number of ionic bonds between the phosphodiester backbone and protonated amine groups located primarily on the N terminus of core histones. These modifications function to weaken the interaction between DNA and core histone and allow enzymes access to the DNA. Portions of the DNA that are actively transcribed are usually in the more open conformation and may also be more accessible to damage from radiation or chemicals.

These effects suggested that we conduct studies to determine whether adduct locations and frequencies of adduction are altered in plasmid DNA reassembled into nucleosomes (reconstituted) relative to naked DNA. This report describes our results, including: (1) BPDE adduct maps for the

5S gene using the 3′ → 5′ exonuclease activity of T4 DNA polymerase, (2) characteristics of reconstituted plasmid using the gel mobility shift assay and restriction digestion, (3) translesional synthesis by DNA polymerases using site-specific BPDE-modified oligomers, and (4) electrospray ionization-mass spectroscopy (ESI-MS) characterization of acetylated histones.

Mapping of BPDE Adducts Using T4 (3′ → 5′) Exonuclease Activity

Plasmid (10 μg) adducted with BPDE was digested with *Eco*RI, dephosphorylated using calf intestinal phosphatase, and 5′-end-labeled with 75 μCi of [γ-^{32}P]-ATP using T4 polynucleotide kinase. After a second digestion with *Hin*dIII, which resulted in a 219-bp fragment containing the 5S rRNA gene with a 5′-labeled template strand, the fragment was purified on a 2% agarose gel. The 219-bp fragment was located on the gel by autoradiography and recovered by centrifugation through 0.45-μm cartridge filters (Rainin, Woburn, MA), with typical yields of 60% to 70%. Digestion with T4 DNA polymerase (3′ → 5′ exonuclease) was done as described by Gale et al. (1987). Digestion of BPDE-adducted DNA with T4 DNA polymerase (exonuclease) resulted in a fragment pattern very similar to a Sequenase ddGTP lane, but shifted 2 or 3 bases longer than the corresponding guanine (Figure 1).

Because most of the DNA fragments are reduced to short oligomers by the T4 digest, the samples were run through NENSORB columns before electrophoresis. This procedure, in addition to amplifying the banding pattern of the adducted samples, also dramatically amplifies the random (nonspecific) pattern in the nonadducted control. Figure 1 (lane 2) shows that the only fragments retained are those not digested to completion. Although the adducted sample had a banding pattern very similar to the G lane, it is apparent that the minor amount of DNA remaining after digestion of the nonadducted sample yielded a much different pattern with very little sequence specificity. Similar to previous mapping results (Thrall et al. 1992), there was a distinct bias for adduction of the 5' end of the poly $d(G)_8$ region

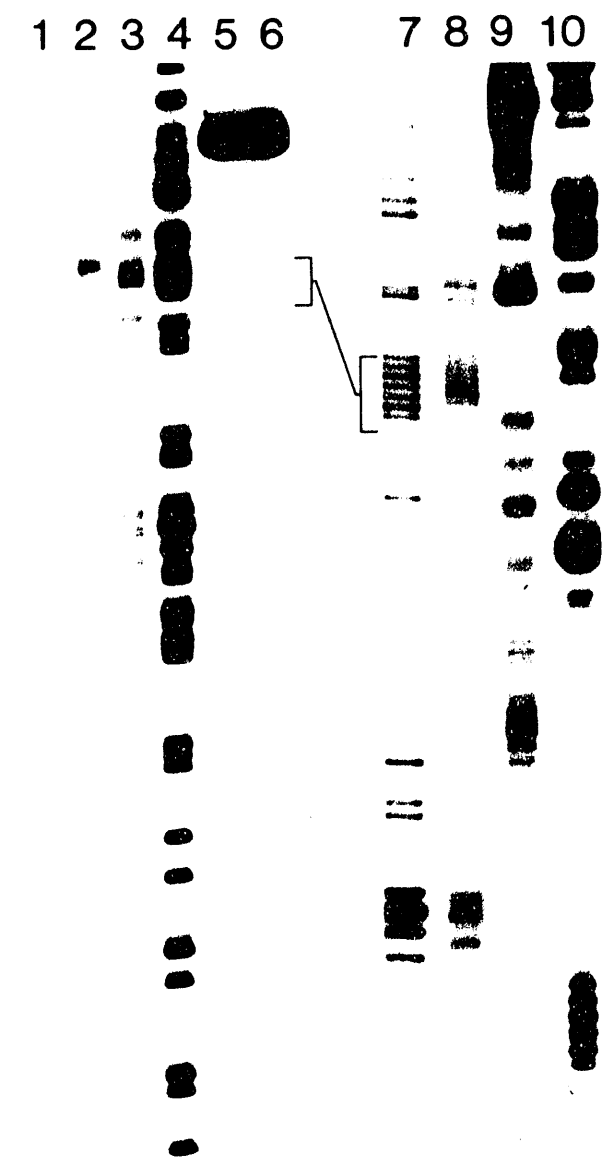

FIGURE 1. T4 DNA Polymerase (Exonuclease) Digestion Map of Adduct Locations in 219-bp Fragment as Determined by Exonuclease Digestion Scheme of Gale et al. (1987). Lane 1: Nonadducted sample digested with T4 polymerase without NENSORB column concentration but with 8-fold radioactivity loaded. Lanes 2 and 3: Nonadducted and BPDE-adducted samples, respectively, digested with T4 polymerase and concentrated with NENSORB. Lane 4: ddGTP Sequencing. Lanes 5 and 6: Nonadducted and BPDE-adducted samples, respectively, not digested with T4 exonuclease. Lane 7: ddGTP Sequencing that corresponds to lane 2. Lane 8: Higher resolution map of BPDE-adducted sample. Lanes 9 and 10: BPDE-adducted and pyrimidine dimers, respectively, show digestive patterns of similar damage. BPDE, benzo[a]-pyrene diolepoxide; GTP, guanosine triphosphate.

(lanes 3-4 and 7-8). Samples that were not digested with T4 polymerase (lanes 5-6) show that nearly all the radioactivity was associated with the 219-bp fragment.

Further comparison of the T4 polymerase-exonuclease digestion pattern was made between the 219-bp DNA fragment containing BPDE adducts and pyrimidine dimers induced by 254-nm UV irradiation. BPDE binds almost exclusively to purines (primarily guanine), and absorption of UV light forms predominantly cyclobutyl dimers at adjacent pyrimidines; the resulting digestion patterns are expected to be quite different. The digestion patterns shown in lanes 9 and 10 of Figure 1 demonstrate this difference, and the stops produced by these two different types of damage closely parallel the locations of guanines (BPDE) or pyrimidines (UV) in the sequence.

In DNA adducted with BPDE, we have found that the progression of both DNA and RNA polymerase, as well as a 3′→5′ exonuclease, was blocked. Such inhibition likely contributes to the cytotoxicity of BPDE and may be involved in its tumorigenic activities. An earlier study (Moore and Strauss 1979) in which primer extension analysis was used suggested that DNA polymerase I (Klenow fragment) was arrested at the base immediately preceding an adducted guanine. In our studies, cloned T7 DNA polymerase (Sequenase) was blocked either at, or one base preceding, an adducted guanine, or both; at the levels of modification used, very few blocks are seen at bases other than guanine (Thrall et al. 1992). Whether the blockage occurred at or one base preceding an adducted guanine varied between different sequences of DNA with no obvious predictable pattern. Different adduct conformations may explain the different positions of polymerase arrest. Energy minimization studies suggest that DNA lesions produced from different enantiomeric forms of BPDE have different spatial orientations. Adducts from (+)-*anti*-BPDE reside predominantly at the N-2 position of guanine in the minor groove, with the pyrenyl moiety thought to be directed toward the 5′ end of the modified strand; however, adducts from (-)-*anti*-BPDE show two possible structures (major and minor groove), both placing the pyrenyl moiety facing the 3′ end of the modified strand (Singh et al. 1991). Such conformational differences may explain the differences in position of the arrested polymerase in DNA modified with racemic (±) BPDE.

We have also found selective modification of guanines at the 5′ end of a poly d(G) region (bases 58 through 65) at all adduction levels analyzed. It is interesting to note that this was found with both the primer extension assay using Sequenase and the T4 exonuclease digestion. Because these two enzymes "read" the DNA damage pattern from opposite directions (5′→3′ and 3′→5′, respectively), this indicates that the bias in adduction of the 5′ end of poly d(G) sequences is not a template artifact. In addition, previous studies using chemical cleavage methods for mapping the distribution of alkali-labile adducts from BPDE suggest that the strongest sequence determinant of adduction at a particular guanine is the presence of 3′ flanking guanines (Rill and Marsch 1990). In terms of defining adduct distributions, comparison of the data for Sequenase and T4 exonuclease indicates that there are advantages and disadvantages in each approach, although both methods provided similar adduct distributions. The exact position of T4 exonuclease blockage is uncertain because the presence of the adduct may alter gel migration. However, the use of T4 exonuclease activity to define adduct positions is more readily adaptable to a variety of DNA targets, whereas the primer extension procedure (Sequenase) performs most efficiently with plasmid DNA and single-stranded templates.

Reconstitution of the pGEM-5S Plasmid

Studies suggest that hot spots for BPDE binding to DNA *in vitro* do not necessarily correlate with the mutations observed *in vivo* (Marien et al. 1989). One reason for this discrepancy may be that the binding patterns of BPDE in nucleosomes and higher order structure may be significantly different than those seen in naked DNA. To address this question, we have developed a plasmid DNA model in which isolated histone cores can be used in the reassembly of nucleosome structure. Briefly, histone cores were isolated by hydroxyapatite chromatography (Stein 1989).

Reconstitution of plasmid DNA with core histone particles was accomplished by stepwise dialysis. Histone core proteins and plasmid were mixed in a 0.5:1 wt/wt ratio (respectively) in buffer containing 1 M NaCl, 20 mM Tris-Cl (pH 7.2), 0.2 mM EDTA, and 0.1 mM phenylmethylsulfonyl fluoride (PMSF). The sample was dialyzed at 4°C in Spectrapore MWCO 8000 dialysis membrane for 8 hr each in buffers containing 0.8, 0.1, and 0.05 M NaCl. Digestion with micrococcal nuclease at 37°C used the final reconstitution buffer and 1 mM $CaCl_2$ with 1 unit of micrococcal nuclease per microgram DNA for 5 min. Restriction digestion and digestion with proteinase K utilized standard buffers and procedures recommended by the supplier (B.R.L.).

Reconstitution was analyzed by electrophoresis in 1% agarose gels in TBE (Figure 2). Migration of the reconstituted plasmid (lane 3) is retarded relative to the native plasmid (lane 2), and removal of the proteins by digestion with proteinase K restores the native migration pattern (lane 4), indicating that the reconstitution procedure did significantly disrupt supercoiling of the plasmid. Partial digestion with micrococcal nuclease (lane 5), which preferentially digests linker (naked) DNA, resulted in a single DNA band that migrates at approximately 146 bp, the size of the nucleosome core. In addition reconstitution of nucleosomes protected the DNA from digestion with the restriction enzymes *Bam*HI and *Pst*1, which cut at sites within the predicted 5S rRNA nucleosome region (Figure 3). Digestion with *Eco*RI, which cleaves at a site approximately 50 bp downstream from the predicted edge of the 5S nucleosome, is also inhibited. This suggests that a nucleosome with a short linker region of

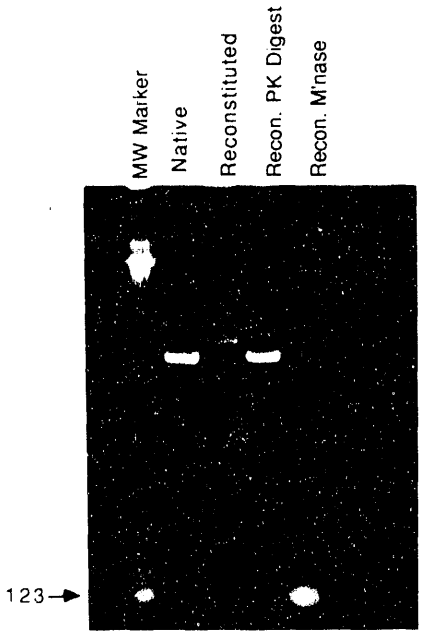

FIGURE 2. Analysis of Reconstituted pGEM-5S by Enzymatic Digestion and Agarose Gel Electrophoresis. Native and reconstituted pGEM-5S samples were subjected to electrophoresis on 1% agarose gel in TBE buffer for 4 hr at 4 V/cm. Lane 1: 123-bp ladder. Lane 2: Native plasmid. Lane 3: Reconstituted sample. Lane 4: Reconstituted sample digested with proteinase K. Lane 5: Reconstituted sample after partial digestion with micrococcal nuclease digest and proteinase K treatment.

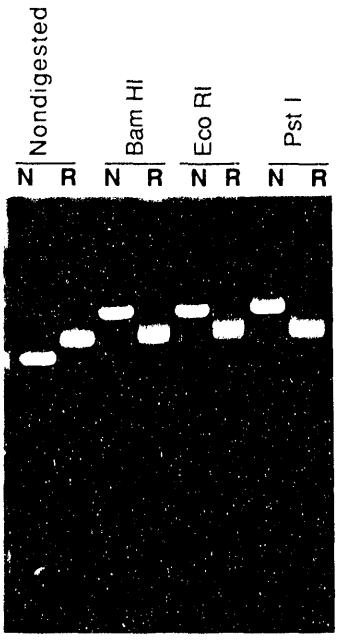

FIGURE 3. Restriction Digestion of Native and Reconstituted pGEM-5S. Native (N) and reconstituted (R) plasmid DNA were digested with 1.25 units of *Bam*HI, *Eco*RI, or *Pst*1 restriction enzymes per microgram DNA for 1 hr and separated on 1% agarose gel in TBE buffer. Shift in gel mobility demonstrates ability of enzyme to linearize only native plasmid samples.

less than 50 bp is formed adjacent to the 5S rRNA nucleosome. The results shown in Figures 2 and 3 demonstrate the formation of nucleosomes within the 5S rRNA region of the plasmid and suggest that adjacent nucleosomes may also be formed in fixed positions.

Figure 4 shows the time course for modification of native and reconstituted plasmid DNA with 10 μM [^{3}H]-(±)-*anti*-BPDE. These results demonstrate that the initial rate of BPDE binding to DNA is inhibited by the presence of nucleosome structures. After 5, 15, and 30 min reaction time, approximately 37% fewer adducts form in the reconstituted sample as compared to native DNA. Because a molar excess of BPDE to DNA molecules of more than 80 fold occurs in the reaction, the number of BPDE molecules available for reaction is not a limiting factor. Thus, it seems unlikely that the large decrease in binding to reconstituted DNA can be explained by binding to histone molecules rather than DNA. These results illustrate the potential importance of nucleosome structure in studies of DNA modification by carcinogens. Studies designed to determine structure in studies of DNA modification by whether nucleosomes alter the distribution of BPDE binding to plasmid DNA are under way.

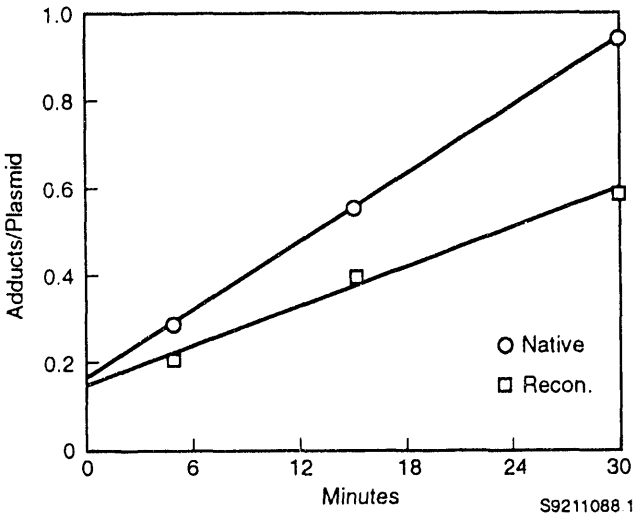

FIGURE 4. Time Course of Benzo[a]pyrene Diolepoxide (BPDE) Adduct Formation in Native and Reconstituted pGEM-5S DNA. Native and reconstituted DNA (250 μg/ml) was incubated with 10 μM [^{3}H]-(±)-*anti*-BPDE for 5, 15, and 30 min on ice in the dark. Reactions were stopped by rapid extraction with phenol:chloroform:isoamyl alcohol (24:24:1) and ethanol precipitation. Samples were then digested with proteinase K, extracted twice with phenol:chloroform:isoamyl alcohol, and again precipitated with ethanol. Level of covalent binding was determined by liquid scintillation analysis and UV spectrophotometry.

Translesional Synthesis by DNA Polymerases in BPDE-Modified DNA

It is clear that bulky adducts such as those produced by BPDE block the progression of both DNA and RNA polymerases. However, the production of a mutation requires that at least a fraction of these interactions result in bypass, or "translesional" synthesis. To investigate this hypothesis, we are using synthetic oligonucleotides modified in a site-specific manner with BPDE. A 17-mer containing a single deoxyguanine residue (5′CTTCGCTTCTCCCTTTC3′) was modified with (±)-*anti*-BPDE and the non-adducted and adducted DNA fragments were separated and purified by reversed-phase HPLC. A complementary 12-base primer was then used to determine the ability of various polymerases to extend the primer one or more bases. As shown in Figure 5, Sequenase (T7 DNA polymerase) was blocked primarily one base before the deoxyguanine in the adducted sample; however, a significant amount of full-length DNA was also produced, suggesting that not all the adducts block the polymerase. Similar analysis using DNA polymerase I (Klenow) revealed the tendency for the enzyme to add an additional base during synthesis, even on nonmodified templates. In addition, the blockage of Klenow in the adducted sample was primarily opposite the deoxyguanine residue, with much less full-length DNA produced, differing from the results obtained with Sequenase. These studies suggest that not all BPDE adducts are absolute blocks to DNA synthesis and that the amount of bypass synthesis depends on the particular polymerase involved. Further characterization of the nucleotides inserted opposite the BPDE adduct are under way.

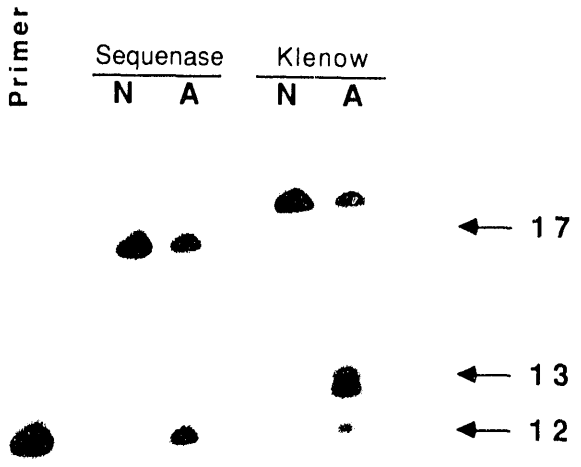

FIGURE 5. Primer Extension Analysis of Nonadducted and Adducted 17-mers. Nonadducted and adducted 17-mers containing a single deoxyguanine at position 13 were annealed with a ^{32}P-end-labeled complementary 12-mer, incubated with Sequenase or Klenow enzyme in presence of deoxynucleotide triphosphates, and separated on 20% denaturing polyacrylamide gel that was exposed to autoradiographic film for 2 hr.

Reconstitution Studies Using Modified Histones

Several lines of evidence indicate that chromatin structure is at least partially controlled by modification of histones. For example, hyperacetylation is a prerequisite to transcription of many genes. Because acetylation of lysine and other basic amino acids decreases the number of ionic interaction between core histones and DNA, this modification may allow enzymes access to genes for transcription, replication, or repair purposes. The goal of this work was to determine whether histone modifications alter the accessibility of DNA to other modification such as covalent binding of bulky chemical adducts or radiation-induced damage.

Initially our approach has been to identify and characterize modified histones by electrospray ionization mass spectrometry (ESI-MS). Core histones were isolated from a human cell line (K562) by extraction of purified nuclei with 0.4 N H_2SO_4. Histone samples were obtained from K562 cells grown in the presence or absence of sodium butyrate, a deacetylase inhibitor that results in hyperacetylated chromatin. Reversed-phase HPLC separation yielded samples of the individual histone, and triton-acid-urea polyacrylamide gel electrophoresis of histone H4 demonstrated that control samples contained predominantly two histone species (probably modified by mono- and di-acetylation), whereas samples from butyrate-treated cells were composed of five species in approximately equal abundance (Figure 6). ESI-MS indicated that the modified H4 species (Figure 7) differed from each other by 42 daltons with measured masses consistent with dimethylated, monoacetylated H4 and further successive additions of acetyl moieties up to a total of five.

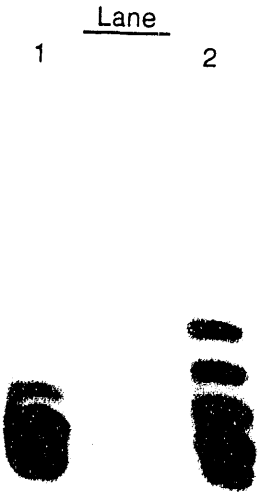

FIGURE 6. Triton-Acid-Urea PAGE Separation of Normal and Modified Histone H4. Histone proteins from human K562 cells grown in either absence (lane 1) or presence (lane 2) of 20 mM sodium butyrate were extracted and electrophoresed on triton-acid-urea polyacrylamide gel that was stained with Coumassie blue.

Our results demonstrate that hyperacetylated histones can be prepared for reconstitution experiments and that ESI-MS provides a valuable new tool to characterize modified histones and other proteins. In addition, histones containing other types of modifications such as methylation, phosphorylation, and ADP ribosylation will be prepared, characterized, and used for reconstitution studies.

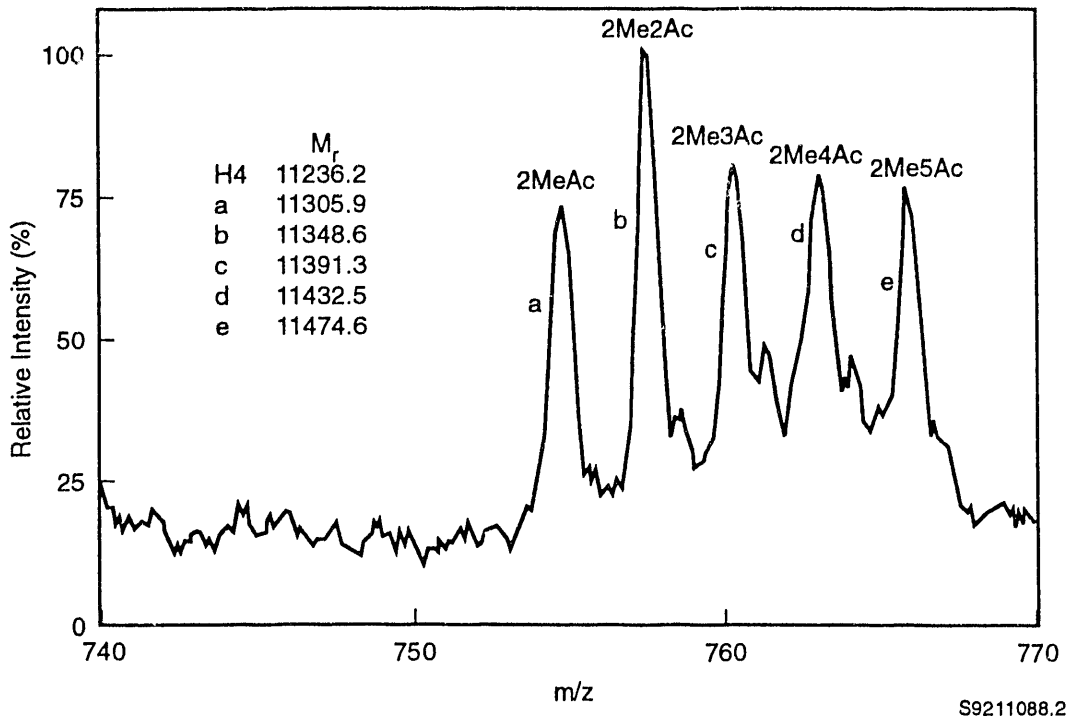

FIGURE 7. Electrospray Ionization Mass Spectrum of Hyperacetylated Histone H4. Portion of spectrum shows $(M+15H)^{15+}$ charge state of molecular ion. Human histone H4 extracted from K562 cells grown in presence of 20 mM sodium buyrate was separated by reversed-phase HPLC and analyzed by ESI-MS. Calculated mass for this protein and measured masses of observed species are tabulated on left.

References Cited

Gale, J. M., K. A. Nissen, and M. J. Smerdon. 1987. UV-induced formation of pyrimidine dimers in nucleosomal core DNA is strongly modulated with a period of 10.3 bases. *Proc. Natl. Acad. Sci. USA* 84:6644-6648.

Marien, K., K. Mathews, K. van Holde, and G. Bailey. 1989. Replication blocks and sequence interaction specificities in the codon 12 region of the c-Ha-*ras* protooncogene induced by four carcinogens *in vitro*. *J. Biol. Chem.* 264:13226-13232.

Moore, P., and B. S. Strauss. 1979. Sites of inhibition of *in vitro* DNA synthesis in carcinogen- and UV-treated øX174 DNA. *Nature* 278:664-666.

Rill, R. L., and G. A. Marsch. 1990. Sequence preferences of covalent binding by anti-(+)- and anti-(-)-benzo[a]pyrene diol epoxides. *Biochemistry* 29:6050-6058.

Singh, S. B., B. E. Hingerty, C. Singh, J. P. Greenberg, N. E. Geacintov, and S. Broyde. 1991. Structures of the (+)- and (-)-*trans*-7,8-dihydroxy-*anti*-9,10-epoxy-7,8,9,10-tetrahydrobenzo(a)pyrene adducts to guanine N_2 in a duplex dodecamer. *Cancer Res.* 51:3482-3492.

Stein, A. 1989. Reconstitution of DNA from purified components. *Methods Enzymol.* 170:585-603.

Straub, K. M., T. Meehan, A. L. Bulingame, and M. Calvin. 1977. Identification of the major adducts formed by reaction of benzo[a]pyrene diol epoxide with DNA *in vitro*. *Proc. Natl. Acad. Sci. USA* 74:5285-5289.

Thrall, B. D., D. B. Mann, M. J. Smerdon, and D. L. Springer. 1992. DNA polymerase, RNA polymerase and exonuclease activities on a DNA sequence modified by benzo[a]pyrene diolepoxide. *Carcinogenesis* 13:1529-1534.

Biochemistry of Free Radical-Induced DNA Damage

Principal Investigator: *A. F. Fuciarelli*

Other Investigators: *E. C. Sisk and J. D. Zimbrick*

Gas chromatography–mass spectrometry and liquid chromatography–thermospray mass spectrometry provide structural and quantitative information for analysis of free radical-induced modifications to DNA. Using these analytical methods and synthetic oligonucleosides of defined base composition, the effects of DNA structure and chemical microenvironment are being examined in irradiated samples of DNA with emphasis on 8,5′-cyclodeoxynucleotide and DNA base damage analysis. Liquid chromatography–thermospray mass spectrometric analysis of an irradiated sample of 2′-deoxyadenosine revealed formation of (R)- and (S)-8,5′-cyclodeoxyadenosine and 8-oxodeoxyadenosine in addition to radiolytic base release. Completion of these analyses, coupled with our ongoing efforts to synthesize 8,5′-cyclodeoxyadenosine, provides the essential background to quantitate these products in irradiated samples of DNA using mass spectrometry. These efforts will permit us to examine the effects of DNA structure and chemical microenvironment on free radical-induced DNA damage.

Assays for Radiation-Induced Molecular Products Generated in DNA

Techniques to assess the products of radiation and free radical-induced damage to nucleic acids include biochemical methods (i.e., enzymatic assays, postlabeling techniques), immunochemical techniques, and assays combining analytical separation and detection methods [i.e., gas chromatography–mass spectrometry (GC/MS), liquid chromatography–mass spectrometry (LC/MS)]. The objectives of these methodologies are similar: to achieve good specificity and high sensitivity for measuring free radical-induced molecular products among numerous other modified DNA constituents and under conditions of high concentrations of unmodified DNA constituents. Mass spectrometric analysis following chromatographic separation provides unequivocal qualitative information and accurate quantitation of components in a complex chemical mixture. These analytical techniques, combined with use of synthetic oligonucleotides of defined base composition, provide a novel experimental approach to address fundamental questions concerning the influence of DNA structure and microenvironment on free radical-induced product formation.

Use of Oligonucleotides of Defined DNA Base Composition for Studies of Radiation-Induced DNA Damage

Although mechanistic information concerning radiation chemical interactions can be obtained in solutions of monomers, in polymers such as DNA the radiation chemical interactions can be quite different. Application of analytical methodologies to characterize and quantitate radiation-induced damage in polymers has been the initial focus of work in our laboratory. This has resulted from our ability to synthesize oligonucleotides of defined composition and subsequent use of these model DNA fragments for probing effects of DNA structure and chemical microenvironment during irradiation of aqueous solutions. As an example of the selectivity and sensitivity required to measure free radical-induced damage to DNA (Figure 1), an oligonucleotide (5′-GCGAAATTTCGC-3′) irradiated to 100 Gy under nitrous oxide (N_2O), was digested to deoxynucleoside constituents using nuclease P1, phosphodiesterase I, and alkaline phosphatase. The constituents were separated with reversed-phase high performance liquid chromatography (HPLC), and using UV detection, the only components observed were unchanged deoxynucleosides (deoxycytidine, thymidine,

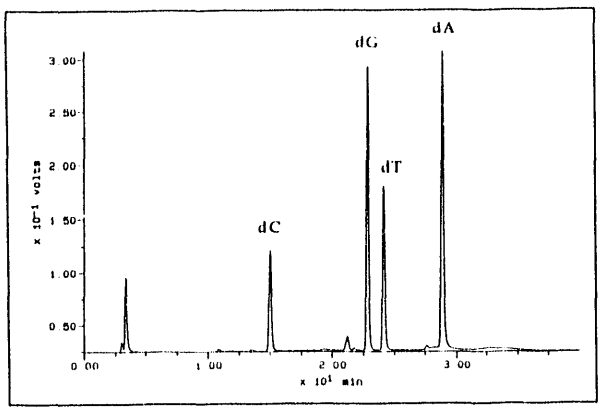

FIGURE 1. HPLC Profile of an Enzymatic Hydrolysis of an Oligonucleotide (5′-GCGAAATTTCGC-3′) Irradiated to 100 Gy Under N_2O Demonstrating Completeness of Conversion to Deoxynucleosides. The undigested oligonucleotide elutes in a single peak at 33 min (not shown).

deoxyadenosine, and deoxyguanosine). However, a plethora of modified DNA constituents, although present in levels that collectively account for less than 5% of the mixture, require "unmasking" from these unchanged DNA constituents. This analytical challenge in studies of free radical-induced DNA damage can be overcome by combining separation–mass spectrometric methodologies.

Gas Chromatography–Mass Spectrometry for Analysis of Radiation-Induced DNA Damage

Gas chromatography–mass spectrometry with selected ion monitoring can selectively "enhance" signals resulting from modified DNA constituents and "remove" signals from unchanged DNA bases in a mass spectrometric ion profile over the chromatographic interval of interest. The oligonucleotide irradiated to 50 Gy with ionizing radiation (see Figure 1) was subjected to acid hydrolysis and chemical derivatization, which liberate DNA bases from the phosphodiester backbone and render them volatile for gas chromatographic separation. The reconstructed ion chromatogram (Figure 2) reveals DNA damage represented by a trimethylsilylated mixture of acid-stable, modified DNA bases. As expected, products formed in our synthetic oligonucleotides are identical to radiation-induced DNA base products that we measured previously using significantly greater quantities of calf thymus DNA (Fuciarelli et al. 1989 1990). A limited fraction of deoxynucleoside products can also be analyzed following enzyme hydrolysis in a volatile buffer system that minimizes undesirable interference during derivatization reactions for GC/MS; for example, measurement of 8,5′-cyclodeoxyadenosine epimers (discussed in more detail later) in enzymatically digested and trimethylsilylated mixtures of irradiated oligonucleotides (5′-GCGAAATTTCGC-3′) (Figure 3).

Liquid Chromatography–Thermospray Mass Spectrometry for Analysis of Radiation-Induced DNA Damage

Deoxynucleoside analysis poses a challenge to GC/MS methodology because samples may be unstable to acid hydrolysis and derivatization reactions. Deoxynucleosides may also vary widely in their degree of volatility and thermal lability. Thus, development of complementary mass spectrometry techniques, particularly those capable of measuring the molecular ion of the deoxynucleoside, is important. Combined liquid chromatography–mass spectrometry (LC/MS) is ideally suited to analysis of products, such as deoxynucleosides, that vary widely in polarity because chemical derivatization is not required. Thermospray mass spectrometry (TSP-MS) has been the most popular LC/MS interface for analysis of DNA bases and nucleosides because the technique yields mass spectra whose molecular ions are nearly always observed for nucleosides, with a few other important peaks such as those representing the purine or pyrimidine base (Edmonds et al. 1985). We initially applied this technology to measurement of radiation-induced DNA damage by examining deoxyadenosine radiolysis products. Under the HPLC chromatographic conditions selected, a reconstructed ion profile (Figure 4) of an irradiated solution of 2′-deoxyadenosine (m/z 252 and 136; 34 min) reveals intense characteristic ions for adenine (m/z 136; 20.5 min), (R)-8,5′-cyclodeoxyadenosine (m/z 250; 22.4 min), (S)-8,5′-cyclodeoxyadenosine (m/z 250; 33 min), and 8-oxodeoxyadenosine (m/z 268; 35.5 min). Synthesis of authentic samples of these products will allow

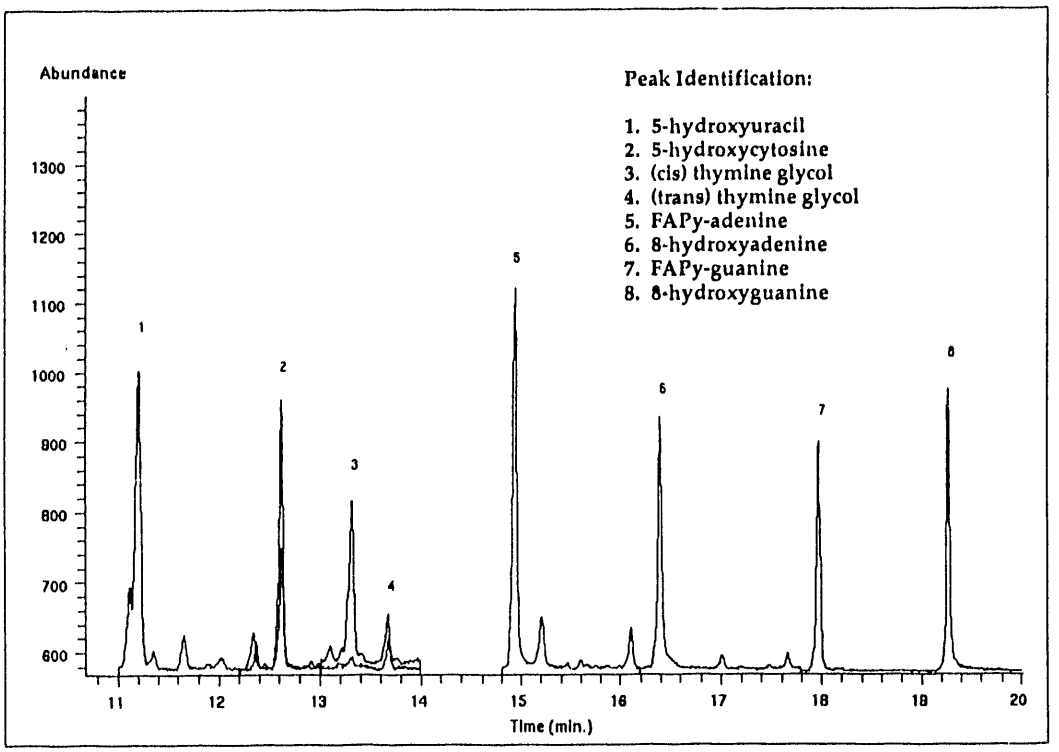

FIGURE 2. Reconstructed Ion Chromatogram from GC/MS Analysis of a Solution of An Oligonucleotide (5′-GCGAAATTTCGC-3′) Irradiated to 50 Gy Following Acid Hydrolysis Illustrating Relative Abundance of the Ions Representing Trimethylsilyl Derivatives of DNA Base Products.

accurate quantitation of product yields in irradiated samples of DNA.

Utilizing DNA Damage as a Molecular Probe of Radiation Biochemistry

Radiation-induced intramolecular cyclization reactions in which a covalent bond is formed between the C(5′) carbon of the deoxyribose moiety and the C(8) position of a purine base result in formation of 8,5′-cyclodeoxypurines. These novel products have served as molecular probes of radiation biochemical events, and changes in product yields as a function of modifications to the aqueous microenvironment have revealed that several characteristics influence product formation. One of the most notable features is the ability of the hydroxyl radical to abstract either of the hydrogen atoms at the C(5′) carbon, leading to formation of either R or S epimers at this position (Raleigh and Fuciarelli 1985; Fuciarelli et al. 1987). Several factors related to the local microenvironment have been shown to influence which hydrogen is abstracted and thus which epimer (R or S) is formed under a given set of experimental conditions. For example, the distribution of charge between the base and sugar moieties can significantly influence the yields of these epimers (Raleigh and Fuciarelli 1985; Fuciarelli et al. 1987). Preferential formation of the R epimer of 8,5′-cycloadenosine in irradiated polyA was found to reflect conformational constraints placed on the polymer chain, and, from these data generated in a single-stranded ribonucleotide polymer, we hypothesized that the R epimer would predominate in double-stranded DNA irradiated in aqueous solution (Fuciarelli et al. 1987). This was supported by our initial molecular models of DNA containing the (R)- and (S)-8,5′-cyclodeoxyadenosine moieties (in collaboration with Dr. Michael Kennedy, University of Washington), which were generated using the

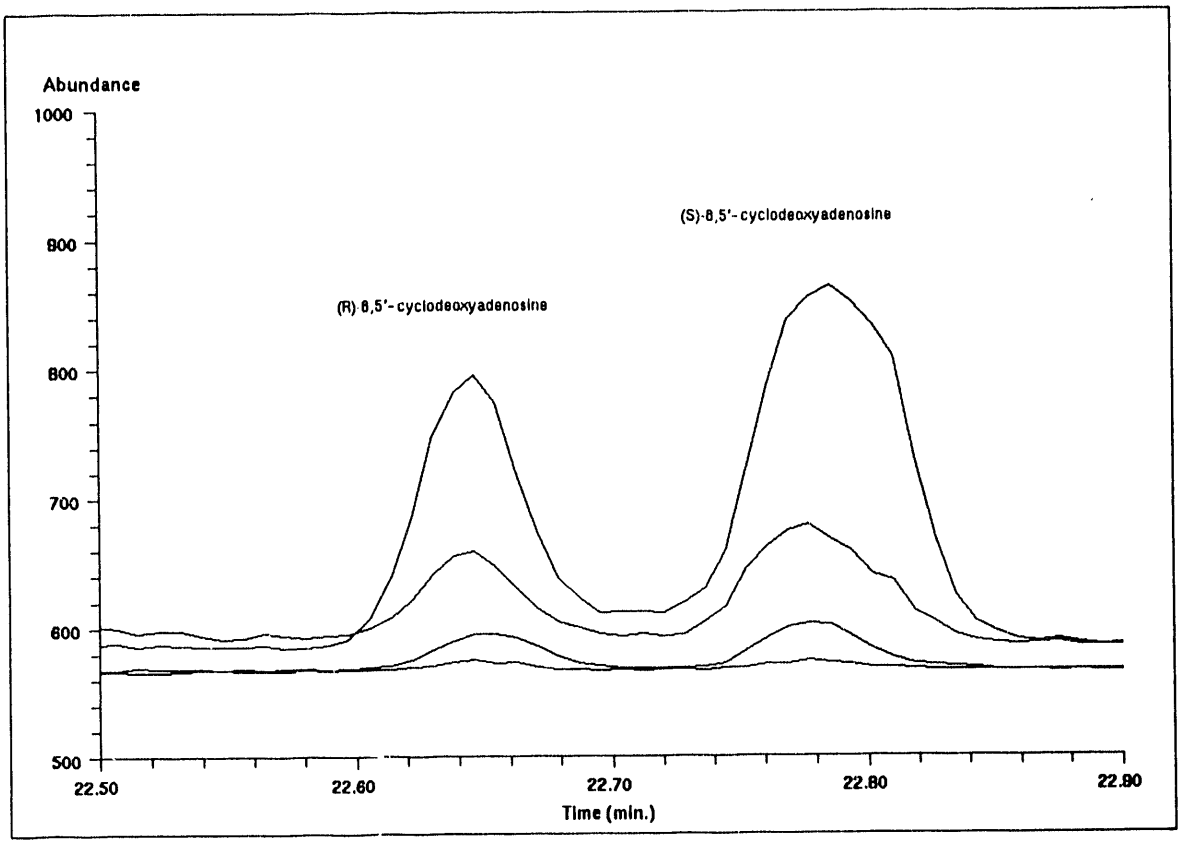

FIGURE 3. Reconstructed Ion Chromatogram from GC/MS Analysis of a Solution of the Oligonucleotide (5′-GCGAAATTTCGC-3′) Irradiated to 100 Gy Following Enzyme Digestion Illustrating the Relative Abundance of the Ions Representing the Trimethylsilyl Derivatives of (R)- and (S)-8,5′-Cyclodeoxyadenosine.

DNA sequence 5′-GTACTA*GCTCGC-3′. These energy-minimization studies indicated that minor perturbations in structure do occur when the R epimer is introduced, but that a major structural distortion affecting the phosphodiester backbone and significant numbers of hydrogen bonds would be required to permit formation of the S epimer (Figure 5). Contrary to these predictions, however, experimental measurements revealed that the R epimer predominated in yield over the S epimer in double-stranded DNA and in synthetic oligonucleotides (see Figure 3). This discrepancy between our hypothesis and experimental data has prompted us to reexamine the question with a combination of molecular dynamic computer simulations (to be performed in collaboration with Drs. Karol Miaskiewicz, John Miller, and Rick Ornstein, PNL) and experimental analysis of irradiated nucleic acid constituents. This combination of molecular modeling and experimental analysis provides an exciting synergism to advance the study of induction and modification of DNA damage caused by the interaction of ionizing radiations.

Effect of DNA Conformation on Radiation-Induced Product Yields

Physical factors in polynucleotides, such as DNA conformation, markedly affect the yields of DNA base products (Fuciarelli et al. 1990). The yields of the pyrimidine products measured in samples of DNA irradiated in the heat-denatured conformation were found to be greater than those measured in native DNA (Fuciarelli et al. 1990). However, this was not observed consistently for the purine products, which were measured simultaneously in each DNA sample during the analysis. To extend our work on the influence of DNA conformation on product yield we measured the

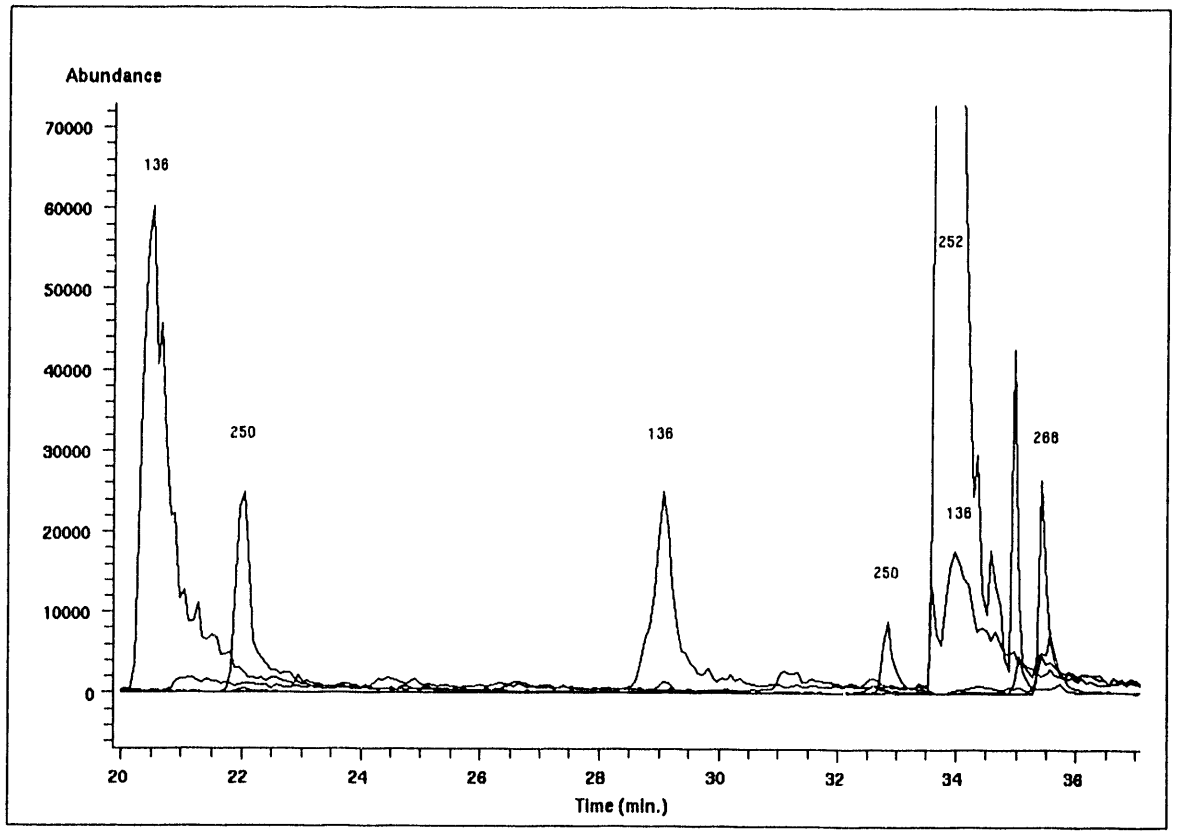

FIGURE 4. Liquid Chromatography-Thermospray Mass Spectrometric Selected-Ion Profile of a Solution of Deoxyadenosine Irradiated to 1000 Gy Under N_2O. Peaks represent ions corresponding to adenine (m/z 136; 20.5 min), (R)-8,5′-cyclodeoxyadenosine (m/z 250; 22.4 min), (S)-8,5′-cyclodeoxyadenosine (m/z 250; 33 min), deoxyadenosine (m/z 252, 136; 34 min), and 7,8-dihydro-8-oxodeoxyadenosine (m/z 268; 35.5 min).

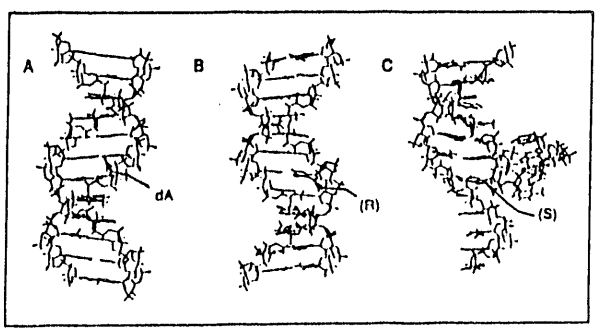

FIGURE 5. Energy-Minimized Diagram Illustrating an Oligonucleotide of the Sequence 5′-GTACTA*GCTCGC-3′ in Which the Central A (**A**) Has Been Replaced with (R)-8,5′-Cyclodeoxyadenosine (**B**) or (S)-8,5′-Cyclodeoxyadenosine (**C**).

spectrum (types and yields) of DNA products observed following exposure of DNA in either the B or Z conformation to ionizing radiation. Specialized nucleotide sequences in DNA may facilitate DNA conformations differing from that of the B form, which may be highly significant during periods of relative inactivity, and during interactions with proteins and other subcellular factors. DNA containing sequences with alternating purines and pyrimidines are known to undergo local changes from the B form to the Z form at high concentrations of salts (4 mol dm^{-3} Na^+); this fact was used to yield DNA with more Z character. We are currently determining from these experimental data whether product formation can differ in B or Z DNA as an example of the effect of DNA structure on product distribution in irradiated nucleic acids.

Future Directions

Understanding mechanisms of DNA radiation biochemistry, including the effects of DNA structure and microenvironment on product yields, is an underlying goal of this newly funded project. These questions are being addressed under controlled experimental conditions using assays of high selectivity and sensitivity. However, an even more challenging goal is to address radiation biochemistry within the cellular environment and to correlate the presence of unrepaired DNA lesions with observable biological effects. Success in this latter area necessitates our increased expertise in sample preparation methods.

References Cited

Edmonds, C. G., M. L. Vestal, and J. A. McCloskey. 1985. Thermospray liquid chromatography-mass spectrometry of nucleosides and of enzymatic hydrolysates of nucleic acids. *Nucleic Acids Res.* 13:8197-8206.

Fuciarelli, A. F., F. Y. Shum, and J. A. Raleigh. 1987. Intramolecular cyclization in irradiated nucleic acids: Correlation between high-performance liquid chromatography and an immunochemical assay for 8,5′-cycloadenosine in irradiated poly(A). *Radiat. Res.* 110:35-44.

Fuciarelli, A. F., B. J. Wegher, W. F. Blakely, and M. Dizdaroglu. 1990. Yields of radiation-induced base products in DNA: Effects of DNA conformation and gassing conditions. *Int. J. Radiat. Biol.* 58:397-415.

Fuciarelli, A. F., B. J. Wegher, E. Gajewski, M. Dizdaroglu, and W. F. Blakely. 1989. Quantitative measurement of radiation-induced base products in DNA using gas chromatography-mass spectrometry. *Radiat. Res.* 119:219-231.

Raleigh, J. A., and A. F. Fuciarelli. 1985. Distribution of damage in irradiated 5′-AMP: 8,5′-Cyclo-AMP, 8-hydroxy-AMP, and adenine release. *Radiat. Res.* 102:165-175.

General
Life Sciences
Research

GnomeView Version 1.0 Beta

Principal Investigator: *R. J. Douthart*

Other Investigators: *J. Pelkey and G. Thomas*

GnomeView is a tool for exploring information generated by the Human Genome Project. GnomeView provides both graphical and textual styles of data presentation. It integrates retrieved database information in such a way that the user can navigate smoothly across databases and between different levels in the mapping hierarchy. Version 1.0 Beta, a test version of the interface with access to Genome Data Base (GDB) and GenBank, is being installed at a number of selected sites.

The architecture of the GnomeView is as generic as possible. Custom X-window widgets that facilitate the drawing of maps (map_widget) and the viewing of detail (zoom_widget) are an integral part of the system. A dominant theme in GnomeView development has been the preservation of pictorial genomic maps.

GnomeView is designed to access data for many different mapping levels such as chromosome, restriction enzyme, contig mapping, and sequence from a variety of databases. Seamless transition among and between various databases harboring information pertinent to genome mapping depends on the integrity of common object definitions and the consistency of cross-referencing.

GnomeView is an interface to databases rather than a data repository. Its evolution into a useful tool depends to a large extent on the existence, condition, and completeness of genome databases that are publicly available.

Database Integration

The two most prominent genome databases are Genome Data Base (GDB) and GenBank. The map_objects in GDB are primarily chromosome loci. The objects in GenBank are DNA sequences. These databases cross-reference one another, and the provided tables are used by GnomeView.

GnomeView Version 1.0 Beta references abstracted versions of GDB and GenBank. Entry into the mapping hierarchy is limited by the objects existing in and defined by these databases. In GnomeView Version 1.0 Beta, entry at the chromosome level is to GDB and entry at the sequence level is to GenBank. Other possible entry levels including restriction enzyme, contig, and linkage mapping are inactive in Version 1.0 Beta. As more cross-referenced databases containing the appropriate data become available, entry at these levels will be incorporated into the system.

Version 1.0 Beta supplies a convenient one-to-one correspondence between map level and database. As GnomeView evolves, this may not always be the case; for example, in the future, GDB may be queried for both chromosome and contig maps.

Database Accommodation

Genome databases have their own "personalities," which reflect either consciously or unconsciously the world view of their curators. Bias occurs in the choice and definition of map_objects keywords and the content of annotations. Although much could be gained by closer cooperation and common formatting, it is not clear that total database homogenization is possible or even desirable.

In GnomeView Version 1.0 Beta, the query options conform to the object definitions of the databases. Entry can be at different mapping levels that send initial queries to different databases. Information trails can be followed through seamless transitions from one database to another. These trails, isolated in separate windows, allow comparisons of similar queries at different entry levels. Cross-referencing inconsistencies and database bias are easily revealed by carefully chosen queries of this nature.

Database Objects

For the GnomeView interface, the following type of objects are defined:

Map_Object: An entity that can be associated with a region or position on a genomic map representation. For example, GDB map_objects include loci and probes. GenBank sequence loci are also map_objects to chromosome representations. GenBank features are map_objects to sequence representations.

Landmarks: Objects that are ordered and, when assembled, contribute to the graphic and metric of a genomic map representation. For example, the bands of a chromosome or the position of restriction enzyme sites are landmark objects.

Queries are sent by a Graphics Users Interface (GUI) for each mapping level. The query can be qualified by a series of buttons (toggles) that define map_objects according to the view of the databases. Figure 1 shows the query window for a chromosome query that accesses GDB. The query objects and the qualifiers are, for the most part, defined by GDB. The notable exceptions are the attribute selections series of buttons. Any number of this set of descriptive attributes are assigned to GDB loci as aids in retrieval. Figure 2 depicts a similar interface to query GenBank sequence loci. There are fewer options for qualifying sequence loci.

The distribution(s) of objects retrieved by query over the genome are indicated graphically by color-coded density maps drawn to the chromosome(s) of interest. The distributions of primary map_objects as delineated by the search criteria are depicted. Primary map_objects can be either loci or probes as defined by GDB or sequence loci as defined by GenBank. Within each database are also associated objects that are linked to other objects. For example, GDB loci have Probes Polymorphisms and Probe Sequences as associated objects, and Probes have Loci and Probe Sequences as associated objects; Sequence Loci from GenBank have Chromosome Loci as associated objects.

As both GnomeView and the databases develop, the number of associated objects will increase. Version 1.0 Beta does not query the sources or contacts fields of GDB, because functionality was limited deliberately to objects more directly associated with the graphics rendition of maps. The first release version, however, will have contacts and sources as associated objects.

The GnomeView Graphic User Interface

Figure 3 shows a generalized diagram of the GnomeView graphics users interface. For Version 1.0, Beta database A can be considered to be either GDB or GenBank. Entry currently is at the chromosome (GDB) or sequence (GenBank) level. Using the templates shown in Figures 1 and 2, the user sends out a qualified query by activating buttons or typing minimal alphanumeric input. An initial results list is returned, tallying the number of hits per selected chromosome. From the initial results list window, the user can then choose to view the results graphically or as a detailed list sorted by chromosome. In the graphics representation, color-coded density maps are displayed next to chromosome representations. The density maps indicate the frequency of occurrence of retrieved objects at various band positions on the chromosomes.

Appropriate lists can be obtained by interaction with the graphics map representations. Region-specific and band-specific lists are available by selecting regions on the graphics representations with the mouse. From these lists, single map_objects can be chosen for more information. The objects on the list are those that

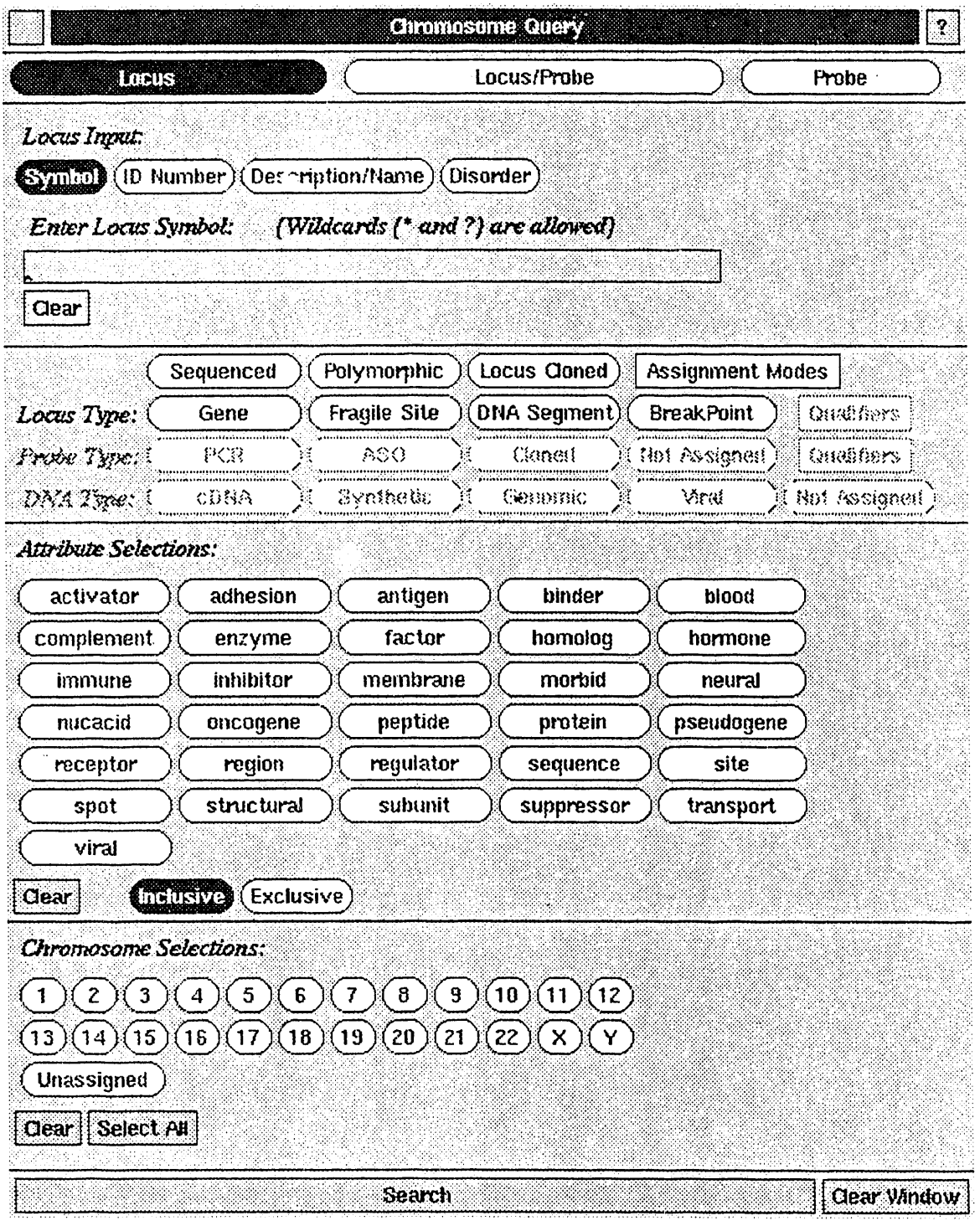

FIGURE 1. Chromosome Query Window When Querying by Locus.

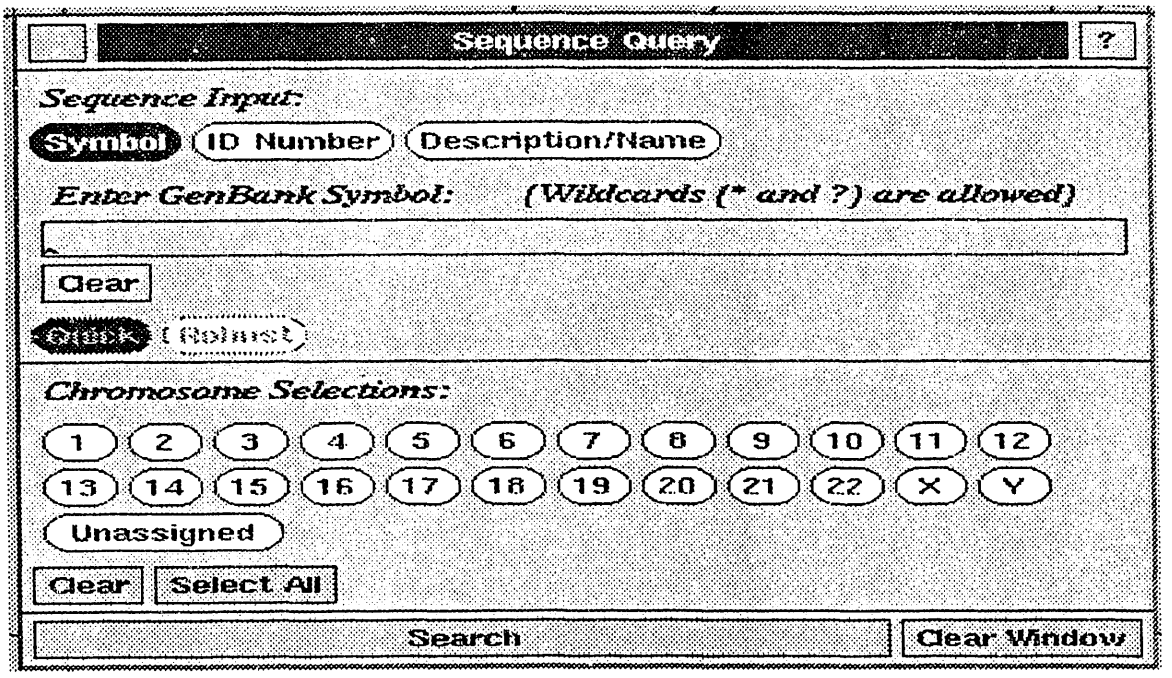

FIGURE 2. Sequence Query Window.

satisfy the criteria of the query. Specific data describing those criteria and other related information are given in the "more information" window of a selected map_object. Viewing and selection are aided by a dynamic zoom capability that is available for all graphics map representations.

The "more information" window also contains buttons for associated map_objects. If associated objects exist for the map_object featured in the window, appropriate buttons will be active. If the user chooses an active associated map_objects button, a list of objects similar to the map_objects list obtained from the initial query is presented. By using associated map_objects lists, almost all the information associated with the primary map_object in the databases can be browsed and represented in color graphics.

If applicable, associated map buttons also may be activated. Choosing chromosome map presents a chromosome representation to which the relevant map_object is mapped as a single object density map. The sequence map button will present a list of GenBank sequence loci associated with the map_object that is the subject of the information window. The associated maps option provides a seamless transition from one database to another. Subsequent information and maps are derived from the referenced database. In Version 1.0 Beta, cross-reference tables from GDB to GenBank and from GenBank to GDB are used to effect these transitions. In Figure 3, this transition is depicted by the arrow to Database B where map type B is obtained.

In Version 1.0 Beta, map type B is a sequence map. A sequence map is a representation of a GenBank sequence loci as a number line with important features for the GenBank header automatically drawn to it. Most chromosome loci to sequence loci references are one to many. This reflects the object definition of the two databases, especially GenBank, where a sequence loci is a single acceptable entry that in most cases does not represent a complete gene or other unit which would tend toward one-to- one mapping with GDB loci.

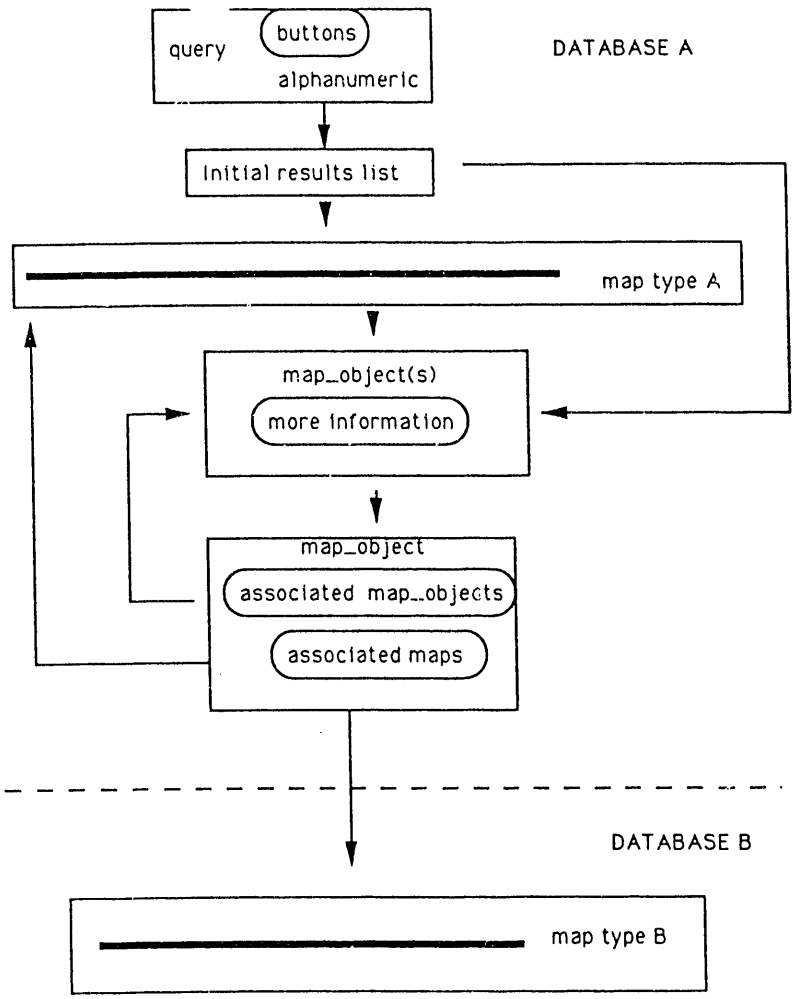

FIGURE 3. GnomeView Implementation.

Future versions of GnomeView will contain some analysis and melding utilities to create longer contiguous DNA sequences from corresponding GenBank loci. It is also anticipated that individual loci will tend toward longer and longer sequences as sequencing procedures improve and more laboratories focus on total sequencing of important genetic regions.

In this context, qualified queries for features as map_objects with the results presented as graphics, color-coded sequence maps will be an important tool in obtaining a holistic understanding of millions of contiguous DNA bases.

Questions about implementation and availability may be addressed to Richard J. Douthart, Pacific Northwest Laboratory, P.O. Box 999, Richland, WA 99352; (509) 375-2653.

Appendix

Appendix

Dose-Effect Studies with Inhaled Plutonium in Beagles

On the following pages (pp. 103-130), data are presented for all dogs assigned to current life-span dose-effect studies with inhaled $^{239}PuO_2$, $^{238}PuO_2$, and $^{239}Pu(NO_3)_4$. Information is presented on the estimated initial lung deposition, based on external thorax counts and on estimated lung weights (0.011 x body weight) at time of exposure. Information is also provided on the current interpretation of the most prominent clinicopathological features associated with the death of animals. For the study involving $^{239}PuO_2$, we report a "Cause of Death" based on a recent review of that study. For the $^{238}PuO_2$ and the $^{239}Pu(NO_3)_4$ studies, the column heading "Comments on Dead Dogs" is used until the study receives final review. These data represent information currently available, and are presented as reference material for scientists who desire to follow in detail the progress of these experiments.

This report differs from previous reports in that actual body weight at time of exposure was used to calculate lung weights and plutonium concentration instead of "ideal weight" at times of exposure used in previous reports. The dogs were then reassigned to dose-level groups based on plutonium concentration (Bq/g lung weight). Also, activity is expressed in SI units (becquerels) instead of nanocuries.

DOSE-EFFECT STUDIES WITH INHALED PU-239 OXIDE IN BEAGLES

DOSE GROUP	DOG IDENT	BIRTH DATE	INITIAL ALVEOLAR DEPOSITION BQ	BQ/G LUNG	BQ/KG	INHALATION EXPOSURE WGT (KG)	AGE (MO)	EXPO DATE	DEATH INFORMATION DEATH DATE	MONTHS POST INH	AGE (MO)	CAUSE OF DEATH
CONTROL	0738 F	4/25/69	0	0.00	0.00	10.3	25.4	6/08/71	8/11/83	146.1	171.5	Hemangiosarcoma {malignant} (Angiosarcoma); Heart
CONTROL	0740 F	4/25/69	0	0.00	0.00	10.8	25.4	6/08/71	6/18/83	144.3	169.8	Lymphoma {malignant}; Ovary
CONTROL	0749 F	6/03/69	0	0.00	0.00	11.2	19.5	1/19/71	9/14/84	163.8	183.4	Inflammation, acute necrotizing; Adrenal gland
CONTROL	0755 M	6/05/69	0	0.00	0.00	11.8	19.5	1/19/71	12/10/82	142.7	162.2	Uremia syndrome; Kidney
CONTROL	0766 M	6/16/69	0	0.00	0.00	11.7	19.1	1/19/71	6/26/84	161.2	180.3	Bronchiolo-alveolar adenocarcinoma {malignant}; Lung Lobe, left diaphragmatic
CONTROL	0775 F	6/28/69	0	0.00	0.00	12.0	18.7	1/19/71	10/05/81	128.5	147.3	Thrombus; Pulmonary artery
CONTROL	0785 M	7/19/69	0	0.00	0.00	12.0	19.5	3/04/71	9/02/87	198.0	217.5	Herniated intervertebral disc; Cervical vertebra
CONTROL	0789 M	7/29/69	0	0.00	0.00	11.6	19.2	3/04/71	7/25/83	148.7	167.9	Lymphoma {malignant}; Spleen
CONTROL	0792 M	9/11/69	0	0.00	0.00	12.5	20.9	6/08/71	4/28/76	58.7	79.5	Melanoma {malignant}; Soft palate
CONTROL	0800 F	10/21/69	0	0.00	0.00	10.1	16.4	3/04/71	11/17/86	188.5	204.9	Pheochromocytoma {malignant}; Adrenal gland
CONTROL	0801 M	10/21/69	0	0.00	0.00	12.5	19.5	6/08/71	2/23/82	128.6	148.1	Bronchiolo-alveolar adenocarcinoma {malignant}; Lung Lobe, left diaphragmatic
CONTROL	0811 F	11/23/69	0	0.00	0.00	11.3	15.3	3/04/71	2/24/85	167.8	183.1	Melanoma {malignant}; Mouth
CONTROL	0846 M	12/19/69	0	0.00	0.00	13.5	18.5	7/06/71	4/08/83	141.1	159.6	Uremia syndrome; Kidney
CONTROL	0861 M	12/29/69	0	0.00	0.00	13.1	18.2	7/06/71	11/18/86	184.4	202.6	Hyperadrenocorticism (Cushings's Disease); Small intestine
CONTROL	0868 F	2/08/70	0	0.00	0.00	9.5	16.9	7/06/71	3/24/87	188.6	205.4	Uremia syndrome; Kidney
CONTROL	0872 F	2/11/70	0	0.00	0.00	7.8	16.8	7/06/71	11/05/82	136.0	152.8	Adenosquamous carcinoma {malignant}; Lung Lobe, right diaphragmatic
CONTROL	0878 M	4/10/70	0	0.00	0.00	12.2	19.0	11/10/71	1/22/85	158.4	177.4	Uremia syndrome; Kidney

DOSE-EFFECT STUDIES WITH INHALED PU-239 OXIDE IN BEAGLES

DOSE GROUP	DOG IDENT	BIRTH DATE	INITIAL ALVEOLAR DEPOSITION BQ	BQ/G LUNG	BQ/ KG	INHALATION EXPOSURE WGT (KG)	AGE (MO)	EXPO DATE	DEATH INFORMATION DEATH DATE	MONTHS POST INH	AGE (MO)	CAUSE OF DEATH
CONTROL	0882 M	4/15/70	0	0.00	0.00	12.4	18.9	11/10/71	11/06/81	119.9	138.7	Hemangiosarcoma {malignant} (Angiosarcoma); Liver
CONTROL	0885 F	5/04/70	0	0.00	0.00	11.4	18.2	11/10/71	2/18/83	135.3	153.5	Sweat gland adenocarcinoma {malignant}; Skin
CONTROL	0903 F	7/14/70	0	0.00	0.00	7.2	15.9	11/10/71	1/30/85	158.7	174.6	Lymphoma {malignant}; Kidney
CONTROL-SAC	0701 F	3/17/69	0	0.00	0.00	9.7	19.8	11/10/70	4/18/79	101.2	121.0	Scheduled sacrifice, no significant pathology;
CONTROL-SAC	0703 M	3/17/69	0	0.00	0.00	14.7	19.8	11/10/70	3/24/77	76.4	96.2	Scheduled sacrifice, no significant pathology;
CONTROL-SAC	0724 M	4/01/69	0	0.00	0.00	13.8	18.8	10/26/70	3/30/78	89.1	107.9	Scheduled sacrifice, no significant pathology;
LOWEST	0756 M	6/05/69	0	0.00	0.00	12.0	19.5	1/19/71	4/21/83	147.0	166.5	Seizure (Epileptic episode); Brain
LOWEST	0847 M	12/19/69	0	0.00	0.00	10.9	18.5	7/06/71	1/23/85	162.6	181.2	Uremia syndrome; Kidney
LOWEST	0858 M	12/29/69	0	0.00	0.00	9.9	18.2	7/06/71	10/01/86	182.9	201.1	Lymphoid leukemia {malignant}; Lymphocytic tissue
LOWEST	0865 F	1/23/70	0	0.00	0.00	9.5	17.4	7/06/71	9/16/86	182.4	199.8	Inflammation, acute, bronchopneumonia; Lung
LOWEST	0879 M	4/10/70	0	0.00	0.00	11.6	17.9	10/07/71	7/27/84	153.7	171.6	Hemangiosarcoma {malignant} (Angiosarcoma); Liver
LOWEST	0886 F	5/04/70	0	0.00	0.00	9.2	18.2	11/10/71	4/04/84	148.8	167.0	Meningioma {malignant}; Brain
LOWEST	0907 F	7/14/70	0	0.00	0.00	9.7	15.9	11/10/71	5/10/86	174.0	189.9	Inflammation, acute, bronchopneumonia; Lung
LOWEST	0904 F	7/14/70	26	0.25	2.76	9.4	15.9	11/10/71	12/19/83	145.3	161.2	Chondrosarcoma {malignant}; Nose
LOWEST	0825 F	12/03/69	52	0.43	4.75	10.9	18.1	6/08/71	11/17/82	137.3	155.5	Hemangioma {benign}; Spleen
LOWEST	0832 F	12/10/69	74	0.72	7.96	9.3	16.5	4/26/71	3/03/86	178.2	194.7	Lymphoma {malignant}; Spleen
LOWEST	0900 M	7/12/70	104	0.80	8.78	11.8	16.0	11/10/71	5/21/82	126.3	142.3	Plasma cell myeloma {malignant}; Subcutaneous tissue
LOWEST	0870 F	2/08/70	141	1.10	12.12	11.6	16.9	7/06/71	5/04/84	154.0	170.8	Inflammation, acute, bronchopneumonia; Lung

DOSE-EFFECT STUDIES WITH INHALED PU-239 OXIDE IN BEAGLES

			INITIAL ALVEOLAR DEPOSITION			INHALATION EXPOSURE			DEATH INFORMATION			
DOSE GROUP	DOG IDENT	BIRTH DATE	BQ	BQ/G LUNG	BQ/ KG	WGT (KG)	AGE (MO)	EXPO DATE	DEATH DATE	MONTHS POST INH	AGE (MO)	CAUSE OF DEATH
LOWEST	0899 F	7/12/70	133	1.14	12.57	10.6	16.0	11/10/71	3/29/81	112.6	128.6	Hemangiosarcoma {malignant} (Angiosarcoma); Spleen
LOWEST	0867 M	1/23/70	174	1.32	14.49	12.0	17.4	7/06/71	2/07/86	175.1	192.5	Lymphoma {malignant}; Mesenteric lymph node
LOWEST	0891 M	7/11/70	211	1.67	18.34	11.5	16.0	11/10/71	6/26/81	115.5	131.5	Sepsis; Prostate
LOWEST	0875 M	2/11/70	281	1.83	20.09	14.0	16.8	7/06/71	5/21/78	82.5	99.3	Lymphoma {malignant}; Kidney
LOWEST	0788 M	7/19/69	296	1.92	21.14	14.0	18.8	2/10/71	4/13/84	158.1	176.8	Uremia syndrome; Kidney
LOWEST	0770 F	6/16/69	222	1.98	21.76	10.2	19.1	1/19/71	11/29/84	166.3	185.5	Uremia syndrome; Kidney
LOWEST	0807 F	11/23/69	296	2.07	22.77	13.0	14.6	2/10/71	7/24/81	125.4	140.0	Adenoma {benign}; Pituitary gland
LOWEST	0850 F	12/28/69	185	2.10	23.13	8.0	21.3	10/07/71	6/06/83	140.0	161.2	Osteosarcoma {malignant}; Maxilla (Upper jaw bone)
LOWEST	0853 M	12/28/69	285	2.16	23.74	12.0	21.3	10/07/71	12/12/84	158.2	179.5	Inflammation, acute, bronchopneumonia; Lung
LOWEST-SAC	0762 M	6/11/69	0	0.00	0.00	12.8	19.3	1/19/71	1/24/77	72.2	91.5	Scheduled sacrifice, no significant pathology;
LOWEST-SAC	0849 F	12/28/69	37	0.33	3.63	10.2	21.3	10/07/71	10/26/72	12.6	33.9	Scheduled sacrifice, no significant pathology;
LOW	0908 M	7/14/70	315	2.55	28.08	11.2	15.9	11/10/71	4/01/80	100.7	116.6	Cause of death undetermined; Topography unknown
LOW	0893 M	7/11/70	318	2.58	28.41	11.2	14.9	10/07/71	7/01/86	176.8	191.7	Inflammation, acute, bronchopneumonia; Lung
LOW	0776 M	6/28/69	370	2.76	30.33	12.2	20.2	3/04/71	9/19/84	162.6	182.7	Inflammation, acute, bronchopneumonia; Lung
LOW	0841 F	12/16/69	222	2.84	31.27	7.1	17.7	6/08/71	4/01/86	177.8	195.5	Lymphoma {malignant}; Mesenteric lymph node
LOW	0767 M	6/16/69	370	3.06	33.64	11.0	18.2	12/21/70	12/09/85	179.6	197.8	Heart failure (Congestive); Heart
LOW	0842 M	12/16/69	385	3.15	34.67	11.1	18.6	7/06/71	5/01/85	165.8	184.5	Bronchiolo-alveolar adenocarcinoma {malignant}; Lung Lobe, left apical
LOW	0862 M	12/29/69	481	3.58	39.43	12.2	17.3	6/08/71	6/25/83	144.6	161.8	Inflammation, acute; Abdomen, peritoneum and retroperitoneum

DOSE-EFFECT STUDIES WITH INHALED PU-239 OXIDE IN BEAGLES

DOSE GROUP	DOG IDENT	BIRTH DATE	INITIAL ALVEOLAR DEPOSITION BQ	BQ/G LUNG	BQ/ KG	INHALATION EXPOSURE WGT (KG)	AGE (MO)	EXPO DATE	DEATH INFORMATION DEATH DATE	MONTHS POST INH	AGE (MO)	CAUSE OF DEATH
LOW	0871 M	2/08/70	481	3.67	40.42	11.9	16.9	7/06/71	7/24/86	180.6	197.5	Melanoma {malignant}; Mouth
LOW	0874 M	2/11/70	596	4.79	52.72	11.3	16.8	7/06/71	4/09/85	165.1	181.9	Uremia syndrome; Kidney
LOW	0845 F	12/19/69	692	5.11	56.25	12.3	17.6	6/08/71	8/09/84	158.1	175.7	Transitional cell carcinoma {malignant}; Urinary bladder
LOW	0748 F	6/03/69	518	6.36	70.00	7.4	19.5	1/19/71	8/19/81	127.0	146.5	*Cause of death undetermined; Topography unknown*
LOW	0754 M	6/05/69	814	6.73	74.00	11.0	19.5	1/19/71	1/10/78	83.7	103.2	Seizure (Epileptic episode); Brain
LOW	0826 F	12/03/69	703	7.02	77.25	9.1	19.1	7/06/71	4/17/84	153.4	172.5	Hemangioma {benign}; Spleen
LOW	0831 F	12/10/69	777	7.51	82.66	9.4	17.9	6/08/71	5/14/84	155.2	173.1	Inflammation, acute, bronchopneumonia; Lung
LOW	0881 F	4/15/70	696	8.21	90.34	7.7	17.7	10/07/71	12/20/86	182.4	200.2	Inflammation, acute, bronchopneumonia; Lung
LOW	0859 M	12/29/69	1295	8.29	91.20	14.2	18.2	7/06/71	4/22/84	153.6	171.8	Transitional cell carcinoma {malignant}; Urinary bladder
LOW	0813 F	11/30/69	1184	8.75	96.26	12.3	15.1	3/04/71	12/15/83	153.4	168.5	Sarcoma {malignant}; Cranial and facial bone
LOW	0876 F	4/10/70	696	9.30	102.29	6.8	17.9	10/07/71	5/05/86	174.9	192.8	Uremia syndrome; Kidney
LOW	0780 F	7/13/69	888	9.50	104.47	8.5	18.2	1/19/71	4/08/82	134.6	152.8	Pheochromocytoma {malignant}; Adrenal gland
LOW	0806 F	11/23/69	962	9.83	108.09	8.9	15.3	3/04/71	10/29/82	139.9	155.2	Melanoma {malignant}; Soft palate
LOW	0757 M	6/05/69	1332	9.84	108.29	12.3	18.5	12/21/70	11/26/86	191.2	209.7	Leiomyosarcoma {malignant}; Kidney
LOW	0769 F	6/16/69	1036	11.08	121.88	8.5	18.2	12/21/70	6/23/78	90.1	108.2	Granulosa cell tumor {malignant}; Ovary
LOW-SAC	0920 M	2/08/71	407	3.19	35.09	11.6	16.0	6/08/72	7/07/72	1.0	16.9	Scheduled sacrifice, no significant pathology;
LOW-SAC	0798 F	10/21/69	592	5.61	61.67	9.6	15.7	2/10/71	8/29/74	42.6	58.3	Scheduled sacrifice, no significant pathology;
MED-LOW	0802 M	10/21/69	1480	13.06	143.69	10.3	18.1	4/26/71	12/28/84	164.1	182.2	Inflammation, acute, bronchopneumonia; Lung
MED-LOW	0877 F	4/10/70	1258	13.15	144.60	8.7	17.9	10/07/71	5/06/86	174.9	192.9	Squamous cell carcinoma {malignant} (epidermoid carcinoma); Lung Lobe, right diaphragmatic

DOSE-EFFECT STUDIES WITH INHALED PU-239 OXIDE IN BEAGLES

DOSE GROUP	DOG IDENT	BIRTH DATE	INITIAL ALVEOLAR DEPOSITION BQ	BQ/G LUNG	BQ/ KG	INHALATION EXPOSURE WGT (KG)	AGE (MO)	EXPO DATE	DEATH INFORMATION DEATH DATE	MONTHS POST INH	AGE (MO)	CAUSE OF DEATH
MED-LOW	0781 F	7/13/69	1776	14.42	158.57	11.2	17.3	12/21/70	2/20/81	122.0	139.3	Hemangiosarcoma {malignant} (Angiosarcoma); Kidney
MED-LOW	0786 M	7/19/69	2294	15.92	175.11	13.1	19.5	3/04/71	5/29/86	182.8	202.3	Adrenal cortical carcinoma {malignant}; Adrenal gland
MED-LOW	0752 M	6/03/69	2294	16.17	177.83	12.9	18.6	12/21/70	2/22/79	98.1	116.7	Papillary adenocarcinoma {malignant}; Lung Lobe, left cardiac
MED-LOW	0823 M	11/30/69	2405	16.44	180.83	13.3	16.8	4/26/71	5/24/84	156.9	173.8	Transitional cell carcinoma {malignant}; Urethra
MED-LOW	0771 F	6/16/69	1628	16.44	180.89	9.0	19.2	1/20/71	11/02/83	153.4	172.6	Bronchiolo-alveolar adenocarcinoma {malignant}; Lung Lobe, left diaphragmatic
MED-LOW	0838 M	12/12/69	2072	17.77	195.47	10.6	17.8	6/08/71	7/20/84	157.4	175.2	Lymphoma {malignant}; Small intestine
MED-LOW	0782 M	7/13/69	2294	18.29	201.23	11.4	19.0	2/10/71	5/27/83	147.5	166.4	Neurofibrosarcoma {malignant}; Brachial plexus, NOS
MED-LOW	0778 M	6/28/69	2738	18.30	201.32	13.6	20.2	3/04/71	8/26/79	101.7	121.9	Thrombus; Lung
MED-LOW	0883 M	4/15/70	2331	18.92	208.13	11.2	17.7	10/07/71	1/25/88	195.6	213.4	Uremia syndrome; Kidney
MED-LOW	0795 F	10/21/69	1998	19.32	212.55	9.4	15.0	1/20/71	9/06/83	151.5	166.5	Adenosquamous carcinoma {malignant}; Lung Lobe, right apical
MED-LOW	0851 F	12/28/69	1961	21.74	239.15	8.2	21.3	10/07/71	12/07/86	182.0	203.3	Carcinoma {malignant}; Thyroid gland
MED-LOW	0834 F	12/12/69	2479	24.77	272.42	9.1	17.8	6/08/71	7/05/79	96.9	114.7	Pyometra; Uterus
MED-LOW	0797 F	10/21/69	3145	30.42	334.57	9.4	16.4	3/04/71	5/16/86	182.4	198.8	Papillary adenocarcinoma {malignant}; Lung Lobe, right diaphragmatic
MED-LOW	0750 M	6/03/69	4366	31.75	349.28	12.5	19.6	1/20/71	6/28/84	161.2	180.8	Papillary adenocarcinoma {malignant}; Lung Lobe, right intermediate
MED-LOW	0827 F	12/03/69	3293	31.85	350.32	9.4	16.7	4/26/71	1/06/85	164.4	181.1	Inflammation, pneumonitis; Lung
MED-LOW	0848 F	12/28/69	2790	32.10	353.14	7.9	21.3	10/07/71	10/02/86	179.8	201.1	Inflammation, acute, bronchopneumonia; Lung

DOSE-EFFECT STUDIES WITH INHALED PU-239 OXIDE IN BEAGLES

DOSE GROUP	DOG IDENT	BIRTH DATE	INITIAL ALVEOLAR DEPOSITION BQ	BQ/G LUNG	BQ/ KG	INHALATION EXPOSURE WGT (KG)	AGE (MO)	EXPO DATE	DEATH INFORMATION DEATH DATE	MONTHS POST INH	AGE (MO)	CAUSE OF DEATH
MED-LOW	0697 M	3/16/69	5180	33.88	372.66	13.9	19.5	10/30/70	5/08/80	114.3	133.7	Heart failure (Congestive); Heart
MED-LOW	0884 M	4/15/70	4551	40.56	446.18	10.2	17.8	10/08/71	9/12/84	155.2	172.9	Squamous cell carcinoma {malignant} (epidermoid carcinoma); Lung Lobe, right diaphragmatic
MED-LOW	0844 F	12/19/69	4995	43.66	480.29	10.4	17.6	6/08/71	8/08/85	170.0	187.6	Uremia syndrome; Kidney
MED-LOW-SAC	0815 M	11/30/69	2516	19.06	209.67	12.0	16.8	4/26/71	5/22/73	24.9	41.7	Scheduled sacrifice, no significant pathology;
MED-LOW-SAC	0918 M	2/08/71	2738	21.64	238.09	11.5	16.0	6/08/72	7/06/72	0.9	16.9	Scheduled sacrifice, no significant pathology;
MEDIUM	0809 F	11/23/69	5809	50.78	558.56	10.4	15.3	3/04/71	5/28/81	122.8	138.1	Cirrhosis; Liver
MEDIUM	0764 F	6/16/69	5846	51.60	567.57	10.3	18.2	12/21/70	7/07/82	138.5	156.7	Adenosquamous carcinoma {malignant}; Lung Lobe, left diaphragmatic
MEDIUM	0814 F	11/30/69	5180	57.43	631.71	8.2	15.1	3/04/71	10/17/79	103.5	118.5	Papillary adenocarcinoma {malignant}; Lung Lobe, right diaphragmatic
MEDIUM	0905 F	7/14/70	4699	58.52	643.70	7.3	15.9	11/10/71	2/07/83	134.9	150.8	Lymphoma {malignant}; Small intestine
MEDIUM	0835 F	12/12/69	6031	58.95	648.49	9.3	16.4	4/26/71	6/25/78	86.0	102.4	Reticulosarcoma {malignant} (Histocytic Lymphosarcoma); Lymphocytic tissue
MEDIUM	0866 M	1/23/70	7400	59.53	654.87	11.3	17.4	7/06/71	6/27/84	155.7	173.1	Adenosquamous carcinoma {malignant}; Lung Lobe, right intermediate
MEDIUM	0836 M	12/12/69	9472	61.95	681.44	13.9	17.8	6/08/71	3/16/81	117.3	135.1	Papillary adenocarcinoma {malignant}; Lung Lobe, right apical
MEDIUM	0839 F	12/16/69	6993	63.57	699.30	10.0	16.3	4/26/71	2/03/86	177.3	193.6	Papillary adenocarcinoma {malignant}; Lung Lobe, left diaphragmatic
MEDIUM	0860 M	12/29/69	9398	65.72	722.92	13.0	17.3	6/08/71	6/24/82	132.5	149.8	Papillary adenocarcinoma {malignant}; Lung Lobe, right diaphragmatic
MEDIUM	0819 F	11/30/69	6031	66.86	735.49	8.2	18.2	6/08/71	8/20/85	170.4	188.6	Papillary adenocarcinoma {malignant}; Lung Lobe, left diaphragmatic

DOSE-EFFECT STUDIES WITH INHALED PU-239 OXIDE IN BEAGLES

			INITIAL ALVEOLAR DEPOSITION			INHALATION EXPOSURE			DEATH INFORMATION			
DOSE GROUP	DOG IDENT	BIRTH DATE	BQ	BQ/G LUNG	BQ/ KG	WGT (KG)	AGE (MO)	EXPO DATE	DEATH DATE	MONTHS POST INH	AGE (MO)	CAUSE OF DEATH
MEDIUM	0824 F	12/03/69	8399	70.70	777.69	10.8	18.1	6/08/71	1/26/81	115.6	133.8	Inflammation, acute, bronchopneumonia; Lung
MEDIUM	0888 M	5/04/70	10138	72.57	798.27	12.7	17.1	10/08/71	7/02/79	92.8	109.9	Papillary adenocarcinoma {malignant}; Lung Lobe, right intermediate
MEDIUM	0833 F	12/10/69	9176	83.42	917.60	10.0	16.5	4/26/71	4/04/83	143.3	159.8	Pyometra; Uterus
MEDIUM	0810 F	11/23/69	11174	94.06	1034.63	10.8	15.3	3/04/71	9/09/81	126.2	141.5	Adenosquamous carcinoma {malignant}; Lung Lobe, right apical
MEDIUM	0808 F	11/23/69	9990	104.39	1148.28	8.7	14.6	2/10/71	9/09/82	138.9	153.5	Papillary adenocarcinoma {malignant}; Lung Lobe, right diaphragmatic
MEDIUM	0805 F	11/23/69	9509	112.27	1234.94	7.7	18.5	6/08/71	7/22/82	133.5	151.9	Papillary adenocarcinoma {malignant}; Lung Lobe, right cardiac
MEDIUM	0794 M	9/11/69	16428	114.00	1254.05	13.1	17.7	3/04/71	2/17/81	119.5	137.2	Adenoma {benign}; Pituitary gland
MEDIUM	0854 M	12/28/69	17205	115.01	1265.07	13.6	21.3	10/08/71	1/25/82	123.6	144.9	Papillary adenocarcinoma {malignant}; Lung Lobe, left apical
MEDIUM	0857 M	12/29/69	17982	132.90	1461.95	12.3	17.3	6/08/71	7/01/80	108.8	126.1	Adenosquamous carcinoma {malignant}; Lung Lobe, right apical
MEDIUM	0892 M	7/11/70	18278	134.00	1474.03	12.4	16.0	11/10/71	10/26/81	119.5	135.5	Bronchiolo-alveolar adenocarcinoma {malignant}; Lung Lobe, left cardiac
MEDIUM	0812 M	11/23/69	16206	137.69	1514.58	10.7	17.1	4/26/71	11/12/79	102.6	119.6	Bronchiolo-alveolar adenocarcinoma {malignant}; Lung Lobe, right apical
MEDIUM	0777 M	6/28/69	20202	158.32	1741.55	11.6	20.2	3/04/71	3/26/80	108.7	128.9	Papillary adenocarcinoma {malignant}; Lung Lobe, right apical
MEDIUM	0787 M	7/19/69	24087	172.42	1896.61	12.7	19.5	3/04/71	2/08/79	95.2	114.7	Bronchiolo-alveolar adenocarcinoma {malignant}; Lung Lobe, left diaphragmatic
MEDIUM	0803 M	10/21/69	20239	175.23	1927.52	10.5	18.1	4/26/71	11/10/77	78.5	96.7	Inflammation, pneumonitis; Lung
MEDIUM-SAC	0478 M	6/08/65	11026	98.27	1080.98	10.2	64.0	10/09/70	10/16/70	0.2	64.3	Scheduled sacrifice, no significant pathology;

DOSE-EFFECT STUDIES WITH INHALED PU-239 OXIDE IN BEAGLES

DOSE GROUP	DOG IDENT	BIRTH DATE	INITIAL ALVEOLAR DEPOSITION BQ	BQ/G LUNG	BQ/ KG	INHALATION EXPOSURE WGT (KG)	AGE (MO)	EXPO DATE	DEATH INFORMATION DEATH DATE	MONTHS POST INH	AGE (MO)	CAUSE OF DEATH
MEDIUM-SAC	0816 M	11/30/69	14726	131.25	1443.73	10.2	16.8	4/25/71	5/11/71	0.5	17.3	Scheduled sacrifice, no significant pathology;
MED-HIGH	0840 F	12/16/69	26011	223.08	2453.87	10.6	17.7	6/08/71	4/29/80	106.7	124.4	Papillary adenocarcinoma {malignant}; Lung Lobe, right cardiac
MED-HIGH	0898 F	7/12/70	26307	223.51	2458.60	10.7	16.0	11/10/71	2/03/81	110.8	126.8	Transitional cell carcinoma {malignant}; Urinary bladder
MED-HIGH	0727 M	4/03/69	27121	224.14	2465.55	11.0	18.8	10/26/70	11/10/76	72.5	91.3	Papillary adenocarcinoma {malignant}; Lung Lobe, left cardiac
MED-HIGH	0856 F	12/29/69	30266	237.19	2609.14	11.6	18.2	7/07/71	5/02/79	93.8	112.1	Papillary adenocarcinoma {malignant}; Lung Lobe, right apical
MED-HIGH	0759 M	6/11/69	29933	256.72	2823.87	10.6	18.3	12/21/70	6/02/75	53.4	71.7	Papillary adenocarcinoma {malignant}; Lung Lobe, left apical
MED-HIGH	0909 M	7/14/70	27269	258.23	2840.52	9.6	15.9	11/10/71	6/04/81	114.8	130.7	Papillary adenocarcinoma {malignant}; Lung Lobe, left apical
MED-HIGH	0864 F	1/23/70	29637	261.58	2877.38	10.3	17.4	7/07/71	11/02/79	99.9	117.3	Papillary adenocarcinoma {malignant}; Lung Lobe, left diaphragmatic
MED-HIGH	0863 F	1/23/70	36260	316.96	3486.54	10.4	17.4	7/07/71	10/21/77	75.5	92.9	Adenosquamous carcinoma {malignant}; Lung Lobe, left apical
MED-HIGH	0837 M	12/12/69	47471	322.06	3542.61	13.4	18.8	7/07/71	7/21/77	72.5	91.3	Papillary adenocarcinoma {malignant}; Lung Lobe, right apical
MED-HIGH	0820 F	11/30/69	31339	360.63	3966.96	7.9	18.2	6/08/71	6/01/79	95.8	114.0	Bronchiolo-alveolar adenocarcinoma {malignant}; Lung Lobe, left diaphragmatic
MED-HIGH	0783 M	7/13/69	51578	366.32	4029.53	12.8	19.0	2/10/71	12/03/75	57.7	76.7	Adenosquamous carcinoma {malignant}; Lung Lobe, right cardiac
MED-HIGH	0804 M	10/21/69	49728	367.54	4042.93	12.3	20.5	7/07/71	8/18/74	37.4	57.9	Bronchiolo-alveolar adenocarcinoma {malignant}; Lung Lobe, right cardiac
MED-HIGH	0880 F	4/15/70	31080	371.77	4089.47	7.6	17.8	10/08/71	12/04/78	85.9	103.7	Adenosquamous carcinoma {malignant}; Lung Lobe, right diaphragmatic

DOSE-EFFECT STUDIES WITH INHALED PU-239 OXIDE IN BEAGLES

DOSE GROUP	DOG IDENT	BIRTH DATE	INITIAL ALVEOLAR DEPOSITION BQ	BQ/G LUNG	BQ/ KG	INHALATION EXPOSURE WGT (KG)	AGE (MO)	EXPO DATE	DEATH INFORMATION DEATH DATE	MONTHS POST INH	AGE (MO)	CAUSE OF DEATH
MED-HIGH	0852 F	12/28/69	43919	383.91	4222.98	10.4	21.3	10/08/71	2/22/78	76.5	97.8	Adenosquamous carcinoma {malignant}; Lung Lobe, right apical
MED-HIGH	0889 F	7/11/70	40293	389.68	4286.49	9.4	16.0	11/10/71	9/20/79	94.3	110.3	Adenosquamous carcinoma {malignant}; Lung Lobe, right apical
MED-HIGH	0873 M	2/11/70	65379	437.03	4807.28	13.6	16.8	7/07/71	9/03/76	61.9	78.7	Bronchiolo-alveolar adenocarcinoma {malignant}; Lung Lobe, left cardiac
MED-HIGH	0760 M	6/11/69	50986	450.01	4950.10	10.3	19.3	1/20/71	8/15/73	30.8	50.1	Inflammation, pneumonitis, radiation induced; Lung
MED-HIGH	0796 F	10/21/69	48766	461.80	5079.79	9.6	15.7	2/10/71	9/17/75	55.2	70.9	Squamous cell carcinoma {malignant} (epidermoid carcinoma); Lung Lobe, left diaphragmatic
MED-HIGH	0761 M	6/11/69	54020	522.44	5746.81	9.4	19.3	1/20/71	11/02/76	69.4	88.7	Bronchiolo-alveolar adenocarcinoma {malignant}; Lung Lobe, right diaphragmatic
MED-HIGH	0772 M	6/16/69	70152	535.92	5895.13	11.9	19.8	2/10/71	6/26/75	52.5	72.3	Bronchiolo-alveolar adenocarcinoma {malignant}; Lung Lobe, left apical
MED-HIGH-SAC	0734 M	4/04/69	33818	267.34	2940.70	11.5	19.2	11/10/70	4/01/71	4.7	23.9	Scheduled sacrifice, no significant pathology;
MED-HIGH-SAC	0709 M	3/24/69	63862	483.80	5321.83	12.0	19.6	11/10/70	3/31/71	4.6	24.2	Scheduled sacrifice, no significant pathology;
MED-HIGH-SAC	0702 F	3/17/69	62234	601.88	6620.64	9.4	19.8	11/10/70	3/31/71	4.6	24.4	Scheduled sacrifice, no significant pathology;
MED-HIGH-SAC	0739 F	4/25/69	55907	736.59	8102.46	6.9	18.5	11/10/70	4/01/71	4.7	23.2	Scheduled sacrifice, no significant pathology;
HIGH	0817 M	11/30/69	117068	858.27	9440.97	12.4	19.2	7/07/71	3/26/73	20.6	39.8	Inflammation, pneumonitis, radiation induced; Lung
HIGH	0829 M	12/03/69	130055	869.35	9562.87	13.6	19.1	7/07/71	9/13/73	26.3	45.3	Inflammation, pneumonitis, radiation induced; Lung
HIGH	0753 F	6/05/69	90576	1069.37	11763.12	7.7	18.5	12/21/70	10/02/76	69.4	87.9	Bronchiolo-alveolar adenocarcinoma {malignant}; Lung Lobe, left diaphragmatic
HIGH	0890 F	7/11/70	114737	1171.98	12891.80	8.9	16.0	11/10/71	6/13/74	31.1	47.1	Inflammation, pneumonitis, radiation induced; Lung

DOSE-EFFECT STUDIES WITH INHALED PU-239 OXIDE IN BEAGLES

			INITIAL ALVEOLAR DEPOSITION			INHALATION EXPOSURE			DEATH INFORMATION			
DOSE GROUP	DOG IDENT	BIRTH DATE	BQ	BQ/G LUNG	BQ/ KG	WGT (KG)	AGE (MO)	EXPO DATE	DEATH DATE	MONTHS POST INH	AGE (MO)	CAUSE OF DEATH
HIGH	0906 F	7/14/70	245384	2348.17	25829.89	9.5	15.9	11/09/71	11/22/72	12.5	28.3	Inflammation, pneumonitis, radiation induced; Lung
HIGH	0896 F	7/12/70	204055	2473.39	27207.33	7.5	16.0	11/10/71	2/12/73	15.1	31.1	Inflammation, pneumonitis, radiation induced; Lung
HIGH	0747 F	6/03/69	276612	3929.15	43220.63	6.4	19.6	1/20/71	1/13/72	11.8	31.3	Inflammation, pneumonitis, radiation induced; Lung
HIGH	0910 M	7/14/70	527879	4323.33	47556.67	11.1	15.9	11/10/71	10/12/72	11.1	27.0	Inflammation, pneumonitis, radiation induced; Lung
HIGH-SAC	0435 F	7/21/64	142080	1207.14	13278.50	10.7	75.5	11/05/70	11/12/70	0.2	75.7	Scheduled sacrifice, no significant pathology;
HIGH-SAC	0913 M	2/04/71	181300	1385.03	15235.29	11.9	17.4	7/19/72	8/18/72	1.0	18.4	Scheduled sacrifice, no significant pathology;

DOSE-EFFECT STUDIES WITH INHALED PU-238 OXIDE IN BEAGLES

DOSE GROUP	DOG IDENT	BIRTH DATE	INITIAL ALVEOLAR DEPOSITION BQ	BQ/G LUNG	BQ/ KG	INHALATION EXPOSURE WGT (KG)	AGE (MO)	EXPO DATE	DEATH INFORMATION DEATH DATE	MONTHS POST INH	AGE (MO)	COMMENTS ON DEAD DOGS
CONTROL	0939 M	5/05/71	0	0.00	0.00	13.3	19.5	12/19/72	10/01/82	117.4	136.9	Transitional Carcinoma, Urinary Bladder
CONTROL	0949 F	5/11/71	0	0.00	0.00	12.1	19.3	12/19/72	10/30/84	142.4	161.7	Malignant Lymphoma
CONTROL	0978 M	5/15/71	0	0.00	0.00	15.4	19.2	12/19/72	4/07/88	183.6	202.8	Herniated Vertebral Disc
CONTROL	0990 F	5/26/71	0	0.00	0.00	7.9	18.8	12/19/72	7/08/79	78.6	97.4	Pyometra
CONTROL	0996 F	5/31/71	0	0.00	0.00	11.7	19.6	1/18/73	7/06/84	137.6	157.2	Malignant Lymphoma
CONTROL	1005 M	5/31/71	0	0.00	0.00	9.8	19.6	1/18/73	2/24/87	169.2	188.8	Lung Tumor
CONTROL	1007 F	6/02/71	0	0.00	0.00	11.2	19.6	1/18/73	3/29/88	182.3	201.9	Chronic Nephropathy
CONTROL	1024 M	6/15/71	0	0.00	0.00	14.5	19.2	1/18/73	7/13/87	173.8	192.9	Transitional Carcinoma, Urethra
CONTROL	1038 M	8/19/71	0	0.00	0.00	14.1	18.2	2/22/73	12/16/86	165.7	183.9	Hemangiosarcoma, Spleen
CONTROL	1045 M	8/20/71	0	0.00	0.00	11.4	18.1	2/22/73	6/08/86	159.5	177.6	Renal Amyloidosis; Hemangiosarcoma, Spleen
CONTROL	1054 F	8/27/71	0	0.00	0.00	9.0	17.9	2/22/73	12/05/88	189.4	207.3	Chronic Nephropathy
CONTROL	1061 F	8/30/71	0	0.00	0.00	13.1	17.8	2/22/73	7/07/81	100.4	118.2	Malignant Lymphoma
CONTROL	1093 M	12/22/71	0	0.00	0.00	14.0	17.3	5/31/73	11/04/83	125.1	142.4	Adenoma, Pituitary; Cushing's Disease
CONTROL	1097 F	1/11/72	0	0.00	0.00	7.6	16.6	5/31/73	9/15/88	183.5	200.1	Nasal Transitional Carcinoma
CONTROL	1112 M	1/19/72	0	0.00	0.00	13.6	16.4	5/31/73	12/02/86	162.1	178.4	Malignant Lymphoma
CONTROL	1116 F	1/27/72	0	0.00	0.00	12.2	16.1	5/31/73	4/07/89	190.2	206.3	Hemangiosarcoma, Omentum
CONTROL	1186 F	8/16/72	0	0.00	0.00	9.4	18.3	2/25/74	7/26/85	137.0	155.3	Transitional Carcinoma, Urinary Bladder
CONTROL	1197 M	8/31/72	0	0.00	0.00	12.2	17.8	2/25/74	4/25/89	181.9	199.8	Pneumonia
CONTROL	1209 M	9/09/72	0	0.00	0.00	12.6	17.5	2/25/74	12/27/88	178.0	195.6	Pulmonary Interstial Fibrosis
CONTROL	1225 F	10/04/72	0	0.00	0.00	7.8	16.8	2/26/74	10/10/87	163.4	180.2	Adenoma, Pituitary

DOSE-EFFECT STUDIES WITH INHALED PU-238 OXIDE IN BEAGLES

			INITIAL ALVEOLAR DEPOSITION			INHALATION EXPOSURE			DEATH INFORMATION			
DOSE GROUP	DOG IDENT	BIRTH DATE	BQ	BQ/G LUNG	BQ/ KG	WGT (KG)	AGE (MO)	EXPO DATE	DEATH DATE	MONTHS POST INH	AGE (MO)	COMMENTS ON DEAD DOGS
CONTROL-SAC	0966 M	5/14/71	0	0.00	0.00	13.0	19.2	12/19/72	4/30/77	52.3	71.6	Sacrificed
CONTROL-SAC	1011 F	6/04/71	0	0.00	0.00	10.8	19.5	1/18/73	6/01/78	64.4	83.9	Sacrificed
CONTROL-SAC	1013 F	6/04/71	0	0.00	0.00	11.5	19.5	1/18/73	5/29/79	76.3	95.8	Sacrificed
CONTROL-SAC	1087 M	12/15/71	0	0.00	0.00	13.6	17.5	5/31/73	12/14/76	42.5	60.0	Sacrificed
CONTROL-SAC	1118 M	1/27/72	0	0.00	0.00	8.4	16.1	5/31/73	1/13/76	31.4	47.5	Sacrificed
CONTROL-SAC	1223 M	9/16/72	0	0.00	0.00	12.2	19.0	4/18/74	5/15/75	12.9	31.9	Sacrificed
CONTROL-SAC	1227 M	10/04/72	0	0.00	0.00	9.5	18.4	4/18/74	12/01/76	31.5	49.9	Sacrificed
CONTROL-SAC	1228 M	10/04/72	0	0.00	0.00	14.4	18.4	4/18/74	10/31/78	54.4	72.9	Sacrificed
LOWEST	0998 M	5/31/71	0	0.00	0.00	10.4	19.6	1/18/73	4/11/86	158.7	178.4	Lung Tumor
LOWEST	1003 M	5/31/71	0	0.00	0.00	12.5	19.6	1/18/73	4/01/87	170.4	190.0	Transitional Carcinoma, Urinary Bladder
LOWEST	1023 F	6/15/71	0	0.00	0.00	11.6	19.2	1/18/73	3/27/88	182.2	201.4	Pneumonia
LOWEST	1039 M	8/19/71	0	0.00	0.00	11.0	17.0	1/18/73	7/04/86	161.5	178.5	Heart Failure
LOWEST	1044 F	8/20/71	0	0.00	0.00	9.9	17.0	1/18/73	8/31/88	187.4	204.4	Epileptic Seizures
LOWEST	1055 M	8/27/71	0	0.00	0.00	10.8	16.8	1/18/73	6/04/87	172.5	189.2	Malignant Melanoma, Oral Cavity
LOWEST	1063 M	8/30/71	0	0.00	0.00	12.3	16.7	1/18/73	11/11/80	93.8	110.4	Brain Tumor
LOWEST	1105 F	1/19/72	0	0.00	0.00	9.8	16.4	5/31/73	2/08/85	140.3	156.7	Malignant Lymphoma
LOWEST	1194 F	8/24/72	0	0.00	0.00	10.2	19.8	4/18/74	12/03/85	139.5	159.3	Malignant Lymphoma
LOWEST	1230 M	10/04/72	0	0.00	0.00	12.1	18.4	4/18/74	9/30/86	149.4	167.9	Hemangiosarcoma, Liver
LOWEST	1008 M	6/02/71	74	0.51	5.65	13.1	19.6	1/18/73	10/24/85	153.2	172.7	Fibrosarcoma, Spleen
LOWEST	0951 M	5/11/71	74	0.52	5.74	12.9	19.3	12/19/72	2/14/83	121.9	141.2	Anesthetic Death

DOSE-EFFECT STUDIES WITH INHALED PU-238 OXIDE IN BEAGLES

DOSE GROUP	DOG IDENT	BIRTH DATE	INITIAL ALVEOLAR DEPOSITION BQ	BQ/G LUNG	BQ/ KG	INHALATION EXPOSURE WGT (KG)	AGE (MO)	EXPO DATE	DEATH INFORMATION DEATH DATE	MONTHS POST INH	AGE (MO)	COMMENTS ON DEAD DOGS
LOWEST	1193 F	8/24/72	74	0.54	5.97	12.4	19.8	4/18/74	1/22/86	141.2	161.0	Immune Hemolytic Anemia
LOWEST	1095 F	1/11/72	74	0.65	7.18	10.3	16.6	5/31/73	8/12/87	170.4	187.0	Chronic Nephropathy
LOWEST	1069 F	11/26/71	74	0.72	7.96	9.3	18.1	5/31/73	6/24/83	120.8	138.9	Malignant Lymphoma
LOWEST	0959 M	5/14/71	111	0.83	9.10	12.2	19.2	12/19/72	6/22/84	138.1	157.3	Liver Abscess
LOWEST	0989 F	5/26/71	111	1.00	10.99	10.1	18.8	12/19/72	3/05/81	98.5	117.3	Bone Tumor
LOWEST	1204 M	9/05/72	222	1.55	17.08	13.0	17.7	2/26/74	2/23/89	179.9	197.6	Transitional Carcinoma, Urethra
LOWEST	0993 F	5/26/71	222	1.63	17.90	12.4	18.8	12/19/72	7/01/86	162.4	181.2	Malignant Lymphoma
LOWEST	1106 F	1/19/72	185	1.65	18.14	10.2	16.4	5/31/73	3/14/83	117.4	133.8	Carcinoma, Adrenal; Osteoarthropathy
LOWEST-SAC	1215 M	9/09/72	0	0.00	0.00	15.0	19.3	4/18/74	4/26/77	36.3	55.5	Sacrificed
LOWEST-SAC	0921 F	4/15/71	115	0.92	10.15	11.3	19.5	11/30/72	12/27/72	0.9	20.4	Sacrificed
LOWEST-SAC	0923 F	4/15/71	111	1.11	12.20	9.1	19.5	11/30/72	1/26/73	1.9	21.4	Sacrificed
LOWEST-SAC	0925 M	4/15/71	185	1.44	15.81	11.7	19.5	11/30/72	2/27/73	2.9	22.5	Sacrificed
LOWEST-SAC	0970 F	5/15/71	222	1.77	19.47	11.4	19.2	12/19/72	1/04/77	48.5	67.7	Sacrificed
LOW	1065 F	11/20/71	222	2.22	24.40	9.1	18.3	5/31/73	4/10/86	154.3	172.6	Malignant Lymphoma; Lung Tumor
LOW	1188 M	8/16/72	407	2.76	30.37	13.4	18.4	2/26/74	1/15/84	118.9	137.0	Metastatic Lung Tumor, Primary Site Unknown
LOW	1082 M	11/29/71	407	2.78	30.60	13.3	18.0	5/31/73	12/04/79	78.1	96.2	Paralysis, Spinal Cord Degeneration
LOW	1084 M	12/15/71	481	3.02	33.17	14.5	17.5	5/31/73	8/19/89	194.6	212.1	Malignant Lymphoma, Heart
LOW	1090 F	12/22/71	370	3.58	39.36	9.4	17.3	5/31/73	5/10/87	167.3	184.6	Heart Failure
LOW	1222 M	9/16/72	555	3.66	40.22	13.8	19.0	4/18/74	3/19/86	143.0	162.0	Malignant Mesothelioma
LOW	0999 F	5/31/71	407	4.20	46.25	8.8	18.7	12/19/72	1/31/86	157.4	176.1	Nasal Sarcoma; Lung Tumor

DOSE-EFFECT STUDIES WITH INHALED PU-238 OXIDE IN BEAGLES

DOSE GROUP	DOG IDENT	BIRTH DATE	INITIAL ALVEOLAR DEPOSITION BQ	BQ/G LUNG	BQ/ KG	INHALATION EXPOSURE WGT (KG)	AGE (MO)	EXPO DATE	DEATH INFORMATION DEATH DATE	MONTHS POST INH	AGE (MO)	COMMENTS ON DEAD DOGS
LOW	0971 F	5/15/71	481	4.42	48.59	9.9	19.2	12/19/72	5/04/83	124.5	143.6	Hemangiosarcoma, Spleen
LOW	1229 M	10/04/72	592	4.45	48.93	12.1	16.8	2/26/74	5/25/84	122.9	139.7	Pneumonia; Carcinoma, Thyroid
LOW	1036 F	8/19/71	592	4.89	53.82	11.0	18.2	2/22/73	5/06/87	170.4	188.6	Malignant Melanoma, Oral Cavity
LOW	1070 M	11/26/71	814	5.48	60.30	13.5	18.1	5/31/73	12/13/83	126.4	144.6	Malignant Lymphoma
LOW	0955 M	5/14/71	629	5.66	62.28	10.1	19.2	12/19/72	1/27/87	169.3	188.5	Lung Tumor; Adenoma, Bile Duct
LOW	1216 M	9/09/72	851	6.85	75.31	11.3	19.3	4/18/74	4/22/87	156.1	175.4	Malignant Lymphoma
LOW	1060 F	8/30/71	814	6.85	75.37	10.8	17.8	2/22/73	12/21/84	141.9	159.7	Pneumonia
LOW	1033 M	7/23/71	629	6.97	76.71	8.2	19.1	2/22/73	12/17/85	153.8	172.8	Lung Tumor
LOW	1050 F	8/22/71	814	8.22	90.44	9.0	18.1	2/22/73	5/14/86	158.7	176.7	Lung Tumor
LOW	1078 F	11/29/71	1073	8.34	91.71	11.7	18.0	5/31/73	11/09/83	125.3	143.3	Malignant Meningioma
LOW	1207 F	9/09/72	814	8.92	98.07	8.3	17.6	2/26/74	8/11/88	173.5	191.0	Herniated Vertebral Disc
LOW	0981 M	5/20/71	1110	9.26	101.83	10.9	19.0	12/19/72	1/12/89	192.8	211.8	Chronic Nephropathy
LOW	1046 M	8/20/71	999	9.46	104.06	9.6	18.1	2/22/73	12/15/87	177.7	195.8	Lung Tumor
LOW	1196 F	8/31/72	1036	11.21	123.33	8.4	17.9	2/26/74	12/26/88	178.0	195.8	Carcinoma, Salivary Gland; Lung Tumor
LOW-SAC	1214 M	9/09/72	629	5.20	57.18	11.0	19.3	4/18/74	5/12/75	12.8	32.0	Sacrificed
LOW-SAC	1189 M	8/16/72	1406	9.47	104.15	13.5	20.0	4/18/74	4/25/79	60.2	80.3	Sacrificed
LOW-SAC	0930 M	4/27/71	1406	9.91	108.99	12.9	19.2	11/30/72	12/28/72	0.9	20.1	Sacrificed
MED-LOW	0972 F	5/15/71	1480	11.80	129.82	11.4	19.2	12/19/72	3/04/86	158.5	177.6	Allergic Bronchitis
MED-LOW	1089 F	12/22/71	1517	13.01	143.11	10.6	17.3	5/31/73	8/21/88	182.7	200.0	Chronic Nephropathy
MED-LOW	1066 M	11/20/71	1998	13.36	146.91	13.6	18.3	5/31/73	6/21/83	120.7	139.0	Malignant Lymphoma

DOSE-EFFECT STUDIES WITH INHALED PU-238 OXIDE IN BEAGLES

DOSE GROUP	DOG IDENT	BIRTH DATE	INITIAL ALVEOLAR DEPOSITION BQ	BQ/G LUNG	BQ/ KG	INHALATION EXPOSURE WGT (KG)	AGE (MO)	EXPO DATE	DEATH INFORMATION DEATH DATE	MONTHS POST INH	AGE (MO)	COMMENTS ON DEAD DOGS
MED-LOW	1219 F	9/16/72	1702	15.02	165.24	10.3	19.0	4/18/74	12/05/86	151.6	170.6	Chronic Nephropathy
MED-LOW	1165 M	5/27/72	2812	18.52	203.77	13.8	17.3	11/06/73	7/21/86	152.4	169.8	Pneumonia
MED-LOW	1158 M	5/15/72	2701	20.13	221.39	12.2	17.7	11/06/73	6/16/88	175.3	193.1	Nasal Carcinoma
MED-LOW	1309 M	8/18/73	2220	20.18	222.00	10.0	18.5	3/04/75	4/22/87	145.6	164.1	Hemangiosarcoma, Liver
MED-LOW	1059 F	8/30/71	2627	20.59	226.47	11.6	17.8	2/22/73	8/08/83	125.5	143.3	Malignant Lymphoma
MED-LOW	1190 F	8/24/72	2627	21.32	234.55	11.2	18.1	2/26/74	5/09/85	134.4	152.5	Lung Tumor
MED-LOW	0960 M	5/14/71	2516	22.21	244.27	10.3	19.2	12/19/72	11/07/80	94.6	113.8	Malignant Lymphoma
MED-LOW	0982 M	5/20/71	2812	23.24	255.64	11.0	19.0	12/19/72	1/29/86	157.3	176.4	Pneumonia; Carcinoma, Thyroid
MED-LOW	1316 M	8/29/73	3108	23.35	256.86	12.1	18.1	3/04/75	12/13/88	165.4	183.5	Ankylosis Spondylitis
MED-LOW	1072 M	11/26/71	3626	25.36	278.92	13.0	18.1	5/31/73	9/22/83	123.7	141.9	Radiation Pneumonitis, Delayed
MED-LOW	1000 F	5/31/71	2590	26.16	287.78	9.0	18.7	12/19/72	12/02/87	179.4	198.1	Transitional Carcinoma, Urinary Bladder
MED-LOW	1040 M	8/19/71	3108	26.41	290.47	10.7	18.2	2/22/73	3/04/81	96.3	114.5	Heart Failure
MED-LOW	1108 F	1/19/72	3108	26.41	290.47	10.7	16.4	5/31/73	1/14/87	163.5	179.8	Posterior Paralysis
MED-LOW	1004 M	5/31/71	4292	31.72	348.94	12.3	19.6	1/18/73	4/30/87	171.3	191.0	Malignant Lymphoma; Lung Tumor; Carcinoma, Bile Duct
MED-LOW	1221 F	9/16/72	4588	32.84	361.26	12.7	19.0	4/18/74	9/30/88	173.4	192.5	Malignant Lymphoma; Carcinoma, Bile Duct
MED-LOW	1026 M	6/15/71	4292	33.35	366.84	11.7	19.2	1/18/73	11/13/85	153.8	173.0	Hepatic Dysplasia
MED-LOW	1056 M	8/27/71	3589	34.34	377.79	9.5	17.9	2/22/73	6/17/86	159.8	177.7	Pneumonia; Carcinoma, Thyroid
MED-LOW	1031 F	7/23/71	2812	35.02	385.21	7.3	19.1	2/22/73	5/04/84	134.3	153.4	Pneumonia
MED-LOW	1043 F	8/20/71	3626	40.70	447.65	8.1	18.1	2/22/73	9/21/81	102.9	121.1	Empyema; Adenoma, Pituitary; Cushing's Disease
MED-LOW-SAC	1312 M	8/18/73	2146	12.59	138.45	15.5	18.5	3/04/75	3/26/79	48.7	67.2	Sacrificed

DOSE-EFFECT STUDIES WITH INHALED PU-238 OXIDE IN BEAGLES

			INITIAL ALVEOLAR DEPOSITION			INHALATION EXPOSURE			DEATH INFORMATION			
DOSE GROUP	DOG IDENT	BIRTH DATE	BQ	BQ/G LUNG	BQ/ KG	WGT (KG)	AGE (MO)	EXPO DATE	DEATH DATE	MONTHS POST INH	AGE (MO)	COMMENTS ON DEAD DOGS
MED-LOW-SAC	1310 M	8/18/73	1998	14.08	154.88	12.9	18.5	3/04/75	4/01/77	24.9	43.4	Sacrificed
MED-LOW-SAC	1311 M	8/18/73	1998	14.77	162.44	12.3	18.5	3/04/75	4/03/78	37.0	55.5	Sacrificed
MED-LOW-SAC	1317 M	8/29/73	2664	18.63	204.92	13.0	18.1	3/04/75	4/01/77	24.9	43.1	Sacrificed
MED-LOW-SAC	1318 M	8/29/73	2479	20.12	221.34	11.2	18.1	3/04/75	3/08/76	12.2	30.3	Sacrificed
MED-LOW-SAC	0929 F	4/27/71	1517	22.61	248.69	6.1	19.2	11/30/72	1/25/73	1.8	21.0	Sacrificed
MED-LOW-SAC	0926 M	4/15/71	2775	23.58	259.35	10.7	19.5	11/30/72	2/28/73	3.0	22.5	Sacrificed
MED-LOW-SAC	1315 M	8/29/73	3330	27.03	297.32	11.2	18.1	3/04/75	3/31/77	24.9	43.0	Sacrificed
MED-LOW-SAC	1319 M	8/29/73	3663	29.47	324.16	11.3	18.1	3/04/75	3/09/76	12.2	30.3	Sacrificed
MEDIUM	1176 M	6/20/72	4773	35.28	388.05	12.3	16.6	11/06/73	12/12/85	145.2	161.7	Hemangioma, Spleen
MEDIUM	1212 F	9/09/72	4107	47.87	526.54	7.8	17.6	2/26/74	6/24/88	171.9	189.5	Hepatocellular Carcinoma
MEDIUM	1053 F	8/27/71	5476	54.71	601.76	9.1	17.9	2/22/73	2/02/85	143.3	161.2	Cushing's Disease
MEDIUM	1195 M	8/24/72	8436	55.98	615.77	13.7	18.1	2/26/74	7/29/87	161.0	179.1	Chronic Nephropathy; Adenoma, Bile Duct
MEDIUM	0997 M	5/31/71	7511	63.81	701.96	10.7	19.6	1/18/73	5/08/86	159.6	179.3	Lung Tumor
MEDIUM	1177 M	6/20/72	9694	65.28	718.07	13.5	16.6	11/06/73	3/12/85	136.1	152.7	Bone Tumor
MEDIUM	0991 F	5/26/71	7178	73.32	806.52	8.9	18.8	12/19/72	6/20/83	126.0	144.8	Transitional Carcinoma, Urinary Bladder
MEDIUM	1103 F	1/14/72	9620	76.05	836.52	11.5	16.5	5/31/73	4/08/83	118.2	134.8	Bone Tumor; Lung Tumor
MEDIUM	1091 F	12/22/71	8991	95.04	1045.47	8.6	17.3	5/31/73	11/10/86	161.3	178.6	Carcinoma, Thyroid
MEDIUM	0973 F	5/15/71	10027	99.08	1089.89	9.2	19.2	12/19/72	10/08/84	141.6	160.8	Bone Tumor
MEDIUM	1114 M	1/19/72	15910	111.26	1223.85	13.0	16.4	5/31/73	4/23/85	142.8	159.1	Bone Tumor; Carcinoma, Bile Duct
MEDIUM	1062 M	8/30/71	16095	113.42	1247.67	12.9	17.8	2/22/73	5/30/84	135.2	153.0	Bone Tumor; Lung Tumor

DOSE-EFFECT STUDIES WITH INHALED PU-238 OXIDE IN BEAGLES

DOSE GROUP	DOG IDENT	BIRTH DATE	INITIAL ALVEOLAR DEPOSITION BQ	BQ/G LUNG	BQ/ KG	INHALATION EXPOSURE WGT (KG)	AGE (MO)	EXPO DATE	DEATH INFORMATION DEATH DATE	MONTHS POST INH	AGE (MO)	COMMENTS ON DEAD DOGS
MEDIUM	1030 F	7/23/71	12580	125.67	1382.42	9.1	19.1	2/22/73	4/14/83	121.7	140.7	Pneumonia; Radiation Pneumonitis
MEDIUM	1081 M	11/29/71	20017	130.92	1440.07	13.9	18.0	5/31/73	1/18/80	79.6	97.6	Hemangiosarcoma, Heart
MEDIUM	0952 F	5/14/71	13505	137.95	1517.42	8.9	19.2	12/19/72	6/03/83	125.4	144.7	Bone Tumor
MEDIUM	1191 F	8/24/72	21867	152.92	1682.08	13.0	19.8	4/18/74	3/21/77	35.1	54.9	Interstitial Pneumonitis
MEDIUM	1198 M	8/31/72	19943	161.88	1780.63	11.2	17.9	2/26/74	9/14/86	150.6	168.4	Pneumonia; Lung Tumor
MEDIUM	1166 M	5/27/72	24901	162.86	1791.44	13.9	17.3	11/06/73	6/23/84	127.5	144.9	Malignant Lymphoma
MEDIUM	1220 F	9/16/72	19166	164.37	1808.11	10.6	19.0	4/18/74	12/09/86	151.7	170.7	Malignant Lymphoma; Addison's Disease
MEDIUM	0983 M	5/20/71	22829	186.97	2056.67	11.1	19.0	12/19/72	12/29/83	132.3	151.3	Carcinoma, Adrenal; Carcinoma, Pituitary
MEDIUM-SAC	1032 M	7/23/71	5994	52.40	576.35	10.4	16.3	11/30/72	12/08/72	0.3	16.6	Sacrificed
MEDIUM-SAC	0932 F	4/28/71	7992	65.45	720.00	11.1	19.1	11/30/72	1/25/73	1.8	21.0	Sacrificed
MEDIUM-SAC	0931 F	4/28/71	10693	92.58	1018.38	10.5	19.1	11/30/72	12/28/72	0.9	20.0	Sacrificed
MEDIUM-SAC	0934 M	4/28/71	16798	116.57	1282.29	13.1	19.1	11/30/72	3/01/73	3.0	22.1	Sacrificed
MED-HIGH	0992 F	5/26/71	20535	172.85	1901.39	10.8	18.8	12/19/72	7/26/84	139.2	158.0	Bone Tumor
MED-HIGH	1157 M	5/15/72	25900	197.86	2176.47	11.9	17.7	11/06/73	3/02/84	123.8	141.6	Bone Tumor
MED-HIGH	1035 F	8/19/71	21127	213.40	2347.44	9.0	18.2	2/22/73	3/04/84	132.3	150.5	Bone Tumor; Cushing's Disease
MED-HIGH	1192 F	8/24/72	27898	262.82	2890.98	9.7	18.1	2/26/74	3/29/83	109.0	127.1	Bone Tumor
MED-HIGH	1140 M	5/01/72	37518	275.06	3025.65	12.4	18.2	11/06/73	12/14/81	97.2	115.4	Bone Tumor
MED-HIGH	1173 M	5/27/72	37851	315.69	3472.57	10.9	17.3	11/06/73	2/09/82	99.1	116.5	Bone Tumor
MED-HIGH	1109 F	1/19/72	41403	324.47	3569.22	11.6	16.4	5/31/73	8/06/80	86.2	102.6	Bone Tumor; Lung Tumor; Addison's Disease
MED-HIGH	1071 M	11/26/71	46953	325.84	3584.20	13.1	18.1	5/31/73	1/09/81	91.3	109.5	Bone Tumor; Lung Tumor

DOSE-EFFECT STUDIES WITH INHALED PU-238 OXIDE IN BEAGLES

DOSE GROUP	DOG IDENT	BIRTH DATE	INITIAL ALVEOLAR DEPOSITION BQ	BQ/G LUNG	BQ/ KG	INHALATION EXPOSURE WGT (KG)	AGE (MO)	EXPO DATE	DEATH INFORMATION DEATH DATE	MONTHS POST INH	AGE (MO)	COMMENTS ON DEAD DOGS
MED-HIGH	1178 M	6/20/72	41625	353.65	3890.19	10.7	16.6	11/06/73	1/06/83	110.0	126.6	Bone Tumor; Lung Tumor
MED-HIGH	1047 M	8/20/71	33300	360.39	3964.29	8.4	18.1	2/22/73	10/05/82	115.4	133.5	Herniated Vertebral Disc
MED-HIGH	1160 F	5/27/72	49728	379.89	4178.82	11.9	17.3	11/06/73	9/22/81	94.5	111.9	Bone Tumor; Lung Tumor
MED-HIGH	1096 F	1/11/72	54612	431.72	4748.87	11.5	16.6	5/31/73	5/08/78	59.2	75.9	Addison's Disease
MED-HIGH	1211 M	9/09/72	65268	452.94	4982.29	13.1	17.6	2/26/74	5/17/82	98.6	116.2	Bone Tumor
MED-HIGH	1092 M	12/22/71	68376	497.28	5470.08	12.5	17.3	5/31/73	10/23/78	64.8	82.0	Bone Tumor
MED-HIGH	0974 F	5/15/71	63566	545.16	5996.79	10.6	20.2	1/18/73	5/24/78	64.1	84.3	Bone Tumor
MED-HIGH	1115 F	1/27/72	69745	561.10	6172.12	11.3	16.1	5/31/73	7/11/78	61.3	77.4	Bone Tumor
MED-HIGH	1027 M	6/15/71	79476	568.90	6257.95	12.7	19.2	1/18/73	12/01/78	70.4	89.6	Bone Tumor; Lung Tumor
MED-HIGH	1218 F	9/16/72	63270	569.49	6264.36	10.1	17.3	2/26/74	4/24/81	85.9	103.2	Bone Tumor
MED-HIGH	1079 M	11/29/71	96940	607.77	6685.52	14.5	18.0	5/31/73	2/12/78	56.4	74.5	Addison's Disease
MED-HIGH	1058 F	8/30/71	70559	647.92	7127.17	9.9	17.8	2/22/73	11/01/79	80.3	98.1	Bone Tumor
HIGH	1002 M	5/31/71	107559	769.93	8469.21	12.7	19.6	1/18/73	1/21/80	84.1	103.7	Bone Tumor; Lung Tumor
HIGH	1057 M	8/27/71	115292	903.54	9938.97	11.6	17.9	2/22/73	3/07/79	72.4	90.3	Bone Tumor
HIGH	1009 M	6/02/71	134310	1080.53	11885.84	11.3	19.6	1/18/73	4/01/78	62.4	82.0	Lung Tumor; Osteoarthropathy
HIGH	1006 F	6/02/71	140970	1144.24	12586.61	11.2	19.6	1/18/73	1/18/79	72.0	91.6	Bone Tumor; Lung Tumor
HIGH	1042 F	8/20/71	109483	1157.33	12730.58	8.6	18.1	2/22/73	11/10/78	68.6	86.7	Bone Tumor; Lung Tumor
HIGH	0994 F	5/31/71	127761	1173.20	12905.15	9.9	19.6	1/18/73	7/04/76	41.5	61.1	Addison's Disease
HIGH	0975 F	5/15/71	146816	1271.13	13982.48	10.5	20.2	1/18/73	7/25/78	66.2	86.3	Bone Tumor; Lung Tumor
HIGH	1037 M	8/19/71	179598	1700.74	18708.13	9.6	18.2	2/22/73	11/21/78	68.9	87.1	Bone Tumor

DOSE-EFFECT STUDIES WITH INHALED PU-238 OXIDE IN BEAGLES

DOSE GROUP	DOG IDENT	BIRTH DATE	INITIAL ALVEOLAR DEPOSITION BQ	BQ/G LUNG	BQ/ KG	INHALATION EXPOSURE WGT (KG)	AGE (MO)	EXPO DATE	DEATH INFORMATION DEATH DATE	MONTHS POST INH	AGE (MO)	COMMENTS ON DEAD DOGS
HIGH	1143 M	5/01/72	284567	2005.41	22059.46	12.9	18.2	11/06/73	12/05/77	49.0	67.2	Bone Tumor; Lung Tumor
HIGH	1025 M	6/15/71	313723	2051.82	22570.00	13.9	19.2	1/18/73	3/17/77	49.9	69.1	Lung Tumor
HIGH	1162 F	5/27/72	257483	2572.26	28294.84	9.1	17.3	11/06/73	12/19/78	61.4	78.8	Bone Tumor; Addison's Disease
HIGH	1064 M	8/30/71	349761	2649.70	29146.75	12.0	16.7	1/18/73	4/14/77	50.8	67.5	Bone Tumor; Lung Tumor
HIGH	1175 F	6/20/72	229437	2979.70	32776.71	7.0	16.6	11/06/73	2/24/78	51.6	68.2	Lung Tumor

INHALED PLUTONIUM NITRATE IN DOGS

DOSE GROUP	DOG IDENT	BIRTH DATE	INITIAL ALVEOLAR DEPOSITION BQ	BQ/G LUNG	BQ/ KG	INHALATION EXPOSURE WGT (KG)	AGE (MO)	EXPO DATE	DEATH INFORMATION DEATH DATE	MONTHS POST INH	AGE (MO)	COMMENTS ON DEAD DOGS
CONTROL	1356 M	5/11/74	0	0.00	0.00	13.0	20.3	1/20/76	4/07/87	134.5	154.9	Carcinoma, Adrenal
CONTROL	1365 M	5/14/74	0	0.00	0.00	10.2	20.2	1/20/76	7/16/88	149.8	170.1	Pneumonia
CONTROL	1376 F	6/17/74	0	0.00	0.00	9.5	19.1	1/20/76	5/11/80	51.7	70.8	Pneumonia
CONTROL	1393 M	6/22/74	0	0.00	0.00	9.6	21.9	4/20/76	6/19/87	133.9	155.9	Pneumonia
CONTROL	1409 M	7/07/74	0	0.00	0.00	12.3	21.5	4/20/76	7/17/89	158.9	180.3	Herniated Vertebral Disc
CONTROL	1418 M	7/16/74	0	0.00	0.00	10.6	23.3	6/23/76	8/26/89	158.1	181.4	Adenoma, Pituitary
CONTROL	1425 M	7/17/74	0	0.00	0.00	15.6	23.2	6/23/76	8/02/82	73.3	96.5	Epileptic Seizures
CONTROL	1455 F	8/05/74	0	0.00	0.00	6.1	20.5	4/20/76	8/20/87	136.0	156.5	Pyometra
CONTROL	1483 F	9/03/74	0	0.00	0.00	9.8	21.7	6/23/76	12/20/91	185.9	207.5	Processing
CONTROL	1516 F	10/05/74	0	0.00	0.00	9.4	20.6	6/23/76	2/24/92	188.1	208.7	Processing
CONTROL	1525 M	10/12/74	0	0.00	0.00	12.5	21.3	7/22/76	11/14/87	135.8	157.1	Transitional Carcinoma, Urethra
CONTROL	1526 M	10/12/74	0	0.00	0.00	10.8	21.3	7/22/76	8/28/90	169.2	190.5	Unknown
CONTROL	1528 F	10/29/74	0	0.00	0.00	10.6	20.8	7/22/76	4/06/87	128.5	149.2	Cerebral Hemorrhage
CONTROL	1543 M	11/03/74	0	0.00	0.00	16.0	20.6	7/22/76	8/12/86	120.7	141.3	Herniated Vertebral Disc
CONTROL	1563 F	9/06/75	0	0.00	0.00	12.0	18.3	3/15/77	2/10/92	178.9	197.2	Adenocarcinoma, Ovary
CONTROL	1572 F	9/09/75	0	0.00	0.00	10.2	19.3	4/19/77	2/01/90	153.5	172.8	Endocarditis
CONTROL	1577 M	9/08/75	0	0.00	0.00	12.2	18.2	3/15/77	4/04/90	156.6	174.9	Hemangioma, Spleen (Ruptured)
CONTROL	1584 F	9/12/75	0	0.00	0.00	12.5	19.2	4/19/77	11/29/88	139.4	158.6	Carcinoma, Thyroid
CONTROL	1594 F	9/13/75	0	0.00	0.00	13.9	19.2	4/19/77	11/02/90	162.5	181.7	Pneumonia; Hepatocellur Carcinoma
CONTROL	1633 F	4/12/76	0	0.00	0.00	11.8	18.9	11/07/77	11/10/86	108.1	126.9	Carcinoma, Thyroid

INHALED PLUTONIUM NITRATE IN DOGS

DOSE GROUP	DOG IDENT	BIRTH DATE	INITIAL ALVEOLAR DEPOSITION BQ	BQ/G LUNG	BQ/KG	INHALATION EXPOSURE WGT (KG)	AGE (MO)	EXPO DATE	DEATH INFORMATION DEATH DATE	MONTHS POST INH	AGE (MO)	COMMENTS ON DEAD DOGS
CONTROL-SAC	1388 M	6/22/74	0	0.00	0.00	12.0	21.9	4/20/76	9/11/81	64.7	86.7	Sacrificed
CONTROL-SAC	1405 M	7/05/74	0	0.00	0.00	10.3	21.5	4/20/76	8/13/84	99.8	121.3	Heart Base Tumor
CONTROL-SAC	1450 F	7/23/74	0	0.00	0.00	13.7	20.9	4/20/76	11/04/81	66.5	87.4	Sacrificed
CONTROL-SAC	1509 M	9/26/74	0	0.00	0.00	11.7	20.9	6/22/76	10/30/86	124.3	145.1	Sacrificed
CONTROL-SAC	1608 M	9/20/75	0	0.00	0.00	12.0	17.8	3/15/77	2/14/91	167.0	184.8	Rhabdomyosarcoma
CONTROL-SAC	1638 F	4/22/76	0	0.00	0.00	9.1	18.5	11/07/77	9/08/87	118.0	136.5	Sacrificed
VEHICLE	1361 M	5/14/74	0	0.00	0.00	14.0	21.0	2/12/76	4/04/89	157.7	178.7	Heart Failure
VEHICLE	1381 F	6/21/74	0	0.00	0.00	8.7	19.7	2/12/76	12/05/89	165.7	185.5	Mammary Tumor
VEHICLE	1392 M	6/22/74	0	0.00	0.00	12.8	22.0	4/22/76	1/16/90	164.8	186.8	Sebaceous Carcinoma, Skin (Lung Metastasis)
VEHICLE	1406 M	7/05/74	0	0.00	0.00	15.5	21.6	4/22/76	1/21/88	141.0	162.6	Malignant Melanoma, Oral Cavity
VEHICLE	1412 F	7/15/74	0	0.00	0.00	8.9	19.0	2/12/76	7/06/89	160.8	179.7	Mammary Tumor
VEHICLE	1421 M	7/16/74	0	0.00	0.00	13.0	23.5	6/29/76	2/26/88	139.9	163.4	Mastocytoma
VEHICLE	1457 F	8/05/74	0	0.00	0.00	11.5	20.6	4/22/76	11/07/89	162.5	183.1	Hypothyroidism
VEHICLE	1491 F	9/05/74	0	0.00	0.00	8.6	21.8	6/29/76	5/10/89	154.3	176.1	Mammary Tumor
VEHICLE	1504 F	9/26/74	0	0.00	0.00	10.2	21.1	6/29/76	2/22/89	151.8	172.9	Malignant Lymphoma
VEHICLE	1514 M	9/26/74	0	0.00	0.00	13.4	21.1	6/29/76	8/06/82	73.2	94.3	Malignant Lymphoma
VEHICLE	1524 M	10/12/74	0	0.00	0.00	12.1	21.5	7/27/76	3/27/88	140.0	161.5	Herniated Vertebral Disc
VEHICLE	1531 F	10/29/74	0	0.00	0.00	8.8	20.9	7/27/76	9/15/91	181.6	202.5	Processing
VEHICLE	1542 M	11/03/74	0	0.00	0.00	12.5	20.8	7/27/76	5/01/89	153.1	173.9	Malignant Lymphoma
VEHICLE	1566 M	9/06/75	0	0.00	0.00	14.5	19.9	5/05/77	1/18/90	152.5	172.4	Malignant Lymphoma

INHALED PLUTONIUM NITRATE IN DOGS

DOSE GROUP	DOG IDENT	BIRTH DATE	INITIAL ALVEOLAR DEPOSITION BQ	BQ/G LUNG	BQ/ KG	INHALATION EXPOSURE WGT (KG)	AGE (MO)	EXPO DATE	DEATH INFORMATION DEATH DATE	MONTHS POST INH	AGE (MO)	COMMENTS ON DEAD DOGS
VEHICLE	1578 M	9/08/75	0	0.00	0.00	10.2	19.9	5/05/77	2/13/90	153.3	173.2	Nephropathy
VEHICLE	1593 F	9/13/75	0	0.00	0.00	11.0	19.7	5/05/77	12/31/90	163.9	183.6	Nephropathy
VEHICLE	1601 F	9/15/75	0	0.00	0.00	7.8	19.6	5/05/77	4/08/90	155.1	174.8	Nephropathy
VEHICLE	1620 M	2/29/76	0	0.00	0.00	13.7	21.1	12/01/77	1/06/87	109.2	130.2	Herniated Vertebral Disc
VEHICLE	1634 F	4/12/76	0	0.00	0.00	10.8	19.6	12/01/77	11/05/92	179.2	198.8	Processing
VEHICLE	1651 F	4/26/76	0	0.00	0.00	9.9	19.2	12/01/77	11/11/92	179.4	198.5	Processing
LOWEST	1416 M	7/16/74	0	0.00	0.00	10.2	22.1	5/20/76	2/15/90	164.9	187.0	Heart Failure
LOWEST	1458 F	8/05/74	0	0.00	0.00	8.5	21.5	5/20/76	9/21/89	160.1	181.6	Malignant Pheochromocytoma, Adrenal
LOWEST	1489 F	9/05/74	0	0.00	0.00	9.5	20.5	5/20/76	8/04/84	98.5	119.0	Carcinoma, Esophagus
LOWEST	1501 M	9/08/74	0	0.00	0.00	12.5	20.4	5/20/76	1/03/84	91.5	111.8	Carcinoma, Thyroid
LOWEST	1513 M	9/26/74	0	0.00	0.00	11.6	19.8	5/20/76	10/08/90	172.6	192.4	Hepatitis; Lung Tumor
LOWEST	1515 M	9/26/74	0	0.00	0.00	11.7	19.8	5/20/76	12/06/90	174.6	194.3	Carcinoma, Urethra; Hepatocellular Carcinoma
LOWEST	1573 M	9/08/75	0	0.00	0.00	11.7	19.4	4/19/77	9/06/90	160.6	179.9	Gastric Dilatation
LOWEST	1581 M	9/10/75	0	0.00	0.00	16.3	19.3	4/19/77	7/31/86	111.4	130.7	Hemangiosarcoma, Spleen
LOWEST	1596 M	9/13/75	0	0.00	0.00	13.9	19.2	4/19/77	7/02/91	170.4	189.6	Senility; Carcinoma, Bile Duct
LOWEST	1600 F	9/14/75	44	0.35	3.83	11.4	19.2	4/19/77	6/27/90	158.3	177.4	Nephropathy
LOWEST	1520 M	10/05/74	47	0.37	4.09	11.4	19.5	5/20/76	5/21/90	168.0	187.5	Carcinoma, Bile Duct
LOWEST	1603 M	9/14/75	61	0.39	4.24	14.4	19.2	4/19/77	12/26/90	164.2	183.4	Nephropathy
LOWEST	1570 F	9/08/75	67	0.60	6.57	10.2	19.4	4/19/77	6/19/87	122.0	141.3	Fibrosarcoma, Stomach
LOWEST	1519 M	10/05/74	84	0.64	7.09	11.8	19.5	5/20/76	7/13/90	169.8	189.2	Nephropathy

INHALED PLUTONIUM NITRATE IN DOGS

DOSE GROUP	DOG IDENT	BIRTH DATE	INITIAL ALVEOLAR DEPOSITION BQ	BQ/G LUNG	BQ/ KG	INHALATION EXPOSURE WGT (KG)	AGE (MO)	EXPO DATE	DEATH INFORMATION DEATH DATE	MONTHS POST INH	AGE (MO)	COMMENTS ON DEAD DOGS
LOWEST	1592 F	9/13/75	142	0.93	10.25	13.9	19.2	4/19/77	10/17/89	149.9	169.1	Pneumonia
LOWEST	1470 F	8/21/74	114	1.06	11.71	9.7	21.0	5/20/76	4/09/84	94.7	115.6	Meningioma
LOWEST	1465 F	8/19/74	154	1.24	13.65	11.3	21.0	5/20/76	5/16/89	155.9	176.9	Nephropathy
LOWEST	1606 F	9/20/75	194	1.31	14.36	13.5	19.0	4/19/77	6/22/90	158.1	177.1	Hemangiosarcoma, Spleen
LOWEST	1466 F	8/19/74	191	1.38	15.18	12.6	21.0	5/20/76	1/04/90	163.5	184.5	Nephropathy
LOWEST	1583 F	9/12/75	139	1.42	15.67	8.9	19.2	4/19/77	10/13/89	149.8	169.0	Carcinoma, Thyroid
LOWEST-SAC	1339 F	5/01/74	74	0.70	7.67	9.7	17.5	10/16/75	11/13/75	0.9	18.4	Sacrificed
LOWEST-SAC	1335 M	4/16/74	178	1.41	15.48	11.5	18.0	10/16/75	11/13/75	0.9	18.9	Sacrificed
LOWEST-SAC	1351 M	5/10/74	248	2.21	24.30	10.2	17.2	10/16/75	11/13/75	0.9	18.1	Sacrificed
LOW	1575 M	9/08/75	100	0.63	6.94	14.4	19.4	4/19/77	12/28/87	128.3	147.6	Transitional Carcinoma, Urethra
LOW	1415 M	7/15/74	86	0.71	7.80	11.0	22.2	5/20/76	12/27/89	163.3	185.4	Transitional Carcinoma, Urinary Bladder
LOW	1507 M	9/26/74	165	1.21	13.31	12.4	19.8	5/20/76	6/07/88	144.6	164.4	Malignant Melanoma, Oral Cavity
LOW	1607 M	9/20/75	167	1.27	13.94	12.0	19.0	4/19/77	7/26/88	135.2	154.2	Hepatocellular Carcinoma
LOW	1590 F	9/13/75	228	1.62	17.81	12.8	19.2	4/19/77	3/18/87	118.9	138.1	Mammary Tumor
LOW	1487 F	9/03/74	222	1.77	19.47	11.4	20.5	5/20/76	7/05/90	169.5	190.0	Gastric Dilatation
LOW	1579 M	9/09/75	308	1.98	21.83	14.1	19.3	4/19/77	6/05/90	157.5	176.9	Hepatocellular Carcinoma
LOW	1585 F	9/12/75	301	2.14	23.50	12.8	19.2	4/19/77	8/31/89	148.4	167.6	Carcinoma, Thyroid
LOW	1565 F	9/06/75	283	2.30	25.31	11.2	19.4	4/19/77	9/28/85	101.3	120.7	Hemangiosarcoma, Spleen
LOW	1591 M	9/13/75	423	2.48	27.31	15.5	19.2	4/19/77	8/15/89	147.9	167.1	Malignant Lymphoma
LOW	1580 F	9/10/75	335	2.62	28.87	11.6	19.3	4/19/77	1/06/92	176.6	195.9	Transitional Carcinoma, Urinary Bladder

INHALED PLUTONIUM NITRATE IN DOGS

DOSE GROUP	DOG IDENT	BIRTH DATE	INITIAL ALVEOLAR DEPOSITION BQ	BQ/G LUNG	BQ/ KG	INHALATION EXPOSURE WGT (KG)	AGE (MO)	EXPO DATE	DEATH INFORMATION DEATH DATE	MONTHS POST INH	AGE (MO)	COMMENTS ON DEAD DOGS
LOW	1567 M	9/06/75	370	2.81	30.86	12.0	19.4	4/19/77	6/15/90	157.9	177.3	Nephritis
LOW	1503 F	9/26/74	324	2.94	32.38	10.0	19.8	5/20/76	12/13/84	102.8	122.6	Carcinoma, Thyroid
LOW	1423 M	7/17/74	356	3.08	33.90	10.5	22.1	5/20/76	6/27/89	157.2	179.4	Panophthalmitis
LOW	1602 M	9/14/75	553	3.31	36.37	15.2	19.2	4/19/77	8/10/86	111.7	130.9	Epileptic Seizures
LOW	1417 M	7/16/74	395	3.33	36.59	10.8	22.1	5/20/76	10/05/89	160.5	182.7	Malignant Lymphoma
LOW	1599 F	9/14/75	381	3.43	37.73	10.1	19.2	4/19/77	3/12/86	106.7	125.9	Carcinoma, Adrenal
LOW	1472 F	8/21/74	374	4.04	44.49	8.4	21.0	5/20/76	11/22/89	162.1	183.1	Nephropathy; Carcinoma, Bile Duct
LOW	1484 F	9/03/74	401	4.14	45.54	8.8	20.5	5/20/76	10/26/90	173.2	193.7	Malignant Lymphoma
LOW	1490 F	9/05/74	581	5.45	59.92	9.7	20.5	5/20/76	10/19/88	149.0	169.5	Mammary Tumor
MED-LOW	1386 M	6/21/74	1266	7.73	84.98	14.9	22.0	4/20/76	1/04/86	116.5	138.5	Hemangiosarcoma, Spleen
MED-LOW	1413 F	7/15/74	1090	8.85	97.36	11.2	18.2	1/20/76	3/01/85	109.3	127.5	Malignant Lymphoma
MED-LOW	1391 M	6/22/74	1991	10.77	118.49	16.8	21.9	4/20/76	7/22/85	111.0	133.0	Carcinoma, Thyroid; Lung Tumor
MED-LOW	1568 M	9/06/75	1702	11.63	127.94	13.3	18.3	3/15/77	12/02/86	116.6	134.9	Pneumonia
MED-LOW	1540 M	10/30/74	2015	12.05	132.57	15.2	20.7	7/22/76	11/25/86	124.1	144.9	Lung Tumor
MED-LOW	1595 M	9/13/75	1850	12.37	136.03	13.6	18.0	3/15/77	1/09/90	153.9	171.9	Nephropathy
MED-LOW	1587 M	9/12/75	1947	12.64	139.09	14.0	18.1	3/15/77	1/14/86	106.0	124.1	Hemangiosarcoma, Subcutis; Lung Tumor
MED-LOW	1574 M	9/08/75	1715	14.43	158.76	10.8	18.2	3/15/77	7/14/90	160.0	178.2	Lung Tumor
MED-LOW	1439 F	7/20/74	1962	15.12	166.31	11.8	21.0	4/20/76	3/30/88	143.3	164.3	Malignant Lymphoma
MED-LOW	1444 F	7/22/74	1831	15.55	171.10	10.7	21.0	4/20/76	5/17/90	168.9	189.8	Transitional Carcinoma, Urinary Bladder
MED-LOW	1380 M	6/17/74	2339	15.75	173.24	13.5	19.1	1/20/76	5/24/87	136.1	155.2	Pneumonia

INHALED PLUTONIUM NITRATE IN DOGS

DOSE GROUP	DOG IDENT	BIRTH DATE	INITIAL ALVEOLAR DEPOSITION BQ	BQ/G LUNG	BQ/ KG	INHALATION EXPOSURE WGT (KG)	AGE (MO)	EXPO DATE	DEATH INFORMATION DEATH DATE	MONTHS POST INH	AGE (MO)	COMMENTS ON DEAD DOGS
MED-LOW	1523 F	10/12/74	2041	17.50	192.50	10.6	21.3	7/22/76	12/21/90	173.0	194.3	Metastatic Melanoma
MED-LOW	1569 F	9/08/75	2152	20.81	228.93	9.4	18.2	3/15/77	9/27/87	126.4	144.6	Lung Tumor
MED-LOW	1582 F	9/12/75	2095	20.93	230.25	9.1	18.1	3/15/77	8/12/88	136.9	155.0	Mammary Tumor; Carcinoma, Bile Duct
MED-LOW	1427 F	7/17/74	2518	23.36	256.96	9.8	21.1	4/20/76	8/23/89	160.1	181.2	Malignant Melanoma, Oral Cavity
MED-LOW	1456 F	8/05/74	2248	27.25	299.75	7.5	20.5	4/20/76	4/21/87	132.0	152.5	Pneumonia
MED-LOW	1363 M	5/14/74	3144	28.30	311.28	10.1	20.2	1/20/76	5/12/87	135.7	155.9	Pneumonia; Carcinoma, Adrenal; Adenoma, Bile Duct
MED-LOW	1530 F	10/29/74	2646	30.84	339.21	7.8	20.8	7/22/76	9/17/86	121.9	142.6	Bone Tumor; Lung Tumor
MED-LOW	1604 M	9/14/75	3145	32.86	361.49	8.7	18.0	3/15/77	4/03/90	156.6	174.6	Encephalopathy
MED-LOW	1422 F	7/17/74	3656	44.32	487.51	7.5	19.1	1/20/76	7/11/90	173.7	191.8	Lung Tumor; Adenoma, Bile Duct
MED-LOW-SAC	1336 M	4/16/74	759	5.35	58.83	12.9	18.0	10/16/75	11/13/75	0.9	18.9	Sacrificed
MED-LOW-SAC	1341 F	5/10/74	692	6.29	69.19	10.0	17.2	10/16/75	11/13/75	0.9	18.1	Sacrificed
MED-LOW-SAC	1605 F	9/20/75	932	7.71	84.76	11.0	17.8	3/15/77	3/24/82	60.3	78.1	Sacrificed
MED-LOW-SAC	1445 F	7/22/74	1252	8.89	97.82	12.8	21.0	4/20/76	5/05/76	0.5	21.5	Sacrificed
MED-LOW-SAC	1389 M	6/22/74	989	9.08	99.86	9.9	21.9	4/20/76	5/04/76	0.5	22.4	Sacrificed
MED-LOW-SAC	1359 M	5/14/74	1850	11.68	128.47	14.4	20.2	1/20/76	1/23/76	0.1	20.3	Sacrificed
MED-LOW-SAC	1390 M	6/22/74	1582	12.29	135.19	11.7	21.9	4/20/76	5/04/76	0.5	22.4	Sacrificed
MED-LOW-SAC	1588 M	9/12/75	1839	12.86	141.48	13.0	18.1	3/15/77	3/22/78	12.2	30.3	Sacrificed
MED-LOW-SAC	1589 F	9/13/75	1526	13.09	143.95	10.6	18.0	3/15/77	6/08/82	62.8	80.8	Sacrificed; Lung Tumor
MED-LOW-SAC	1344 F	5/10/74	1531	13.64	150.07	10.2	17.2	10/16/75	11/14/75	1.0	18.2	Sacrificed
MED-LOW-SAC	1529 F	10/29/74	1586	13.86	152.48	10.4	20.8	7/22/76	10/19/76	2.9	23.7	Sacrificed

INHALED PLUTONIUM NITRATE IN DOGS

DOSE GROUP	DOG IDENT	BIRTH DATE	INITIAL ALVEOLAR DEPOSITION BQ	BQ/G LUNG	BQ/ KG	INHALATION EXPOSURE WGT (KG)	AGE (MO)	EXPO DATE	DEATH INFORMATION DEATH DATE	MONTHS POST INH	AGE (MO)	COMMENTS ON DEAD DOGS
MED-LOW-SAC	1375 F	6/17/74	1850	15.29	168.18	11.0	19.1	1/20/76	1/23/76	0.1	19.2	Sacrificed
MED-LOW-SAC	1564 F	9/06/75	1479	15.64	172.01	8.6	18.3	3/15/77	3/20/78	12.2	30.4	Sacrificed
MED-LOW-SAC	1539 M	10/30/74	2398	17.58	193.41	12.4	20.7	7/22/76	10/20/76	3.0	23.7	Sacrificed
MED-LOW-SAC	1576 M	9/08/75	2601	19.71	216.79	12.0	18.2	3/15/77	3/17/82	60.1	78.3	Sacrificed
MED-LOW-SAC	1407 F	7/07/74	1850	21.29	234.18	7.9	18.5	1/20/76	1/23/76	0.1	18.6	Sacrificed
MED-LOW-SAC	1571 F	9/08/75	2533	23.26	255.82	9.9	18.2	3/15/77	3/21/78	12.2	30.4	Sacrificed
MED-LOW-SAC	1522 F	10/12/74	2880	27.56	303.17	9.5	21.3	7/22/76	10/18/76	2.9	24.2	Sacrificed
MED-LOW-SAC	1598 F	9/14/75	3448	42.94	472.38	7.3	18.0	3/15/77	3/10/82	59.8	77.8	Sacrificed
MEDIUM	1404 M	7/05/74	9620	51.44	565.88	17.0	21.5	4/20/76	2/03/84	93.5	115.0	Pleuritis
MEDIUM	1637 M	4/12/76	7100	56.62	622.80	11.4	18.9	11/07/77	11/28/88	132.7	151.6	Lung Tumor
MEDIUM	1521 F	10/12/74	7570	61.45	675.91	11.2	21.3	7/22/76	6/07/85	106.5	127.8	Bone Tumor; Lung Tumor
MEDIUM	1379 M	6/17/74	10280	61.89	680.82	15.1	19.1	1/20/76	1/20/88	144.0	163.1	Carcinoma, Bile Duct; Lung Tumor; Bone Tumor
MEDIUM	1656 M	4/26/76	7816	62.88	691.67	11.3	18.4	11/07/77	1/02/91	157.8	176.2	Pneumonia; Lung Tumor
MEDIUM	1362 M	5/14/74	9879	63.25	695.70	14.2	20.2	1/20/76	12/20/88	155.0	175.2	Bone Tumor; Hepatocellular Carcinoma; Carcinoma, Bile Duct; Lung Tumors
MEDIUM	1534 M	10/28/74	10900	76.23	838.48	13.0	20.8	7/22/76	5/26/85	106.1	126.9	Heart Failure
MEDIUM	1645 F	4/23/76	9520	77.28	850.04	11.2	18.5	11/07/77	8/07/86	105.0	123.5	Lung Tumor
MEDIUM	1639 F	4/22/76	9188	78.80	866.78	10.6	18.5	11/07/77	12/24/89	145.5	164.1	Radiation Pneumonitis; Lung Tumor
MEDIUM	1385 M	6/21/74	13794	79.36	873.01	15.8	19.0	1/20/76	7/12/84	101.7	120.7	Bone Tumor; Lung Tumor
MEDIUM	1640 M	4/22/76	11344	85.94	945.35	12.0	18.5	11/07/77	3/20/84	76.4	94.9	Lung Tumor
MEDIUM	1618 F	2/29/76	10239	88.65	975.14	10.5	20.3	11/07/77	7/12/89	140.1	160.4	Bone Tumor

INHALED PLUTONIUM NITRATE IN DOGS

DOSE GROUP	DOG IDENT	BIRTH DATE	INITIAL ALVEOLAR DEPOSITION BQ	BQ/G LUNG	BQ/ KG	INHALATION EXPOSURE WGT (KG)	AGE (MO)	EXPO DATE	DEATH INFORMATION DEATH DATE	MONTHS POST INH	AGE (MO)	COMMENTS ON DEAD DOGS
MEDIUM	1414 F	7/15/74	8610	92.08	1012.93	8.5	18.2	1/20/76	8/14/86	126.8	145.0	Bone Tumor; Lung Tumor; Carcinoma, Bile Duct
MEDIUM	1647 M	4/23/76	10863	98.75	1086.28	10.0	18.5	11/07/77	1/13/90	146.2	164.7	Lung Tumor; Carcinoma, Bile Duct
MEDIUM	1446 F	7/22/74	13099	112.34	1235.73	10.6	21.0	4/20/76	8/10/86	123.7	144.6	Pyometra; Adenoma, Bile Duct
MEDIUM	1408 F	7/07/74	12240	115.30	1268.35	9.7	18.5	1/20/76	10/12/83	92.7	111.2	Bone Tumor
MEDIUM	1535 F	10/30/74	12758	115.98	1275.76	10.0	20.7	7/22/76	10/06/86	122.5	143.2	Bone Tumor; Lung Tumor
MEDIUM	1428 F	7/17/74	13986	116.65	1283.12	10.9	21.1	4/20/76	10/28/85	114.3	135.4	Bone Tumor; Lung Tumor
MEDIUM	1364 M	5/14/74	17146	135.54	1490.94	11.5	20.2	1/20/76	8/02/84	102.4	122.6	Lung Tumor
MEDIUM	1387 F	6/22/74	12769	181.37	1995.11	6.4	19.0	1/20/76	8/13/80	54.8	73.7	Bone Tumor
MED-HIGH	1648 M	4/23/76	30014	216.55	2382.10	12.6	18.5	11/07/77	7/11/85	92.1	110.6	Bone Tumor; Lung Tumor
MED-HIGH	1659 F	4/29/76	36641	254.28	2797.06	13.1	18.3	11/07/77	8/19/83	69.4	87.7	Bone Tumor
MED-HIGH	1636 M	4/12/76	44851	302.03	3322.33	13.5	18.9	11/07/77	5/03/83	65.8	84.7	Bone Tumor
MED-HIGH	1646 F	4/23/76	39255	346.47	3811.14	10.3	18.5	11/07/77	11/11/82	60.1	78.6	Bone Tumor
MED-HIGH	1621 M	2/29/76	49343	358.86	3947.46	12.5	20.3	11/07/77	11/19/84	84.4	104.7	Bone Tumor; Lung Tumor
MED-HIGH	1641 M	4/22/76	47171	366.52	4031.74	11.7	18.5	11/07/77	6/28/85	91.7	110.2	Lung Tumor
MED-HIGH	1429 M	7/17/74	50912	370.27	4072.96	12.5	23.2	6/23/76	5/29/81	59.2	82.4	Bone Tumor; Lung Tumor
MED-HIGH	1660 M	4/29/76	56149	392.65	4319.15	13.0	18.3	11/07/77	9/05/84	81.9	100.2	Bone Tumor; Lung Tumor
MED-HIGH	1508 M	9/26/74	63503	395.41	4349.53	14.6	20.9	6/23/76	1/24/80	43.0	63.9	Bone Tumor
MED-HIGH	1655 M	4/26/76	40481	432.95	4762.42	8.5	18.4	11/07/77	3/18/85	88.3	106.7	Lung Tumor; Bone Tumor
MED-HIGH	1652 F	4/26/76	48822	452.89	4981.79	9.8	18.4	11/07/77	7/20/83	68.4	86.8	Bone Tumor; Lung Tumor
MED-HIGH	1619 F	2/29/76	55148	477.47	5252.20	10.5	20.3	11/07/77	1/21/83	62.5	82.7	Bone Tumor

INHALED PLUTONIUM NITRATE IN DOGS

DOSE GROUP	DOG IDENT	BIRTH DATE	INITIAL ALVEOLAR DEPOSITION BQ	BQ/G LUNG	BQ/ KG	INHALATION EXPOSURE WGT (KG)	AGE (MO)	EXPO DATE	DEATH INFORMATION DEATH DATE	MONTHS POST INH	AGE (MO)	COMMENTS ON DEAD DOGS
MED-HIGH	1419 M	7/16/74	57683	524.39	5768.30	10.0	23.3	6/23/76	10/22/82	76.0	99.2	Bone Tumor; Lung Tumor
MED-HIGH	1512 M	9/26/74	89192	526.52	5791.70	15.4	20.9	6/23/76	12/23/79	42.0	62.9	Bone Tumor
MED-HIGH	1498 F	9/08/74	74666	678.78	7466.60	10.0	21.5	6/23/76	4/09/82	69.5	91.0	Bone Tumor; Lung Tumor
MED-HIGH	1502 F	9/26/74	111289	717.53	7892.81	14.1	20.9	6/23/76	1/21/81	55.0	75.9	Bone Tumor; Lung Tumor
MED-HIGH	1471 F	8/21/74	92781	795.72	8752.94	10.6	22.1	6/23/76	5/01/79	34.2	56.3	Radiation Pneumonitis
MED-HIGH	1492 F	9/05/74	91516	875.75	9633.24	9.5	21.6	6/23/76	10/16/80	51.8	73.4	Bone Tumor
MED-HIGH	1459 F	8/05/74	97865	926.75	10194.27	9.6	22.6	6/23/76	9/25/80	51.1	73.7	Radiation Pneumonitis; Lung Tumor
MED-HIGH	1485 F	9/03/74	86210	955.76	10513.41	8.2	21.7	6/23/76	12/30/80	54.2	75.9	Bone Tumor
MED-HIGH-SAC	1329 F	4/16/74	13420	123.23	1355.55	9.9	18.0	10/16/75	11/14/75	1.0	19.0	Sacrificed
MED-HIGH-SAC	1346 M	5/10/74	24272	158.74	1746.19	13.9	17.2	10/16/75	11/14/75	1.0	18.2	Sacrificed
MED-HIGH-SAC	1347 F	5/10/74	25463	257.21	2829.27	9.0	17.2	10/16/75	11/14/75	1.0	18.2	Sacrificed
HIGH	1518 M	10/05/74	131905	1142.03	12562.38	10.5	20.6	6/23/76	12/18/79	41.8	62.4	Radiation Pneumonitis; Lung Tumor
HIGH	1420 M	7/16/74	142080	1254.02	13794.17	10.3	23.3	6/23/76	7/12/78	24.6	47.9	Radiation Pneumonitis
HIGH	1517 F	10/05/74	191845	1797.99	19777.84	9.7	20.6	6/23/76	11/02/77	16.3	36.9	Radiation Pneumonitis
HIGH	1510 F	9/26/74	257860	2056.30	22619.33	11.4	20.9	6/23/76	11/09/77	16.6	37.5	Radiation Pneumonitis
HIGH	1424 M	7/17/74	284204	2609.77	28707.52	9.9	23.2	6/23/76	8/31/77	14.3	37.5	Radiation Pneumonitis

Publications and Presentations

Publications

1991

Badger, C. C., J. Rasey, C. Nourigat, D. R. Fisher, T. E. Hui, Z. M. Wu, and I. D. Bernstein. 1991. WR2721 Protection of bone marrow in ^{131}I-labeled antibody therapy. *Radiat. Res.* 128:320-324.

Badger, C. C., J. Davis, C. Nourigat, Z. M. Wu, T. E. Hui, D. R. Fisher, H. Shulman, F. R. Appelbaum, J. F. Eary, K. A. Krohn, D. C. Matthews, and I. D. Bernstein. 1991. Biodistribution and dosimetry following infusion of antibodies labeled with large amounts of ^{131}I. *Cancer Res.* 51:5921-5928.

Bailey, M. R., A. Birchall, R. G. Cuddihy, A. C. James, and M. Roy. 1991. Respiratory tract clearance model for dosimetry and bioassay of inhaled radionuclides. *Radiat. Prot. Dosim.* 38(3/4)153-158.

Birchall, A., M. R. Bailey, and A. C. James. 1991. LUDEP: A lung dose evaluation program. *Radiat. Prot. Dosim.* 38(3/4):167-175.

Birchall, A., A. C. James, and C. R. Muirhead. 1991. Adequacy of personal air samplers for measuring plutonium intakes. *Radiat. Prot. Dosim.* 37(3):179-188.

Cross, F. T. 1991. A review of experimental animal radon health effect data. In: *Radiation Research, A Twentieth-Century Perspective,* Proceedings of the 9th International Congress of Radiation Research, Vol. 1, Congress Abstracts, W. C. Dewey and G. F. Whitmore, eds., p. 54 (abstract). Academic Press, San Diego.

Cross, F. T. 1991. Experimental studies on lung carcinogenesis and their relationship to future research on radiation-induced lung cancer in humans. In: *The Future of Human Radiation Research* (Section 2, Lung Cancer), G. B. Gerber, D. M. Taylor, E. Cardis, and J. W. Thiessen, eds., pp. 27-35. Report 22, British Institute of Radiology, London. Medical Physics Publishing, Madison, Wisconsin.

Cross, F. T. 1991. PNL research ranges from rocks to cancers. *Radon Research Notes* 6:1-3.

Cross, F. T. 1991. Pacific Northwest research focuses on toxicology of exposure. *Radon Research Notes* 6:3-4.

Cross, F. T. (co-author). 1991. *State of Washington, Radon Health Effects Committee/Radon Task Force Findings Report.* State of Washington, Olympia, Washington.

Dagle, G. E. 1991. Physicochemical interactions and tumor induction in bones by inhaled $^{239}Pu(NO_3)_4$. In: *Proceedings of the Joint Bone Radiology Workshop*, N. J. Parks, chairman, pp. 45-46 (abstract). USDOE Report UCD-472-136, Laboratory for Energy-Related Health Research, Institute of Toxicology and Environmental Health, University of California, Davis.

Dagle, G. E., J. F. Park, R. E. Weller, E. S. Gilbert, and R. L. Buschbom. 1991. Health effects of inhaled plutonium in dogs. In: *Radiation Research, A Twentieth-Century Perspective*, Proceedings of the 9th International Congress of Radiation Research, Vol. 1, Congress Abstracts, W. C. Dewey and G. F. Whitmore, eds., p. 321 (abstract). Academic Press, San Diego, California.

Finch, G. L., W. T. Lowther, M. C. Hoover, and A. L. Brooks. 1991. Effects of beryllium metal particles on the viability and function of cultured rat alveolar macrophages. *J. Toxicol. Environ. Health* 34:103-114.

Fisher, D. R., T. E. Hui, and A. C. James. 1991. Model for assessing radiation dose to epithelial cells of the human respiratory tract from radon progeny. *Radiat. Prot. Dosim.* 38(1/3):73-80.

Fisher, D. R., R. L. Kathren, and M. J. Swint. 1991. Modified biokinetic model for uranium from analysis of acute exposure to UF_6. *Health Phys.* 60(3):335-342.

Fisher, D. R., C. C. Badger, H. Breitz, J. F. Eary, J. S. Durham, T. E. Hui, R. L. Hill, and W. B. Nelp. 1991. Internal radiation dosimetry for clinical testing of radiolabeled monoclonal antibodies. *Antibody Immunoconj. Radiopharmaceut.* 4(4):655-664.

Fuciarelli, A. F., B. J. Wegher, W. F. Blakely, and M. Dizdaroglu. 1991. Radical-induced base damage in aqueous DNA solutions. In: *The Early Effects of Radiation on DNA*, E. M. Fielden and P. O. O'Neill, eds., pp. 405-408. NATO ASI Series, Vol. H54, Springer-Verlag, Berlin.

Gies, R. A., F. T. Cross, G. E. Dagle, and R. L. Buschbom. 1991. The influence of exposure rate and level on the incidence and type of primary lung tumors in rats exposed to radon. *Health Phys.* 60 (Suppl. 2):S32 (abstract).

James, A. C. 1991. Dosimetry of the respiratory tract and other organs: Implications for risk. In: *Radiation Research, A Twentieth-Century Perspective*, Proceedings of the 9th International Congress of Radiation Research, Vol. 1, Congress Abstracts, W. C. Dewey and G. F. Whitmore, eds., p. 53 (abstract). Academic Press, San Diego.

James, A. C., and A. Birchall. 1991. Implications of the ICRP Task Group's proposed lung model for internal dose assessments in the mineral sands industry. In: *Minesafe International, 1990,* Proceedings of an International Conference on Occupational Health and Safety in the Minerals Industry, September 10-14, 1990, Perth, Australia, pp. 210-222. Chamber of Mines and Energy of Western Australia, Perth.

James, A. C., J. R. Johnson, and D. R. Fisher. 1991. ICRP Task Group's dosimetry model for the respiratory tract: Implications for uranium. *Health Phys.* 60(2):S14 (abstract).

James, A. C., W. Stahlhofen, G. Rudolf, M. J. Eagan, W. Nixon, P. Gehr, and J. K. Briant. 1991. The respiratory tract deposition model proposed by the ICRP Task Group. *Radiat. Prot. Dosim.* 38(3/4):159-166.

James, A. C., P. Gehr, R. Masse, R. G. Cuddihy, F. T. Cross, A. Birchall, J. S. Durham, and J. K. Briant. 1991. Dosimetry model for bronchial and extrathoracic tissues of the respiratory tract. *Radiat. Prot. Dosim.* 37(4):221-230.

Jostes, R. F., T. E. Hui, A. C. James, F. T. Cross, J. L. Schwartz, J. Rotmensch, R. W. Atcher, H. H. Evans, J. Mencl, G. Bakele, and P. S. Rao. 1991. *In vitro* exposure of mammalian cells to radon: Dosimetric considerations. *Radiat. Res.* 127:211-219.

Leung, F. C. 1991. Growth factor and growth factor receptor in radiation carcinogenesis. *Radiat. Environ. Biophys.* 30:191-194.

Leung, F. C., L. R. Bohn, and G. E. Dagle. 1991. Elevated epidermal growth factor receptor binding in plutonium-induced lung tumors from dogs. *Proc. Soc. Exp. Biol. Med.* 196:385-389.

Leung, F. C., L. R. Bohn, and G. E. Dagle. 1991. Elevated epidermal growth factor receptor binding in dog lung tumors. In: *Proceedings, Eighth International Congress of Endocrinology*, July 17-23, 1988, Kyoto, Japan.

Mahaffey, J. A., J. R. Johnson, and C. L. Sanders. 1991. Robust estimation of nonlinear lung kinetics in animals exposed to alpha-emitting radionuclides. In: *The Analysis, Communication, and Perception of Risk: Advances in Risk Analysis, Vol. 9*, B. J. Garrick and W. C. Gekler, eds., pp. 401-410. Plenum, New York.

Mahaffey, J. A., F. T. Cross, J. R. Johnson, and M. C. Baechler. 1991. Prevention of lung cancer by remediation of residential exposure to radon daughters. *Radiat. Prot. Dosim.* 36:335-339.

Meznarich, H. K., L. A. Braby, and M. R. Sikov. 1991. Altered fibronectin levels in irradiated mouse blastocysts. *Fed. Am. Soc. Exp. Biol. J.* 5:1617A (abstract).

Meznarich, H. K., L. A. Braby, and M. R. Sikov. 1991. Expression of fibronectin in mouse blastocysts following irradiation. *Proc. Soc. Exp. Biol. Med.* 196(1):115A (Abstracts, Northwest Section).

Press, O. W., J. F. Eary, C. C. Badger, P. J. Martin, F. R. Appelbaum, W. B. Nelp, K. A. Krohn, D. Fisher, B. Porter, E. D. Thomas, R. Miller, S. Brown, R. Levy, and I. D. Bernstein. 1991. High-dose radioimmunotherapy of B cell lymphomas. In: *Frontiers of Radiation Therapy and Oncology, Vol. 24, The Present and Future Role of Monoclonal Antibodies in the Management of Cancer*, J. M. Vaeth and J. L. Meyer, eds., pp. 204-213. Karger, Basel, Switzerland.

Samet, J. M., R. E. Albert, J. D. Brain, R. A. Guilmette, P. K. Hopke, A. C. James, and D. G. Kaufman. 1991. *Comparative Dosimetry of Radon in Mines and Homes.* National Academy Press, Washington, D.C.

Sanders, C. L. 1991. Carcinogenesis in the lung following inhalation of $^{239}PuO_2$. In: *Proceedings, Primer Congreso Regional Sobre Seguridad Radiologica y Nuclear*, Buenas Aires, Argentina. *Seguridad Radiologica* 5:10.

Sanders, C. L., K. E. Lauhala, and G. E. Dagle. 1991. Brain tumors in the rat following inhalation of $^{239}PuO_2$. In: *Radiation Research: A Twentieth-Century Perspective,* Proceedings of the 9th International Congress of Radiation Research, Vol. 1, Congress Abstracts, W. C. Dewey and G. F. Whitmore, eds., p. 257. Academic Press, San Diego.

Sever, L. E. 1991. Low-level ionizing radiation: Paternal exposure and children's health. *Health Environ. Digest* 5(1):1-3.

Sever, L. E. 1991. Parental radiation exposure and children's health: Are there effects on the second generation? *Occup. Med. State of the Art Rev.* 6(4):613-627.

Sikov, M. R., H. K. Meznarich, and R. J. Traub. 1991. Comparison of placental transfer and localization of cesium, strontium, and iodine in experimental animals and women. In: Meeting Report, CEIR/MRC Forum—Radionuclides and External Irradiation: Implications for the Embryo and Fetus. *Int. J. Radiat. Biol.* 60(3):553-555.

Sikov, M. R., F. T. Cross, T. J. Mast, H. E. Palmer, and A. C. James. 1991. Developmental toxicology and dosimetry studies of prenatal radon exposures in rats. *Proc. Soc. Exp. Biol. Med.* 196(1) (Abstracts, Northwest Section).

Thrall, B. D., and G. G. Meadows. 1991. Induction of glutathione content in murine melanocytes by transformation with c-H-*ras* oncogene. *Carcinogenesis* 12(7):1319-1323.

Thrall, B. D., G. Raha, D. L. Springer, and G. G. Meadows. 1991. Differential sensitivity of murine melanocytes and melanoma cells to glutathione depletion. *Pigm. Cell Res.* 4:234-239.

Watson, C. R., J. C. Prather, and S. K. Smith. 1991. *National Radiobiology Archives Distributed Access User's Manual.* PNL-8777, Pacific Northwest Laboratory, Richland, Washington.

Wolff, S. F., R. Jostes, F. T. Cross, T. E. Hui, V. Afzal, and J. K. Wiencke. 1991. Adaptive response of human lymphocytes for the repair of radon-induced chromosomal damage. *Mutat. Res.* 250:299-306.

1992

Arnold, G. E., A. K. Dunker, S. J. Johns, and R. J. Douthart. 1992. Use of conditional probabilities for determining relationships between amino acid sequence and protein secondary structure. *Proteins Struct. Funct. Genet.* 12:382-399.

Benson, J. M., A. L. Brooks, and R. F. Henderson. 1992. Comparative in vitro cytotoxicity of nickel compounds to pulmonary alveolar macrophages and to rat lung epithelial cells. In: *Nickel and Human Health: Current Perspectives*, E. Nieboer and J. O. Nriagu, eds., pp. 319-330. Wiley, New York.

Briant, J. K., and M. Lippman. 1992. Particle transport through a hollow canine airway cast by high-frequency oscillatory ventilation. *Exp. Lung Res.* 18:385-407.

Briant, J. K., D. D. Frank, A. C. James, and L. L. Eyler. 1992. Numerical simulation of aerosol particle transport by oscillating flow in respiratory airways. *Ann. Biomed. Eng.* 20:573-581.

Brooks, A. L., R. M. Kitchin, N. F. Johnson, and E. S. Gilbert. 1992. The role of cellular and molecular studies in evaluation of health effects from combined radiation and chemical exposure. *Radiat. Res.* 113:121-122.

Brooks, A. L., K. E. McDonald, B. B. Kimsey, and R. M. Kitchin. 1992. Radioadaptive response *in vivo* in Chinese hamsters injected with alpha- or beta/gamma-emitting radionuclides. In: *Low Dose Irradiation and Biological Defense Mechanisms, Excerpta Med. Int. Congr. Ser.*, T. Sugahara, L. A. Sagan, and T. Aoyama, eds., pp. 319-322. Elsevier, New York.

Brooks, A. L., C. J. Mitchell, C. Lloyd, K. E. McDonald, and N. F. Johnson. 1992. Genotoxic effects of silicon carbide fibers. *In Vitro Toxicol.* 5(1):51-58.

Brooks, A. L., K. Rithidech, N. F. Johnson, D. G. Thomassen, and G. J. Newton. 1992. Evaluating chromosome damage to estimate dose to tracheal epithelial cells. In: *Indoor Radon and Lung Cancer: Reality or Myth?*, F. T. Cross, ed., Part 2, pp. 601-614, Proceedings of the 29th Hanford Symposium on Health and the Environment, Richland, Washington. Battelle Press, Columbus, Ohio.

Brooks, A. L., R. A. Guilmette, P. J. Haley, F. F. Hahn, B. A. Muggenberg, J. A. Mewhinney, and R. O. McClellan. 1992. Distribution and biological effects of inhaled $^{239}Pu(NO_3)_4$ in cynomolgus monkeys. *Radiat. Res.* 130:79-87.

Cross, F. T. 1992. A review of experimental animal radon health effects data. In: *Radiation Research: A Twentieth-Century Prospective*, Proceedings of the 9th International Congress of Radiation Research, Vol. 2, W. C. Dewey, M. Edington, R. J. M. Fry, E. J. Hall, and G. F. Whitmore, eds., pp. 476-481. Academic Press, New York.

Cross, F. T., ed. 1992. *Indoor Radon and Lung Cancer: Reality or Myth?*, Proceedings of the 29th Hanford Symposium on Health and the Environment, Richland, Washington. Battelle Press, Columbus, Ohio.

Cross, F. T., G. E. Dagle, R. A. Gies, L. G. Smith, and R. L. Buschbom. 1992. Experimental animal studies of radon and cigarette smoke. In: *Indoor Radon and Lung Cancer: Reality or Myth?*, F. T. Cross, ed., Part 2, pp. 821-844, Proceedings of the 29th Hanford Symposium on Health and the Environment, Richland, Washington. Battelle Press, Columbus, Ohio.

Cross, F. T., G. E. Dagle, M. E. Foreman, R. A. Gies, E. S. Gilbert, A. C. James, R. F. Jostes, F. C. Leung, S. H. Moolgavkar, and L. G. Smith. 1992. Mechanisms of radon injury/inhalation hazards to uranium miners. In: *DOE FY 1991 Radon Research Program Report*, pp. 213-218. DOE/ER-0536P, NTIS, Springfield, Virginia.

Dagle, G. E., F. T. Cross, and R. A. Gies. 1992. Morphology of respiratory tract lesions in rats exposed to radon progeny. In: *Indoor Radon and Lung Cancer: Reality or Myth?*, F. T. Cross, ed., Part 2, pp. 659-676, Proceedings of the 29th Hanford Symposium on Health and the Environment, Richland, Washington. Battelle Press, Columbus, Ohio.

Dagle, G. E., E. P. Moen, R. A. Adee, T. E. Hui, A. C. James, R. E. Filipy, and R. L. Kathren. 1992. Microdistribution and microdosimetry of thorium deposited in the liver. *Health Phys.* 63(1):41-45.

Egert, G. H., R. L. Kathren, F. T. Cross, and M. A. Robkin. 1992. The effect of home weatherization on indoor radon concentrations. In: *Indoor Radon and Lung Cancer: Reality or Myth?*, F. T. Cross, ed., Part 1, pp. 51-54, Proceedings of the 29th Hanford Symposium on Health and the Environment, Richland, Washington. Battelle Press, Columbus, Ohio.

Fisher, D. R., T. E. Hui, V. P. Bond, and A. C. James. 1992. Microdosimetry of radon progeny: Application to risk assessment. In: *Indoor Radon and Lung Cancer: Reality or Myth?*, F. T. Cross, ed., Part 1, pp. 307-323, Proceedings of the 29th Hanford Symposium on Health and the Environment, Richland, Washington. Battelle Press, Columbus, Ohio.

Foreman, M. E., L. S. McCoy, and M. E. Frazier. 1992. Involvement of oncogenes in radon-induced lung tumors in rats. In: *Indoor Radon and Lung Cancer: Reality or Myth?*, F. T. Cross, ed., Part 2, pp. 649-658, Proceedings of the 29th Hanford Symposium on Health and the Environment, Richland, Washington. Battelle Press, Columbus, Ohio.

Gies, R. A., F. T. Cross, G. E. Dagle, and R. L. Buschbom. 1992. The histomorphologic effects of inhaled radon, uranium ore dust, and cigarette smoke in the tracheal epithelium of the rat. In : *Abstracts, 37th Annual Meeting of the Health Physics Society*, June 21-22, Columbus, Ohio.

Gilbert, E. S., F. T. Cross, C. L. Sanders, and G. E. Dagle. 1992. Models for comparing lung-cancer risks in radon- and plutonium-exposed experimental animals. In: *Indoor Radon and Lung Cancer: Reality or Myth?*, F. T. Cross, ed., Part 2, pp. 783-802, Proceedings of the 29th Hanford Symposium on Health and the Environment, Richland, Washington. Battelle Press, Columbus, Ohio.

Hulla, J. E. 1992. The rat genome contains a p53 pseudogene: Detection of a processed pseudogene using PCR. *PCR Methods and Applications* 1:251-254.

James, A. C. 1992. Dosimetry of radon and Thoron exposures: Implications for risks from indoor exposure. In: *Indoor Radon and Lung Cancer: Reality or Myth?*, F. T. Cross, ed., Part 1, pp. 167-200, Proceedings of the 29th Hanford Symposium on Health and the Environment, Richland, Washington. Battelle Press, Columbus, Ohio.

James, A. C., D. R. Fisher, T. E. Hui, J. K. Briant, K. D. Thrall, R. F. Jostes, and F. T. Cross. 1992. Dosimetry of radon progeny. In: *DOE FY 1991 Radon Research Program Report*, pp. 137-140. DOE/ER-0536P, NTIS, Springfield, Virginia.

Johnson, N. F., M. D. Hoover, D. G. Thomassen, Y. S. Cheng, A. Dalley, and A. L. Brooks. 1992. In vitro activity of silicon carbide whiskers in comparison to other industrial fibers using four cell culture systems. *Am. J. Ind. Med.* 21:807-823.

Jostes, R. F., E. W. Fleck, R. A. Gies, T. E. Hui, T. L. Morgan, J. L. Schwartz, J. K. Wiencke, and F. T. Cross. 1992. Cytotoxic, clastogenic, and mutagenic response of mammalian cells exposed in vitro to radon and its progeny. In: *Indoor Radon and Lung Cancer: Reality or Myth?*, F. T. Cross, ed., Part 2, pp. 555-568, Proceedings of the 29th Hanford Symposium on Health and the Environment, Richland, Washington. Battelle Press, Columbus, Ohio.

Leung, F. C., G. E. Dagle, and F. T. Cross. 1992. Involvement of growth factors and their receptors in radon-induced rat lung tumors. In: *Indoor Radon and Lung Cancer: Reality or Myth?*, F. T. Cross, ed., Part 2, pp. 615-626, Proceedings of the 29th Hanford Symposium on Health and the Environment, Richland, Washington. Battelle Press, Columbus, Ohio.

Loo, J. A., R. R. Ogorzalek, D. R. Goodlett, R. D. Smith, A. F. Fuciarelli, D. L. Springer, B. D. Thrall, and C. G. Edmonds. 1992. Elucidation of covalent and non-covalent association of proteins by electrospray ionization mass spectrometry. In: *Techniques in Protein Chemistry*, Vol. 4, R. H. Angellette, ed. Academic Press, New York.

Lutze, L. H., R. A. Winegar, R. Jostes, F. T. Cross, and J. E. Cleaver. 1992. Radon-induced deletions in human cells: Role of nonhomologous strand rejoining. *Cancer Res.* 52:5126-5129.

Minnick, M. F., L. C. Stilwell, J. M. Heineman, and G. L. Stiegler. 1992. A highly repetitive DNA sequence possibly unique to canids. *Gene* 110:235-238.

Perry, R. E., R. E. Weller, R. L. Buschbom, G. E. Dagle, and J. F. Park. 1992. Radiographically determined growth dynamics of primary lung tumors in dogs by inhalation of plutonium. *Am. J. Vet. Res.* 53(10):1740-1743.

Russell, M. J., R. White, E. Patel, W. R. Markesbery, C. R. Watson, and J. W. Geddes. 1992. Familial influence on plaque formation in the beagle brain. *NeuroReport* 3:1093-1096.

Sanders, C. L. 1992. Life-span studies in rats exposed to $^{239}PuO_2$ aerosol. II. Nonpulmonary tumor formation in control and exposed groups. *J. Environ. Pathol. Toxicol. Oncol.* 11(5,6):265-277.

Sanders, C. L. 1992. Pleural mesothelioma in the rat following exposure to $^{239}PuO_2$. *Health Phys.* 63(6):695-697 (Note).

Sanders, C. L., and K. E. McDonald. 1992. Malignancy of proliferative pulmonary lesions in the Syrian hamster following inhalation of $^{239}PuO_2$. *J. Environ. Pathol. Toxicol. Oncol.* 11(3):151-156.

Sanders, C. L., G. E. Dagle and J. A. Mahaffey. 1992. Incidence of brain tumors in rats exposed to an aerosol of $^{239}PuO_2$. *Int. J. Radiat. Biol.* 62:97-102.

Schwartz, J. L., J. Rotmensch, R. W. Atcher, R. F. Jostes, F. T. Cross, T. E. Hui, D. Chen, S. Carpenter, H. H. Evans, J. Mencl, G. Bakale, and P. S. Rao. 1992. Interlaboratory comparison of different alpha particle and radon sources: Cell survival and relative biological effectiveness. *Health Phys.* 62(5):458-461.

Sikov, M. R. 1992. *Effects of Low-Level Fetal Irradiation on the Central Nervous System* (proceedings of a workshop). PNL-8009, Pacific Northwest Laboratory, Richland, Washington.

Sikov, M. R. , R. J. Traub, and H. K. Meznarich. 1992. Comparative placental transfer, localization, and effects of radionuclides in experimental animal and human pregnancies. In: *Proceedings of the AECL Fetal Dosimetry Workshop Conference*, E. S. Lamothe, ed., pp. 1-26, Chalk River, Ontario. AECL-10578, Health Physics Branch, Chalk River, Ontario.

Sikov, M. R., R. J. Traub, T. E. Hui, H. K. Meznarich, and K. D. Thrall. 1992. *Contribution of Maternal Radionuclide Burdens to Prenatal Radiation Doses.* NUREG/CR-5631, PNL-7445, Rev. 1. Prepared for the U.S. Nuclear Regulatory Commission, Washington, D.C., by Pacific Northwest Laboratory, Richland, Washington.

Sikov, M. R., F. T. Cross, T. J. Mast, H. E. Palmer, A. C. James, and B. D. Thrall. 1992. Developmental toxicology of radon exposures. In: *Indoor Radon and Lung Cancer: Reality or Myth?*, F. T. Cross, ed., Part 2, pp. 677-692, Proceedings of the 29th Hanford Symposium on Health and the Environment, Richland, Washington. Battelle Press, Columbus, Ohio.

Smith, S. K., J. C. Prather, E. K. Ligotke, and C. R. Watson. 1992. *National Radiobiology Archives Distributed Access User's Manual Version 1.1, Rev. 1.* PNL-7877, Pacific Northwest Laboratory, Richland, Washington.

Stark, P., B. D. Thrall, G. G. Meadows, and M. M. Abdel-Monem. 1992. Synthesis and evaluation of novel spermidine derivatives as targeted chemotherapeutic agents. *J. Med. Chem.* 35:4264-4269.

Thrall, B. D., and D. L. Springer. 1992. Sequence-specific blocks in DNA/RNA polymerases induced by benzo[a]pyrene diolepoxide. *Toxicologist* 12:251 (abstract).

Thrall, B. D., D. B. Mann, M. J. Smerdon, and D. L. Springer. 1992. DNA polymerase and exonuclease activities on a DNA sequence modified by benzo[*a*]pyrene diolepoxide. *Carcinogenesis* 13(9):1529-1534.

Wasiolek, P. T., P. K. Hopke, and A. C. James. 1992. Assessment of exposure to radon decay products in realistic living conditions. *J. Exposure Anal. & Environ. Epidemiol.* 2:309-322.

Weller, R. E. 1992. Intrathoracic neoplasia: Epidemiology and etiology. In: *Proceedings of the 10th American College of Veterinary Internal Medicine Forum*, pp. 652-654, San Diego, California. Omnipress, Madison, Wisconsin.

Weller, R. E. 1992. Paraneoplastic syndromes. In: *Handbook of Small Animal Practice*, 2nd Ed., R. V. Morgan, ed., pp. 813-822. Churchill Livingstone, New York.

Weller, R. E., and W. E. Hoffman. 1992. Renal function in dogs with lymphosarcoma and associated hypercalcemia. *J. Small Anim. Pract.* 33:61-66.

Weller, R. E., G. E. Dagle, R. E. Perry, and J. F. Park. 1992. Primary pulmonary chondrosarcoma in a dog. *Cornell Vet.* 82(4):447-452.

Zangar, R. C., D. L. Springer, and D. R. Buhler. 1992. Alterations in cytochrome P-450 levels in adult rats following neonatal exposure to xenobiotics. *J. Toxicol. Environ. Health.* 38:43-55.

Zangar, R. C., D. L. Springer, J. A. McCrary, R. F. Novak, T. Primiano, and D. R. Buhler. 1992. Changes in adult metabolism of aflatoxin B_1 in rats neonatally exposed to diethystilbestrol. Alterations in α-class glutathione S-transferases. *Carcinogenesis* 13:2375-2379.

1993

Hulla, J. E., and R. P. Schneider. 1993. Structure of the rat p53 tumor suppressor gene. *Nucleic Acids Res.* 21(3):723-717.

In Press

Brooks, A. L., K. E. McDonald, C. Mitchell, D. S. Culp, A. Lloyd, N. F. Johnson, and R. M. Kitchin. The combined genotoxic effects of radiation and occupational pollutants. In: *Current Topics in Occupational Health*, T. S. Tenforde, ed., Proceedings of the 30th Hanford Symposium on Health and the Environment, Richland, Washington. *Appl. Occup. Hyg. J.* (in press).

Cross, F. T. Evidence of cancer risk from experimental animal radon studies. In: *Pedagogical Symposium: Radiation and Society*, Proceedings of the 203rd National Meeting of the American Chemical Society, April 5-10, 1992, San Francisco, California (in press).

Cross, F. T. Experimental, statistical, and biological models of radon carcinogenesis. *Radiat. Prot. Dosim.* (in press).

Cross, F. T., J. Lubin, R. Masse, J. Samet, and G. A. Swedjemark. Inputs to the quantification of risk. In: *CEC/DOE Radon-Related Risk Recommendations Report*, Chapter 4 (in press).

Hoover, M. D., F. A. Seiler, G. L. Finch, P. J. Haley, A. F. Eidson, J. A. Mewhinney, D. E. Bice, A. L. Brooks, and R. K. Jones. Beryllium toxicity: An update. In: *Proceedings, Sixth Symposium on Space Nuclear Power Systems* (in press).

Hui, T. E., A. L. Brooks, and A. C. James. Microdosimetry of micronuclei induction and cell killing in mammalian cells irradiated in vitro by alpha particles. *Int. J. Radiat. Biol.* (in press).

Hui, T. E., F. T. Cross, A. C. James, R. F. Jostes, J. L. Schwartz, and K. L. Swinth. Evaluation of an alpha probe detector for *in vitro* cellular dosimetry. *Health Phys.* (in press).

Jostes, R. F., T. E. Hui, and F. T. Cross. Use of the single-cell gel technique to support hit probability calculations in mammalian cells exposed to radon and radon progeny. *Health Phys.* (in press).

Mahaffey, J. A., M. A. Parkhurst, A. C. James, F. T. Cross, H. E. Palmer, M. C. R. Alavanja, S. Ezrine, P. Henderson, and R. Brownson. Feasibility study to evaluate affixing CR-39 to glass artifacts for estimating cumulative exposure to radon. *Health Phys.* (in press).

Sanders, C. L. Lifespan studies in rats exposed to $^{239}PuO_2$ aerosol. I. Dosimetry. *Health Phys.* (in press).

Sanders, C. L., and G. E. Dagle. A threshold model of pulmonary carcinogenesis: Carcinoma in the rat after deposition of plutonium or quartz. In: *Current Topics in Occupational Health*, T. S. Tenforde, ed., Proceedings of the 30th Hanford Symposium on Health and the Environment, Richland, Washington. *Appl. Occup. Environ. Hyg. J.* (in press).

Sanders, C. L., G. E. Dagle, and J. A. Mahaffey. Incidence of brain tumors in rats exposed to an aerosol of $^{239}PuO_2$. *Int. J. Radiat. Biol.* (in press).

Sanders, C. L., R. A. Guilmette, and R. L. Kathren. Autoradiographic examination of soft tissues in a human case of acute ^{241}Am exposure. *Health Phys.* (in press).

Wolff, S., V. Afzal, R. Jostes, and J. K. Wiencke. Indications of repair of radon-induced chromosome damage in human lymphocytes: An adaptive response induced by low doses of x rays. *Environ. Health Perspect.* (in press).

Presentations

1991

Briant, J. K., A. C. James, and M. A. Parkhurst. 1991. Design and Calibration of an Ultrafine Radon Progeny Size-Spectrometer Utilizing Etched Tracks in CR-39 Plastic. Presented at the 1991 Meeting of the American Association for Aerosol Research, October 7-11, 1991, Traverse City, Michigan.

Blakely, W. F., G. Iliakis, D. M. Mosbrook, and A. F. Fuciarelli. Studies on Hydrogen Peroxide-Induced Cell Killing Using Chinese Hamster V79 Cells. Presented at the 9th International Congress of Radiation Research, July 7-12, 1991, Toronto, Canada.

Brooks, A. L. 1991. Use of *In Vitro/In Vivo* Models of Carcinogenesis. Presented at the National Cancer Institute and Cancer Biology — Immunology Contracts Committee Review, October 6-9, 1991, Bethesda, Maryland.

Brooks, A. L., K. E. McDonald, and R. M. Kitchin. 1991. Influence of Internally Deposited ^{239}Pu on Chromosome Aberration Frequency Induced by Acute Exposure to ^{60}Co in Bone Marrow of the Chinese Hamster. Presented at the 9th International Congress of Radiation Research, July 7-12, 1991, Toronto, Canada.

Brooks, A. L., R. F. Kitchin, K. E. McDonald, and A. Vinson. 1991. Genotoxic Damage from Combined Exposures to Organic Solvents and Radiation. Presented at the Environmental Mutation Society Meeting, April 6-10, 1991, Orlando, Florida.

Brooks, A. L., K. E. McDonald, B. B. Kimsey, and R. M. Kitchin. 1991. The Induction of Chromosome Damage in Bone Marrow of Chinese Hamsters Following Combined Acute Gamma Ray Exposure and Internally Deposited ^{239}Pu. Presented at the 9th International Congress of Radiation Research, July 7-12,1991, Toronto, Canada.

Brooks, A. L., D. S. Culp, A. L. Lloyd, K. E. McDonald, and R. M. Kitchin. 1991. Lack of Interaction Between Damage Produced by ^{60}Co Gamma Rays and Organic Solvents Methyl Isobutyl Ketone or Tributyl Phosphate on Cell Killing and Micronuclei. Presented at the Annual Meeting of the Pacific Northwest Association of Toxicologists, September 6, 1991, Seattle, Washington.

Brooks, A. L., K. E. McDonald, C. Mitchell, A. Lloyd, N. F. Johnson, and R. M. Kitchin. 1991. The Combined Genotoxic Effects of Radiation and Occupational Pollutants. Presented at the 30th Hanford Symposium on Health and the Environment, "Current Topics in Occupational Health," October 29-November 1, 1991, Richland, Washington.

Cross, F. T. 1991. NIH Core Project Overview and Development and Application of the Animal Model. Presented at the NIH Radon Proposal Review Site Visit, February 21, 1991, Richland, Washington.

Cross, F. T. 1991. Experimental Studies on Lung Carcinogenesis and Their Relationship to Future Research in Radiation-Induced Lung Cancer in Humans. Presented at the Workshop on The Future of Human Radiation Research, March 4-8, 1991, Schloss Elmau, Germany.

Cross, F. T. 1991. Overview of the DOE/RERF/I-ARC/CEC Schloss Elmau Workshop. Presented at the Meeting of the Washington State Radon Health Effects Committee/Radon Task Force, March 12, Seattle, Washington.

Cross, F. T. 1991. Can Animal Data Apply to Man? Presented at the DOE Science Writers' Workshop, "Radon Today: The Science and the Politics," April 25-26, 1991, Bethesda, Maryland.

Cross, F. T. 1991. A Review of Experimental Animal Radon Health Effects Data. Presented at the 9th International Congress of Radiation Research, July 7-12, 1991, Toronto, Canada.

Cross, F. T. 1991. Evidence of Risk from Animal Studies. Presented at the 1991 DOE/OHER Radon Contractors' Meeting, August 25-27, 1991, Albuquerque, New Mexico.

Cross, F. T. 1991. Progress on Risk in "Inhalation Hazards to Uranium Miners" and "Mechanisms of Radon Injury" Projects. Presented at the 1991 DOE/OHER Radon Contractors' Meeting, August 25-27, 1991, Albuquerque, New Mexico.

Cross, F. T. 1991. Experimental, Statistical, and Biological Models of Radon Carcinogenesis. Presented at the 5th International Symposium on the Natural Radiation Environment, September 22-28, 1991, Salzburg, Austria.

Cross, F. T. 1991. Radon Health Effects Data in Animals and Their Relationship to Human Data. Presented at the 5th Annual Conference of the American Association of Radon Scientists and Technologists, October 9-12, 1991, Rockville, Maryland.

Cross, F. T. 1991. Experimental Radon Health-Effect Studies. Presented to the Radiological Sciences Course 501, Biological Effects of Ionization Radiation, November 7, 1991, Washington State University Tri-Cities Campus, Richland, Washington.

Cross, F. T. 1991. The DOE and PNL Radon Program with Emphasis on Experimental Animal Studies. Presented at the Cellular and Mammalian Biology Section Meeting, November 7, 1991, Richland, Washington.

Cross, F. T. 1991. A Review of Experimental Animal Radon Health Effects Data. Presented at the 2nd IAEA/UNESCO/UNIDO/ICTP Workshop on Radon Monitoring in Radioprotection, Environmental and/or Earth Sciences, November 25-December 6, 1991, Trieste, Italy.

Cross, F. T., and G. E. Dagle. 1991. Lung Cancer in Rats Exposed to Radon/Radon Progeny. Presented at the 1991 International Symposium on Radon and Radon Reduction Technology, April 2-5, 1991, Philadelphia, Pennsylvania.

Dagle, G. E. 1991. Physicochemical Interactions and Tumor Induction in Bones by Inhaled $^{239}Pu(NO3)_4$. Presented at the Joint Bone Radiology Workshop, July 12-13, 1991, Toronto, Canada.

Dagle, G. E., J. F. Park, R. E. Weller, E. S. Gilbert, and R. L. Buschbom. 1991. Health Effects of Inhaled Plutonium in Dogs. Presented at the 9th International Congress of Radiation Research, July 7-12, 1991, Toronto, Canada.

Douthart, R. D. 1991. Computer Graphics as a Tool in Understanding Genomic Structures. Presented at the workshop "Computer-Based Analysis of Nucleic Acids and Protein Sequences," January 19, 1991, University of Washington Medical Center, Seattle, Washington (invited presentation).

Douthart, R. D. 1991. Graphics Sequence Representation and Analysis. Presented at the workshop, "Computer-Based Analysis of Nucleic Acids and Protein Sequences," January 19, 1991, University of Washington Medical Center, Seattle, Washington.

Douthart, R. D. 1991. Computer Visualization of Large Genomic Structures. Presented at BBN, Inc., March 4, 1991, Cambridge, Massachusetts.

Douthart, R. D. 1991. "Metacodes in DNA and Protein Sequence," the Telluride Workshop on Open Problems of Computational Molecular Biology, June 2-8, 1991, Telluride, Colorado.

Douthart, R. D., and D. A. Thurman. 1991. GnomeView: A Computer Graphics Window into the Human Genome. Presented at the Human Genome Workshop III, October 22, 1991, San Diego, California.

Douthart, R. D., D. A. Thurman, and J. E. Pelkey. 1991. GnomeView: A Genome Graphics Interface. Presented at the Human Genome Workshop, February 19, 1991, Santa Fe, New Mexico.

Elston, R. A. 1991. Future of the Coastal Shellfish Resource. Presented at the Washington Department of Fisheries Information Fair, January 17, 1991, Long Beach, Washington.

Hulla, J. E. 1991. Evidence of the Occurrence of a Processed p53 Pseudogene Within the Rat Genome. Presented at the Radiation Research Society Special Workshop, "Oncogenic Mechanisms in Radiation-Induced Cancer," January 16-19, 1991, Fort Collins, Colorado.

James, A. C. 1991. ICRP Lung Dosimetry – Status of the ICRP Task Group Proposals. Seminar presented to the Atomic Energy Control Board, April 22, 1991, Ottawa, Canada.

James, A. C. 1991. Developments in Lung and Body Organ Dosimetry for Radon, Thoron, and Their Short-Lived Progeny – What Are They Telling Us? Seminar presented to the National Radiological Protection Board, October 3, 1991, Chilton, England.

James, A. C., and J. K. Briant. 1991. Proposed New Concepts in ICRP Respiratory Tract Dosimetry with Application to Gases and Vapors. Presented at the 30th Hanford Symposium on Health and the Environment, "Current Topics in Occupational Health," October 29-November 1, 1991, Richland, Washington.

James, A. C., and K. D. Thrall. 1991. General Biokinetic Model for Radon, Thoron, and Their Short-Lived Progeny – What Are They Telling Us? Presented at the Annual Meeting of DOE/OHER Research Contractors, August 25-27, 1991, Albuquerque, New Mexico.

James, A. C., J. R. Johnson, and D. R. Fisher. 1991. ICRP Task Group Dosimetry Model for the Respiratory Tract: Implications for Uranium. Presented at the 36th Annual Meeting of the Health Physics Society, July 21-26, 1991, Washington, D.C.

Jostes, R. F., T. L. Morgan, E. W. Fleck, and F. T. Cross. 1991. Radiation-Induced Mutation Studies. Presented at the 1991 DOE/OHER Radon Contractors' Meeting, August 25-27, 1991, Albuquerque, New Mexico.

Kitchin, R. M., K. E. McDonald, and A. L. Brooks. 1991. The Induction of Chromosome Damage in Bone Marrow and Liver Cells of Chinese Hamsters Following Combined Exposure to Acute Gamma Ray Exposures and Internally Deposited ^{144}Ce. Presented at the 9th International Congress of Radiation Research, July 7-12, 1991, Toronto, Canada.

Kitchin, R. M., K. E. McDonald, B. B. Kimsey, and A. L. Brooks. 1991. Influence of Internally Deposited ^{144}Ce – ^{144}Pr on Chromosome Aberration Frequency Induced by Acute Exposure to ^{60}Co in Bone Marrow and Liver of Chinese Hamsters. Presented at the 9th International Congress of Radiation Research, July 7-12, 1991, Toronto, Canada.

Meznarich, H. K. 1991. Altered Fibronectin Levels in Irradiated Mouse Blastocysts. Presented at the Annual Meeting of the Federation of American Societies for Experimental Biology, April 1991, Atlanta, Georgia.

Meznarich, H. K. 1991. Fibronectin in Prenatally Irradiated Mouse Brains. Presented at the Regional Meeting for the Pacific Northwest Association of Toxicologists, September 1991, Seattle, Washington.

Morgan, T. L., L. A. Braby, E. W. Fleck, R. F. Jostes, and F. T. Cross. 1991. Model of Radiation Mutagenesis. Presented at the 24th Radiological and Chemical Physics Contractors Meeting, April 1991, New York, New York.

Sanders, C. L., and G. E. Dagle. 1991. A Threshold Model of Pulmonary Carcinogenesis: Carcinoma in the Rat After Deposition of Plutonium or Quartz. Presented at the 30th Hanford Symposium on Health and the Environment, "Current Topics in Occupational Health," October 29-November 1, 1991, Richland, Washington.

Sanders, C. L., G. E. Dagle, J. A. Mahaffey, and K. E. Lauhala. 1991. Increased Incidence of Brain Tumors in Rats Exposed to Plutonium Aerosol. Presented at the 9th International Congress of Radiation Research, July 7-12, 1991, Toronto, Canada.

Shum, F. Y., A. F. Fuciarelli, and J. A. Raleigh. 1991. Hydrated Electron Reaction with 8,5′-Cycloadenosine-5′-Monophosphate: 5′-Deoxy-5′-Dihydro-8,5′-Cycloadenosine. Presented at the 9th International Congress of Radiation Research, July 7-12, 1991, Toronto, Canada.

Sikov, M. R. 1991. Hazards and Risks Associated with Prenatal Irradiation: Emphasis on Internal Radionuclide Exposures. Invited presentation at DOE/CEC/EULEP Workshop on Age-Dependent Factors in the Biokinetics and Dosimetry of Radionuclides, November 1991.

Springer, D. L., C. G. Edmonds, D. M. Sylvester, and R. J. Bull. 1991. Hemoglobin Adducts as Biomarkers of Chemical Exposure. Presented at the 1991 Annual Meeting of the Society for Risk Analysis, December 8-11, 1991, Baltimore, Maryland.

Springer, D. L., S. C. Goheen, C. G. Edmonds, M. McCulloch, D. M. Sylvester, C. L. Sanders, and R. J. Bull. 1991. Presented at the 30th Annual Meeting of the Society of Toxicology, February 25-March 1, 1991, Dallas, Texas.

Stiegler, G. E. 1991. Evidence for *ras* Oncogene Activation in Radiation-Induced Carcinogenesis. Presented at the Radiation Research Society Special Workshop, "Oncogenic Mechanisms in Radiation-Induced Cancer," January 16-19, 1991, Fort Collins, Colorado.

Stiegler, G. L., L. C. Stillwell, E. C. Sisk, and M. F. Minnick. 1991. Evidence for *ras*-Oncogene Activation in Radiation-Induced Oncogenesis. Presented at the 9th Annual Meeting of the Pacific Northwest Association of Toxicologists, September 6-7, 1991, Seattle, Washington.

Thrall, B., and D. L. Springer. 1991. Altered Transcription by SP6 Polymerase. Presented at the 82nd Annual Meeting of the American Association for Cancer Research, May 15-18, 1991, Houston, Texas.

Thrall, B., M. J. Smerdon, and D. L. Springer. 1991. Sequence-Specific Modification of DNA by Benzo[a]pyrene Diol Epoxide Determined by Inhibition of Polymerase Activities. Presented at the American Association for Cancer Research Special Conference, "Cellular Responses to Environmental DNA Damage," December 1-6, 1991, Banff, Alberta, Canada.

Watson, C. R. 1991. Workshop on "Future Directions for Radium Dial Painter Studies." Presented at Argonne National Laboratory, June 3-5, 1991, Argonne, Illinois.

Watson, C. R. 1991. National Radiobiology Archives. Presented at the 36th Annual Meeting of the Health Physics Society, July 21-26, 1991, Washington, D.C.

Watson, C. R., Chairman. 1991. "The Control Beagle Workshop," convened by the National Radiobiology Project, December 16-17, 1991, Salt Lake City, Utah.

Weller, R. E. 1991. Canine Lymphoma: What's Old? What's New? Presented to the Southeast Washington Veterinary Medical Association, October 15, 1991, Pasco, Washington.

Zangar, R. C., D. R. Buhler, and D. L. Springer. 1991. Developmental Regulation of Cytochrome P450 IIC11 Enzyme Activity Correlates with mRNA Levels in DES-Imprinted Rats. Presented at the 30th Annual Meeting of the Society of Toxicology, February 25-March 1, 1991, Dallas, Texas.

1992

Briant, J. K. 1992. Computational Modeling of Aerosol Bolus Dispersion and Deposition During Breathhold. Presented at the Inhalation Toxicology Research Institute, May 12, 1992, Albuquerque, New Mexico.

Briant, J. K. 1992. Particle Transport by Cardiogenic Air Motion in Mammalian Lung Airways: A Computational Model. Presented at the American Association for Aerosol Research, October 16, 1992, San Francisco, California.

Brooks, A. L. 1992. Radioadaptive Response In Vivo in Chinese Hamsters Injected with Alpha- (^{239}Pu) or Beta-Gamma- (^{144}Ce) Emitting Radionuclides. Presented at the International Conference on Low Dose Irradiation and Biological Defense Mechanisms, July 11-19, 1992, Kyoto, Japan.

Brooks, A. L. 1992. Use of Cell and Molecular Techniques in Risk Assessment. Presented at the Hanford Technical Exchange Program on Human Health and Ecological Risk: Science and Policy Issues Important to the DOE Approach to Environmental Cleanup, October 14, 1922, Richland, Washington.

Brooks, A. L., M. A. Khan, R. F. Jostes, and F. T. Cross. 1992. Metaphase Chromosome Aberrations as Markers of Radiation Exposure and Dose. Presented at the 31st Hanford Symposium on Health and the Environment, "The Laboratory and Epidemiology: The Development and Application of Biomarkers to the Study of Human Health Effects," October 19-23, 1992, Richland, Washington.

Brooks, A. L., R. M. Kitchin, N. F. Johnson, and E. S. Gilbert. 1992. The Role of Cellular and Molecular Studies in Evaluation of Health Effects from Combined Radiation and Chemical Exposures. Presented at the American Statistical Association Conference on Radiation and Health, June 28-July 2, 1992, Hilton Head Island, South Carolina.

Brooks, A. L., M. R. Raju, M. K. Murphy, W. F. Harvey, G. J. Newton, and R. Guilmette. 1992. Comparison of the Effectiveness of Collimated and Non-Collimated Random ^{238}Pu Sources on the Induction of Micronuclei and Cell Killing in Lung Epithelial Cells. Presented at the 40th Annual Meeting of the Radiation Research Society, March 15-18, 1992, Salt Lake City, Utah.

Brooks, A. L., J. Adelstein, B. Boecker, K. Kase, A. Kronenburg, B. McNeil, R. Shore, and W. Templeton. 1992. Identification of Research Needs in Radiation Protection. Presented at the 40th Annual Meeting of the Radiation Research Society, March 15-18, 1992, Salt Lake City, Utah.

Cross, F. T. 1992. DOE and PNL Programs on Risk of Environmental Radon Exposure. Presented at the Florida Institute of Phosphate Research October 16, 1992, Bartow, Florida.

Cross, F. T. 1992. Evidence of Cancer Risk from Experimental Animal Radon Studies. Presented at the Pedagogical Symposium of the 203rd National Meeting of the American Chemical Society: "Radiation and Society," April 5-10, 1992, San Francisco, California.

Dagle, G. E., F. T. Cross, R. A. Gies, and R. Buschbom. 1992. Lung Tumors in Rats Exposed to Inhaled Uranium Ore Dust and Radon Progeny. Presented at the European Society for Radiation Biology Meeting, October 4-8, 1992, Erfurt, Germany.

Gies, R. A., F. T. Cross, G. E. Dagle, R. L. Buschbom, and J. C. Aryan. 1992. The Histomorphologic Effects of Inhaled Radon, Uranium Ore Dust, and Cigarette Smoke in the Tracheal Epithelium of the Rat. Presented at the 37th Annual Meeting of the Health Physics Society, June 21-25, 1992, Columbus, Ohio.

Jostes, R. F., Jr., T. E. Hui, R. A. Gies, and F. T. Cross. 1992. Use of the Single Cell Gel Technique to Confirm Hit Probability Calculations in Mammalian Cells Exposed to Radon and Radon Progeny. Presented at the 40th Annual Meeting of the Radiation Research Society, March 14-18, 1992, Salt Lake City, Utah.

Dagle, G. E., F. T. Cross, R. A. Gies, and R. Buschbom. 1992. Lung Tumors in Rats Exposed to Inhaled Uranium Ore Dust and Radon Progeny. Presented at the 24th Annual Meeting of the European Society for Radiation Biology, October 4-8, 1992, Erfurt, Germany.

Douthart, R. J. 1992. A Computer Graphics Window to the Human Genome. Presented at Baylor College of Medicine, Houston, Texas.

Douthart, R. J. 1992. GnomeView: Human Genome Data Base Integration with Color Graphics. Presented at Washington State University, Pullman.

Douthart, R. J. 1992. The Insulin Gene That Wasn't. Presented at the Biotechnology Training Program Workshop, Washington State University, Pullman.

Douthart, R. J. 1992. Invited lecture and GnomeView demonstration given at the Human Genome Informatics Workshop, Lawrence Berkeley Laboratory, Berkeley, California.

Douthart, R. J. 1992. Invited lecture and GnomeView demonstration given at the Johns Hopkins University Medical School, Baltimore, Maryland.

Edmonds, C. G., D. L. Springer, D. M. Sylvester, S. C. Goheen, and R. J. Bull. 1992. Characterization of Acrylamide Adducted Hemoglobin and Proteolytically Derived Peptides Based on Electrospray Ionization Mass Spectrometry. Presented at the 40th ASMS Conference on MS and Allied Topics, May 31-June 5, 1992, Washington, D.C.

Edmonds, C. G., J. A. Loo, R. D. Smith, A. F. Fuciarelli, B. T. Thrall, J. D. Morris, and D. L. Springer. 1992. Evaluation of Histone Sequence and Modifications by Electrospray Ionization Mass Spectrometry and Tandem Mass Spectrometry. Presented at the 31st Hanford Symposium on Health and the Environment, "The Laboratory and Epidemiology: The Development and Application of Biomarkers to the Study of Human Health Effects," October 19-23, 1992, Richland, Washington.

Edmonds, C. G., J. A. Loo, R. D. Smith, A. F. Fuciarelli, B. T. Thrall, J. D. Morris, and D. L. Springer. 1992. Evaluation of Histone Sequence and Modifications by Electrospray Ionization Mass Spectrometry and Tandem Mass Spectrometry. Presented at the Pacific Conference on Chemistry and Spectroscopy, October 21, 1992, Foster City, California.

Fuciarelli, A. F., E. C. Sisk, and J. D. Zimbrick. 1992. Measurement of Free Radical-Induced Base Damage in DNA. Presented at the 31st Annual Meeting of the Society of Toxicology, February 23-27, 1992, Seattle, Washington.

Fuciarelli, A. F., E. C. Sisk, and J. D. Zimbrick. 1992. 5-Bromouracil Radiolysis as a Molecular Indicator of Electron Migration in Aqueous Solutions of DNA. Presented at the 40th Annual Meeting of the Radiation Research Society, March 14-18, 1992, Salt Lake City, Utah.

Fuciarelli, A. F., E. C. Sisk, and J. D. Zimbrick. 1992. Electron Transfer in Irradiated Solutions of DNA. Presented at the 9th Annual Meeting of the Pacific Northwest Association of Toxicologists (PANWAT), September 24-25, 1992, Richland, Washington.

Fuciarelli, A. F., M. Kennedy, J. D. Zimbrick, and J. A. Raleigh. 1992. Radiation-Induced Intramolecular Cyclization Reactions in DNA: Molecular Modeling and Experimental Analysis. Presented at the conference "Pathways to Radiation Damage in DNA," June 14-18, 1992, Oakland University, Rochester, Michigan.

Gies, R. A., F. T. Cross, G. E. Dagle, R. L. Buschbom, and J. C. Aryan. 1992. The Histomorphologic Effects of Inhaled Radon, Uranium Ore Dust, and Cigarette Smoke in the Tracheal Epithelium of the Rat. Presented at the 37th Annual Meeting of the Health Physics Society, June 21-25, 1992, Columbus, Ohio.

James, A. C. 1992. Implications of a New ICRP Lung Model for the Uranium and Sand Mining Industries. Overview presented at the International Workshop on the Health Effects of Inhaled Radionuclides: Implications for Radiation Protection in Mining, September 1992, Jabiru, Northern Territory, Australia (keynote address).

James, A. C. 1992. The ICRP Task Group's New Lung Model for Dosimetry and Bioassay. Overview presented at the 17th Annual Meeting of the Australian Radiation Protection Society, September 21-23, 1992, Darwin, Northern Territory, Australia.

Jarvis, M. G., K. D. Thrall, T. E. Hui, J. R. Johnson, J. A. Leonowich, T. T. Jarvis, and J. V. Mohatt. 1992. The Integrated Use of Instrumentation and PBPK Models to Establish Occupational Exposure. Presented at the 31st Hanford Symposium on Health and the Environment, "The Laboratory and Epidemiology: The Development and Application of Biomarkers to the Study of Human Health Effects," October 19-23, 1992, Richland, Washington.

Jostes, R. F., Jr., T. E. Hui, R. A. Gies, and F. T. Cross. 1992. Use of the Single-Cell Gel Technique to Confirm Hit Probability Calculations in Mammalian Cells Exposed to Radon and Radon Progeny. Presented at the 40th Annual Meeting of the Radiation Research Society, March 14-18, 1992, Salt Lake City, Utah.

Khan, M. A., R. F. Jostes, F. T. Cross, K. Rithidech, and A. L. Brooks. 1992. Micronucleus: A Biomarker of Genotoxic Damage Induced *in Vivo* and *in Vitro* from Radiation and Chemical Exposure. Presented at the 31st Hanford Symposium on Health and the Environment, "The Laboratory and Epidemiology: The Development and Application of Biomarkers to the Study of Human Health Effects," October 19-23, 1992, Richland, Washington.

Khan, M. A., R. F. Jostes, J. E. Morris, R. A. Gies, and A. L. Brooks. 1992. The Induction and Repair of Micronuclei in Deep Lung Fibroblasts of Rats from *in Vitro* and *in Vivo* Radon-Progeny Exposure. Presented at the 9th Annual Meeting of the Pacific Northwest Association of Toxicologists (PANWAT), September 24-25, 1992, Richland, Washington.

Loo, J. A., R. R. Ogorzalek-Loo, R. D. Smith, A. F. Fuciarelli, D. L. Springer, and C. G. Edmonds. 1992. Evaluation of Covalent Modifications and Non-Covalent Associations in Proteins by Electrospray Ionization-Mass Spectrometry. Presented at the 6th Symposium of the Protein Society, July 25-29, 1992, San Diego, California.

Lucus, J. N., M. Poggensee, A. B. Cox, J. McLean, and A. L. Brooks. 1992. Chromosome Translocation Studies in Irradiated Primates Using Fluorescence *in Situ* Hybridization. Presented at the 40th Annual Meeting of the Radiation Research Society, March 14-18, 1992, Salt Lake City, Utah.

Meznarich, H. K., L. S. McCoy, and M. R. Sikov. 1992. Brain Fibronectin Expression in Prenatally Irradiated Mice. Presented at the 31st Hanford Symposium on Health and the Environment, "The Laboratory and Epidemiology: The Development and Application of Biomarkers to the Study of Human Health Effects," October 19-23, 1992, Richland, Washington.

Miller, R. T., R. J. Douthart, and A. K. Dunker. 1992. Learning an Objective Alphabet of Amino Acid Conformations. Presented at the 6th Annual Meeting of the Protein Society, San Diego, California.

Miller, R. T., A. K. Dunker, and R. J. Douthart. 1992. Amino Acid Conformations as a Alphabet. Presented at the West Coast Theoretical Chemistry Conference, Richland, Washington.

Sanders, C. L. 1992. Spatial Distribution of Inhaled $^{239}PuO_2$ and Pulmonary Carcinogenesis in Three Strains of the Rat. Presented at the 40th Annual Meeting of the Radiation Research Society, March 14-18, 1992, Salt Lake City, Utah.

Sanders, C. L. 1992. Inhaled Plutonium and Lung Cancer in an Animal Model. Seminar presented to Physics Applications, Westinghouse Hanford, Richland, Washington.

Sanders, C. L. 1992. Is Inhaled Plutonium Really All That Toxic? Seminar presented to the Department of Environmental Science, Washington State University Tri-Cities Campus, Richland, Washington.

Sanders, C. L. 1992. Microdosimetric and Cellular Basis for a Lung Tumor Threshold Following Inhalation of $^{239}PuO_2$. Presented at the EULEP Symposium on Acute and Late Effects on the Lungs from Inhaled Radioactive Materials and External Irradiation, Erfurt, Germany.

Sanders, C. L. 1992. Pulmonary Carcinogenesis of Inhaled Plutonium. Seminar given at the Department of Pharmacology/Toxicology, Washington State University, Pullman.

Sanders, C., D. M. Sylvester, and D. L. Springer. 1992. Recognition of Acrylamide Adducts in Peptides from Hemoglobin. Presented at the 31st Annual Meeting of the Society of Toxicology, February 23-27, 1992, Seattle, Washington.

Springer, D. L., C. G. Edmonds, D. M. Sylvester, C. Sanders, and R. J. Bull. 1992. Partial Characterization of Proteolytically Derived Peptides from Acrylamide-Adducted Hemoglobin. Presented at the 31st Annual Meeting of the Society of Toxicology, February 23-27, 1992, Seattle, Washington.

Thrall, B., and D. L. Springer. 1992. Sequence-Specific Blocks in DNA/RNA Polymerases Induced by Benzo[a]pyrene Diol Epoxide. Presented at the 31st Annual Meeting of the Society of Toxicology, February 23-27, 1992, Seattle, Washington.

Thrall, B. D., C. G. Edmonds, and D. L. Springer. 1992. Translesional Synthesis by Model DNA Polymerases on an Oligonucleotide Modified by Benzo[a]pyrene Diol Epoxide. Presented at the 9th Annual Meeting of the Pacific Northwest Association of Toxicologists (PANWAT), September 24-25, 1992, Richland, Washington.

Thrall, K., J. Johnson, M. Jarvis, E. Hui, and T. Jarvis. 1992. Use of Models to Establish Occupational Exposure to Chemicals and/or Radioactivity. Presented at the Joint Meeting of the International Society of Exposure Analysis and the International Society of Environmental Epidemiology, August 26-29, Cuernavaca, Morelos, Mexico.

Weller, R. E. 1992. Intrathoracic Neoplasia: Epidemiology and Etiology. Presented at the 10th American College of Veterinarians Internal Medicine Forum, May 30, 1992, San Diego, California.

Zimbrick, J. 1992. Implications of Radiation Repair Genes for Radiation Protection. Presented at the 37th Annual Meeting of the Health Physics Society, June 21-25, 1992, Columbus, Ohio.

Zimbrick, J. D. , C. M. Beach, E. C. Sisk, and A. F. Fuciarelli. 1992. Electron Migration in 5-Bromouracil-Substituted DNA and Oligonucleotides in Irradiated Aqueous Solutions. Presented at "Pathways to Radiation Damage in DNA," June 14-18, 1992, Oakland University, Rochester, Michigan.

Author Index

Author Index

Distribution

Distribution

OFFSITE

S. Addison
Radiological Safety Division
University of Washington
GS-05
Seattle, WA 98105

R. E. Albert, Professor
& Chairman
Department of Environmental
Health
University of Cincinnati
Medical Center
3223 Eden Avenue
Cincinnati, OH 45267-0056

E. L. Alpen
University of California
230 Donner Laboratory
Berkeley, CA 94720

A. Andersen
Center for Devices &
Radiological Health
Food & Drug Administration
5600 Fishers Lane, HFZ-100
Rockville, MD 20857

D. Anderson
ENVIROTEST
1108 NE 200th Street
Seattle, WA 98155-1136

G. Anderson
Department of Oceanography
University of Washington
Seattle, WA 98115

V. E. Archer
Rocky Mountain Center for
Occupational & Environmental
Health - Building 512
University of Utah
50 North Medical Drive
Salt Lake City, UT 84112

Assistant Secretary
Environment, Safety & Health
EH-1, FORS
U.S. Department of Energy
Washington, DC 20585

O. Auerbach
VA Hospital
East Orange, NJ 97919

J. A. Auxier
Auxier & Associates, Inc.
111 Mabry Hood Road
Suite 500
Knoxville, TN 37922

F. I. Badgley
13749 NE 41st Street
Seattle, WA 98125

R. E. Baker
8904 Roundleaf Way
Gaithersburg, MD 20879-1630

R. W. Barber
EH-33, GTN
U.S. Department of Energy
Washington, DC 20585

W. W. Barker, Chairman
Department of Biology
Central Washington University
Ellensburg, WA 98926

B. J. Barnhart
Office of Energy Research
U.S. Department of Energy
ER-72, GTN
Washington, DC 20585

N. F. Barr
ER-72, GTN
U.S. Department of Energy
Washington, DC 20585

M. M. Bashor, Ph.D.
ATSDR, Mail Stop E-28
1600 Clifton Road NE
Atlanta, GA 30333

J. W. Baum
Brookhaven National
Laboratory
Building 703-M
Upton
Long Island, NY 11973

J. R. Beall
ER-72, GTN
U.S. Department of Energy
Washington, DC 20585

P. M. Beam
EM-451/Trevion II
U.S. Department of Energy
Washington, DC 20585-0002

S. Benjamin
Director, CRHL
Foothills Campus
Colorado State University
Fort Collins, CO 80523

G. L. Bennett
Code RP
National Aeronautics & Space
Administration
Washington, DC 20585

R. P. Berube
EH-20, Forrestal
U.S. Department of Energy
Washington, DC 20585

M. H. Bhattacharyya
BIM Div., Bldg. 202
Argonne National Laboratory
9700 South Cass Avenue
Argonne, IL 60439

PNL-8500, Pt. 1
UC-408

R. W. Bistline
Rockwell International
Rocky Flats Plant
P. O. Box 464
Golden, CO 80401

B. B. Boecker
Inhalation Toxicology Research Institute
The Lovelace Foundation for Medical Education & Research
P. O. Box 5890
Albuquerque, NM 87185

V. P. Bond
Life Sciences, Chemistry and Safety
Brookhaven National Laboratory
Building 460
Upton, NY 11973

R. Borders
Health Protection Division
U.S. Department of Energy
P.O. Box 5400
Albuquerque, NM 87115

C. M. Borgstrom
Acting Director, NEPA
EH-25, Room 3E080
U.S. Department of Energy
1000 Independence Avenue SW
Washington, DC 20585

Dr. H. Box, Director
Biophysics
Roswell Park Cancer Institute
Elm & Carlton Streets
Buffalo, NY 14263-0001

J. D. Brain
Professor of Physiology
Director, Harvard Pulmonary Specialized Center of Research
Harvard University School of Public Health
665 Huntington Avenue
Boston, MA 02115

B. D. Breitenstein
Brookhaven National Laboratory
P.O. Box 83
Upton, NY 11973

F. W. Bruenger
Division of Radiobiology
Building 586
University of Utah
Salt Lake City, UT 84112

D. R. Buhler, Chairman
Toxicology Program
Oregon State University
Corvallis, OR 97331

R. J. Bull
Associate Professor of Pharmacology/Toxicology
College of Pharmacy
Pullman, WA 99164-6510

G. Burley
Office of Radiation Programs, ANR-458
Environmental Protection Agency
Washington, DC 20460

L. K. Bustad
College of Veterinary Medicine
Washington State University
Pullman, WA 99163

C. E. Carter
National Institute of Environmental Health Sciences
P.O. Box 12233
Research Triangle Park, NC 27709

H. W. Casey, Chairman
Department of Veterinary Pathology
School of Veterinary Medicine
Louisiana State University
Baton Rouge, LA 70803

R. J. Catlin
U.T. Health Science Center-Houston
13307 Queensbury Lane
Houston, TX 77079

N. Cohen
New York University Medical Center
P.O. Box 817
Tuxedo, NY 10987

W. Cool
Nuclear Regulatory Commission
Washington, DC 20585

D. K. Craig
Savannah River Laboratories
P.O. Box 616
Aiken, SC 29802

E. P. Cronkite
Medical Department
Brookhaven National Laboratory
Upton, NY 11973

J. Crowell
The Maxima Corporation
107 Union Valley Road
Oak Ridge, TN 37830

G. Davis
Vice President & Chairman
Medical Sciences Division
Oak Ridge Associated Universities
P.O. Box 117
Oak Ridge, TN 37830-0117

G. DePlanque, Director
U.S. Nuclear Regulatory Commission
Washington, DC 20555

G. P. Dix
3028 St. Tropex Street
Las Vegas, NV 89128

T. J. Dobry, Jr.
DP-221, GTN
U.S. Department of Energy
Washington, DC 20585

DOE/Office of Scientific & Technical Information (12)

DOE - Savannah River Operations Office
Environmental Division
P.O. Box A
Aiken, SC 29801

D. Doyle
Argonne National Laboratory
9700 South Cass Avenue
Argonne, IL 60439

H. Drucker
Argonne National Laboratory
9700 South Cass Avenue
Argonne, IL 60439

J. A. Louis Dubeau
Urological Cancer Research Laboratory
USC Comprehensive Cancer Center
University of Southern California
Los Angeles, CA 90033-0800

A. P. Duhamel
ER-74, GTN
U.S. Department of Energy
Washington, DC 20585

D. Dungworth
Associate Dean of Research and Professor & Chairman
Department of Veterinary Pathology
School of Veterinary Medicine
University of California
Davis, CA 95616

Dr. Patricia W. Durbin
Division of Biology and Medicine
Lawrence Berkeley Laboratory
University of California
Berkeley, CA 94704

K. F. Eckerman
Health Studies Section
Health and Safety Research Division
Oak Ridge National Laboratory
P.O. Box 2008
Oak Ridge, TN 37831-6383

C. W. Edington, Director
National Academy of Sciences
JH 554
2101 Constitution Avenue, NW
Washington, DC 20418

G. R. Eisele
Medical Division
Oak Ridge Associated Universities
P.O. Box 117
Oak Ridge, TN 37830

M. Eisenbud
711 Bayberry Drive
Chapel Hill, NC 27514

N. B. Everett
Department of Biological Structure
University of Washington
School of Medicine
Seattle, WA 98105

H. Falk, M.D.
CDC
CEHIC/EHHE
1600 Clifton Road NE
Atlanta, GA 30333

K. P. Ferlic
Office of Scientific & Engineering Recruitment, Training & Development
TR-1
U.S. Department of Energy
Washington, DC 20585

B. H. Fimiani
Battelle, Pacific Northwest Laboratories
Washington Operations
370 L'Enfant Promenade, Suite 900
901 D Street, SW
Washington, DC 20024

M. E. Frazier
Office of Health and Environment
Office of Energy Research
U.S. Department of Energy
ER-72, GTN
Germantown, MD 20875

H. L. Friedell
Biochemical Oncology
Case-Western Reserve University
2058 Abington Road
Wearn B21
Cleveland, OH 44106

PNL-8500, Pt. 1
UC-408

T. Fritz
Argonne National Laboratory
9700 South Cass Avenue
Argonne, IL 60439

D. J. Galas
Office of Energy Research
ER-63
U.S. Department of Energy
Washington, DC 20585

D. E. Gardner
Northrop Services, Inc.
P.O. Box 12313
Research Triangle Park,
NC 27709

T. F. Gesell
Idaho State University
Campus Box 8106
Pocatello, ID 83209

R. D. Gilmore, President
Environmental Health
Sciences, Inc.
Nine Lake Bellevue Building
Suite 220
Bellevue, WA 98005

M. Goldman
Department of Radiological
Sciences (VM)
University of California
Davis, CA 95616

R. Goldsmith, Director
Office of Epidemiology & Health
Surveillance, EH-42
U.S. Department of Energy
Washington, DC 20585

G. Goldstein
Office of Epidemiology & Health
Surveillance
EH-42
U.S. Department of Energy
Washington, DC 20585

J. A. Graham
ECAO, Mail Drop 52
Environmental Protection
Agency
Research Triangle Park,
NC 27711

R. A. Griesemer, Director
National Toxicology Program
National Institutes of Health
P.O. Box 12233
Research Triangle Park,
NC 27709

G. H. Groenewold
Energy and Mineral Research
Center
University of North Dakota
Box 8123, University Station
Grand Forks, ND 58202

F. F. Hahn
Lovelace Inhalation Toxicology
Research Institute
P.O. Box 5890
Albuquerque, NM 87115

E. J. Hall
Radiological Research
Laboratory
Columbia University
630 West 168th Street
New York, NY 10032

R. Hamlin
Department of Veterinary
Physiology
The Ohio State University
1900 Coffey Road
Columbus, OH 43201

W. Happer
ER-1, FORS
U.S. Department of Energy
Washington, DC 20585

J. W. Healy
51 Grand Canyon Drive
White Rock, NM 87544

C. H. Hobbs
Inhalation Toxicology Research
Institute
The Lovelace Foundation for
Medical Education & Research
P.O. Box 5890
Albuquerque, NM 87185

L. M. Holland
Los Alamos National
Laboratory
P.O. Box 1663
Los Alamos, NM 87545

R. Hornung
DSHEFS, NIOSH
Robert A. Taft Laboratories
4676 Columbia Parkway
Cincinnati, OH 45220

R. O. Hunter, Jr.
ER-1, FORS
U.S. Department of Energy
1000 Independence Avenue SW
Washington, DC 20585

F. Hutchinson
Department of Therapeutic
Radiology, HRT 315
Yale University
School of Medicine
333 Cedar Street
New Haven, CT 06510-8040

H. Ishikawa, General Manager
Nuclear Safety Research
Association
P.O. Box 1307
Falls Church, VA 22041

E. D. Jacobson
Center for Devices & Radiological Health
Food & Drug Administration
5600 Fishers Lane, HFZ-100
Rockville, MD 20857

A. W. Johnson
San Diego State University
6310 Alvardo Court, Suite 110
San Diego, CA 92120

Dr. B. M. Jones
V-243 Carolina Meadows
Chapel Hill, NC 27514

R. K. Jones
The Lovelace Foundation for Medical Education & Research
Building 9200, Area Y
Sandia Base
Albuquerque, NM 87108

G. Y. Jordy, Director
ER-30, GTN
U.S. Department of Energy
Washington, DC 20585

C. M. Kelly
Air Products and Chemicals, Inc.
Corporate Research and Development
P.O. Box 538
Allentown, PA 18105

R. T. Kratzke
NP-40
U.S. Department of Energy
Germantown, MD 20875

W. Lowder
U.S. Department of Energy-EMEL
375 Hudson Street
New York, NY 10014-3621

W. M. Leach
Food & Drug Administration
5600 Fishers Lane, HFZ-100
Rockville, MD 20857

Librarian
Documents Department — The Libraries
Colorado State University
Ft. Collins, CO 80523

Librarian
Electric Power Research Institute
3412 Hillview Avenue
P.O. Box 10412
Palo Alto, CA 94303

Librarian
Health Sciences Library, SB-55
University of Washington
Seattle, WA 98195

Librarian
Los Alamos National Laboratory
Report Library, MS P364
P.O. Box 1663
Los Alamos, NM 87545

Librarian
Oregon Regional Primate Research Center
505 NW 185th Avenue
Beaverton, OR 97006

Library
Serials Department (#80-170187)
University of Chicago
1100 East 57th Street
Chicago, IL 60637

Librarian
Washington State University
Pullman, WA 99164-6510

J. B. Little
Department of Physiology
Harvard School of Public Health
665 Huntington Avenue
Boston, MA 02115

A. B. Lovins
Rocky Mountain Institute
1739 Snowmass Creek Road
Snowmass, CO 81654-9199

D. L. Lundgren
Inhalation Toxicology Research Institute
P.O. Box 5890
Albuquerque, NM 87185

O. R. Lunt
Laboratory of Biomedical & Environmental Sciences
University of California
900 Veteran Avenue
Los Angeles, CA 90024-1786

J. R. Maher
ER-65, GTN
U.S. Department of Energy
Washington, DC 20585

T. D. Mahony
750 Swift Boulevard
Richland, WA 99352

S. Marks
8024 47th Place West
Mukilteo, WA 98275

D. R. Mason
Nuclear Safety Branch
U.S. Department of Energy
P.O. Box A
Aiken, SC 29801

W. H. Matchett
Graduate School
New Mexico State University
Box 3G
Las Cruces, NM 88003-0001

H. M. McCammon
ER-74, GTN
U.S. Department of Energy
Washington, DC 20585

R. O. McClellan, President
Chemical Industry Institute of Toxicology
P.O. Box 12137
Research Triangle Park,
NC 27709

J. F. McInroy
Los Alamos National Laboratory
Mail Stop K484
P.O. Box 1663
Los Alamos, NM 87545

Medical Officer
Monsanto Research Corp.
Mound Laboratory
P.O. Box 32
Miamisburg, OH 45342

T. Meinhardt
DSHEFS, NIOSH
Robert A. Taft Laboratories
4676 Columbia Parkway
Cincinnati, OH 45220

C. B. Meinhold
National Council on Radiation Protection
7910 Woodmont Avenue
Suite 800
Bethesda, MD 20814

H. Menkes
Assistant Professor of Medicine & Environmental Medicine
The John Hopkins University
Baltimore, MD 21205

D. B. Menzel
Southern Occupational Health Center
University of California, Irvine
Irvine, CA 92717

C. Miller
P.O. Box 180
Watermill, NY 11976

S. Miller
Department of Radiobiology
University of Utah
Salt Lake City, UT 84112

K. Z. Morgan
1984 Castleway Drive
Atlanta, GA 30345

P. E. Morrow
Department of Biophysics
Medical Center
University of Rochester
Rochester, NY 14642

O. R. Moss
Chemical Industry Institute of Toxicology
P.O. Box 12137
Research Triangle Park,
NC 27709

W. F. Mueller
New Mexico State University
Box 4500
Las Cruces, NM 88003-4500

D. S. Nachtwey
NASA-Johnson Space Center
Mail Code SD-5
Houston, TX 77058

R. Nathan
Battelle Project Management Division
505 King Avenue
Columbus, Ohio 43201

National Library of Medicine
TSD-Serials
8600 Rockville Pike
Bethesda, MD 20014

N. S. Nelson
Office of Radiation Programs (ANR-461)
Environmental Protection Agency
401 M Street SW
Washington, DC 20460

P. Nettesheim
National Institutes of Environmental Health Sciences
Research Triangle Park,
NC 27711

W. R. Ney, Executive Director
National Council on Radiation Protection and Measurements
7910 Woodmont Avenue
Suite 800
Bethesda, MD 20814

S. W. Nielsen
Department of Pathology
New York State Veterinary College
Cornell University
Ithaca, NY 14850

R. A. Nilan
Division of Sciences
Washington State University
Pullman, WA 99164

M. Nolan
10958 Rum Cay Court
Columbia, MD 21044

Nuclear Regulatory Commission
Advisory Committee on Reactor Safeguards
Washington, DC 20555

A. F. Perge
RW-43, FORS
U.S. Department of Energy
Washington, DC 20585

D. F. Petersen
Los Alamos National Laboratory
P.O. Box 1663
Los Alamos, NM 87545

G. R. Petersen, Director
Epidemiologic Studies Division
Office of Epidemiology and Health Surveillance, EH-42
U.S. Department of Energy
Washington, DC 20585

L. E. Peterson
Epidemiology Research Unit/UTSPH
P.O. Box 20186
Houston, TX 77225

H. J. Pettengill
Deputy Assistant Secretary of Health
EH-40, GTN
U.S. Department of Energy
Washington, DC 20585

H. Pfuderer
Oak Ridge National Laboratory
P.O. Box X
Oak Ridge, TN 37830

O. G. Raabe
Laboratory for Energy-Related Health Research
University of California
Davis, CA 95616

R. Rabson
Division of Biological Energy Research
ER-17, GTN
U.S. Department of Energy
Washington, DC 20585

D. P. Rall, Director
National Institutes of Environmental Health Sciences
P.O. Box 12233
Research Triangle Park, NC 27709

R. D. Reed, Chief
Rocky Flats Area Office
Albuquerque Operations Office
U.S. Department of Energy
P.O. Box 928
Golden, CO 80402-0928

C. R. Richmond
Oak Ridge National Laboratory
4500N, MS-62523
P.O. Box 2008
Oak Ridge, TN 37831-6253

B. Robinson
Monsanto Research Corp.
Mound Laboratory
P.O. Box 32
Miamisburg, OH 45342

S. L. Rose
ER-72, GTN
U.S. Department of Energy
Washington, DC 20585

G. Runkle, Chief
U.S. Department of Energy, AL
HPB/EHD
P.O. Box 5400
Albuquerque, NM 87115

G. Saccomanno
Pathologist and Director of Laboratories
St. Marys and V. A. Hospitals
Grand Junction, CO 81501

U. Saffiotti
Laboratory of Experimental Pathology
National Cancer Institute
Building 41, Room C-105
Bethesda, MD 20892

L. Sagan
Electric Power Research Institute
3412 Hillview Avenue
P.O. Box 10412
Palo Alto, CA 94304

M. Sage
CDC (F-28)
CEHIC
1600 Clifton Road NE
Atlanta, GA 30333

J. M. Samet
New Mexico Tumor Registry
University of New Mexico
Cancer Research and Treatment Center
Albuquerque, NM 87131

R. A. Scarano
Mill Licensing Section
Nuclear Regulatory Commission
Washington, DC 20585

R. A. Schlenker
Environmental Health and Safety Department
Building 201
Argonne National Laboratory
9700 South Cass Avenue
Argonne, IL 60439

C. R. Schuller
Battelle - Seattle
4000 NE 41st Street
Seattle, WA 98105

PNL-8500, Pt. 1
UC-408

M. Schulman
ER-70, GTN
U.S. Department of Energy
Washington, DC 20585

T. M. Seed
BIM 202
Argonne National Laboratory
9700 South Cass Avenue
Argonne, IL 60439

R. B. Setlow
Brookhaven National Laboratory
Upton, NY 11973

R. Shikiar
Battelle - Seattle
4000 NE 41st Street
Seattle, WA 98105

H. P. Silverman
Beckman Instruments
2500 Harbor Blvd.
Fullerton, CA 92634

W. K. Sinclair
National Council on Radiation Protection
7910 Woodmont Avenue
Suite 800
Bethesda, MD 20814

D. H. Slade
ER-74, GTN
U.S. Department of Energy
Washington, DC 20585

D. A. Smith
ER-72, GTN
U.S. Department of Energy
Washington, DC 20585

G. S. Smith
New Mexico State University
Box 3-I
Las Cruces, NM 88003-0001

J. M. Smith
CDC
CEHIC
1600 Clifton Road NE
Atlanta, GA 30333

M. Smith
Department of Ecology
NUC Waste Library
PV-11 Building 99
South Sound
Olympia, WA 98504

Dr. H. Spitz
Department of Mechanical, Industrial, & Nuclear Engineering
University of Cincinnati
MS 072
Cincinnati, OH 45267

J. N. Stannard
17441 Plaza Animado #132
San Diego, CA 92128

R. W. Starostecki
U.S. Department of Energy
1000 Independence Ave. SW
Washington, DC 20585

R. J. Stern
EH-10, FORS
U.S. Department of Energy
Washington, DC 20585

K. G. Steyer
Nuclear Regulatory Commission
Washington, DC 20555

E. T. Still
Kerr-McGee Corporation
P.O. Box 25861
Oklahoma City, OK 73125

B. Stuart
Brookhaven National Laboratory
Upton, NY 11973

D. Swanger
Biology Department
Eastern Oregon State College
La Grande, OR 97850

J. Swinebroad
PE-43, GTN
U.S. Department of Energy
Washington, DC 20585

M. Tanaka
Physics Library
510A
Brookhaven National Laboratory
Upton, NY 11973

G. N. Taylor
Division of Radiobiology
Building 351
University of Utah
Salt Lake City, UT 84112

Technical Information Service
Savannah River Laboratory
Room 773A
E. I. duPont de Nemours & Company
Aiken, SC 29801

R. G. Thomas
Argonne National Laboratory
Environmental Res. Bldg. 203
9700 South Cass Avenue
Argonne, IL 60439

T. Thomas
Health Physics and Industrial Hygiene
EH-41
U.S. Department of Energy
Washington, DC 20585

L. H. Toburen
Board of Radiation Research
Room 342
2101 Constitution NW
Washington, DC 20318

P. W. Todd
Center for Chemical Engineering
National Bureau of Standards (773.10)
325 Broadway
Boulder, CO 80303

Trend Publishing, Inc.
National Press Building
Washington, D.C. 20045

G. E. Tripard
Acting Director, NRC
Washington State University
Pullman, WA 99164-1300

P. T'so
Division of Biophysics
Room 3120
School of Hygiene & Public Health
The Johns Hopkins University
615 North Wolfe Street
Baltimore, MD 21205

A. C. Upton
New York University Medical Center
Institute of Environmental Medicine
P. O. Box 817
Tuxedo, NY 10987

B. Valett
NORCUS
390 Hanford Street
Richland, WA 99352

E. J. Vallario
15228 Red Clover Drive
Rockville, MD 20853

R. L. Van Citters, Dean
Research and Graduate Programs
University of Washington
Seattle, WA 98105

Dr. C. R. Vest
Marymount University
2807 North Glebe Road
Arlington, VA 22207

G. J. Vodapivc
DOE - Schenectady Naval Reactors Office
P.O. Box 1069
Schenectady, NY 12301

G. L. Voelz
Los Alamos National Laboratory
MS-K404
P.O. Box 1663
Los Alamos, NM 87545

B. W. Wachholz
Radiation Effects Branch
National Cancer Institute
Executive Plaza North
6130 Executive Blvd.
Rockville, MD 20842

N. Wald
School of Public Health
University of Pittsburgh
Pittsburgh, PA 15213

A. Waldo
U.S. Department of Energy (EH-231)
1000 Independence Avenue SW
Washington, DC 20585

P. Watson
Associate Professor
Department of Chemistry
Oregon State University
Corvallis, OR 97331

M. E. Weaver
Professor of Anatomy
University of Oregon Health Science Center
School of Dentistry
Portland, OR 97201

M. H. Weeks
U.S. AEHA, Bldg. 2100
Edgewood Arsenal
Aberdeen Proving Ground, MD 21014

I. Wender
Department of Chemical Engineering
1249 Benedum Hall
University of Pittsburgh
Pittsburgh, PA 15261

W. W. Weyzen
Electric Power Research Institute
3412 Hillview Avenue
P.O. Box 10412
Palo Alto, CA 94303

K. Wilzbach
Argonne National Laboratory
9700 South Cass Avenue
Argonne, IL 60439

F. J. Wobber
U.S. Department of Energy
ER-75, GTN
Germantown, MD 20875

R. W. Wood
PTRD, OHER
ER-71, GTN
U.S. Department of Energy
Washington, DC 20585

M. E. Wrenn
Environmental Radiation & Toxicology Laboratory
University of Utah
1771 South 900 W. #10
Salt Lake City, UT 84104

Dr. Chui-hsu Yang
NASA Johnson Space Center
NASA Road 1
Mail Code: SD4
Houston, TX 77058

Dr. S. Yaniv
18 Cedarwood Court
Rockville, MD 20852

P. L. Ziemer, Ph. D.
Assistant Secretary
Environment, Safety and Health
EH-1, Forrestal
U.S. Department of Energy
Washington, DC 20585

FOREIGN

Dr. Asker Aarkrog
Riso National Laboratory
ECO/MIL
DK-4000 Roskilde
DENMARK

G. E. Adams, Director
Medical Research Council
Radiobiology Unit
Harwell, Didcot
Oxon OX11 ORD
ENGLAND

A. L. Alejandrino, Head
Biomedical Research, ARD
Republic of the Philippines
Philippine Nuclear Research Institute
P.O. Box 932
Manila
THE PHILIPPINES

M. Anderson
Library
Department of National Health & Welfare
Ottawa, Ontario
CANADA

Atomic Energy of Canada, Ltd.
Scientific Document Distribution Office
Station 14
Chalk River Nuclear Laboratories
Chalk River, Ontario KOJ 1JO
CANADA

D. C. Aumann
Institut für Physikalische Chemie
Universität Bonn
Abt. Nuklearchemie
Wegelerstraße 12
5300 Bonn 1
GERMANY

M. R. Balakrishnan, Head
Library & Information Services
Bhabha Atomic Research Centre
Bombay-400 085
INDIA

G. W. Barendsen
Laboratory for Radiobiology
AMC, FO 212
Meibergdreef 9
1105 AZ Amsterdam
THE NETHERLANDS

A. M. Beau, Librarian
Département de Protection Sanitaire
Commissariat à l'Énergie Atomique
BP 6
F-92265 Fontenay-aux-Roses
FRANCE

G. Bengtsson
Director-General
Statens Stralskyddsinstitut
Box 60204
S-104 01 Stockholm
SWEDEN

D. J. Beninson
Director, Licenciamento de Instalaciones Nulceares
Comisión Nacional de Energía Atómica
Avenida del Libertador 8250
2° Piso Of. 2330
1429 Buenos Aires
ARGENTINA

A. Bianco
Viale Seneca, 65
10131 Torino
ITALY

J. Booz
KFA Jülich Institut für Medezin
Kernsforschungsanlage Jülich
Postfach 1913
D-5170 Jülich
GERMANY

M. J. Bulman, Librarian
Medical Research Council
Radiobiology Unit
Harwell, Didcot
Oxon OX11 ORD
ENGLAND

M. Calamosia
ENEA-LAB Fisica E Tossicologia Aerosol
Via Mazzini 2
I-40138 Bologna
ITALY

Cao Shu-Yuan, Deputy Head
Laboratory of Radiation Medicine
North China Institute of Radiation Protection
P.O. Box 120
Tai-yuan, Shan-Xi
PEOPLE'S REPUBLIC OF CHINA

M. Carpentier
Commission of the European Communities
200 Rue de la Loi
J-70 6/16
B-1049 Brussels
BELGIUM

M. W. Charles
Nuclear Electric PLC
Radiological Protection Branch
Berkeley Nuclear Laboratories, Berkeley
Gloucestershire GL 13 9PB
ENGLAND

Chen Xing-An
Laboratory of Industrial Hygiene
Ministry of Public Health
2 Xinkang Street
Deshengmenwai, Beijing
PEOPLE'S REPUBLIC OF CHINA

R. Clarke
National Radiological Protection Board
Harwell, Didcot
Oxon OX11 ORQ
ENGLAND

G. F. Clemente, Director
Radiation Toxicology Laboratory
National Committee of Nuclear Energy (CNEN)
Casaccia Centre for Nuclear Studies (CSN)
Casella Postale 2400
I-00100 Roma
ITALY

H. Coffigny
Institut de Protection et de Sûreté Nucléaire
Département de Protection Sanitaire
Service de Pathologie Expérimentale
BP 6
F-92265 Fontenay-aux-Roses
FRANCE

Commission of the European Communities
DG XII - Library SDM8 R1
200 Rue de la Loi
B-1049 Brussels
BELGIUM

M. S. Davies
Medical Research Council
20 Park Crescent
London W1N 4AL
ENGLAND

Deng Zhicheng
North China Institute of Radiation Protection
Tai-yuan, Shan-Xi
PEOPLE'S REPUBLIC OF CHINA

M. Di Paola
ENEA, PAS/VALEPID
C.R.E. Casaccia
Casella Postale 2400
I-00100 Roma
ITALY

Director
Commissariat à l'Énergie Atomique
Centre d'Etudes Nucléaires
Fontenay-aux-Roses (Seine)
FRANCE

Director
Laboratorio di Radiobiologia Animale
Centro di Studi Nucleari Della Casaccia
Comitate Nazionale per l'Energia Nucleare
Casella Postale 2400
I-00100 Roma
ITALY

D. Djuric
Institute of Occupational and Radiological Health
11000 Beograd
Deligradoka 29
YUGOSLAVIA

M. Dousset
Health Ministry
Frue de la Gruerie
F-91190 Gifsur Yvette
FRANCE

J. Eapen
Biochemistry Division
Bhabha Atomic Research Centre
Bombay-400 085
INDIA

Estacão Agronómica Nacional
Biblioteca
2780 Oeiras
PORTUGAL

L. Feinendegen, Director
Institut für Medezin
Kernsforschungsanlage Jülich
Postfach 1913
D-5170 Jülich
GERMANY

PNL-8500, Pt. 1
UC-408

T. M. Fliedner
Institut für Arbeits- u. Sozialmedizin
Universität Ulm
Oberer Eselsberg M 24, 309
D-7900 Ulm
GERMANY

L. Friberg
The Karolinska Institute
Stockholm
SWEDEN

R. M. Fry, Head
Office of the Supervising Scientist for the Alligator Rivers Region
P.O. Box E348
Queen Victoria Terrace
PARKES ACT 2600
AUSTRALIA

A. Geertsema
Sasol Technology (Pty), Ltd.
P.O. Box 1
Sasolburg 9570
REPUBLIC OF SOUTH AFRICA

T. Giuseppe
ENEA-PAS-FIBI-AEROSOL
Via Mazzini 2
I-40138 Bologna
ITALY

H. L. Gjørup, Head
Health Physics Department
Atomic Energy Commission
Research Establishment
Risø, Roskilde
DENMARK

A. R. Gopal-Ayengar
73-Mysore Colony
Mahul Road, Chembur
Bombay-400 074
INDIA

C. L. Greenstock
Radiation Biology
AECL Research
Chalk River, Ontario
KOJ 1JO
CANADA

R. V. Griffith
International Atomic Energy Agency
Wagramerstraße 5
P.O. Box 200
A-1400 Vienna
AUSTRIA

Y. Hamnerius
Applied Electron Physics
Chalmers University of Technology
S-412 96 Göteborg
SWEDEN

G. P. Hanson, Chief
Radiation Medicine Unit
World Health Organization
CH-1211 Geneva 27
SWITZERLAND

J. L. Head
Department of Nuclear Science & Technology
Royal Naval College, Greenwich
London SE10 9NN
ENGLAND

W. Hofmann
Division of Biophysics
University of Salzburg
Hellbrunner Str 34
A-5020 Salzburg
AUSTRIA

J. Inaba, Director
Division of Comparative Radiotoxicology
National Institute of Radiological Sciences
9-1, Anagawa-4-chome
Chiba-shi 260
JAPAN

International Atomic Energy Agency
Documents Library
Attn: Mrs. Javor
Kaerntnerring 11
A-1010 Vienna 1
AUSTRIA

E. Iranzo
Jefe, División Protección Radiológica
Junta de Energia Nuclear
Cuidad Universitari
Madrid 3
SPAIN

W. Jacobi
Institut für Strahlenschutz
Post Schleissheim
Ingolstadter Landstrasse 1
D-8042 Neuherberg
GERMANY

K. E. Lennart Johansson
Radiofysiska Inst.
Regionsjukhuset
S-901-82 Umeå
SWEDEN

A. M. Kellerer
Institut für Strahlen biologie, GSF
Ingolstadter Landstrasse 1
D-8042 Neuherberg b. München
GERMANY

T. Kivikas
Studsvik Nuclear
S-611 82 Nyköping
SWEDEN

H.-J. Klimisch
BASF Aktiengesellschaft
Abteilung Toxikologie, Z470
D-6700 Ludwigshafen
GERMANY

H. E. Knoell
Battelle-Institut e.V.
Am Römerhof 35
Postfach 900160
D-6000 Frankfurt am Main 90
GERMANY

T. Kumatori
National Institute of
Radiological Sciences
9-1, Anagawa-4-chome
Chiba-shi 260
JAPAN

Dr. L. Lafuma
Department de Protection
Sanitair
Commissariate a l'Energie
Atomique
92260 Fontenay-Aux-Roses
FRANCE

J. R. A. Lakey
Department of Nuclear Science
& Technology
Royal Naval College
Greenwich Naval college
SW10 9NN
ENGLAND

Li De-Ping
Professor and Director of North
China
Institute of Radiation
Prctection, NMI
P.O. Box 120
Tai-yuan, Shan-Xi
PEOPLE'S REPUBLIC OF
CHINA

Librarian
Alberta Environmental Centre
Bag 4000
Vegreville, Alberta T9C 1T4
CANADA

Librarian
Centre d'Etudes Nucléaires de
Saclay
P.O. Box 2, Saclay
Fig-sur-Yvette (S&O)
FRANCE

Librarian
CSIRO
314 Albert Street
P.O. Box 89
East Melbourne, Victoria
AUSTRALIA

Librarian
CSIRO
Division of Wildlife and Ecology
P.O. Box 84
Lyneham, ACT 2602
AUSTRALIA

Librarian
HCS/EHE
World Health Organization
CH-1211 Geneva 27
SWITZERLAND

Librarian
Kernforschungzentrum
Karlsruhe
Institut für Strahlenbiologie
Postfach 3640
D-75 Karlsruhe 1
GERMANY

Librarian
Max-Planck Institut für
Biophysics
Forstkasstraße
D-6000 Frankfurt/Main
GERMANY

Librarian
Medical Research Council
Radiobiology Unit
Chilton
Oxon OX11 ORD
ENGLAND

Librarian
Ministry of Agriculture,
Fisheries & Food
Fisheries Laboratory
Lowestoft, Suffolk NR33 OHT
ENGLAND

Librarian
National Institute of
Radiological Sciences
9-1, Anagawa-4-chome
Chiba-shi 260
JAPAN

Librarian
Supervising Scientist for the
Alligator Rivers Region
Level 23, Bondi Junction Plaza
P.O. Box 387
Bondi Junction NSW 2022
AUSTRALIA

Library
Atomic Energy Commission of
Canada, Ltd.
Whiteshell Nuclear Research
Establishment
Pinawa, Manitoba ROE 1L0
CANADA

Library
Department of Meteorology
University of Stockholm
Arrhenius Laboratory
S-106 91 Stockholm
SWEDEN

B. Lindell
National Institute of Radiation Protection
Fack S-104 01
Stockholm 60
SWEDEN

J R. Maisin
Radiobiology Department
C.E.N. - S.C.K.
Mol
BELGIUM

A. M. Marko
9 Huron Street
Deep River, Ontario KOJ 1PO
CANADA

R. Masse
Institut de Protection et de Sûreté Nucléaire
Département de Protection Sanitaire
Service d'Etudes Appliquées de Protection Sanitaire
BP No. 6
F-92260 Fontenay-aux-Roses
FRANCE

H. Matsudaira,
Director General
National Institute of Radiological Sciences
9-1, Anagawa-4-chome
Chiba-shi 260
JAPAN

O. Matsuoka
Research Consultant
Abiko Research Laboratory
Central Research Institute of Electric Power Industry
1646, Abiko, Abiko City
Cniba-ken 270-11
JAPAN

N. Matsusaka
Department of Veterinary Medicine
Faculty of Agriculture
Iwate University
Ueda, Morioka
Iwate 020
JAPAN

S. Mattsson
Department of Radiation Physics
Malmö General Hopsital
S-214 01 Malmö
SWEDEN

R. G. C. McElroy
Atomic Energy Commission of Canada, Ltd.
Dosimetric Research Branch
Chalk River, Ontario KOJ 1JO
CANADA

F.-I. S. Medina
Cytogenetics Laboratory
Biomedical Research Division
A.R.C.
Philippine Atomic Energy Commission
P.O. Box 932
Manila
THE PHILIPPINES

M. L. Mendelsohn
Radiation Effects Research Foundation
1-8-6 Nakagawa
Nagasaki 850
JAPAN

Meng Zi-Qiang
Department of Environmental Science
Shanxi University
Tai-Yuan, Shan-xi
PEOPLE'S REPUBLIC OF CHINA

P. Metalli
ENEA-PAS
CRE Casaccia
Casella Postale 2400
I-00100 Roma
ITALY

H. J. Metivier
Institut de Protection et de Sûreté Nucléaire
Centre d'Études de Service de Fontenay-aux-Roses
BP 6
F-92265 Fontenay-aux-Roses
FRANCE

A. R. Morgan
Biotechnology
Building 353
AEA Technology
Harwell, Didcot
Oxfordshire OX11 ORA
ENGLAND

Y. I. Moskalev
Institute of Biophysics
Ministry of Public Health
Givopisnaya 46
Moscow
RUSSIA

J. Muller
7 Millgate Crescent
Willowdale, Ontario M2K 1L5
CANADA

D. K. Myers, Head
Radiation Biology Branch
Atomic Energy Commission of Canada, Ltd.
Chalk River, Ontario
CANADA

J. C. Nénot, Deputy Director
Département de Protection
Centre d' Etudes Nucléaires
BP 6
F-92260 Fontenay-aux-Roses
FRANCE

R. Osborne
Atomic Energy Commission of Canada, Ltd.
Biology and Health Physics Division
Chalk River Nuclear Laboratories
P.O. Box 62
Chalk River, Ontario KOJ 1JO
CANADA

J. Pacha
Silesian Medical School
Fac. of Pharmacy
Ul. Jagiellonska 4
41-200 Sosnowiec
POLAND

H. G. Paretzke
GSF Institut für Strahlenschutz
Ingolstadter Landstraße 1
D-8042 Neuherberg
GERMANY

N. Parmentier
Département de Protection Sanitaire
Centre d'Etudes Nucléaires
BP 6
F-92260 Fontenay-aux-Roses
FRANCE

G. Patrick
Medical Research Council
Radiobiology Unit
Harwell, Didcot
Oxon OX11 ORD
ENGLAND

O. Pavlovski
Institute of Biophysics
Ministry of Public Health
Givopisnaya 46
Moscow D-182
RUSSIA

G. Premazzi
Commission of the European Communities
Joint Research Centre
Ispra Establishment
I-21020 Ispra
ITALY

V. Prodi
Department of Physics
University of Bologna
Via Irnerio 46
I-40126 Bologna
ITALY

O. Ravera
Commission of the European Communities, C.C.R.
I-21020 Ispra (Varese)
ITALY

REP Instituutes TNO
TNO Division of Health Research Library
P.O. Box 5815
151 Lange Kleiweg
2280 HV Rijswijk
THE NETHERLANDS

Reports Librarian
Harwell Laboratory,
Building 465
UKAEA
Harwell, Didcot
Oxon OX11 ORB
ENGLAND

P. J. A. Rombout
Inhalation Toxicology Department
National Institute of Public Health and Environmental Protection
P.O. Box 1
NL-3720 BA Bilthoven
THE NETHERLANDS

M. Roy
Institut de Protection et de Sûreté Nucléaire
Département de Protection Sanitaire
Service d'Etudes Appliquées de Protection Sanitaire
BP 6
F-92260 Fontenay-aux-Roses
FRANCE

F. A. Sacherer
Battelle-Institut e.V.
Am Römerhof 35
Postfach 900160
D-6000 Frankfurt am Main 90
GERMANY

W. Seelentag, Chief Medical Officer
Radiation Health Unit
World Health Organization
CH-1211 Geneva 27
SWITZERLAND

J. Sinnaeve
Biology, Radiation Protection Medical Research
Commission of the European Communities
200 Rue de la Loi
B-1049 Brussels
BELGIUM

H. Smith
International Commission on Radiological Protection
P.O. Box 35
Didcot
Oxon OX11 ORJ
ENGLAND

J. W. Stather
National Radiological Protection Board
Building 383
Chilton, Didcot
Oxon OX11 ORQ
ENGLAND

PNL-8500, Pt. 1
UC-408

M. J. Suess
Regional Officer for
Environmental Hazards
World Health Organization
8, Scherfigsvej
DK-2100 Copenhagen
DENMARK

Sun Shi-quan, Head
Radiation-Medicine Department
North China Institute of
Radiation Protection, MNI
P.O. Box 120
Tai-yuan, Shan-Xi
PEOPLE'S REPUBLIC OF
CHINA

G. Tarroni
EHEA-AMB-BIO-FITS
Viale G. B. Ercolani 8
I-40138 Bologna
ITALY

D. M. Taylor
5 Branwen Close
The Sanctuary
Culverhouse Cross
Cardiff CF5 4NE
ENGLAND

K. H. Tempel
Institut für Pharmakologie,
Toxikologie und Pharmazie
Fachbereich Tiermedizin der
Universität München
Veterinärstraße 13
D-8000 München 22
GERMANY

J. W. Thiessen
Radiation Effects Research
Foundation
1-8-6 Nakagawa
Nagasaki 850
JAPAN

United Nations Scientific
Committee on the Effects of
Atomic Radiation
Vienna International Center
P.O. Box 500
A-1400 Vienna
AUSTRIA

D. Van As
Atomic Energy Corporation
P.O. Box 582
Pretoria 0001
REPUBLIC OF SOUTH AFRICA

Dame Janet Vaughan
1 Fairlawn End
First Turn
Wolvercote
Oxon OX2 8AP
ENGLAND

J. Vennart
Bardon, Ickleton Road,
Wantage
Oxon OX12 9OA
ENGLAND

Vienna International Centre
Library
Gifts and Exchange
P.O. Box 100
A-1400 Vienna
AUSTRIA

V. Volf
Kernforschungzentrum
Karlsruhe
Institut für Genetik und
Toxikologie von Spaltstoffen
Postfach 3640
D-7500 Karlsruhe 1
GERMANY

G. Walinder
Unit of Radiological Oncology
University of Agricultural
Sciences
P.O. Box 7031
S-750 07 Uppsala
SWEDEN

Wang Hengde
North China Institute of
Radiation Protection
P.O. Box 120
Tai-yuan, Shan-Xi
PEOPLE'S REPUBLIC OF
CHINA

Wang Renzhi
Institute of Radiation Medicine
27# Tai Ping Road
Beijing 100850
PEOPLE'S REPUBLIC OF
CHINA

Wang Ruifa, Associate Director
Laboratory of Industrial Hygiene
Ministry of Public Health
2 Xinkang Street
P.O. Box 8018
Deshengmenwai, Beijing
100088
PEOPLE'S REPUBLIC OF
CHINA

Wang Yibing
North China Institute of
Radiation Protection
P.O. Box 120
Tai-yuan, Shan-Xi
PEOPLE'S REPUBLIC OF
CHINA

Wei Lü-Xin
Laboratory of Industrial
Hygiene
Ministry of Public Health
2 Xinkang Street
Deshengmenwai, Beijing 100088
PEOPLE'S REPUBLIC OF
CHINA

J. Wells
Radiobiology Laboratory
Radiation Biophysics
Nuclear Electric
Berkeley Nuclear Laboratories
Berkeley
Gloucestershire GL 13 9PB
ENGLAND

B. C. Winkler, Director of Licensing
Raad Op Atomic
Atoomkrag Energy Board
Privaatsk X 256
Pretoria 0001
REPUBLIC OF SOUTH AFRICA

Wu De-Chang
Institute of Radiation Medicine
27# Tai Ping Road
Beijing
PEOPLE'S REPUBLIC OF CHINA

Yao Jiaxiang
Laboratory of Industrial Hygiene
2 Xinkang Street
Deshengmenwai, Beijing
100088
PEOPLE'S REPUBLIC OF CHINA

Kenjiro Yokoro, Director
Research Institute for Nuclear Medicine & Biology
Hiroshima University
Kasumi 1-2-3, Minami-ku
Hiroshima 734
JAPAN

V. Zelenv
Institute of Experimental Biology and Genetics
Czechoslovak Academy of Sciences
Bidekpvocla 1-83
Prague 4
CZECHOSLOVAKIA

Zhu Zhixian
China Research Institute of Radiation Protection
Ministry of Nuclear Industry
P.O. Box 120
Tai-yuan, Shan-Xi
PEOPLES REPUBLIC OF CHINA

ONSITE

DOE Richland Operations Office (4)

D. R. Segna A5-90
P. W. Kruger A5-90
E. C. Norman A5-16
Public Reading Room A1-65

WSU Tri-Cities University Center

H. R. Gover, Librarian H2-52

Hanford Environmental Health Foundation (3)

S. E. Dietert H2-52
R. L. Kathren H2-52
T. Henn H1-01

U. S. Testing

V. H. Pettey H2-51

Westinghouse Hanford Co.

D. E. Simpson B3-55

Pacific Northwest Laboratory (222)

R. R. Adee P8-13
R. C. Adams K6-52
L. E. Anderson K4-28
R. W. Baalman K1-50 (20)
J. F. Bagley K1-66
W. J. Bair K1-50 (2)
L. A. Braby P8-47
J. K. Briant P7-53
A. L. Brooks P7-53
J. A. Buchanan P7-82
R. L. Buschbom P7-82
D. P. Chandler K4-13
T. D. Chikalla P7-75
B. J. Chou K4-10
J. M. Christensen P7-58 (2)
T. T. Claudson K1-66
J. A. Creim K4-28
F. T. Cross K4-13
G. E. Dagle P7-53
J. R. Decker K4-16
H. S. DeFord K4-16
J. A. Dill K4-16
R. J. Douthart K4-13
R. D. DuBois P8-47
C. G. Edmonds P8-19
C. E. Elderkin K6-11
J. J. Evanoff K6-91
D. R. Fisher K3-53
L. G. Florek K4-16
W. C. Forsythe K4-16
A. F. Fuciarelli P7-56
K. M. Gideon K4-10
R. A. Gies K4-13
A. W. Gieschen K4-16
E. S. Gilbert P7-82
M. F. Gillis K1-50
W. A. Glass K4-13
B. J. Greenspan K4-16
D. K. Hammerberg P8-29
B. K. Hayden K4-16
J. M. Heineman P7-56
L. A. Holmes K1-29
M. G. Horstman K4-10
V. G. Horstman P7-58
J. R. Houston A3-60
T. E. Hui K3-70
A. C. James K3-51
A. E. Jarrell K4-12
J. R. Johnson K3-53
R. F. Jostes K4-13
M. T. Karagianes P7-58
M. Knotek K1-48
E. G. Kuffel K4-16
W. W. Laity K2-50
K. E. Lauhala P7-58
F. C. Leung K4-13

PNL-8500, Pt. 1
UC-408

M. K. Lien P8-47
E. K. Ligotke P7-82
C. C. Lumetta P7-58 (5)
J. A. Mahaffey P7-82
D. D. Mahlum P7-56
E. M. Maloney K1-51
D. B. Mann P7-56
T. J. Mast K4-10
J. C. McDonald P7-03
P. W. Mellick K4-10
D. L. Miller P7-53
J. H. Miller P8-47
M. C. Miller P7-41
R. A. Miller K4-10
C. E. Mitchell P7-53
J. E. Morris P7-53
D. A. Nelson P8-38
J. M. Nelson P8-47
J. F. Park P7-52 (50)
M. A. Parkhurst K3-57
J. E. Pelkey K7-22
R. W. Perkins P7-35
J. T. Pierce K4-10
G. J. Powers P7-53
J. C. Prather P7-82
H. A. Ragan K4-13
R. A. Renne K4-10
D. N. Rommereim K4-28
R. L. Rommereim K4-10
C. O. Romsos K4-10
E. J. Rossignol K4-16
S. E. Rowe K4-13
P. S. Ruemmler K4-10
J. L. Ryan P7-25
C. L. Sanders H2-52
L. B. Sasser P7-53
G. F. Schiefelbein P8-38
J. E. Schmaltz K7-22
L. C. Schmid K1-34
R. P. Schneider P7-56
L. E. Sever BSRC
B. D. Shipp K1-73
M. R. Sikov P7-53
J. C. Simpson K7-34
E. C. Sisk P7-56
L. G. Smith P7-58
S. K. Smith P7-82
D. L. Springer P7-56
J. G. Stephan K6-84
R. G. Stevens P7-82
D. L. Stewart K6-96
G. L. Stiegler P7-56
L. C. Stillwell P7-56
G. M. Stokes K1-74
K. L. Swinth K3-55
W. L. Templeton K1-30
T. S. Tenforde K1-50 (10)
G. S. Thomas K7-22
R. M. Thomas P7-53
R. C. Thompson P7-58
B. D. Thrall P7-50
K. D. Thrall K3-54
H. R. Udseth P8-19
B. E. Vaughan K1-66
R. A. Walters K1-50
C. R. Watson P7-82
R. J. Weigel K4-16
R. E. Weller P7-52
R. B. Westerberg K4-16
T. J. Whitaker K2-21
E. L. Wierman K7-98
R. E. Wildung P7-54
W. E. Wilson P8-47
J. D. Zimbrick P7-58
Health Physics Department Library
Life Sciences Library (2)
Publishing Coordination
Technical Report Files (5)

☆U.S. GOVERNMENT PRINTING OFFICE: 1993-792-877

END

DATE
FILMED
9/2/93